The design of a synthetic, bioactive dermal scaffold to assist the healing of chronic, non-healing wounds

Daniel John Gilmartin

A thesis submitted for the degree of

Doctor of Philosophy

UCL

Declaration

I, Daniel John Gilmartin, confirm that the work presented in this thesis is my own. Where information has been derived from other sources, I confirm that this has been indicated in the thesis.

Signed: **Date:**

Acknowledgements

I would like to express my greatest thanks to the members of my laboratory who provided both scientific discussion and moral support throughout my PhD. Thank you to Nikki Davis, Jessica Sutcliffe, Katie Heath, Ming Hou and Beverley Bright.

I would also like to extend my gratitude to members of the data analysis team at the UCL Confocal Imaging department at UCL for their much valued support during my use of the equipment in the facility. This includes Tim Robson, Chris Thrasivoulou, Daniel Ciantar and Jane Pendjiky.

I also appreciate the scientific input and direction provided by my supervisors Prof David Becker and Dr Suwan Jayasinghe throughout the course of my PhD, as well as from Anthony Phillips of CoDa Therapeutics Inc. in New Zealand.

Lastly, I would like to extend my sincere gratitude to all of my family and friends, without whom I could have never made it this far!

Abstract

Chronic ulcers are painful, hard-to-heal wounds. To assist the healing of full-thickness ulcers and burns, engineers have designed scaffolds; synthetic skin substitutes intended to act as a temporary structure to support cell growth and wound regeneration. Remarkably few studies have investigated the effect of scaffolds on healing at the cellular level, however. Owing to the lack of clear evidence, the initial project aim was to investigate the function of scaffolds *in vivo*, with the hypothesis "scaffolds do not promote healing of full-thickness wounds." After applying fabricated collagen scaffolds to full-thickness wounds, scaffolds appeared to integrate with the wound edge poorly. Wound edge keratinocytes were found to express markedly elevated levels of the gap junction proteins connexin 43 (Cx43) and Cx26, surprisingly similar to chronic wounds. In an effort to improve integration, scaffolds were bioactivated through local application of a Cx43 antisense sequence (asODN). This significantly reduced wound edge Cx43 expression, epithelial thickening and inflammation of the surrounding tissue compared to using ordinary scaffolds, yet healing still occurred underneath scaffolds without matrix integration. An alternative hypothesis was formulated; that "scaffolds could instead be used to deliver drugs to render them beneficial in ulcer treatment." To achieve this, scaffolds were polymer coated with Cx43 asODN using an emulsion technique, and asODN elution was confirmed *in vitro* to occur over several days using UV spectrophotometry. Application of coated Cx43 asODN scaffolds significantly improved wound re-epithelialisation, even over untreated wounds, and prevented scaffold-associated adverse effects. Incorporation of novel Cx26 antisense sequences also significantly reduced wound edge Cx26 levels and improved re-epithelialisation. Wounds treated with combined Cx26 and Cx43 asODN scaffolds typically re-epithelialised further still, such that using both sequences may be synergistic. These findings support the use of coated scaffolds as drug delivery mechanisms that could be developed to treat chronic wounds.

Abbreviations

asODN	Antisense Oligodeoxynucleotide
Cx	Connexin
DFU	Diabetic foot ulcer
ECM	Extracellular matrix
EGF	Epidermal growth factor
FBS	Foetal bovine serum
FGF	Fibroblast growth factor
FRET	Förster resonance energy transfer
GJIC	Gap junctional intercellular communication
H&E	Haematoxylin and eosin
IL	Interleukin
MMP	Matrix metalloproteinase
ODN	Oligodeoxynucleotide
PCL	Polycaprolactone
PDGF	Platelet-derived growth factor
PLGA	Poly(lactic-co-glycolic acid)
PMN	Polymorphonuclear leukocyte
PU	Pressure ulcer
ROS	Reactive oxygen species
SEM	Scanning electron microscopy (or in statistical references - Standard error of the mean)
sODN	Sense oligodeoxynucleotide
STZ	Streptozotocin
TGF-ß	Transforming growth factor beta
TIMP	Tissue inhibitor of metalloproteinase
TNF- α	Tumour necrosis factor alpha
VEGF	Vascular endothelial growth factor
VLU	Venous leg ulcer
α-SMA	Alpha smooth muscle actin

Table of Contents

Declaration & Acknowledgements 2

Abstract 3

Abbreviations 4

Table of Contents 5

Table of Figures 14

List of Tables 18

Introduction 19

1.1 – The structure and function of skin 20

1.11 – Epidermis 20

1.12 – Gap junctions 23

1.13 – Dermis 25

1.14 – Hypodermis 26

1.2 – Acute wound healing 27

1.21 – Haemostasis and inflammation 27

1.22 – Re-epithelialisation 29

1.23 – Granulation tissue formation 30

1.24 – Wound closure and remodelling 31

1.3 – Connexins in wound healing 32

1.31 – Connexins in intact skin 33

1.32 – Connexins in acute wounds 34

1.4 – Chronic and diabetic wound healing 36

1.41 – Ulcer aetiology 37

Diabetic foot ulcers 37

Venous leg ulcers 38

Pressure ulcers 38

1.42 – Shared features of chronic ulcers 39

1.43 – Connexin expression in chronic ulcers and diabetic wounds 40

1.5 – Chronic wound treatment 42

1.51 – Conventional treatments 42

1.52 – Surgery 43

1.53 – Scaffolds as a chronic ulcer treatment 45

1.54 – Antisense oligodeoxynucleotide therapy 47

1.6 – Aims of the study 50

Materials and Methods 52

Introduction 53

2.1 – Scaffold materials and design 53

2.11 – Collagen scaffolds 53

2.12 – Alginate microspheres 54

2.13 – Commercial scaffold materials 54

2.14 – Scanning electron microscopy assessment of scaffold structure 54

2.2 – Scaffold bioactivation 55

2.21 – Infusion with Pluronic gel containing Cx43 asODN 55

2.22 – Application of polymer coatings containing Cx43 asODN 56

2.3 – *In vitro* analysis of coated scaffolds 57

2.31 – Quantification of asODN elution 57

2.32 – Förster Resonance Energy Transfer (FRET) analysis 57
2.4 – Animal procedures 59
2.41 – Rodent strains 59
2.42 – *In vivo* full-thickness wounding 59
2.5 – Histology procedures 60
2.51 – Harvesting wounds 60
2.52 – Haematoxylin and eosin staining 60
2.53 – Immunofluorescence staining 61
2.6 – Light microscopy 61
2.61 – Epidermal measurements 61
2.62 – Polymorphonuclear cell quantification 61
2.63 – Measurement of granulation tissue area 62
2.64 – Assessment of smooth muscle actin area 62
2.7 – Confocal microscopy 63
2.71 – Confocal image analysis 63
2.8 – Statistical analysis 64
2.81 – Power analysis 64
2.82 – Normality tests 64
2.83 – Statistical tests 64
Design and application of a bioactive scaffold 65
3.1 – Introduction 66
3.2 – Materials and methods 70
3.21 – Scaffold preparation 70

Scaffold and microsphere fabrication 70
Commercial scaffold materials 70
Investigation of scaffold porosity 70
Scaffold infusion with Cx43 asODN 70
3.22 – Surgery 71
3.23 – Processing and histology 71
Tissue collection 71
Haematoxylin and eosin staining 71
Immunofluorescence staining 72
3.24 – Analysis 72
Imaging 72
Epidermal thickening measurements 72
Connexin 26 and 43 protein quantification 73
Polymorphonuclear leukocyte quantification 73
Statistical analyses 73
3.3 – Development of a collagen scaffold for *in vivo* use 74
Scaffolds impede full-thickness wound repair 74
3.31 – Scaffolds inhibit wound closure 74
3.32 - Scaffolds induce aberrant thickening of wound edge keratinocytes 76
3.33 - Thickened epidermal bulbs contain elevated levels of connexins 43 and 26 78
3.4 – Modification of scaffolds 80
3.41 - Collagen scaffold design 80
3.42 – Investigation into the effect of alginate applications on wound healing 80
3.5 - Bioactivation of collagen scaffolds using Cx43 asODN 81

3.51 – Bioactivated scaffolds macroscopically appear to integrate with wounds..... 81

3.52 – Bioactivated scaffolds do not induce wound edge epidermal thickening 82

3.53 – Cx43 and Cx26 expression is downregulated following application of Cx43 asODN bioactivated scaffolds..... 86

3.6 – The effect of scaffold bioactivation on inflammation..... 86

3.7 – Discussion..... 88

Conclusions..... 92

Development of a Cx43 asODN sustained release scaffold..... 94

4.1 – Introduction..... 95

4.2 – Materials and Methods..... 98

4.21 – Scaffold fabrication..... 98

4.22 – Application of polymer coatings containing Cx43 asODN to scaffolds..... 98

4.23 – Surgery..... 99

4.24 – Processing and histology..... 99

Harvesting wounds..... 99

Haematoxylin and eosin staining..... 100

Immunofluorescence staining..... 100

4.25 – *In vitro* assays..... 100

Quantification of asODN elution..... 100

Förster Resonance Energy Transfer analysis..... 101

4.26 – Analysis..... 102

Imaging..... 102

Epidermal thickening measurements..... 102

Connexin 26 and 43 protein quantification..... 102

Polymorphonuclear cell quantification 103

Measurement of granulation tissue area 103

Assessment of smooth muscle actin area 103

Statistical analyses 103

4.3 – Design of a drug eluting polymer coating 104

4.31 – Investigation into coating properties 104

4.32 – Analysis of asODN degradation in scaffold coatings 106

4.4 – Using coated scaffolds to deliver Cx43 asODN to wounds 109

4.41 – Macroscopic analysis of wounds 109

4.42 – Re-epithelialisation analysis following scaffold placement 111

4.43 – Local inflammatory response following Cx43 asODN scaffold application 116

4.44 – Cx26 and 43 expression in wound edge keratinocytes following scaffold application 119

4.5 – The effect of Cx43 asODN coated scaffolds on the late stages of wound healing 128

4.51 – Granulation tissue formation following scaffold application 128

4.52 – Application of Cx43 asODN coated scaffolds reduces the region of wound alpha smooth muscle actin (α-SMA) at D10 131

4.7 – Discussion 133

Conclusions 139

Targeting Cx26 expression using scaffolds 141

5.1 – Introduction 142

5.2 – Materials and Methods 144

5.21 – Scaffold fabrication 144

5.22 – Application of polymer coatings containing Cx26 or Cx43 asODN to scaffolds 145

5.23 – Surgery 146

5.24 – Processing and histology 146

Harvesting wounds 146

Haematoxylin and eosin staining 146

Immunofluorescence staining 147

5.25 – Analysis 147

Imaging 147

Epidermal thickening and re-epithelialisation measurements 147

Connexin 26 and 43 protein quantification 148

Polymorphonuclear cell quantification 148

Measurement of granulation tissue area 148

Assessment of smooth muscle actin area 148

Statistical analyses 149

5.3 – Wound healing response to a Cx26 asODN coated scaffold 149

5.31 – Evaluation of macroscopic wound closure 149

5.32 – Cx26 asODN coated scaffolds significantly improve wound re-epithelialisation 151

5.33 - The effect of Cx26 asODN coated scaffolds on the local inflammatory cell response 157

5.5 – Cx26 asODN promotes wound edge Cx26 downregulation 160

5.6 – The effect of Cx26 asODN coated scaffolds on the late stages of wound healing. 168

5.61 – Granulation tissue area measurements at D10 and 15. 168

5.62 – The effect of the combined Cx26/43 asODN scaffold on the presence of myofibroblasts 168

5.7 – Discussion 173

Conclusions 177

Discussion 178

6.1 – Introduction 179

6.2 – Comparing project findings with the literature 179

6.21 - Downregulation of connexins 43 and 26 179

6.22 – Scaffold design 181

6.23 – Wound closure 183

6.24 – Inflammation and the foreign body reaction 186

6.3 – Additional therapeutic candidates for scaffold bioactivation 188

6.31 – Growth factors 188

6.32 – Peptide therapy 190

6.33 – Antisense therapy 191

6.4 – A revised role for dermal scaffolds in wound healing 193

6.41 - Study limitations 194

6.5 – Future experiments 196

6.51 – Performing a systematic review of scaffold-related literature 196

6.52 – Establishment of a novel chronic wound model 204

Assessments 205

6.53 – Continued development of the polymer coated drug-eluting scaffold 209

6.6 – Conclusions 211

Publications and presentations 213

Bibliography.....214

Table of Figures

CHAPTER 1 - Introduction

Figure 1. 1 – The structure of human skin 21

Figure 1. 2 – Vertebrate connexin structure and gap junction assembly 24

Figure 1. 3 – Haemostasis and the early inflammatory response in acute wound healing ... 27

Figure 1. 4 – The late inflammatory, re-epithelialisation and proliferation phases of acute wound healing 29

Figure 1. 5 – The remodelling phase of acute wound healing 31

Figure 1. 6 – Examples of commercial cellular, acellular and extracellular matrix-derived scaffolds. 46

Figure 1. 7 – Antisense oligodeoxynucleotide mode of action 49

CHAPTER 2 - Materials and Methods

Figure 2. 1 – A simplified diagram illustrating the principles of FRET. 58

CHAPTER 3 - Design and application of a bioactive scaffold

Figure 3. 1 – Electrospinning a collagen scaffold 74

Figure 3. 2 – Scaffold application to wounds 75

Figure 3. 3 – Epithelial and Connexin response to scaffolds. 77

Figure 3. 4 – Wound edge Connexin 43 expression is elevated across all different collagen scaffold applications. 79

Figure 3. 5 – Connexin 43 expression in alginate treated wounds..... 81

Figure 3. 6 – The *in vivo* effect of Cx43 asODN bioactivation of scaffolds. 83

Figure 3. 7 – The microscopic effects of Cx43 asODN bioactivation of scaffolds 3 days after wounding. 84

Figure 3. 8 – The microscopic effects of Cx43 asODN bioactivation of scaffolds 5 days after wounding. 85

Figure 3. 9 – The effect of scaffolds on polymorphonuclear cell recruitment. 87

CHAPTER 4 - Development of a Cx43 asODN sustained release scaffold

Figure 4. 1 – Coating of collagen scaffolds with a Cx43 asODN and PLGA emulsion. ... 104

Figure 4. 2. – Cx43 asODN elution from differing combinations of scaffold coatings..... 105

Figure 4. 3 – Cx43 asODN elution from differing combinations of scaffold coatings..... 108

Figure 4. 4 – Macroscopic wound evaluation following coated scaffold placement..... 110

Figure 4. 5 – D1 full-thickness wound healing following application of Cx43 asODN polymer coated scaffolds..... 113

Figure 4. 6 – D3 full-thickness wound healing following application of Cx43 asODN polymer coated scaffolds..... 114

Figure 4. 7 – D5 full-thickness wound healing following application of Cx43 asODN polymer coated scaffolds.....115

Figure 4. 8 – Leading edge epidermal thickening following Cx43 asODN scaffold application. 116

Figure 4. 9 – The effect of Cx43 asODN scaffold application on the dermal infiltration of polymorphonuclear cells 118

Figure 4. 10 – D1 Cx26 expression in the epidermal wound edge of scaffold-treated wounds.....120

Figure 4. 11 – D1 Cx43 expression in the epidermal wound edge of scaffold-treated wounds.....121

Figure 4. 12 – D3 Cx26 expression in the epidermal wound edge of scaffold-treated wounds.....124

Figure 4. 13 – D3 Cx43 expression in the epidermal wound edge of scaffold-treated wounds.....125

Figure 4. 14 – D5 Cx26 expression in the epidermal wound edge of scaffold-treated wounds.....126

Figure 4. 15 – D5 Cx43 expression in the epidermal wound edge of scaffold-treated wounds.....127

Figure 4. 16 – Full-thickness wounds treated with scaffolds at D10.....129

Figure 4. 17 – Full-thickness wounds treated with scaffolds at D15.....130

Figure 4. 18 – α-SMA expression in D10 scaffold-treated wounds.....132

Figure 5. 1 – Effect of scaffold application on macroscopic wound appearance 150

Figure 5. 2 – D1 full-thickness wound healing following application of scaffolds coated with Cx26 asODN 152

Figure 5. 3 – D3 full-thickness wound healing following application of scaffolds coated with Cx26 asODN 153

Figure 5. 4 – D5 full-thickness wound healing following application of scaffolds coated with Cx26 asODN 155

Figure 5. 5 – Thickening of the nascent epidermis following Cx26 asODN scaffold application. 156

Figure 5. 6 – The effect of Cx26 asODN scaffold application on the number of polymorphonuclear cells (PMNs) infiltrating the unwound dermis 159

Figure 5. 7 – D1 Cx26 expression in the epidermal wound edge of scaffold-treated wounds. 162

Figure 5. 8 – D1 Cx43 expression in the epidermal wound edge of scaffold-treated wounds. 163

Figure 5. 9 – D3 Cx26 expression in the epidermal wound edge of scaffold-treated wounds. 164

Figure 5. 10 – D3 Cx43 expression in the epidermal wound edge of scaffold-treated wounds. 165

Figure 5. 11 – D5 Cx26 expression in the epidermal wound edge of scaffold-treated wounds. 166

Figure 5. 12 – D5 Cx43 expression in the epidermal wound edge of scaffold-treated wounds. 167

Figure 5. 13 – Full-thickness wounds treated with scaffolds at D10.....170

Figure 5. 14 – Full-thickness wounds treated with scaffolds at D15.....171

Figure 5. 15 – α-SMA expression in D10 scaffold-treated wounds 172

CHAPTER 6 - Discussion

Figure 6. 1 – Interpretation of the function of uncoated and bioactive scaffolds.....195

List of Tables

CHAPTER 1 - Introduction

Table 1. 1 – Connexin expression in the uninjured skin of humans and rodents 33

Table 1. 2 – Changes in rodent connexin expression in injured keratinocytes, wound fibroblasts and proximal epidermal appendages up to 7 days after acute wounding.....35

CHAPTER 1

Introduction

1.1 – The structure and function of skin

The skin is the largest organ in the body and serves an essential role to protect against stresses such as desiccation, injury and infection (Margadant et al., 2010). It is comprised of multiple distinct layers, each providing the skin with a number of different properties.

1.11 – Epidermis

The epidermis comprises the topmost layer of skin and the predominant cell type present in it is the keratinocyte. The primary role of keratinocytes is to form a tightly adherent layer of cells that has the important role of establishing a stratified squamous epithelial barrier (Figure 1. 1). Keratinocytes in the epidermis can be segregated into 4 distinct layers, each of which differs in shape and function. From the bottom layer upwards, keratinocytes in the epidermis can be categorised as belonging to the basal, spinous, granular or cornified layers (Haake et al., 2001). Many keratinocytes in the lowermost basal layer are capable of proliferation and are cuboidal in shape. Basal keratinocytes are a single layer and have the important function of anchoring the epidermis to the underlying basement membrane as well as supplementing the epidermis with additional keratinocytes (Martin, 1997). The former is achieved through the expression of cell-matrix junctional proteins termed hemidesmosomes on the cell membrane of basal keratinocytes, which bind to anchoring filaments contained within the underlying basal lamina (Figure 2. 1, top left). As new cells are produced, existing keratinocytes can delaminate from the basement membrane and progress upwards throughout the layers in a process termed terminal differentiation (Fuchs and Byrne, 1994). As well as keratinocytes, around 5-10% of cells in the basal layer of adult human skin are melanocytes. Melanocytes are responsible for the production of melanin, necessary to absorb UV radiation to afford a level of protection against DNA damage (Costin and Hearing, 2007). This is demonstrated in albino individuals, who are deficient in melanin production and prone to sun-mediated skin damage. Merkel cells are also prevalent within the basal layer of mammalian epidermis, and are associated with light touch discrimination of shape and texture. As such, they are more common in touch-sensitive areas such as the fingertips (Maricich et al., 2009).

The layer directly above the basal layer is the spinous layer, and is usually around 8-10 rows of keratinocytes thick (Haake et al., 2001). Interspersing these keratinocytes are

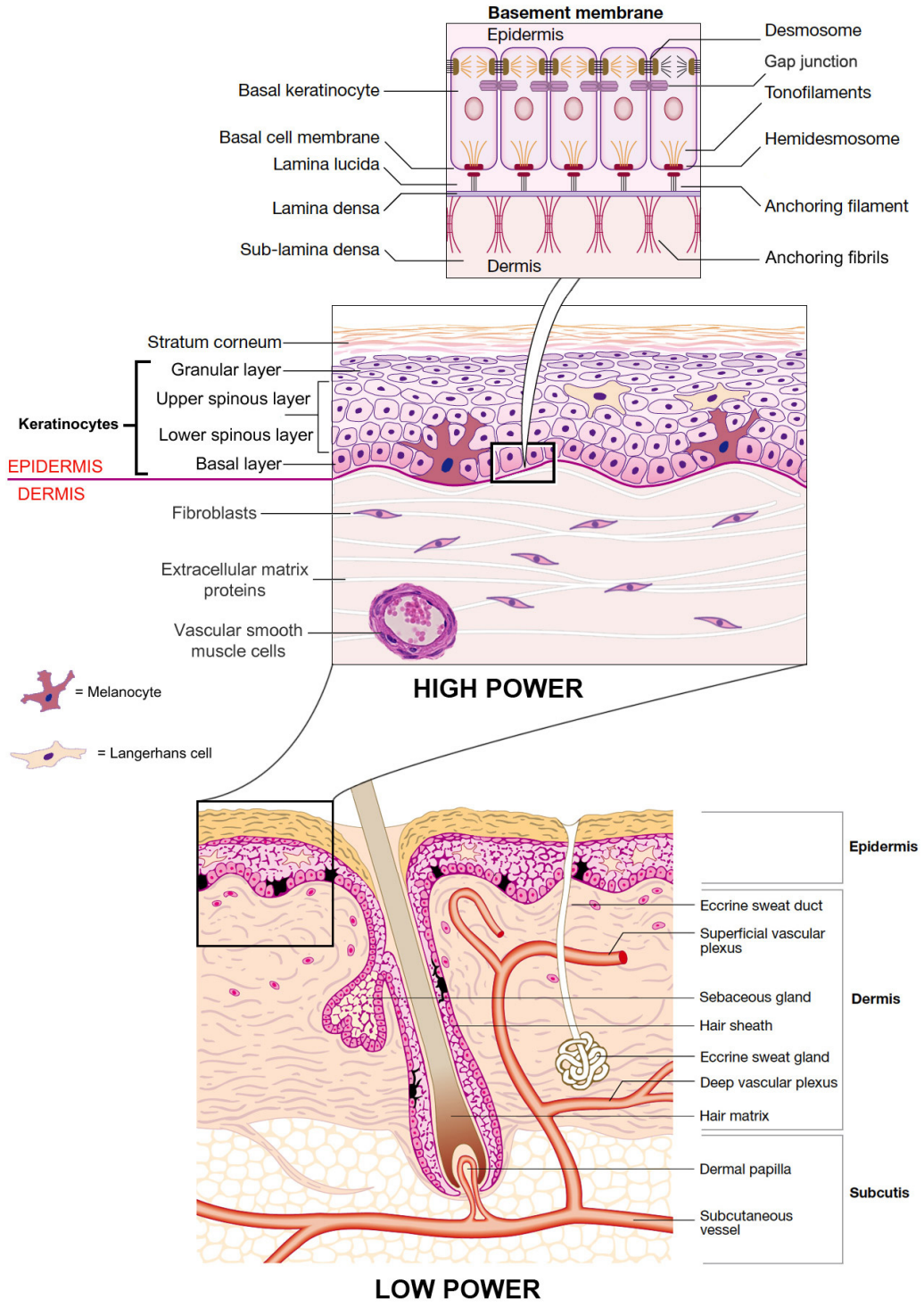

Figure 1. 1 – The structure of human skin

The skin is comprised of multiple layers of functionally distinct cells, and each layer can differ in the types of cells and cell junctions present. The structure of skin is shown both at a low power (bottom) and high power (middle). The major membrane bound channels present on keratinocytes are illustrated in the topmost illustration (image adapted from Colledge et al., 2010 using Goliger and Paul, 1995).

Langerhans cells. Langerhans cells are dendritic cells that function as antigen-presenting cells in the case of infection (Cella et al., 1997). The epidermal region of skin also contributes to the development of hair follicles, an appendage exclusive to mammals. These epithelial organs project downwards into the territory of the dermis and are accompanied by arrector pili muscles which can contract to elevate hair, as well as sebaceous glands to secrete sebum to lubricate and waterproof the skin (Paus and Cotsarelis, 1999). Keratinocytes in the spinous layer additionally express desmosome junctions on the surface of the cell membrane. Unlike hemidesmosomes, the extracellular domain of desmosomes anchors the cells to desmosomes of adjacent cells, while the intracellular domain binds to the intracellular keratin filaments within the cell cytoplasm (Green and Jones, 1996). Desmosomes are formed by an aggregation of adhesion associated cadherin proteins, and function primarily to mechanically adhere cells to one another. Formation of a barrier is also assisted by the presence of adherens junctions. These are assembled from transmembrane proteins of the cadherin family. Cadherins also bind to each other on neighbouring cells, while the internal domain bind to members of the catenin family of proteins. Catenins then anchor the cell to the actin cytoskeleton within the cell cytoplasm, resulting in a strong mechanical attachment between cells (Niessen, 2007). The closest contact formed between keratinocytes is due to the presence of tight junctions on the surface of the cell membrane. These are multiprotein complexes found only in epithelial cells and anchor the apical region of cells to one another. Tight junctions prevent the liberal diffusion of molecules between cells, thus allowing the establishment of distinct compartments. This is particularly important in the case of a lumen, such as in a blood vessel wall, and plays a crucial role in establishing apical to basal cell polarity. Three main protein families form tight junctions: occludins, claudins and junctional adhesion molecules (Niessen, 2007).

Directly above the spinous keratinocyte layer is the granular layer. This is usually around 3-5 rows of flattened keratinocytes thick and the cells are highly differentiated from those in the basal layer. Granular keratinocytes contain keratohyalin granules filled with histadine- and proline-rich proteins, resulting in classification of the layer as 'granular' (Haake et al., 2001). These proteins are considered responsible for binding keratin filaments to one another. While being displaced from the granular to stratum corneum layers, keratinocytes secrete lamellar bodies that contain lipids and proteins to create a hydrophobic lipid barrier of protection for the skin (Schmitz and Muller, 1991). Additionally, during the process of

keratinocyte displacement in an upwards direction, the stratum corneum cells flatten further, enucleate and lose their cytoplasmic organelles and water. These terminally differentiated flattened cells, termed corneocytes, form the thick stratum corneum layer of skin which can comprise several layers (Candi et al., 2005). The number of layers depends on the location within the body; thick-skinned areas such as the soles of feet and palms contain the most layers (Caspers et al., 2003). Corneocytes, while biologically dead, are still filled with water-retaining keratin bundles. Corneocytes lie within a cornified protein envelope and are responsible for many of the barrier-related functions of skin (Kalinin et al., 2002). Corneocytes in the bottom layers of the stratum corneum attach to one another through corneodesmosomes, which are variants of regular desmosomes (Haftek et al., 1998). As lower layers of corneocytes are displaced, protease degradation of these junctions allows dead skin cells to be shed through desquamation (Caubet et al., 2004). The total time taken between generation of a basal keratinocyte to it shedding from the stratum corneum is approximately 6 weeks (Haake et al., 2001). The shedding of skin is a finely tuned process where skin shedding occurs at approximately the same rate as keratinocyte replenishment. This balance is particularly important, since perturbations to the cycle have been frequently noted in painful hyperproliferative skin conditions (Bauer and Boezeman, 1986, Weinstein et al., 1984).

1.12 – Gap junctions

Also embedded in the membranes of multiple cells throughout the epidermis and dermis in skin are gap junctions. Gap junctions are crucial for cell to cell communication and are formed by proteins of the connexin (Cx) family. These are structurally related four-pass transmembrane proteins found throughout a diverse number of cell types (Makowski et al., 1977). Connexins have a cytoplasmic loop and two extracellular loops, as well as cytoplasmic facing C and N termini (Figure 1. 2). There are currently 21 known connexins in humans and 20 in mice, and the naming of connexin proteins refers to the molecular weight of the protein (Sohl and Willecke, 2004). In invertebrates, a group of proteins called innexins instead form gap junctions, which share homology with mammalian pannexins. Unlike connexins, pannexins are not thought to form gap junctions (Bauer et al., 2005, Panchin et al., 2000). In mammals, six Cx subunits assemble to form a connexon hemichannel embedded within the plasma membrane of a cell (Goodenough, 1975, Makowski et al., 1977). Individual connexon hemichannels on a cell surface can alone

function to allow the transport of ions between the cell and the environment (Goodenough, 1975). However, connexons on opposing cells can also dock to form a gap junction. Gap junctions formed by docking of two connexons can either be homotypic (both connexons are composed of the same connexin proteins), heterotypic (individual connexons are composed of one type of connexin, but the connexin in question is different between the two connexons), or heteromeric (an asymmetrical assortment of 6 connexin proteins makes up each connexon) (Sosinsky, 1995). Direct cell communication through gap junctions that cluster as plaques on cells can then be achieved through the passage of ions, metabolites and second messengers under 1 kDa in size (Yeager and Nicholson, 1996). Gap junctions are found throughout multiple tissues and have been demonstrated to function across a number of processes, including heart contraction (Sohl and Willecke, 2004), corneal homeostasis (Yuan et al., 2009) and wound healing (Coutinho et al., 2003). The prevalence of different connexin proteins differs between cell types and species, as well as the different layers of the epidermis, and this expression can change during processes such as wound healing (connexins are described in detail in section 2.3) (Coutinho et al., 2003).

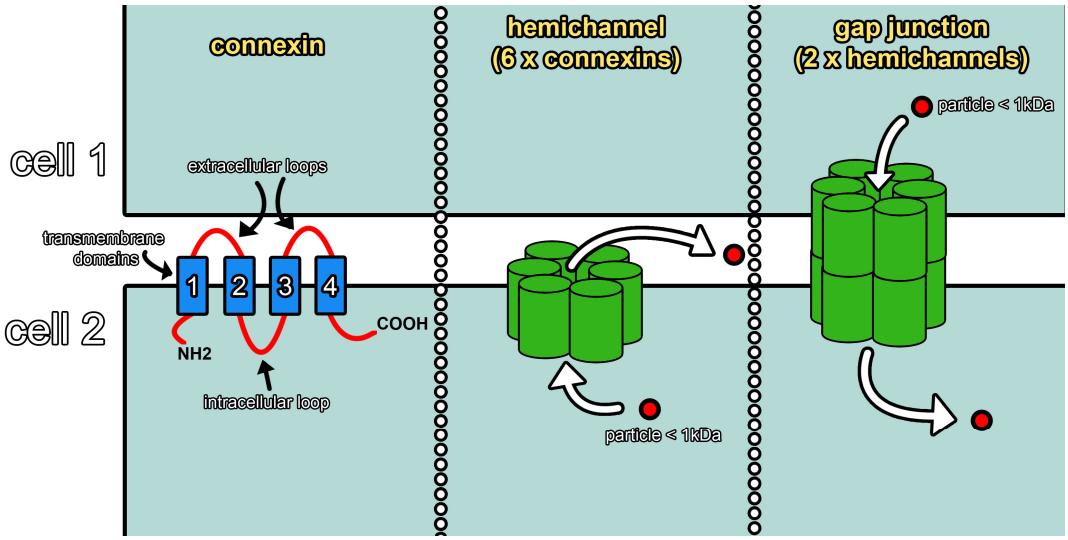

Figure 1. 2 – Vertebrate connexin structure and gap junction assembly
Left: the simplified structure of a single connexin transmembrane protein. Middle: six connexin subunits group to form an active connexin hemichannel that can function to transport small molecules under 1 kDa in size. Right: hemichannels on neighbouring cells can dock to form a gap junction, allowing transport to take place between cells (figure created using information from Wagner, 2008).

1.13 – Dermis

In humans and pigs, keratinocytes in the epidermis protrude into the underlying dermis as finger-like projections referred to as rete pegs. These strengthen the attachment of the epidermis to the dermis, although through the process of ageing the protrusions flatten and the epidermis thins, reducing skin resistance to shearing (Bank and Nix, 2006). In contrast to the epidermis, the dermis is a considerably thicker layer yet has a much lower cell density. The dermis functions as the connective tissue component of the skin and provides skin with elasticity and tensile strength (Vogel, 1974). The most common cell type in the dermis is the fibroblast. Fibroblasts are responsible for synthesis of many of the connective tissue components of the skin, the most abundant of which are collagen and elastin. In the case of the latter, elastin is often lost as the individual ages, resulting in a loss of elasticity and wrinkling (Narayanan et al., 1989, Sephel and Davidson, 1986). Collagen is the most prevalent protein, and in fact accounts for 75% of the dry weight of the human body. There are around 20 genetically distinct collagens, but the majority found within native dermal tissue belongs to type I, III and V. Of this, approximately 80-90% is type I and 8-12% is type III (Weber et al., 1984). The various collagen species differ in the makeup of the 3 chains that form each collagen molecule. Collagen is synthesised through chain glycosylation, assembly into procollagen molecules and bonding to rough endoplasmic reticulum, where it is then destined for secretion into the extracellular space (Lodish H et al., 2000). There it is proteolytically cleaved by matrix metalloproteinase (MMP) enzymes, resulting in the formation of banded collagen fibrils and filament networks.

Within the dermis, glycosaminoglycans, glycoproteins and proteoglycans together form a gel referred to as 'ground substance' through which migration can occur over, and it also provides a structure for the embedding of fibrous components. Skin proteoglycans are large molecules of around 100-2500 kDa in size and can bind up to 1000 times their own volume and regulate dermal volume (Archer, 2008). Glycosaminoglycans such as hyaluronan, on the other hand, are polymers that are formed of repeating disaccharides and provide a link to components of the overlying basement membrane (Brown et al., 2001). The glycoproteins present in the extracellular matrix include fibronectin, thrombospondin, tenascin and vitronectin, and similar to the other components of the dermis like collagen, they provide a substrate for cell adhesion and interaction through integrin receptors (Midwood et al., 2004). Many of the components in the dermis are not distributed evenly,

however, leading to the establishment of distinct layers within the dermis. The topmost layer of the dermis is labelled the papillary dermis. This contains the rete peg protrusions from the epidermis as well as small bundles of fine collagen fibrils and immature elastic fibres (Fore, 2006). The structural properties of the papillary dermis confer the ability to resist mechanical stress upon the skin. The layer also contains a large proportion of active fibroblasts that have the ability to synthesise proteoglycans to regulate dermal volume (Imai et al., 1992, Midwood et al., 2004). The papillary dermis also contains capillaries extending from the subpapillary plexus, which project into and terminate at the dermal rete pegs. These capillaries are necessary for nutrient exchange to both dermal and epidermal layers (Pasyk et al., 1989). Below the papillary layer is the significantly thicker reticular layer. Unlike the papillary dermis, this layer contains a far greater proportion of mature, large diameter collagen fibrils that are woven into a mesh network. Elastic fibres wrap around the collagen fibrils to form a combined structure, and provide the skin with a considerably strong level of mechanical stress resistance and elasticity (Silver et al., 2001).

1.14 – Hypodermis

Also referred to as subcutaneous tissue or subcutis, the hypodermis resides below the dermis and above tissue and bodily organs. The hypodermis is responsible for insulating the body as well as providing a shock resistant cushion to the skin (Tobin, 2006). The predominant tissue in the hypodermis is adipose tissue, and is often referred to as subcutaneous fat. The numerous adipocytes in this layer provide the body with an energy reserve for the body under starving conditions. The layer of fat is not present in all tissues, however; it is absent from multiple regions of the body including the scalp, eyelids and foreskin. (Hausman et al., 1981). The hypodermis is also highly vascularised, such that the layer is often selected for drug injection (Dominguez-Delgado et al., 2010). Also within the layer are apocrine and eccrine sweat glands responsible for release of sweat, as well as hair follicles that can extend deep into the hypodermis (Wilke et al., 2007). Unique to the hypodermis in certain areas of the body is the panniculus carnosus. This is a continuous striated sheet of muscle found in areas such as the scalp, face and hand, and is responsible for twitch contractions, and in the face allows the performance of certain facial expressions. In animals such as mice and rats the panniculus carnosus is considerably more extensive and covers larger areas of the body such as the back (Treuting et al., 2012).

1.2 – Acute wound healing

In order to maintain the highly organised structure of skin following injury a complex series of events are triggered to restore the epithelial barrier and tensile strength of the tissue.

1.21 – Haemostasis and inflammation

When the skin is wounded a cascade of events to halt blood loss and repair the wound is initiated (Nurden et al., 2008, Figure 1. 3). In order to halt blood loss platelets are drawn to injury-induced extravasated blood and deposit a temporary fibrin-rich clot to plug the wound. Platelets also secrete platelet-derived growth factor (PDGF) and transforming growth factor ß1 (TGF-ß1) (Grainger et al., 1995). PDGF acts as a powerful chemoattractant, recruiting neutrophils, monocytes and macrophages, as well as the fibroblasts required for deposition of new ECM proteins (Hosgood, 1993). TGF-ß1 stimulates macrophages to secrete inflammatory cytokines such as interleukin-1 (IL-1)

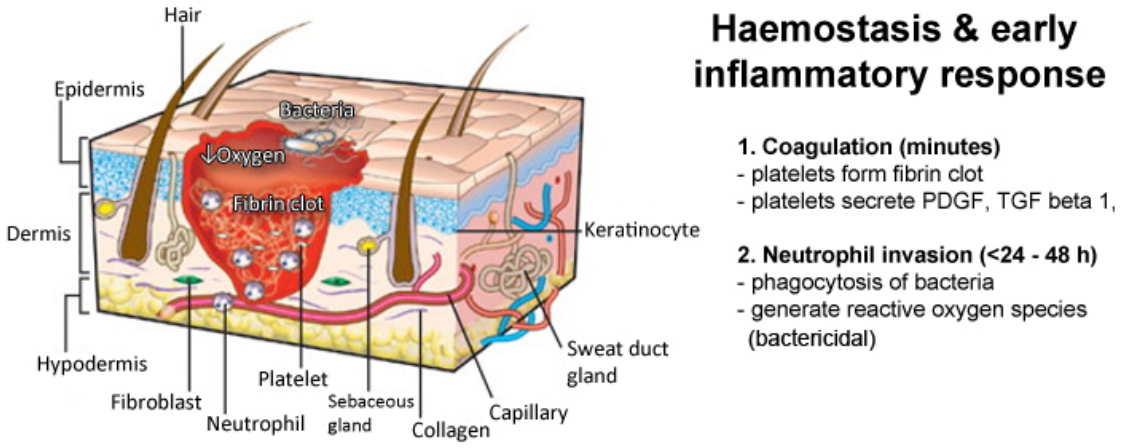

Figure 1. 3 – Haemostasis and the early inflammatory response in acute wound healing

Shortly after wounding, platelets are recruited and form a fibrin blood clot to prevent blood loss. Platelets secrete factors to attract neutrophils within the first 24 h, which are the first line of defence against infection (image derived from Stein and Kuchler, 2013).

and tumour necrosis factor α (TNFα), as well as additional PDGF to promote further chemotaxis of fibroblasts (Nurden et al., 2008). Characterisation of inflammation in response to a wound has been documented as far back as the Romans, who noted the signs of *rubor* (redness), *tumor* (swelling), *calor* (heat) and *dolor* (pain) (Shah, 2011).

Within the first 24 h of injury, neutrophils that have been activated by pro-inflammatory cytokines undergo diapedesis to exit the capillaries close to the wound and begin to phagocytose dead cells, bacteria and debris (Lingen, 2001, Figure 1. 3). Neutrophil diapedesis is dependent on expression of various adhesion molecules on endothelial cells including endothelial P- and E-selectins as well as ICAM-1 and -2. In turn, these interact with integrins on the neutrophil surface, including CD18, CD11b and CD11c (Abbassi et al., 1993, Jones et al., 1993, Smits et al., 2000). Neutrophil recruitment is also promoted through the degranulation of mast cells to release a cocktail of pro-inflammatory cytokines. Indeed, studies of mast cell deficient mice indicated a decreased level of neutrophil recruitment (Egozi et al., 2003). As well as polymorphonuclear neutrophils, monocytes arrive at the wound site and are activated by TGF-ß1 as well as the ECM to develop into macrophages (Figure 1. 4). Neutrophil recruitment typically subsides after 2-3 days, while macrophages appear from around 2-3 days onwards. As monocytes mature, they can be differentially activated to become either M1 or M2 macrophage subtypes. M1 macrophages adopt a pro-inflammatory role, secreting inflammatory cytokines such as interferon gamma (IFN-γ), IL-1, IL-6, and IL-23, as well as reactive oxygen species (ROS). These are responsible for the targeted destruction and phagocytosis of pathogens and spent neutrophils (Diegelmann and Evans, 2004). M2 macrophages, on the other hand, instead express mediators that promote angiogenesis and tissue regeneration. These include IL-10, TGF-ß1 and low levels of IL-12. Macrophages are also responsible for the release of various mitogens, including PDGF and vascular endothelial growth factor (VEGF) (Mosser and Edwards, 2008, Strassmann et al., 1994). For this reason, some have argued that macrophage recruitment and function is crucial for efficient wound healing to occur, and macrophage depletion has been reported to result in a reduced wound healing capacity (DiPietro and Polverini, 1993). However, further evidence suggests that macrophages, and even neutrophils, may not be essential to wound healing. Wounds made in neonatal PU.1 knockout mice that are deficient in macrophages and neutrophils re-epithelialise faster with an absence of fibrosis (Martin et al., 2003). While macrophages and neutrophils are important in targeting pathogens it is possible that beyond this, their main function is to

regulate scarring and fibrosis, as opposed to wound re-epithelialisation. If this is the case, anti-inflammatory therapies could improve the healing of even acute wounds (Martin and Leibovich, 2005).

1.22 – Re-epithelialisation

The re-epithelialisation stage consists of the proliferation and outward migration of epidermal keratinocytes to cover the open wound (Figure 1. 4). This step is initiated within 24 h and coincides with the inflammatory phase (Winter, 1962). Re-epithelialisation is first triggered by TGF-ß1 release from activated macrophages, keratinocytes and macrophages which acts to drive keratinocyte integrin expression (Gailit et al., 1994). Desmosome and hemidesmosome adhesion complexes dissolve and peripheral cytoplasmic actin forms, allowing cell migration to take place (Chen et al., 1993). Re-arrangement of these actin bundles confers cell polarity and allows for the formation of a protruding lamellipodia used for migration. E-cadherin, required for adherens junction formation, has also been noted

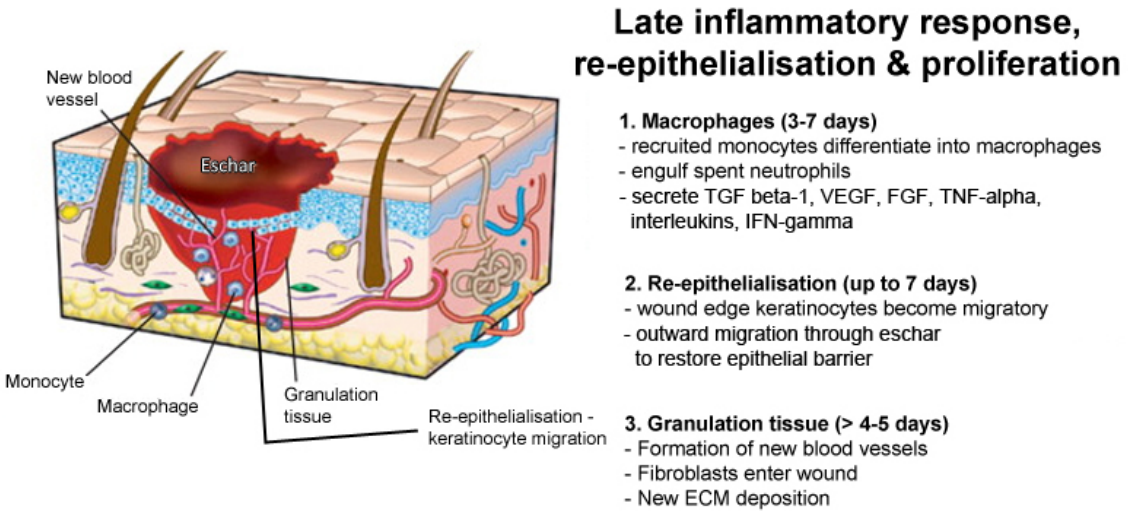

Figure 1. 4 – The late inflammatory, re-epithelialisation and proliferation phases of acute wound healing

A few days into wound healing, monocytes are recruited that differentiate into macrophages. Macrophages release a number of factors that promote angiogenesis, fibroblast recruitment and ECM deposition, resulting in granulation tissue formation. Throughout wound healing and usually up to 7 days, keratinocytes at the wound edge become migratory to restore the epithelial barrier (image derived from Stein and Kuchler, 2013).

to vanish from the leading edge keratinocytes in mouse wounds (Kuwahara et al., 2001). The expression of various integrins prior to re-epithelialisation prepares keratinocytes for migration and adhesion to the temporary wound matrix, consisting of fibronectin, vitronectin, tenascin and collagen (Gailit et al., 1994). Since keratinocytes are required to migrate through granulation tissue they enzymatically convert plasminogen at the clot to plasmin, which degrades a pathway for cell advancement (Pepper, 2001). Around 24-72 h after migration commences, a dramatic increase in the proliferation of keratinocytes behind the migratory leading edge occurs (Usui et al., 2005). This, alongside contributions from epidermal stem cells in hair follicles, supplies keratinocytes to repair the broken epidermis. Migrating keratinocytes also deposit laminin to help reconstitute the basal membrane (Nguyen et al., 2000). Once the epithelial barrier is restored at around 5-7 days, keratinocytes once again adopt a flattened morphology and reform cell-cell junctions. Re-stratification then occurs, leaving behind an epidermis similar to that in uninjured tissue. This re-epithelialisation process is affected by dynamic changes in Cx43. Cx43 downregulation at the wound is necessary in keratinocytes and fibroblasts in order to adopt a migratory phenotype (discussed in further detail in section 1.32; Goliger and Paul, 1995, Coutinho et al., 2003, Mendoza-Naranjo et al., 2012a).

1.23 – Granulation tissue formation

Around three to five days after injury granulation tissue rich in vascular endothelial cells, macrophages and fibroblasts is formed at the wound (Tonnesen et al., 2000, Figure 1. 4). The proliferation and subsequent migration of fibroblasts into the tissue is due to the release of cytokines and growth factors from active macrophages and platelets, including PDGF and TGF-ß1 (Schreier et al., 1993). Fibroblasts adhere to and migrate along the fibrin matrix laid down by platelets and monocytes, into the wound space. The main function of fibroblasts in the early proliferative phase is to rapidly synthesise collagen III, providing structural support to the wound (Klinge et al., 2000). This is largely regulated by TGF-ß1, which increases fibroblast transcription of collagen- and protease-related genes, as well as the downregulation of MMP activity by inducing expression of tissue inhibitors of metalloproteinases (TIMPs) (Hall et al., 2003).

Newly formed tissue must obtain a blood supply. Components of the recently deposited ECM, particularly fibrin, have been shown to promote angiogenesis (Knighton et al., 1982).

Macrophages and fibroblasts also secrete cytokines that promote proliferation and chemotaxis of vascular endothelial cells, such as fibroblast growth factor 2 (FGF2), TGF-α, vascular endothelial growth factor (VEGF) angiopoietin and TNFα (Li et al., 2003). Expression of the $\alpha_V\beta_3$ integrin on cells has also been linked to promotion of migration and blood vessel elongation (Brooks et al., 1994). Localised hypoxia is also an important trigger of angiogenesis. Hypoxia Inducible Factor (HIF)-1, a heterodimeric transcription factor, accumulates under hypoxic conditions (Semenza, 2001). Accumulated HIF-1 subsequently assembles as heterodimers which then go on to drive transcription of pro-angiogenesis factors such as VEGF.

1.24 – Wound closure and remodelling

Re-epithelialisation is not the only contributor to wound closure. Fibroblasts at the wound edge can also differentiate into specialised contractile cells termed myofibroblasts, and are most numerous around 4-14 days after wounding (Darby et al., 1990, Figure 1. 5). This differentiation can be induced by various soluble factors including TGF-ß1, PDGF, TNFα and IL1. Myofibroblasts primarily differ from fibroblasts by their accumulation of large bundles of alpha smooth muscle actin along the cytoplasmic face of the plasma membrane

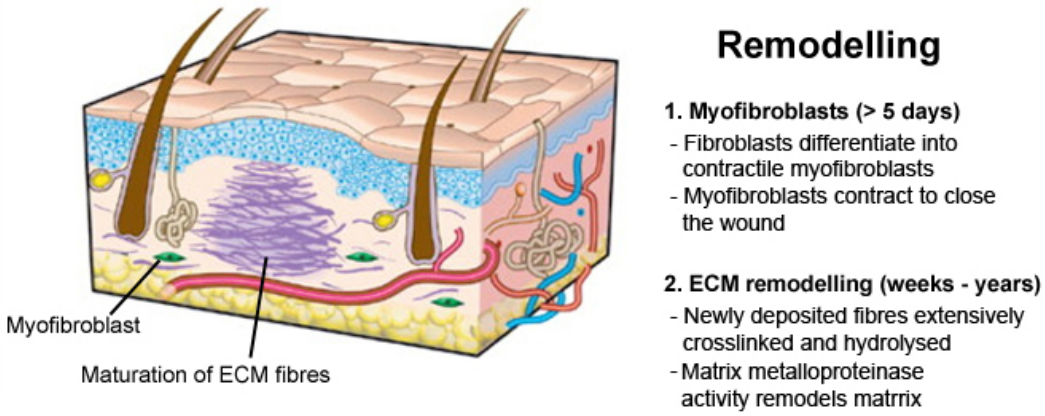

Figure 1. 5 – The remodelling phase of acute wound healing
From around 5 days onwards, fibroblast differentiation into myofibroblasts results in a contractile cell capable of promoting wound closure. Newly deposited ECM fibres are continuously crosslinked and processed through activity of matrix metalloproteinases for up to 2 years (image derived from Stein and Kuchler, 2013).

(Thannickal et al., 2003). These bundles function to allow contraction in conjunction with ongoing re-epithelialisation to pull the wound margins together. Initially appearing close to the wound margins, myofibroblasts eventually reside close to the centre of wounds around 7-14 days after wounding. Interestingly, targeted knockdown of Cx43 has been shown to advance the differentiation of fibroblasts to myofibroblasts by around 1-2 days, resulting in acceleration of wound closure and loss of myofibroblasts from the edge of wounds (Mori et al., 2006). In contrast to this, a different study made use of skin implants that release lithium chloride, a known gap junction intercellular communication (GJIC) inducer, and found that there was an increased amount of granulation tissue deposited, and that collagen fibres were more mature (Moyer et al., 2002). After the two migrating epithelial sheets have fused many myofibroblasts show signs of apoptosis (Desmouliere et al., 1995). This may be necessary for optimal healing, as persistence of myofibroblasts has been found in keloid scars where collagen deposition is extreme (Ladin et al., 1998). The ECM is then remodelled for up to 2 years to enhance the tensile strength of the new skin (Gurtner et al., 2008, Figure 1. 5). During this time the type III collagen deposited by fibroblasts is gradually degraded by MMPs and replaced with the more versatile type I collagen (Klinge et al., 2000). MMP activity reduces the collagen density found in the provisional matrix, after which a fine balance between synthesis and degradation of further collagen is established (Witte et al., 1998). The most time-consuming stage of remodelling is the continuous crosslinking of matrix proteins, resulting in an end restoration of about 70-80% of the original tissue tensile strength (Diegelmann and Evans, 2004). In adults, this method of remodelling results in formation of a fibrous scar (Stadelmann et al., 1998). This is not the case in the developing embryo where healing is privileged and occurs without scarring (Martin, 1997). This is in part due to healing occurring solely by actin contraction in cells at the wound in a purse string method (Redd et al., 2004).

1.3 – Connexins in wound healing

The structural components of gap junctions, connexins, have been implicated throughout development and a number of other biological processes. These include heart contraction (Jalife et al., 1999), CNS signalling (Dermietzel et al., 1991), mammary gland differentiation (El-Sabban et al., 2003), inflammation (Mori et al., 2006) and wound re-epithelialisation

(Wang et al., 2007, Qiu et al., 2003). The variations between different connexins occur primarily through variations in the cytoplasmic loop and the C-terminus of the protein structure, and have given rise to the 21 different connexin proteins in humans. Specifically in skin, expression profiling of these individual connexin proteins in both intact and wounded skin reveals distinct localisation and function of the different connexin types.

1.31 – Connexins in intact skin

In rodents there are at least 4 connexins that are differentially expressed in the skin during the wound healing process; Cx43, Cx26, Cx30 and Cx31.1 (Risek et al., 1992, Goliger and Paul, 1995). Cx43 is the most ubiquitous connexin and also the most studied. It has been implicated in a number of processes including inflammation, wound re-epithelialisation, differentiation and proliferation (Becker et al., 2012, Mori et al., 2006, Qiu et al., 2003). In intact skin, Cx43 is expressed in the epidermis, dermal fibroblasts, hair follicles, vascular smooth muscle cells and sebaceous glands (Table 1. 1). In rodent epidermis Cx43 expression tends to be localised to the basal layer, while in humans Cx43 is also present

Structure	Human	Rodent
Stratum corneum	none	none
Granular layer	31.1^{++}, 26^{low}, 31^{++}, 37, 30.3^{+++}, 40^{++}	26^{low}, 30^{low}, 31.1^{+}, 31, 37
Spinous layer (upper)	30^{+}, 31.1^{+}, 26^{low}, 37, 31^{+}, 30.3^{+}, 45^{low}	31, 37
Spinous layer (lower)	43^{++}, 30^{+}, 31.1^{+}, 37, 31	31, 37
Basal layer	43^{+}, 32^{+}	43^{++}, 37, 40
Fibroblasts	43^{+}, 40^{low}, 45^{low}	43^{+}
Blood vessels	43^{+++}, 26^{++}, 30^{+}	43^{+++}, 26^{++}, 30^{+}
Sebaceous glands	43^{++}	43^{+}
Hair follicles	43^{+++}, 26^{++}, 30^{+}, 31.1^{low}	43^{+++}, 26^{++}, 30^{+}, 31.1^{low}

Table 1. 1 – Connexin expression in the uninjured skin of humans and rodents
The expression of a number of different connexins is localised to specific regions of the skin. In the order of highest relative expression to lowest: +++ > ++ > + > low. Connexins whose levels of expression have not accurately been determined for individual compartments have not been assigned a symbol (table constructed using information from Richard, 2000 and Coutinho et al., 2003).

within the lower and upper rows of keratinocytes within the spinous layer (Di et al., 2001). While Cx43 expression is strongly expressed in the epidermis, both Cx26 and Cx30 are expressed at barely detectable levels in the granular layer of rodent skin as well as at moderate levels in the hair follicles and blood vessels (Coutinho et al., 2003, Goliger and Paul, 1995). In the thicker human skin, both connexins are also present at low levels within the upper spinous layer of keratinocytes. Cx31.1 is detectable at low levels within the granular layer in rodents, as well as at very low levels within hair follicles. As Cx31.1 appears to be confined to the granular layer in which keratinocytes undergo apoptosis to produce dead cells in the cornified layer, Cx31.1 may have a role in co-ordinating cell-death signals between these cells (Coutinho et al., 2003, Goliger and Paul, 1995). Indeed, in ovarian follicles undergoing atresia through apoptosis, Cx31.1 expression is restricted to atretic follicles, lending credence to the possibility that Cx31.1 can mediate the communication of apoptotic signals (Wright et al., 2001). While around 10 connexin genes are found to be expressed in human adult skin (Table 1. 1), it is unclear exactly how each one is involved in maintenance of the skin physiology. Of these connexins, Cx43, 26, 30 and 31.1 have been linked to the process and resolution of wound healing, and are dynamically regulated following injury (Coutinho et al., 2003, Goliger and Paul, 1995).

1.32 – Connexins in acute wounds

Following injury, within the first 6-24 h there is a strong downregulation of Cx43 as well as Cx31.1 in leading edge keratinocytes of the basal layer in rodent skin (Table 1. 2). At around 1-2 days the level is reduced to the extent that it is almost undetectable (Coutinho et al., 2003, Goliger and Paul, 1995). At the same time, keratinocytes flatten, extend lamellipodial protrusions and migrate outwards across the wound bed. These two occurrences have been linked, as knockdown of Cx43 experimentally has been found to accelerate cell migration while overexpression has found to slow it (Mendoza-Naranjo et al., 2012b, Qiu et al., 2003). There are a number of possibilities as to why Cx43 downregulation may be necessary during wound healing. The cytoplasmic tail of Cx43 is capable of interacting with cytoskeletal proteins both directly through a PDZ domain as well as through adhesion associated proteins like ZO-1, Cadherins and both α- and β-catenin. The cytoplasmic tail has also been found to interact with actin and microtubules (Butkevich et al., 2004, Giepmans et al., 2001a, Shaw et al., 2007, Theiss and Meller, 2002,

Wei et al., 2005). Indeed, a wide array of protein interactions with Cx43 have been reviewed, including those mediated by the C-terminus of Cx43 (Herve et al., 2012). While this could affect adhesion and cell migration directly, the sequestration of transcription factors such as β-catenin could also influence gene expression. In this way it has been suggested that Cx43 may form a nexus, acting as a regulator of other genes in a separate capacity to its role in forming gap junctions (Iacobas et al., 2007, Spray et al., 2002). Cx43 expression in the dermis also changes following wounding. Cx43 downregulation occurs in dermal fibroblasts at around 24-48 h and this has been shown to result in enhanced migration both *in vitro* and *in vivo* (Mendoza-Naranjo et al., 2012b, Mori et al., 2006). This enhancement may be due to a decrease in fibroblast adhesion since Cx43 downregulation was observed in conjunction with activation of the small GTPases Rac1 and RhoA. RhoA has a role in regulation fibroblast lamellipodial protrusion, while Rac1 can help stabilise newly extended protrusions (Machacek et al., 2009, Mendoza-Naranjo et al., 2012a). In

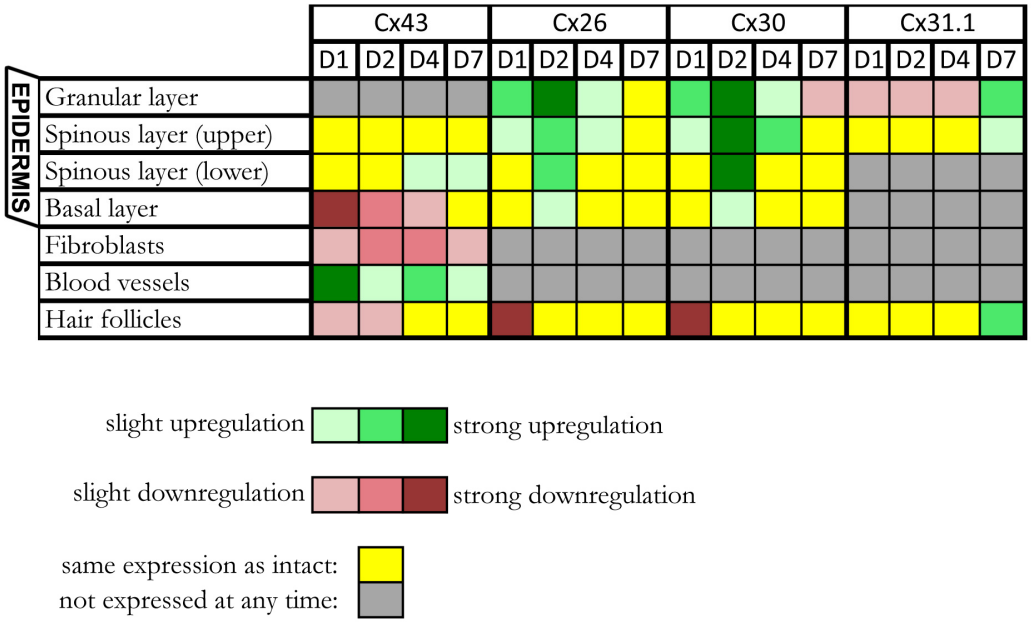

Table 1. 2 – Changes in rodent connexin expression in injured keratinocytes, wound fibroblasts and proximal epidermal appendages up to 7 days after acute wounding

The table illustrates the expression of connexin proteins at the leading edge in the case of epidermal keratinocytes. Connexin levels increase (green), decrease (red) or do not differ from the level of intact cells (yellow). Grey is used where a particular connexin is never expressed in that particular compartment (table constructed using immunofluorescence staining data from Coutinho et al., 2003).

contrast, Cx43 levels increase in blood vessels surrounding the wound within the first few hours as they become leaky due to inflammation. This leakiness results in blood extravasation, which delivers additional inflammatory cells and platelets to the site of damage (Coutinho et al., 2003, Cronin et al., 2008). While Cx43 is downregulated in the leading cells, just a short distance away cells are actively proliferating and around 4 days post wounding they overexpress Cx43 (Coutinho et al., 2003). This raises the possibility that during wound healing, keratinocytes at the wound edge may form a communication compartment distinct from cells in the same layer that are just a short distance away.

This concept is further supported by the role of Cx26 and 30 during wound healing. Unlike Cx43, Cx26 and 30 are expressed at almost undetectable levels in the granular layer of epidermis in rodent skin. However, during wound healing the keratinocytes at the wound edge undergo rapid upregulation of these connexins throughout the granular and spinous layers (Coutinho et al., 2003). The exact function of Cx26 and 30 in wound healing is unclear; although it has been shown that ectopic overexpression of Cx26 is associated with hyperproliferative conditions and a delay in barrier reformation (Djalilian et al., 2006). As previously discussed, gap junctions can be either heterotypic or heteromeric and thus can be comprised of more than one type of connexin subunit. However, Cx43 cannot form channels with Cx26 and 30 due to differences in coupling properties (Marziano et al., 2003). This presents a scenario in which the leading edge keratinocytes express connexins that are incompatible with connexins a short distance back, such that leading edge cells may not be able to communicate in a manner such as receiving signals relating to adhesion.

1.4 – Chronic and diabetic wound healing

A small wound will typically re-epithelialise within 5-7 days; at which point the migrating keratinocytes fuse to restore the epithelial barrier. In some situations, however, hard-to-heal wounds may develop in which the normal series of events leading to restoration of the epithelial barrier is perturbed. These chronic ulcers commonly appear on the feet of diabetics (diabetic foot ulcers; 'DFUs'), as venous ulcers on the legs of the elderly (venous leg ulcers; 'VLUs') and also as pressure ulcers on bedbound patients ('PUs'). Chronic ulcers place a huge burden on healthcare organisations and result in a significant deterioration of

patient quality of life. A conservative estimate made for the 2005-2006 period projected the cost of ulcer management in the UK to be £2.3-3.1 billion, accounting for 3% of total health expenditure. Around 200,000 patients in the UK were estimated to have a chronic ulcer at any one time, the majority of which are VLUs. These figures are expected to increase considerably due to the ulcer risk factors of age and diabetes. In the US, the World Health Organisation (WHO) anticipates that one third of all US adults will be diabetic by 2050. Of these, around 2.5-10.7% of diabetics are likely to develop a DFU. DFUs can be particularly detrimental to quality of life since in 1.8% of diabetics the lead to foot amputation (Centers for Disease Control & Prevention, 2011, Hunt, 2011). The ageing population is also a factor, with the worldwide population of over 60s expected to exceed 2 billion by 2050 (WHO, 2011). PUs alone amount to an annual £1.4 – 2.1 billion cost, over 90% of which is spent on nursing (Bennett et al., 2004).

1.41 – Ulcer aetiology

Diabetic foot ulcers

The development of effective chronic wound treatments requires investigation into the aetiology of chronic ulcers. The causes of chronic ulcers vary between VLUs, DFUs and PUs. In diabetic individuals, the presence of neuropathies allows minor abrasions to remain unchecked by the patient, such that they can develop into larger non-healing DFUs. Neuropathies also prevent the release of neuropeptides such as nerve growth factor, which promote cell chemotaxis and growth factor production (Galkowska et al., 2006). Once wounds have been formed, diabetics are at a disadvantage compared to normal individuals. Under hyperglycaemic conditions, excess glucose is converted to sorbitol at the cost of NADPH (Yagihashi et al., 2007). NADPH is necessary for the production of antioxidant reducing equivalents nitric oxide and reduced glutathione. With reduced levels of antioxidants at the wound the balance between reactive oxidant species (ROS) and antioxidants in the wound is lost, resulting in accumulation of ROS that can cause tissue harm and prolong the duration of healing (Vincent et al., 2004). Fibroblasts derived from hyperglycaemic patients have also been found to divide more slowly, while the ability of leukocytes to phagocytose and destroy bacteria was markedly reduced (Loots et al., 1999, Mowat and Baum, 1971). Capillary blood flow is also reduced in diabetic individuals and

can contribute to hypoxic damage of tissue and a poor healing environment (Jorneskog et al., 1995).

Venous leg ulcers

In contrast to DFUs, the underlying causes of VLUs relate to venous insufficiency in the legs. In healthy individuals, the hydrostatic pressure in the deep veins of the leg when standing approximates to 80 mm Hg (Falanga, 1993). Movement of the leg causes the calf muscle to contract, causing deep veins to compress and transiently elevate blood pressure in order to propel blood in an anterior direction. As pressure rises in the deep veins, valves close to prevent retrograde flow of blood. As the deep vein system empties, deep vein pressure drops to between 0-10 mm Hg, allowing valves to re-open and for blood to re-enter the deep vein system (Gourdin and Smith, 1993). Venous hypertension, which precedes development of VLUs, occurs as a result of perturbation to this series of events. This can be caused either by valvular incompetence resulting in retrograde blood flow, or calf muscle dysfunction which results in insufficient clearance of blood (Gourdin and Smith, 1993, Falanga, 1993). In either case, the fall in pressure normally experienced following deep vein emptying is not achieved, resulting in the condition described as venous hypertension. Ultimately, this results in the pooling of hypoxic blood in the legs, which in turn promotes the death of tissue and the development of an inflammatory response.

Pressure ulcers

PUs occur as a result of mechanical stress and subsequent ischaemia reperfusion damage, commonly in bedridden individuals (Berlowitz and Brienza, 2007). They commonly form as localised areas of necrosis in response to compression of soft tissue between a bony prominence and an external surface for prolonged periods. Typical sites where PUs can occur are the heels, back and elbows, due to prolonged resting on these areas in a setting such as a hospital or nursing home. The constant resting on one particular area can raise the interstitial pressure of capillaries in that region. Normal capillary pressure ranges between 12-32 mm Hg (Kosiak et al., 1958). Pressures over 32 mm Hg result in compromises to oxygenation and circulation, which is of particular concern since lying on a hospital bed can generate pressures of up to 150 mm Hg (Daniel et al., 1981). Studies also suggest that considerable durations of hypoxia followed by repeated reperfusion events can

in fact cause more damage than hypoxia alone (Peirce et al., 2000). While just 2 hours of constant pressure at 70 mm Hg on a single region can cause cell death, intermittent relief of pressure can avoid damage to the tissue that would otherwise occur (Kosiak, 1959). The likelihood of developing PUs can also be promoted through friction, shearing forces and moisture (such as in patients with urinary incontinence) (Herman and Rothman, 1989). As such, the prevention of PUs in many cases is dependent on the effective management of bedbound patients in hospitals and care homes.

1.42 – Shared features of chronic ulcers

While the underlying causes of the three main types of ulcers differ, a number of features are present in all cases. Chronic ulcers are invariably associated with an elevated inflammatory response that does not typically resolve within the usual 1 week associated with acute wounds. One common cause of inflammation is the excessive colonisation of wounds with bacteria and sometimes fungi. Regardless of the type of bacteria present, a level greater than 10^6 organisms per gram of tissue is associated with impaired healing (Bendy et al., 1964). Chronic ulcers are also frequently found to develop biofilms containing the bacteria *P. aeruginosa*. Biofilms are complex communities of bacteria that envelope within a self-secreted polysaccharide matrix. This protects bacteria from neutrophils and may also explain the failure of some antibiotics to heal chronic wounds (Bjarnsholt et al., 2008). Inflammation is also accelerated by the repeat ischaemic events in most of the ulcer conditions. In VLUs, venous insufficiency results in the retention of deoxygenated blood, resulting in a hypoxic environment. Reperfusion also increases the incidence of oedema, which increases the distance between capillaries and renders the environment even more hypoxic (J et al., 2010). In a hypoxic environment of under 40 mm Hg pO_2, neutrophils have been shown to lose their bactericidal properties, further increasing the likelihood of developing infections (Hohn et al., 1976). The same hypoxic insults are experienced repeatedly in PUs, since extended pressure applied to regions of soft tissue reduces blood flow to the region. Readjustment of posture later on then results in blood reperfusion of the affected area. Diabetics are known to suffer from a number of microvascular diseases that also contribute to hypoxia, including reduction in capillary size, thickening of the basement membrane and arterial thickening (hyalinosis).

The repeated occurrence of hypoxia followed by reperfusion events results in the continuous delivery of blood containing leukocytes that are activated in response to the

hypoxic environment to release ROS and pro-inflammatory cytokines (Woo et al., 2007). The generation of ROS also affects the availability of growth factors such as VEGF in the wound, inhibiting the level of angiogenesis occurring in chronic ulcers. In the hypoxic stage of an acute wound immediately following injury, the transcription factor hypoxia inducible factor (HIF)-1α is constitutively expressed which triggers fibroblasts to release VEGF. Excessive ROS have been shown to degrade HIF-1 α at the post-transcriptional level, resulting in reduced VEGF levels in the ulcer (Zou and Cowley, 2003). Following hypoxia, the reperfusion of oxygen to oxygen-starved cells can then also result in cell apoptosis, leading to further tissue damage within the chronic ulcer. Inflammation also drives the destruction of the underlying dermal integrity of skin. The upregulation of pro-inflammatory cytokines IL-1, IL-6 and TNF-α in turn cause upregulation of MMPs, particularly MMP-2 and MMP-9 (Han et al., 2001, Raffetto and Marston, 2011). MMP-2 was also reported to be increased 3-fold in DFUs (Lobmann et al., 2005). MMP activity is crucial in acute wound healing to degrade and remodel the newly deposited ECM. Normally MMP function is tightly regulated by Tissue Inhibitors of Metalloproteinases (TIMPs) within the wound. However, the rise of MMP activity and the reduction of TIMP levels in chronic ulcers results in considerable degradation of ECM proteins laid down in the wound, including collagen types I and III and fibronectin (Chen and Rogers, 2007, Muller et al., 2008). MMPs also act to degrade growth factors and their receptors, compromising wound regeneration (Ren et al., 2014). The loss of ECM is particularly detrimental to wound healing as it behaves as a substrate for migration and proliferation of tissue regenerative fibroblasts as well as restoring tensile strength and integrity to the skin.

1.43 – Connexin expression in chronic ulcers and diabetic wounds

In diabetics, wound healing is compromised, and hyperglycaemia appears to affect the level of connexin expression throughout numerous cells. In the endothelial cells of diabetics, some reports suggest that the expression levels of Cx37, Cx40 and Cx43 do not differ from normoglycaemic cells, while others argue that the levels are reduced. There is a general agreement that Cx43 expression and GJIC is decreased diabetic blood vessels, however, which occurs in conjunction with vessel breakdown and cell death (Zhang et al., 2006a, Muto et al., 2014, Makino et al., 2008, Inoguchi et al., 2001, Bobbie et al., 2010). Diabetic vascular endothelial cells as well as those cultured *in vitro* in hyperglycaemic conditions have also been found to have reduced gap junctional communication but an increase in

Cx43 phosphorylation (Kuroki et al., 1998, Inoguchi et al., 2001). Within the intact epidermis, studies of streptozotocin (STZ) diabetes-induced rats indicate that Cx43 and Cx26 protein expression as well as GJIC is significantly reduced (Wang et al., 2007). Hyperglycaemia does not appear to downregulate connexin levels across the board, however, since conflicting reports indicate Cx43 expression is both increased and decreased in diabetic kidney tubules (Zhang and Hill, 2005, Satriano et al., 2010, Poladia et al., 2005). Recent studies also suggest that Cx43 protein levels are instead increased in the hyperglycaemic dermis, with a positive linear relationship between blood glucose concentration and Cx43 expression in dermal fibroblasts identified (Mendoza-Naranjo et al., 2012b). Gap junction intercellular communication (GJIC) was also found to be increased in the diabetic dermis (Wang et al., 2007). Hyperglycaemia appears to affect cells differently and the reasons for these differences are not completely understood.

During wound healing it is necessary for Cx43 downregulation to occur within 24 h in wound edge keratinocytes in order for cells to become migratory to reform the epithelial barrier (Wang et al., 2007, Qiu et al., 2003). The pre-established low levels of Cx43 in diabetic epidermis do not confer an advantage to wound healing, however, as studies of wounds in STZ rats have highlighted. Full-thickness wounds made to the dorsum of STZ rats form thickened non-migratory bulbs of keratinocytes at the wound edge which contain a high level of Cx43 protein (Wang et al., 2007). In those diabetic wounds Cx43 was only downregulated around 48 h after wounding, at which point keratinocytes began to migrate properly. Similar results have also been found in a human study of diabetic ulcers, in which ulcer wound edge keratinocytes were found not to downregulate Cx43 (Brandner et al., 2004). These findings have been contested by a later study, however, which investigated human diabetic ulcer biopsies and found no significant change in Cx43 and Cx26 mRNA and protein levels (Brandner et al., 2008). Additionally, keratinocytes and fibroblasts cultured from diabetic ulcer biopsies showed similar localisation and levels of Cx43 following immunostaining and western blotting (Pollok et al., 2011). The reason for these conflicting reports is unclear, but could be due to differences in chronic ulcer severity and subsequent cell culture conditions.

Unlike Cx43, Cx26 expression in the STZ rats did not elevate above the high levels normally encountered in acute wound edge keratinocytes but expression was elevated further back from the wound edge, and over a larger area (Wang et al., 2007). Cx26 is

strongly associated with hyperproliferative skin conditions (Thomas et al., 2003). Cx26 has been found to be directly involved in regulating thickness of the epidermis, as mutations in the Cx26 gene *GJB2* have resulted in a thicker epidermis both within the human population and using *in vitro* organotypic models (Man et al., 2007). These mutations can frequently go on to cause deafness. Cx26 upregulation has also been found to occur in hyperthickened psoriatic lesions (Labarthe et al., 1998). Experimentally, it has been shown that inducing Cx26 overexpression using an involucrin promoter in mouse keratinocytes increased ATP release which delayed re-epithelialisation, promoted hyperproliferation of the epidermis and caused invasion of inflammatory cells (Djalilian et al., 2006).

1.5 – Chronic wound treatment

1.51 – Conventional treatments

Chronic ulcers have multiple underlying problems that existing therapeutic solutions attempt to address. Conventional approaches to treating ulcers often attempt to address the high levels of pressure that can cause ulcers to form as well as deal with oedema. Particularly in DFUs and VLUs, a common mode of treatment is to employ the method of offloading to reduce pressure. This includes bed rest, wheelchair use, wearing leg casts or elastic stockings and the wearing of therapeutic shoes (Wu et al., 2008). Elevation of the leg is also practiced in conjunction with compression therapy to improve the return flow of blood to the heart as well as reduce fluid buildup (Abu-Own et al., 1994). Compression therapy is a slow process, however, and although it can help reduce oedema, after 24 weeks of practice in one study it was found to be successful in only 30-60% of cases (Margolis et al., 2000). In contrast to applying pressure through compression, negative pressure treatments have also been practiced. Controlled negative pressure can be applied using a vacuum-assisted closure device to remove excess fluid released from open wounds. While there are indications that this practice may help reduce wound size and volume, it has been noted that there is not currently sufficient evidence or high quality data to support its use in ulcer management (Ubbink et al., 2008).

Dressings are also typically applied to wounds in order to provide a temporary barrier against infection and also to keep the wound moist. Since the 1960s, it has generally been

accepted that wounds benefit from a moist environment as oppose to air drying, so a number of dressings have been developed to keep wounds moist (Hinman and Maibach, 1963). Multilayer compression bandaging is routinely practiced in VLU treatment and dressings are usually placed on the ulcer before compression bandages and wrappings are applied (Fletcher et al., 1997). These wound dressings include foams, hydrocolloids, hydrogels, transparent films, gauzes and alginates (Fonder et al., 2008). The choice of dressing is often based on the level of exudate released from the ulcer, as well as based on the level of infection and necrotic tissue present in a wound. While dry gauzes have historically been a popular choice of dressing, evidence suggests that they can desiccate the wound base and that moist wound dressings may have a greater effect on wound healing (Callen et al., 2009, Bolton et al., 2004). Dry wounds are often the target of water-based hydrogel applications such as ActivHeal in order to create a moist wound environment, while wounds with heavy exudate may receive highly absorbent alginate or foam dressings (Jones and Milton, 2000, Fonder et al., 2008). Wounds that are particularly prone to infection may be treated with a transparent adhesive film, which provides a barrier against bacterial infection while also trapping internal moisture. Incorporation of silver have also been noted for their antimicrobial properties, but are not considered cost effective (Lo, 2010). Transparent dressings can lead to discharge, however, and are not recommended for use in wounds with heavy exudate (Fonder et al., 2008). Hydrocolloids dressings such as Tagasorb are occlusive dressings that combine a gel-forming agent with an adhesive. They can be applied for a longer amount of time than regular dressings but are expensive relative to other dressing types (Singh et al., 2004). Despite the diverse number of dressings tailored to seemingly suit any type of ulcer, a comprehensive BMJ review of 254 dressing studies concluded that there was no convincing data that suggested the advanced dressings conferred any statistical improvement to ulcer healing (Palfreyman et al., 2007). This highlights the lack of scientific studies into the function of dressings and may also indicate that they are not actually that effective in promoting the healing of ulcers.

1.52 – Surgery

Conventional pressure therapy in conjunction with dressing application has a 71-80% chance of healing acute ulcers that are less than 3 months old. For ulcers that have been present for more than 3 months and are considered chronic, the chance of the wound healing falls to just 22% (Nelson et al., 2000). The prevalence of chronic ulcers highlights

the need for research into novel treatments as well surgical intervention. Chronic ulcers containing large amounts of necrotic tissue, bacteria and debris may be eligible for debridement in order to expose the receptive cells at the wound edge. This can be performed as sharp debridement using a scalpel or using biological methods such as the application of larvae (Dumville et al., 2009, Lebrun et al., 2010). While the rationale for debridement is logical, there is a need for convincing evaluations of undebrided versus debrided wounds. A review of five DFU studies of debrided wounds found that studies often lacked meaningful observations of wound healing following debridement and a lack of statistical significance testing (Lebrun et al., 2010). A second review of studies that employed debridement in VLU management concluded that, similarly, there was a need for accurate assessment of the effect of debridement on wound healing relative to undebrided wounds (Collins and Seraj, 2010). Despite this, debridement is commonly performed in DFU management alongside management of infection and offloading practices (Alexiadou and Doupis, 2012).

A significant problem present in chronic ulcers is the overactivity of MMPs in the wound, resulting in proteolytic degradation of the epidermal basement membrane and dermal ECM. This results in a loss of wound integrity and can significantly reduce the potential for the ulcer to heal. In order to address large ulcers, another surgical approach is to perform autografting to cover the ulcer with healthy tissue. (An et al., 1995). This can be impractical in diabetic patients, however, since healing is often compromised in individuals such that it is unfeasible to create additional wounds in order to harvest tissue. This can also be true in the case of significant burns, where extensive damage to the body can leave too small an amount of viable tissue from which to derive grafts (Vacanti et al., 1998). One method to generate more tissue from a patient is to culture donor grafts in the laboratory. However, this method has significant drawbacks; it requires weeks of cell culture and the graft take success rate can be low. The chance of patient graft take can vary between 15-85%, with an average of just 53% for full-thickness wounds (Atiyeh and Costagliola, 2007, Paddle-Ledinek et al., 1997). Skin grafting can also be ineffective when there is persistent oedema, which can often be the case in VLUs (Jones and Nelson, 2007). The practice of allografting in which donor tissue is derived from another person can also be employed, yet studies suggest that these may only act as temporary barriers within the host. DNA analysis of healed wounds in one study indicated that the healed tissue did not contain the DNA of the allograft donor (Roseeuw et al., 1990, Phillips and Gilchrest, 1991).

1.53 – Scaffolds as a chronic ulcer treatment

The unsuitability of grafting in many ulcer patients has led to the production of epidermal and dermal mimicking devices termed 'scaffolds'. These are typically inserted into the full-thickness ulcer or burn and are intended to function similar to the skin components they mimic (Shevchenko et al., 2010). Unlike dressings, which serve primarily as a means to control wound hydration and minimise infection, scaffolds are intended to be functional by either integrating with the wound or serving literally as a scaffold for cell adhesion and proliferation (Shevchenko et al., 2010). A range of commercial scaffolds have been made developed to treat full-thickness wounds (Figure 1. 6). Arguably the most complex types of scaffolds include Apligraf (Organogenesis website, 2011) and Orcel (Forticell Bioscience website, 2011). These are bilayer arrangements of human keratinocytes over an animal-derived ECM containing human fibroblasts. Cell seeded scaffolds that comprise only epidermal (e.g. Epicel) or dermal (e.g. Dermagraft) layers are also commercially available. While improved wound closure rates using Apligraf have been reported, cellular scaffolds have several disadvantages: they are both expensive and time consuming to produce, and there is a potential risk of rejection of the incorporated allogenic cells (Schonfeld et al., 2000). Apligraf in particular was estimated to cost about $30 per square cm in 2002 (Bouchie, 2002). While reports detailing rejection of Apligraf are scarce, it was found that the scaffolds did not actually integrate with wounds as an autograft would, contrary to the original manufacturer claims made regarding the product. It was instead proposed that these this type of scaffold may instead promote wound healing by stimulating growth factor production (Ehrenreich and Ruszczak, 2006). Cellular scaffolds may therefore not be acting as substitutes for skin.

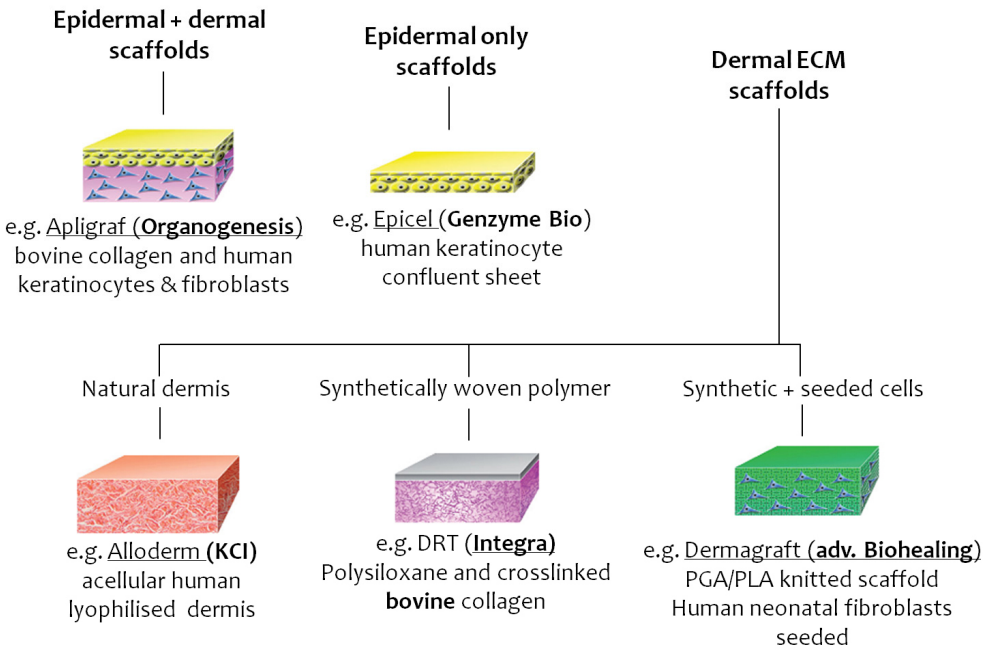

Figure 1. 6 – Examples of commercial cellular, acellular and extracellular matrix-derived scaffolds.

Scaffold information and diagram adapted from Shevchenko et al., 2010.

Due to the drawbacks associated with cellular scaffolds, a number of scaffolds have been manufactured that are acellular, either as lyophilised extracellular matrix extracts (Oasis, Alloderm) or synthesised from scratch using synthetic components such as nylon (DRT, Integra) (Shevchenko et al., 2010). Dermal scaffolds have also been experimentally fabricated from ECM-derived polymers including collagen (Torres-Giner et al., 2009), fibrinogen (McManus et al., 2007) and hyaluronic acid (Ji et al., 2006), as well as from synthetic polymers such as polycaprolactone (PCL) (Garcia-Giralt et al., 2008) and polylactic-co-glycolic acid (PLGA) (Yang et al., 2009). These polymers have also been fabricated as solid microspheres and aqueous hydrogels in addition to large sheet structures (Ashton et al., 2007).

The scope of current scaffold studies is limited, however, to the point that it is not clear whether most scaffolds actually improve wound healing. It appears that many wound healing studies involving scaffolds focus simply on whether wound closure occurs, with little exploration into the effect of scaffolds on cells at the wound (Gholipour Kanani and Hajir Bahrami, 2010, Rho et al., 2006, Sabolinski et al., 1996, Wainwright, 1995). Many

clinical studies also investigate the effect of scaffolds long after the wound has closed and the scaffold has degraded, often 30 days or more after the scaffold was initially applied. Additionally, studies using electrospun scaffolds are frequently performed by engineers who typically use cells as opposed to *in vivo* models to assess the function and biocompatibility of scaffolds, which does not accurately recapitulate the conditions of a wound (Chong et al., 2007, Zhang et al., 2005). The studies that assess wound healing at early time points often do not focus on the leading edge cells at the wound, and when images are captured they can often be at a low magnification where it is difficult to assess the reaction to scaffolds (Blackwood et al., 2008, Khil et al., 2003, Powell and Boyce, 2006). The efficacy of scaffolds has also been called into question following in-depth reviews of wound healing devices. A recent report investigated 60 studies that used venous leg ulcer advanced dressings, which included both ordinary dressings as well as cellular and acellular dermal scaffolds. They found the majority of scaffold studies to be flawed, concluding that that they could not prove that they significantly improved healing over controls (Zenilman et al., 2013). There is therefore a clear need to assess the effects of scaffolds on wound healing to determine whether they are suitable for use in healing chronic ulcers.

1.54 – Antisense oligodeoxynucleotide therapy

Due to the upregulation of Cx43 in chronic ulcers (Mendoza-Naranjo et al., 2012a, Mendoza-Naranjo et al., 2012b) and STZ diabetic rat wound edge keratinocytes (Wang et al., 2007), the concept of downregulating Cx43 as a potential chronic ulcer treatment has recently been explored. Antisense therapeutic approaches allow the targeting of individual components through the design of DNA and RNA molecules. These include ribozymes, which are engineered, catalytically active RNA molecules that can cleave the target mRNA sequence (Scherer and Rossi, 2003). Similar to RNAzymes are DNAzymes, which also target and directly cleave mRNA transcripts, but are instead engineered DNA molecules (Santoro and Joyce, 1997). RNA interference is another RNA-based approach that can result in effective gene silencing. In this method, the design of short interfering RNA sequences can result in the targeted degradation of specific mRNA transcripts (Soutschek et al., 2004).

Research performed in the Becker lab, however, has led to the focus on single stranded antisense oligodexoynucleotides (asODN) as a method to downregulate Cx43, since it is typically overexpressed in chronic ulcers and models of perturbed wound healing

(Mendoza-Naranjo et al., 2012a, Mendoza-Naranjo et al., 2012b, Wang et al., 2007). The first successful use of ODN in gene therapy was by Zamecnik Stephenson in 1978, using a 13-mer ODN complementary to the terminal sequences of the Rous sarcoma virus 35S RNA (Stephenson and Zamecnik, 1978). Using this approach, they demonstrated a 99% reduction in reverse transcriptase activity and a decrease in cellular transformation. The principle by which asODN silences protein expression is outlined in Figure 1. 7. In this method of silencing expression, a single stranded DNA sequence of typically no more than 30 base pairs in length is designed that is complimentary to a length of the target mRNA sequence. Following gene transcription in the target cells to produce mRNA, the ODN sequence then binds to it (Akhtar, 1998). It has been suggested that asODN can prevent protein translation of the mRNA by two or more different ways. The first is that asODN prevents ribosome binding to the mRNA through steric interference, which has been supported by the finding that asODN directed against ribosome assembly regions had the greatest effect on translation (Boiziau et al., 1991, Goodchild, 1989). The second is through induction of RNaseH activity to degrade the mRNA. This occurs because RNaseH specifically recognises DNA-RNA duplexes such as those formed between mRNA and asODN. Silencing has also been found to take place following asODN entry into the nucleus to inhibit splicing, as well as prevent pre-mRNA processing or mRNA exit from the nucleus.

The design of effective asODN sequences is critical in order to achieve effective silencing. There are two main methods employed to design ODN sequences. The first method is a more conventional approach, often referred to as a 'walk-the-gene' strategy (Akhtar, 1998). A series of ODN sequences that are complimentary to sites along the length of the mRNA sequence are immediately evaluated both *in vitro* and *in vivo*. This approach is particularly time consuming and not entirely exhaustive, leading to some dependence on chance (Akhtar, 1998). The second approach involves the use of RNaseH mapping (Ho et al., 1996). In this method, a random or semi-random library of ODN sequences are hybridised to the mRNA sequence of interest, after which RNaseH is used to cleave only the duplexed structures. The resulting fragments are then analysed on a gel to identify accessible sites for designing asODN.

Silencing protein expression using asODN has certain limitations, however. The most limiting factor regarding asODNs is their short duration of activity owing to their swift

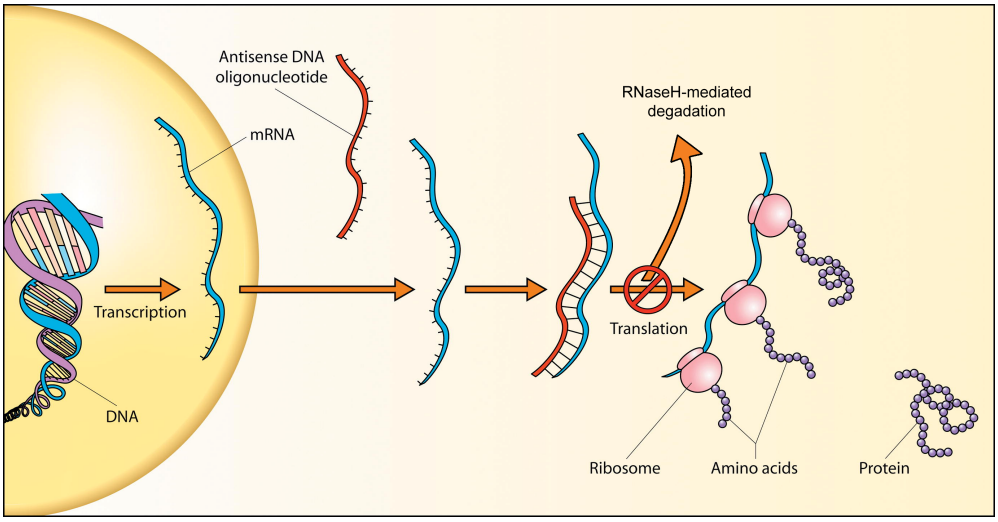

Figure 1. 7 – Antisense oligodeoxynucleotide mode of action.
Antisense oligodeoxynucleotide (asODN) sequences are designed complimentary to a section of the target mRNA sequence. These sequences bind to the mRNA and prevent protein translation, as well as inducing catalytic breakdown of the mRNA sequence via RNaseH activity (image derived and adapted from Robinson, 2004).

degradation by exo- and endonucleases, both in the wound and within the cell cytoplasm (Agrawal, 1996). Specific 3' and 5' modifications, such as phosphorothioate modification, have been shown to increase the stability of asODN against nuclease damage (Shaw et al., 1991). However, modifications have been shown to come at the cost of efficacy, and have also been demonstrated to increase both cell cytotoxicity and the chance of non-specific events occurring (Agrawal, 1996). High affinity is also particularly important in order to achieve effective silencing. Longer asODN sequences tend to result in greater affinity binding, as well as higher numbers of guanine-cytosine pairs (Hoke et al., 1991).

Despite the short half-life of unmodified asODN sequences, application of asODN using a Pluronic hydrogel vector to prolong asODN longevity has been found to result Cx43 knockdown for up to 2-3 days in the spinal cord, where Cx43 is not normally downregulated (Cronin et al., 2006). Cx43 protein has a short half-life of 1.5 h, such that the effects of preventing new protein production can be quickly observed (Leithe et al., 2006). Using a 30-mer sequence directed against the rodent Cx43 mRNA, knockdown of Cx43 was accelerated in mouse wound edge keratinocytes. Within 2 h of wounding Cx43 expression in wound edge keratinocytes had decreased, which is 4 h sooner than in untreated wounds (Goliger and Paul, 1995, Qiu et al., 2003). While Cx43 is normally

downregulated at the wound edge, the application of Cx43 asODN appeared to accelerate this downregulation, alongside increasing the rate of wound re-epithelialisation (Mori et al., 2006, Qiu et al., 2003). Downregulation with Cx43 asODN also significantly reduced Cx43 expression in diabetic rat wounds that expressed high levels of Cx43, similar to chronic wounds (Wang et al., 2007). The effects of the same Cx43 asODN sequence were also confirmed in another study which found that the inflammatory response was reduced, while fibroblast migration and wound closure was also significantly accelerated (Mori et al., 2006). Given the positive results obtained *in vivo*, a human Cx43 asODN sequence is currently being tested as the drug Nexagon® to treat chronic ulcers and has passed stage 2 clinical trials. In the trials it was found that there was a 69% reduction in VLU size following treatment with the drug (CoDa Therapeutics Inc. official webpage, 2011). Treatment of wounds with other asODN sequences to different targets has also been found to have an effect. In a different study, asODN against the glycoprotein osteopontin was found to significantly downregulate expression of the protein in wounds, as well as enhance the rate of wound re-epithelialisation, reduce fibrosis and dampen inflammation (Mori et al., 2008). The use of asODN sequences therefore appears to be a valid method to address the deregulated expression of specific proteins in perturbed healing. While asODN delivered using Pluronic gel is still degraded within hours, the incorporation of asODN into drug-eluting stents has indicated that alternative methods may afford a level of protection to DNA in a nuclease-rich environment (Zhang et al., 2004).

1.6 – Aims of the study

Dermal scaffolds are purported to promote wound healing by acting as a substitute extracellular matrix for cell adhesion and proliferation. Despite this, there is little conclusive evidence to support these claims, and particularly not at the cellular level or at the early stages of wound healing. Owing to a lack of supporting evidence, this led to the initial null hypothesis for the project, that: *'scaffolds do not promote healing of full-thickness wounds'*. If this hypothesis were accepted, the next stage was to assess why this was the case and whether scaffolds could be optimised to promote wound healing.

To test this hypothesis it required the fabrication of scaffolds similar to those used in wound healing studies, followed by application to full-thickness wounds using animal *in*

vivo models. Upon application, the reaction of wound edge keratinocytes could be assessed. Following the findings of the first results chapter (chapter 3), the hypothesis was considered to be correct. Scaffolds appeared to exert a negative effect on wound healing across a number of different observations. Attempts to optimise this scaffold using Cx43 asODN to overturn the upregulation of Cx43 appeared only somewhat effective, yet it appeared that scaffolds may better function as a reservoir of Cx43 asODN through infusion of the structures with the drug.

As such, a method of coating scaffolds in a similar way to sustained drug delivery stents was devised as a technique to deliver Cx43 asODN over time. Using this method, the aim was to improve the rate of wound re-epithelialisation and scaffold integration through delivery of Cx43 asODN to the wound. It also became apparent that Cx26 was also implicated in perturbed healing, and the availability of two new Cx26 asODN meant that Cx26 overexpression could be targeted as a second means to improve wound healing. Altogether, the aims of the project were to first investigate the effects of scaffolds on wound healing and then to design a scaffold capable of delivering asODN sequences beneficial to the healing of full-thickness wounds.

<u>The summarised aims for the project were therefore as follows:</u>

1. To produce a dermal scaffold for application to full-thickness wounds, to verify whether scaffolds promoted or inhibited the healing of full-thickness wounds at the cellular level.

2. After scaffolds appeared to inhibit wound healing, the aim was to devise a novel coating method to coat scaffolds with Cx43 asODN, in order to assess whether scaffolds could function instead as a Cx43 asODN delivery device to promote wound healing.

3. Following positive results using coated scaffolds, the final aim was to address whether scaffolds coated in the same manner but with novel asODN sequences to Cx26 mRNA could also improve *in vivo* wound healing, and whether combined Cx26 and Cx43 asODN coated scaffolds could further promote wound healing.

CHAPTER 2

Materials and Methods

Introduction

In this chapter, the techniques and materials used to carry out the experiments in chapters 3-5 will be described.

2.1 – Scaffold materials and design

2.11 – Collagen scaffolds

The method used to generate the scaffolds used throughout this study was electrospinning. This technique was chosen following a short review of the literature, in which it was found to be one of the most commonly used techniques to produce scaffolds (Huang et al., 2003). The primary aim of this study was to produce a scaffold comparable to those produced in other studies, such that the results and observations made throughout the first chapter of this thesis would be relevant to the engineers producing, but not thoroughly testing, their scaffolds. Electrospinning was also selected because it is relatively inexpensive and capable of producing micro-scale spun fibres similar to those found in commercial scaffolds (Shevchenko et al., 2010). Another significant factor governing the choice of scaffold fabrication method was our existing lab collaboration with Dr Suwan Jayasinghe, who had both the relevant experience and apparatus to produce scaffolds. Following a further search into the literature and the advice of Dr Jayasinghe, collagen was selected as the major scaffold fabrication material due to its abundance in the native matrix, routine use in biomaterials studies, biodegradability and ease at which it can be electrospun (Buttafoco et al., 2006, Huang et al., 2003). The method of electospinning used in a study by Torres-Giner et al. (2009) was further modified over 6 months as this study thoroughly characterised the fibres produced with detailed methods, and was well cited by other sources (cited by 38 other publications). Collagen scaffolds were fabricated by electrospinning acid-soluble bovine collagen (>99% purity, Kensey Nash, PA, USA) blended with poly-ε-caprolactone (>99% purity, Sigma Aldrich, Poole, UK) at a 10:1 weight ratio, respectively. The electrospinning work was carried out in Dr Jayasinghe's laboratory in the Department of Mechanical Engineering at UCL. Blended polymers were dissolved in hexafluoropropan-2-ol (HFP, 99% purity, Apollo Scientific, UK) at 10%

(wt./v.). In this study, scaffolds were electrospun at a flow rate of 5 ml/hour, with a needle to collector distance of 130 mm and using an output voltage of 13 kV.

In total, 30 ml of polymer solution was spun onto a 9 cm^2 foil sheet to produce scaffolds with an average thickness of 0.8 mm. To generate thinner scaffolds with an average thickness 0.4 mm, 14 ml of polymer solution was electrospun (Figure 3. 4 only). Uncoated electrospun scaffolds in this study (but not coated scaffolds) were crosslinked by immersion in either a high (15% wt./v.) or a low (0.15% wt./v.) concentration of N-(3-Dimethylaminopropyl)-N'-ethylcarbodiimide (EDC) hydrochloride (99.5% purity, Apollo Scientific) in a 1:10 water to acetone solution. Scaffolds were washed for 20 min with sterile PBS, sterilised for 1 h using 70% ethanol, and washed 3 times with sterile PBS. Scaffold discs were then punched out using a 6 mm biopsy punch to match the size and shape of excisional wounds.

2.12 – Alginate microspheres

Alginate microspheres were produced in the same laboratory as the electrospun scaffolds. Microspheres were produced by electrospraying medium 2% (wt./v.) viscosity alginic acid powder Phosphtate buffered saline (PBS) solution (Sigma, A2033). The electrospraying process was carried out to a previously described specification (Klokk and Melvik, 2002). The polymer mixture was electrosprayed at a distance of 10 cm from the collector, using a voltage of 8 kV and a flow rate of 10 ml/hour. Microspheres were sprayed into a gelling bath containing a 200 μM concentration of calcium chloride dehydrate solution (≥98% purity, Sigma) to become crosslinked. The average sphere diameter generated using this method was measured as 685 μm using a phase contrast microscope at a 10 X objective.

2.13 – Commercial scaffold materials

Both alginate hydrogel and dressing materials under the brand name ActivHeal were kindly provided for use by Prof David Becker. This is produced by Advanced Medical Solutions (website: http://www.activheal.com).

2.14 – Scanning electron microscopy assessment of scaffold structure

Collagen scaffolds were air dried for 3 h at room temperature, snapped, and mounted onto aluminium stubs. Samples were sputter coated and subsequently imaged using a JEOL JSM

7401F electron microscope system set at 2.0 kV. Images were acquired at 800 X magnification.

2.15 – Investigation of scaffold porosity

Scaffold porosity was assayed by submerging scaffolds in a Pluronic gel solution comprising 30% (wt./v.) Pluronic® F-127 powder (Sigma Aldrich, UK) and 5% Fluorescein isothiocyanate (FITC) in water at 4 ºC overnight. The Pluronic F-127 structure is comprised of propylene oxide and ethylene oxide blocks that form a triblock structure resulting in a molecular weight of between 9,840–14,600. Pluronic gel is a liquid at 4 ºC and below, yet above this temperature it forms a gel with a toothpaste consistency. The gelling of Pluronic is thought to be due to the formation of micelles as a result of polypropylene oxide block dehydration. As temperature increases, micelles come into contact with each other and no longer have space to spread out. The restriction of micelle movement is believed to underlie the gelling of the solution (Machado et al., 2013). Scaffolds were then placed under a Leica MZ8 dissection microscope and excited using the FITC filter set to confirm the presence of FITC. The presence of fluorescence throughout the scaffold structure was confirmed and considered an indicator of scaffold permeability, such that the entirety of the scaffold was considered permeable to the vector.

2.2 – Scaffold bioactivation

2.21 – Infusion with Pluronic gel containing Cx43 asODN

Rat Cx43 antisense oligodeoxynucleotides (Cx43 asODN), sequence 5'-GTA ATT GCG GCA GGA GGA ATT GTT TCT GTC-3' (Sigma Genosis), were dissolved in molecular grade water to make a 1 mM stock. They were then diluted into a 30% (wt./v.) Pluronic gel solution to a 30 μM concentration. Pluronic gel is liquid at 1-4°C but sets to a toothpaste consistency when above about 4°C. Collagen scaffolds of 6 mm diameter were immersed in 20 μl of either Pluronic gel containing Cx43 asODN or PBS at 4°C overnight. Alginate microspheres were soaked in a volume of Cx43 asODN Pluronic gel equal to the volume of polymer used in electrospraying at 4°C, which was 5 ml.

2.22 – Application of polymer coatings containing Cx43 asODN

Unlike the Pluronic gel infusion method, both Cx43 and Cx26 asODN sequences were incorporated into polymer coatings using an emulsion technique. The same rat Cx43 asODN sequence that was used in Pluronic gel delivery (section 2.21) was used for the purpose of coating scaffolds and had the sequence 5'-GTA ATT GCG GCA GGA GGA ATT GTT TCT GTC-3'. A non-functional sense (sODN) sequence to this Cx43 asODN was also incorporated to create one of the control scaffold treatments, and had the sequence: 5'- GAC AGA AAC AAT TCC TCC TGC CGC AAT TAC-3'. A modified version of this Cx43 asODN sequence was also separately obtained that had the fluorophores Cy3 and Cy5 conjugated at the 5' and 3' ends, respectively.

In the case of Cx26 asODN, two different novel sequences had been developed by the laboratory at CoDa Therapeutics Inc in New Zealand and preliminary testing in the UCL laboratory suggested they were promising leads from previous *in vivo* data. These asODN sequences were both 20-mers, termed 'AS3' and 'AS6' (sequences currently undisclosed at the suggestion of CoDa Therapeutics Inc.). These sequences were entered into a multiple sequence analyser to confirm that the sequences did not bind each other or themselves (available at: www.thermoscientificbio.com/webtools/multipleprimer). Due to the limited time remaining in the PhD to examine each individually, both of these Cx26 sequences were instead combined into one coating mixture. The asODN sequences were first dissolved in nuclease-free water to a 10 mM concentration. Either PCL or Poly(D, L-lactice-co-glycolide) (PLGA) was then dissolved in the solvent dimethyl carbonate (Sigma 517127) at 10% wt./v. using gentle rocking. The PLGA selected had a lactide : glycolide content ratio of 65:35 ratio (Sigma, P2066). The aqueous asODN solutions were pipetted into the dissolved polymer solution to either a 100 μM final concentration (in the case of the initial coating experiments) or 300 μM, as used everywhere else. These two immiscible layers were then processed for 10 seconds using a handheld T8.01 Netzgerat IKA Labortechnik homogenizer (Janke and Kunkel, Staufen, Germany) on setting 4 (medium) at room temperature to produce an emulsion. After preparing the coating mixture, individual 6 mm collagen scaffolds were dipped for 1 second in the desired polymer-asODN solutions and immediately placed in a tube of liquid nitrogen. Coated scaffolds were lyophilised in an Edwards (model name 'Modulyo') freeze-drier attached to an Edwards high vacuum pump (model EZM2) overnight to remove the solvent from the

scaffolds in order to maintain the structure of the scaffold. In the later scaffold experiments, this coating process, from dipping to freeze drying, was repeated 3 times to produce 4 layers of polymer + asODN, or 7 times in the case of 8-layer 'double coated' scaffolds, which in total received 4 coating layers of PCL + asODN followed by 4 layers of PLGA + asODN.

2.3 – *In vitro* analysis of coated scaffolds

2.31 – Quantification of asODN elution

Scaffolds coated in asODN using the emulsion method were assayed for asODN release rate *in vitro*. Three coated scaffolds were immersed in 40 µl of nuclease free water at 37°C. At daily intervals, 1.5 µl of liquid was removed and assayed using a NanoDrop 2000 UV spectrophotometer under the 'ssDNA' setting to determine DNA concentration. Scaffolds were placed in a fresh 40 µl of water to compensate for the reduction in volume following water removal for assays. Individual time point elution data was collected to produce both cumulative and daily asODN elution graphs.

2.32 – Förster Resonance Energy Transfer (FRET) analysis

The integrity of asODN incorporated into scaffolds was assessed using a Förster Resonance Energy Transfer (FRET) imaging technique (Hu et al., 2009). Scaffolds coated with Cx43 asODN conjugated at either end to fluorophores Cy3 and Cy5 using the previously detailed emulsion method was used in this technique. Scaffolds were either left untreated or submerged in 37°C sterile foetal bovine serum (FBS) for up to 7 days. Samples were removed every 24 h then snap frozen in Tissue-Tek® Optimal Cutting Temperature (OCT) medium (Sakura Finetek, UK), and sectioned to a thickness of 10 µm using a Leica cryostat. Scaffold sections were then washed briefly with PBS and mounted with a size 1 coverslip using Citifluor AF1 mountant (Citifluor Ltd, UK). Samples were imaged using a Leica SP8 confocal microscope using the FRET wizard package available within the Leica LAS AF software. Scaffolds were assessed using a FRET acceptor bleaching technique. Using this method, six randomly selected areas of FRET coated

scaffolds per time point were bleached for the Cy5 acceptor fluorophore using a 633 nm laser. After the Cy5 acceptor is bleached, an increase in donor Cy3 excitation can indicate that FRET was occurring since energy used to excite the Cy3 was previously resonating to the Cy5 fluorophore (Figure 2. 1). A marked increase in Cy3 signal emission at 570 nm post-bleaching was considered to be indicative of FRET activity, since energy was no longer transferring to the acceptor fluorophore via FRET. The detected change in donor emission intensity was acquired and interpreted by the software package to calculate a FRET efficiency percentage ($FRET_{eff}$). The formula to calculate the $FRET_{eff}$ is stated in the software package and is as follows:

$$FRET_{eff} = (D_{post} - D_{pre}) / D_{post}$$

In this formula, D_{post} is the fluorescence intensity of the donor after photobleaching and D_{pre} is the donor fluorescence intensity prior to photobleaching. A minimum percentage of 15-20% has been considered indicative of genuine FRET occurring in other studies (Lai et al., 2014)., and the average percentage obtained in this study was 21.4%. Images captured

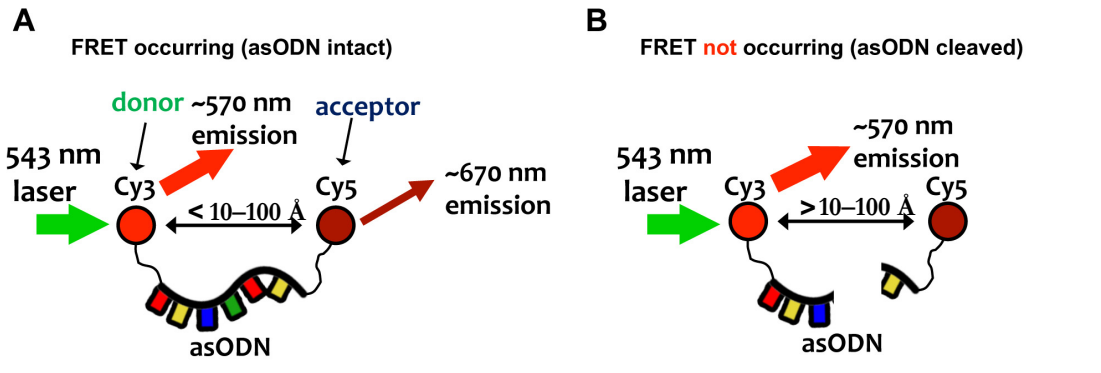

Figure 2. 1 – A simplified diagram illustrating the principles of FRET.
(A): When an asODN sequence tagged with both Cy3 and Cy5 fluorophores at either end is intact, fluorophores are less than 10–100 Å apart (Sekar and Periasamy, 2003). When the donor fluorophore (Cy3) is excited using a 543 nm wavelength laser a portion of this energy may transfer resonate to the proximally located acceptor fluorophore (Cy5), resulting in light emissions at both 570 nm and 670 nm wavelengths. **(B)**: When the asODN sequence is degraded, the fluorophores are no longer within range to permit FRET to occur, resulting in emission largely at 570 nm when excited with a 543 nm laser.

were 8-bit single optical sections with a resolution of 1024 by 1024 pixels. To determine the potency of serum in degrading asODN the wavelength emission spectra of 6 asODN regions per time point were generated by performing xyλ-mode scans on FRET labelled asODN that had been incubated in FBS at 37°C. Individual λ-scans were performed using a 543 nm laser excitation, with 19 equally sized detection steps occurring between the wavelengths of 550 nm to 730 nm. Emission values were output using the LAS AF software.

2.4 – Animal procedures

All animal procedures and experiments were performed under the terms of a UK Home Office License and in accordance with the UK Animals (Scientific Procedures) Act, 1986. All animals were housed in individual cages at the Biological Service Unit at University College London. Animals obtained from suppliers were kept on site for 7 days to allow adjustment prior to experimentation.

2.41 – Rodent strains

ICR (CD-1) outbred mice were obtained from Harlan Laboratories and used in experiments at 6 weeks old. Sprague Dawley rats were reared on site at the BSU and also used at 6 weeks old. Animal weights were measured prior to surgery to calculate drug doses.

2.42 – *In vivo* full-thickness wounding

Anaesthesia was induced using 4% isoflurane, 20% oxygen and 10% nitrous oxide, and maintained using 1.5% isoflurane. Animals were injected subcutaneously with 0.03 mg/ml buprenorphine (Vetergesic®) before operation. The rodent dorsum was initially shaved then covered in a thin layer of Nair® hair removal cream (Church and Dwight, UK), after which both the cream and hair was removed using a warm moistened gauze pad. Animals were then placed on a heated mat for the duration of the procedure. Four full-thickness excisional biopsy punch wounds were made using a 6 mm medical biopsy punch to rodent backs, two on each side of the dorsal midline. Collagen scaffolds (coated or uncoated), alginate microspheres, commercial products (either an ActivHeal® brand alginate dressing or hydrogel; Advanced Medical Solutions, Winsford, UK) or 20 µl pluronic gel containing microspheres were applied directly to wounds, and covered with Tegaderm™ film (3M,

UK). Post-procedure, animals were kept in a heated chamber and monitored for recovery. Once recovered, animals were rehoused in individual cages and monitored regularly.

2.5 – Histology procedures

2.51 – Harvesting wounds

Animals were culled by cervical dislocation at 1, 3, 5, 10 or 15 days post wounding. A large sheet of back skin containing the wounds was first excised to allow macroscopic imaging of individual wounds using a Leica MZ8 dissection microscope at 0.63 X magnification (D1-5). Wounds were subsequently excised and fixed by immersion in a 4% paraformaldehyde (PFA)-PBS solution for 24 h at 4°C. Samples were washed 3 times for 1 h in PBS then transferred to 20% sucrose-PBS solution for 24 h at 4°C. Wounds were bisected and one half was snap frozen in OCT medium, then sectioned using a cryostat at a thickness of either 5 μm (mice) or 10 μm (both mice and rats). For mouse tissue, 5 μm thick tissue cryosections were stained with haematoxylin and eosin whilst 10 μm sections were used for immunostaining.

2.52 – Haematoxylin and eosin staining

Frozen tissue sections were thawed for 5 min then covered completely in tap water for 5 min at room temperature. Slides were submerged in Harris' haematoxylin solution (HHS16, Sigma) for 30 seconds followed by immersion in a container full of running tap water for 5 min. Background staining was reduced by dipping the slides in a container full of 1% acid alcohol (1% glacial hydrochloric acid, 70% ethanol, 29% distilled water) for 3 seconds, after which slides were immersed in a container of running tap water for a further 5 min. Samples were then submerged for 15 seconds in a container full of eosin B solution (2853, Sigma), followed by immersion for 5 seconds in a container full of tap water to rinse away excess stain. Slides were then immersed in 70% ethanol for 2 min, 100% ethanol for 2 min and a second container of 100% ethanol for a further 2 min, to dehydrate the sections. Slides were then submerged in a container full of xylene for 5 min, then a second container of xylene for an additional 5 min. Slides were then individually removed and covered with approximately 1 ml of xylene based DPX mounting media (06522, Sigma), then sealed using a number 1 coverslip.

2.53 – Immunofluorescence staining

Tissue sections were permeabilised in cold acetone for 5 min and then blocked against non-specific antigen binding for 30 min using a 0.1 M L-lysine (Sigma, L5501) PBS solution containing 0.1% Triton-X-100 (L5501, Sigma). This was known as the 'blocking solution', and all antibodies were made up in this solution. Sections were stained using polyclonal rabbit antibodies to Cx43 (Sigma C6219, 1:2000 dilution), Cx26 (for mouse tissue this was the anti-Cx26 antibody 'GAP28' used at 1:200 dilution, generated in a study by (Diez et al., 1999), and for rat tissue was Millipore AB8143 at 1:600) or mouse monoclonal alpha smooth muscle actin (α-SMA; Sigma A2547, 1:200) for 1 h, followed by 3 x 5 min washes using blocking solution. Goat anti-rabbit Alexa 488 secondary antibody (Invitrogen UK, A11008) or goat anti-mouse Alexa 488 (Invitrogen UK, A11001) was applied at a 1:400 dilution for 1 h followed by a 5 min counterstain using Hoechst solution (Hoechst 33528 and Hoechst 33342 dyes each diluted to 1:50,000 in PBS, Sigma). Tissue sections were washed 2 x 5 min in PBS and then mounted with a size 1 coverslip using Citifluor AF1 mountant (Citifluor Ltd., UK).

2.6 – Light microscopy

2.61 – Epidermal measurements

H&E stained tissue sections were examined using a Leica DMLB light microscope and images were captured at either 10 X or 20 X magnifications using the Leica IM50 software. The thickness of the epidermis at the wound edge was determined by measuring the thickest point along the axis from the basal to spinous layer within the end 100 μm (mice) or 150 μm (rats) of nascent epidermis using ImageJ. The length of nascent epidermis growing out from the wound edge was measured for rats at either side of the wound using ImageJ and averaged to return a re-epithelialisation distance measurement for each sample.

2.62 – Polymorphonuclear cell quantification

H&E stained tissue sections were examined using a Leica DMLB light microscope and polymorphonuclear leukocytes (PMNs) were identified and counted in a single field of view

700 μm from the wound edge in the lower dermis using a 40 X objective. For mice, high quality images of PMNs and scaffolds used in figures were captured using a Hamamatsu Nanozoomer 2.0 slide scanner using the 20 X objective using brightfield to generate automatically stitched montage images. For rats, high quality figure images were captured using a Zeiss Axio Scan.Z1 automated slide scanner using a 20 X objective and the brightfield image acquisition wizard settings. Images were automatically stitched together to form a montage.

2.63 – Measurement of granulation tissue area

Rat wounds harvested at D10 and D15 were H&E stained and loaded into a Zeiss Axio Scan.Z1 automated slide scanner. Brightfield images were captured using a 20 X objective using the image acquisition wizard settings, and were then automatically stitched together to form a montage. Montages were then exported to JPEG format and quantified for granulation tissue area using ImageJ. The granulation tissue (or wound area) was defined as the new area of tissue within the wound margins yet above the muscle and panniculus carnosus layers, and was measured using the freehand line tool within the program.

2.64 – Assessment of smooth muscle actin area

Rat wounds that had been harvested at D10 were loaded into the Zeiss Axio Scan.Z1 slide scanner and imaged using a 20 X objective using the built in image acquisition wizard. Both Hoechst and Alexa 488 fluorophores were excited using the image acquisition wizard settings and montages containing both channels were generated and overlaid. The Zeiss slide scanner proprietary ZEN 2012 Lite software was then used to open the montage images. The α-SMA staining in the green channel was then thresholded in the software to a level that allowed visualisation of both α-SMA positive blood vessels as well as a positive staining region in the wound gap, above the panniculus carnosus. This area was drawn around using a marker tool within the proprietary software and an area in square microns was displayed. This approach was applied in the same manner to each of the 8 samples in each treatment group.

2.7 – Confocal microscopy

Single optical section images of Cx43 or Cx26 immunostained wound and tissue sections were acquired using a Leica SP2 confocal microscope using a 40 X oil objective. Fluorophores were excited sequentially (Hoechst using both 351 and 364 nm wavelength lasers, Alexa 488 using a 488 nm wavelength laser). 8-bit images were acquired using a frame average of 4 at a resolution of 1024 by 1024 pixels. Image acquisition settings remained identical between each treatment in order to allow comparisons to be made during image analysis.

2.71 – Confocal image analysis

Connexin protein expression was quantified by counting positive pixels on binary images of wound edges using ImageJ software using the method outlined in a study by (Wang et al., 2007). Images from each experiment were identically thresholded prior to analysis. Only the number of connexin positive pixels contained within the end 100 μm (for mouse) or 150 μm (for rat) of nascent epidermis was assessed in order to gauge only protein expression at the wound edge. Connexin levels were also expressed per square micron of epidermis to compensate for variations in epidermal thickness between samples. In order to account for variations in connexin levels between individual animals, wound edge expression was normalised to connexin levels at a distal site away from the wound edge and expressed as a percentage change from distal levels. In the case of Cx26 stained tissue, distal levels were extremely low, to the extent that small fluctuations between samples could result in large differences between values. For this reason, Cx26 distal levels were averaged and these values were used to calculate the change in wound edge Cx26 expression.

2.8 – Statistical analysis

2.81 – Power analysis

Sample size was determined using power analysis software G*Power. The effect size value used in the formula was derived from previous lab *in vivo* wound healing data obtained by a previous Masters student.

2.82 – Normality tests

All data amenable to statistical analysis was subjected to Kolmogorov-Smirnov tests using GraphPad Prism 5.0 software to ascertain normality. Data is classified as normal using this test when a significance value of over 0.05 is returned. All data was normally distributed and therefore subjected to parametric statistical tests.

2.83 – Statistical tests

After confirming normality, data was subjected to one-way ANOVA testing followed by a Tukey's post-hoc test to investigate individual statistical significance differences. GraphPad Prism 5.0 software was used to perform all statistical analyses. A significance value of 0.05 was used as the lowest threshold of significance.

CHAPTER 3

Design and application of a bioactive scaffold

Associated publication: (Gilmartin et al., 2013)

3.1 – Introduction

Chronic ulcers are hard-to-heal wounds that typically contain elevated numbers of inflammatory cells, reduced levels of growth factors, damage or loss of the dermal extracellular matrix (ECM) and the misexpression of specific proteins (Seah et al., 2005, Muller et al., 2008, Brandner et al., 2004). In particular, both chronic ulcers and diabetic rat wounds have been found to contain high levels of the gap junction protein connexin 43 (Cx43) (Wang et al., 2007, Brandner et al., 2004). During acute wound healing Cx43 is normally downregulated in the first 6 h in keratinocytes at the wound edge and remains low until re-epithelialisation of the wound completes around days 5-7 (Coutinho et al., 2003). However, in chronic wounds Cx43 expression is reported to either fail to downregulate (Brandner et al., 2004) or may instead be upregulated (Mendoza-Naranjo et al., 2012a, Mendoza-Naranjo et al., 2012b) (Sutcliffe et al., submitted publication), a feature accompanied by a lack of epithelial migration to restore the epithelial barrier. The identification of Cx43 as a drug target has led to the development of an antisense oligodeoxynucleotide (asODN) sequence specific to Cx43 which, when applied to both diabetic and acute wounds, was found to downregulate Cx43 expression and accelerate re-epithelialisation (Wang et al., 2007, Qiu et al., 2003). Cx43 asODN has also been demonstrated to promote fibroblast migration *in vitro* as well as reduce wound size. Additionally, Cx43 asODN has been noted to dampen the inflammatory response (Mori et al., 2006).

While the use of Cx43 asODN addresses a number of problems pertinent to chronic ulcers, the frequently occurring damage to or loss of the underlying dermal ECM is not one of them. The loss of regular ECM is associated with over-activity of MMP enzymes, particularly MMP-2 and MMP-9. These normally function to degrade excess matrix proteins such as collagen and fibrinogen. A reduction in TIMPs, as well as MMP stimulation through inflammatory cytokines IL-1, IL-6 and TNF-alpha contribute to the degradative state of chronic ulcers (Raffetto and Marston, 2011, Han et al., 2001).

Wounds that are significant in depth and result in the loss of both epidermal and dermal compartments are termed full-thickness wounds, and pose a difficult challenge in treatment. In terms of substituting significantly damaged tissue, autografts are considered to be the gold standard to heal large skin wounds (An et al., 1995). However, in the case of

chronic ulcer patients, healing is often compromised throughout the individual such that removal of donor skin from other parts of the body is not feasible due to the risk of generating additional non-healing wounds. This can also be true in the case of significant burns, where extensive damage to the body can leave too small an amount of viable tissue from which to derive donor grafts (Vacanti et al., 1998). One method to generate more tissue from a patient is to culture donor grafts. This method has its limitations, as it requires several weeks of cell culture and the success rate can be low. The chance of patient graft take is variable at 15-85%, while for full-thickness burns this has been estimated to be around 53% (Atiyeh and Costagliola, 2007, Paddle-Ledinek et al., 1997).

The lack of suitability of grafts for many patients with significant full-thickness wounds has led to increased research into engineered scaffolds; substrates that are placed in the full-thickness wound and are intended to mimic the native skin or dermal matrix (Shevchenko et al., 2010). The method to produce scaffolds varies considerably, from cell-cultured constructs to artificially synthesised polymer matrices. All types are intended to serve a similar purpose, which is to behave as scaffolds for cell attachment and proliferation in the missing wound bed (Rho et al., 2006). In an effort to most accurately recreate both the epidermal and dermal layers of normal skin, cellular scaffolds have been engineered such as the branded products Apligraf (Organogenesis webpage, 2012) and Orcel (Forticell Bioscience webpage, 2012). These comprise a bilayer arrangement of human keratinocytes over an animal-derived extracellular matrix. There are three major disadvantages to these scaffold types, however – they are expensive, time consuming to produce and there is a risk of patient rejection of allogenic cells (Schonfeld et al., 2000).

As mentioned in chapter 1, these limitations have led to the development of a number of acellular scaffolds, including lyophilised extracellular matrix from animal skin, (Oasis, Alloderm) and synthetic nylon structures. (Integra) (Shevchenko et al., 2010). Recently, scaffolds have also been experimentally fabricated from matrix-derived polymers including collagen (Torres-Giner et al., 2009) and fibrinogen (McManus et al., 2007) as well as synthetic polymers such as polycaprolactone (PCL) (Garcia-Giralt et al., 2008) and polylactic-co-glycolic acid (PLGA) (Yang et al., 2009). In these studies, the scaffolds contain one layer and are intended to only substitute the extracellular matrix. It is anticipated that the wound is then encouraged to re-epithelialise over the artificial scaffold matrix to close the wound. As well as woven structures, various polymers have also been

used to synthesise solid microspheres and aqueous hydrogels in addition to large sheet structures (Ashton et al., 2007).

While cell-based and freeze-dried dermal scaffolds may more closely mimic the existing skin architecture, the time and cost required to develop these devices, as well as the potential biocompatibility issues, make acellular options particularly more attractive from a commercial point of view. It is therefore the family of scaffolds fabricated using naturally derived polymers that appear to hold particular promise as a quick and affordable method to fill the damaged dermal layer in a full-thickness wound. A method commonly employed to fabricate fibrous acellular scaffolds is the technique of electrospinning. Using this method, a wide variety of polymers can be dissolved in a solvent and extruded through a syringe into an electric field to generate a mesh network of polymer fibres (Rho et al., 2006). This technique is both affordable and highly customisable, with alterations to the applied voltage, volume of polymer used or the distance between the syringe and collector plate all resulting in differences in the output scaffold fibres. Importantly, this technique offers potential as an 'off-the-shelf' solution that could be ready for immediate application to a patient.

However, although dermal scaffolds lack cells that could cause biocompatibility issues *in vivo*, there has been very little investigation into whether these types of devices actually promote healing of wounds. Much of the research into electrospun scaffolds has only been followed up with *in vitro* testing, commonly in the form of cell adhesion or migration assays. And while many studies have reported clinical outcomes using scaffolds, the vast majority pay little microscopic attention to the early stages of the healing process, and most observations at the macroscopic level (Gholipour Kanani and Hajir Bahrami, 2010, Rho et al., 2006, Sabolinski et al., 1996, Wainwright, 1995). When microscopic evaluation of wounds is performed, images taken have often been at a low magnification such that the behaviour of cells at the wound edge cannot be clearly characterised. Additionally, microscopic assessments are again typically performed at late time points after scaffolds have broken down or wounds have re-epithelialised (Rho et al., 2006). Furthermore, a recent report investigating 60 venous leg ulcer scaffold trials found the majority of studies to be flawed, concluding that the scaffolds in the studies were not proven to improve wound healing (Zenilman et al., 2013). Owing to the lack of clear evidence that acellular

polymer-based scaffolds adopted a supportive role *in vivo*, this led to an initial null hypothesis for the project, that: *scaffolds do not promote healing of full-thickness wounds*.

In order to test the primary hypothesis, an electrospinning technique was used to generate a scaffold using collagen, one of the most commonly used natural polymers in biomaterials (Shevchenko et al., 2010). A source of purified acid-soluble bovine collagen had been identified that had been processed by the manufacturer in an effort to reduce the chance of potential adverse reactions (Kensey-Nash, 2014). Following fabrication and processing of scaffolds, they were then applied to full-thickness excision wounds made to the dorsum of mice. In this way, wounds could both be examined macroscopically and microscopically to assess the cellular response to scaffolds. In the latter case, wound re-epithelialisation and inflammatory cell association in response to scaffold application could be visualised following high power examination of haematoxylin and eosin staining tissue sections. Since Cx43 is found to be upregulated at the wound edge in more than one situation when wound healing is perturbed, it seemed possible that if scaffolds instead had a detrimental effect on healing that Cx43 expression analysis might be a useful tool to help detect such an occurrence. Cx26 expression has also been linked to hyperproliferative skin conditions and hard-to-heal wounds and its overexpression could also be indicative of poorly healing wounds.

Aims

The aims of this chapter were to:

1. Produce a fibrous collagen scaffold that could be applied to a series of full-thickness mouse wounds *in vivo*.
2. Macroscopically characterise the wounds to determine whether the scaffolds inhibited or promoted wound healing.
3. Microscopically assess wound re-epithelialisation, inflammatory cell response and Cx43 and Cx26 expression in cells at the wound edge, in order to characterise the effect of scaffolds on the wound the wound healing response.

3.2 – Materials and methods

See Chapter 2 for a detailed description of the individual methods and materials employed. A condensed explanation of the methods used in this chapter is listed below.

3.21 – Scaffold preparation

Scaffold and microsphere fabrication

Collagen scaffolds were fabricated by electrospinning a 20:1 ratio of acid-soluble bovine collagen with poly-ε-caprolactone (PCL) as described in Chapter 2. Scaffolds were electrospun to thicknesses of both 0.8 mm and 0.4 mm and crosslinked by immersion in either a high (15% wt./v.) or a low (0.15% wt./v.) concentration of N-(3-Dimethylaminopropyl)-N'-ethylcarbodiimide (EDC) hydrochloride in a 1:10 water to acetone solution. Scaffolds were washed as outlined in Chapter 2 and cut out of the scaffold sheet using a 6 mm biopsy punch to match the size and shape of excisional wounds. Alginate microspheres were produced by electrospraying medium 2% (wt./v.) viscosity alginic acid powder PBS solution using the method described in Chapter 2.

Commercial scaffold materials

Both alginate hydrogel and dressing materials under the brand name ActivHeal® were provided for use by Prof David Becker.

Investigation of scaffold porosity

Scaffold porosity was assayed by submerging scaffolds overnight in a solution of 30% (wt./v.) Pluronic® F-127 powder dissolved in water (herein referred to as 'Pluronic gel') that had been supplemented with 5% fluorescein isothiocyanate (FITC). Scaffolds were excited using blue light to confirm the presence of FITC under a dissection microscope.

Scaffold infusion with Cx43 asODN

Cx43 antisense oligodeoxynucleotides (Cx43 asODN), sequence 5'-GTA ATT GCG GCA GGA GGA ATT GTT TCT GTC-3' were dissolved in nuclease free water and diluted Pluronic gel to a 30 μM concentration. Collagen scaffolds were immersed in 20 μl of either Cx43 asODN containing Pluronic gel or PBS at 4°C overnight. Alginate microspheres were

soaked in a volume of Cx43 asODN Pluronic gel equal to the volume of polymer used in electrospraying.

3.22 – Surgery

Six week old male imprinting control region (CD-1) outbred mice were anaesthetised via a nose cone using 4% isoflurane, 20% oxygen and 10% nitrous oxide, and maintained using 1.5% isoflurane. Animals were injected subcutaneously with 0.03 mg/ml buprenorphine (Vetergesic) before operation. Mouse backs were shaved and covered in a thin layer of Nair® hair removal cream, after which both the cream and hair was removed using a warm moistened gauze pad. Animals were placed on heated mats for the operation. Four full-thickness excisional biopsy punch wounds were made using a 6 mm medical biopsy punch to rodent backs, two on each side of the dorsal midline. Scaffold treatments were applied directly to wounds, after which the back was covered with a sheet of Tegaderm™ film. Post-procedure, animals were kept in a heated chamber and monitored for recovery. Once recovered, animals were re-housed in standard individual cages.

3.23 – Processing and histology

Tissue collection

Animals were culled by cervical dislocation at 1, 3 or 5 days post wounding. Wounds were macroscopically imaged as outlined in chapter 2 then excised and fixed in 4% paraformaldehyde (PFA)-PBS solution for 24 h at 4°C. Tissue was immersed in 20% sucrose overnight then washed in PBS, after which wounds were bisected. Half of each wound was snap frozen in OCT medium, then sectioned using a cryostat at a thickness of either 5 μm (for H&E staining) or 10 μm (for immunofluorescence staining).

Haematoxylin and eosin staining

Frozen tissue sections were thawed for 5 min then covered completely in tap water for 5 min at room temperature. Slides were submerged in Harris' haematoxylin solution for 30 seconds followed by immersion in a container full of running tap water for 5 min. Background staining was reduced by dipping the slides in a container full of 1% acid alcohol (1% glacial hydrochloric acid, 70% ethanol, 29% distilled water) for 3 seconds, after which slides were immersed in a container of running tap water for a further 5 min.

Samples were then submerged for 15 seconds in a container full of eosin B solution, followed by immersion for 5 seconds in a container full of tap water to rinse away excess stain. Slides were then immersed in 70% ethanol for 2 min, 100% ethanol for 2 min and a second container of 100% ethanol for a further 2 min, to dehydrate the sections. Slides were then submerged in a container full of xylene for 5 min, then a second container of xylene for an additional 5 min. Slides were then individually removed and covered with DPX mounting media, then sealed using a coverslip.

Immunofluorescence staining

Tissue sections were permeabilised in cold acetone for 5 min and then using a 0.1 M L-lysine PBS solution containing 0.1% Triton-X-100. Sections were stained for 1 h using a rabbit polyclonal antibody to Cx43 (1:2000 dilution, C6219, Sigma Aldrich UK) or Cx26 (1:200 dilution, (Diez et al., 1999). Sections were then stained using a goat anti-rabbit Alexa 488 secondary antibody (A11008, Invitrogen UK) at a 1:400 dilution for 1 h. Tissue was counterstained using Hoechst solution (both Hoechst 33528 and Hoechst 33342 dyes at 1:50,000 dilution, Sigma Aldrich UK).

3.24 – Analysis

Imaging

Wounds were macroscopically and microscopically imaged as outlined in Chapter 2. Collagen scaffolds were sputter coated with tungsten and imaged using scanning electron microscopy (SEM) at 800 X magnification. Tissue sections immunostained for Cx26/43 and Hoechst were imaged using confocal microscopy. Single optical section 8-bit images were acquired at the wound edge and at a distal region of skin at 1024 by 1024 pixels. Image settings were consistent between treatments.

Epidermal thickening measurements

Epidermal thickness was measured on H&E stained tissue and determined by measuring the thickest point along the basal to spinous layer axis within the end 100 μm (mice) or 150 μm (rats) of nascent epidermis using ImageJ. The length of nascent epidermis outgrowing from the wound margin was measured in rats at either side of the wound using ImageJ and averaged to return a re-epithelialisation distance measurement for each sample.

Connexin 26 and 43 protein quantification

Cx43 and Cx26 protein expression was quantified by counting positive pixels on binary images of wound edges using ImageJ software using the method outlined in a study by Wang et al. (2007). Images from each experiment were identically thresholded and the number of connexin positive pixels within the end 100 μm quantified. Connexin levels were expressed per square micron of epidermis and normalised to distal levels to reduce sample-to-sample variation. In the case of Cx26, distal levels were extremely low, to the extent that small variations in distal expression could strongly impact the calculated percentage change from distal to wound edge levels. For this reason, at each time point distal epidermal Cx26 levels for each sample were averaged to produce a single value. This averaged distal expression value was then used to calculate individual percentage increases in expression for each wound.

Polymorphonuclear leukocyte quantification

Polymorphonuclear leukocytes (PMNs) were identified 700 μm away from the wound edge in the lower dermis using a 63 X objective on a light microscope (see chapter 2 for full details). PMNs were counted in one field of view using a 40 X objective. Images displayed in figures were captured using a Hamamatsu Nanozoomer 2.0 slide scanner using the 20 X objective using brightfield to generate automatically stitched montage images.

Statistical analyses

Sample size was determined using power analysis software G*Power as described in Chapter 2. Data was subjected to Kolmogorov-Smirnov tests using GraphPad Prism 5.0 software to ascertain normality, then to one-way ANOVA tests followed by Tukey's post-hoc tests to determine statistical significance.

3.3 – Development of a collagen scaffold for *in vivo* use

Collagen scaffolds were fabricated using an electrospinning technique that had been employed by other groups to produce an uneven mesh network of fibres (Figure 3. 1A). Use of this method resulted in the generation of fibres with a diameter range of 0.03 - 4.12 µm. SEM revealed a porous structure when viewed from above (Figure 3. 1B) and the side (Figure 3. 1C). This closely mirrored the scaffolds fabricated in other studies, which were designed to mimic the fibre diameter and porosity contained within native ECM (Torres-Giner et al., 2009, Nishida et al., 1988).

Scaffolds impede full-thickness wound repair

3.31 – Scaffolds inhibit wound closure

In order to assess the effect of scaffolds on wound healing, 6 mm diameter scaffold discs were biopsy punched out of the electrospun collagen mats and applied to same-size full-thickness wounds made to the dorsum of mice (Figure 3. 2A-B). Cull time points of 3 and

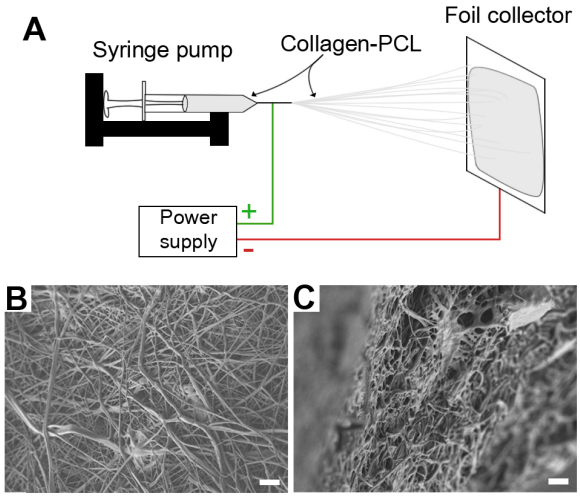

Figure 3. 1 – Electrospinning a collagen scaffold.
Electrospun collagen scaffolds were fabricated by the method of electrospinning a blend of collagen and PCL to produce a mesh network of fibres Scaffolds were electrospun **(A)** and imaged using a scanning electron microscope (800 X magnification) from above **(B)** and side-on **(C)**. Scale bar = 10 µm. Images shown are representative of triplicate observations of a minimum of n = 3 scaffolds.

5 days were selected to investigate re-epithelialisation and granulation tissue formation between treatments.

Visual assessment of wounds at D3 and D5 (Figure 3. 2C) indicated scaffold application resulted in a clear decrease in the wound closure rate. It was also possible to occasionally observe re-epithelialisation over the wound site in control wounds (marked by a dotted line), but not over scaffolds. Wound contraction, a prominent feature in healing rodent wounds, was severely impeded by the presence of a solid scaffold. While scaffolds are intended to integrate with wounds, at D3 the applied scaffolds were typically disassociated from the wound edge and showing little or no integration. However, it was not clear whether wounds treated with scaffolds were re-epithelialising into the scaffolds or underneath them without further microscopic assessment.

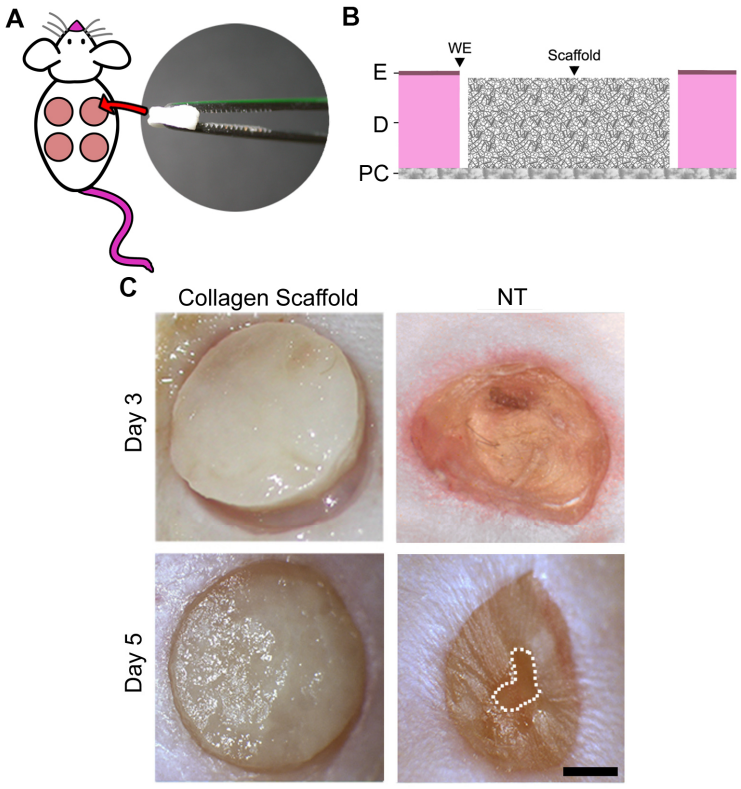

Figure 3. 2 – Scaffold application to wounds.
(A-B): Collagen scaffolds were applied to full-thickness wounds and compared to wounds left untreated. **(C)**: Macroscopic images of wounds were taken at D3 and D5 post wounding. The white dotted line outlines a visible leading edge of re-epithelialisation. Images are typical representations across all mice (n = 7), Scale bar = 1.5 mm.

3.32 - Scaffolds induce aberrant thickening of wound edge keratinocytes

Following macroscopic assessment it seemed possible that scaffolds may actually delay healing, which is a feature more commonly associated with chronic wounds. In chronic ulcers and diabetic wounds, cells at the wound edge upregulate Cx43 (Mendoza-Naranjo et al., 2012a, Mendoza-Naranjo et al., 2012b, Wang et al., 2007). The epidermis at the chronic wound edge has also been found to thicken extensively and contain elevated levels of Cx26 (Sutcliffe et al., submitted publication). In order to assess whether scaffolds were inducing features characteristic of chronic wounds, the excised tissue was histologically examined.

At both D3 and D5 time points, scaffold application caused keratinocytes at the wound edge to form thickened, non-migratory bulbs compared to the thin tongues of cells formed in the rapidly healing untreated wounds (Figure 3. 3A-B). At D3 the average thickness of the nascent epidermis of scaffold-treated wounds was 106 ± 24 μm (mean +/- SEM); a significant 73% increase from the 33 ± 5 μm of untreated wounds ($P < 0.01$, Figure 3. 3C).

At D5 there was a similar 57% increase in epidermal thickness in scaffold treated wounds ($P < 0.05$, Figure 3. 3D). Microscopically, there was no visual evidence of keratinocyte entry into or over the scaffolds. Keratinocyte and fibroblast migration instead appeared by D5 to occur down the side and underneath scaffolds, similar to how re-epithelialisation occurs under a scab (Figure 3. 3B). Scaffolds were also typically surrounded by polymorphonuclear cells with a morphology characteristic of neutrophils at both D3 and D5. By D5, in the majority of cases scaffolds had degraded considerably. This failure to develop a thinning epithelial tongue in scaffold treated wounds appeared to suggest that scaffolds were inducing a negative effect on healing.

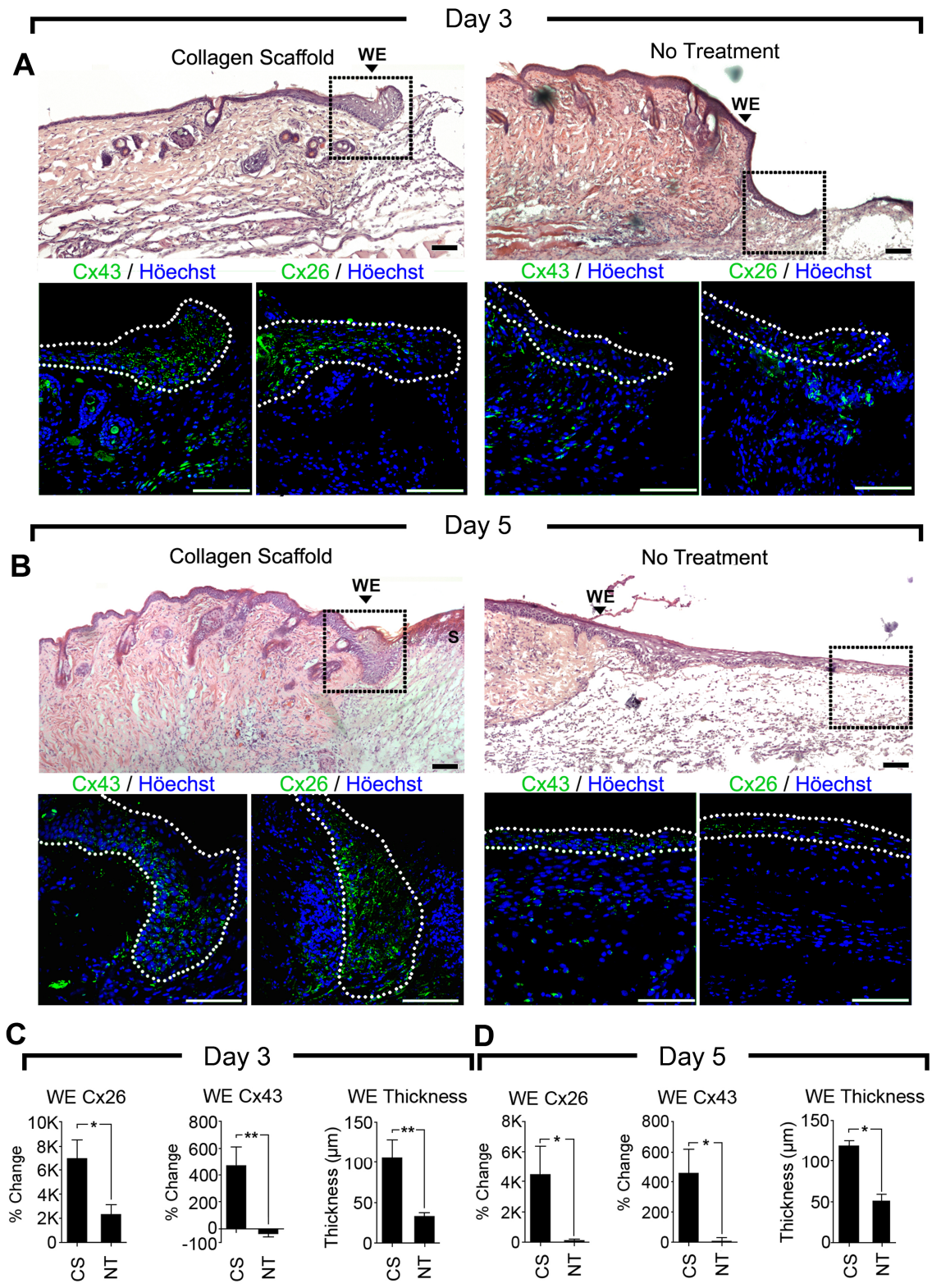

Figure 3. 3 – Epithelial and Connexin response to scaffolds.

H&E and Cx43 staining of D3 **(A)** and D5 **(B)** mouse full-thickness wounds following either no treatment or application of collagen scaffolds. Boxed areas of representative H&E stained wound edges are magnified below in high power confocal images of sister

sections. Expression of Cx26, Cx43 and epithelial thickness was quantified in keratinocytes at the wound edge at D3 **(C)** and D5 **(D)**. Dotted white lines mark the epidermis. Scale bar = 100 μm, n = 7 samples per group, data is plotted as mean + SEM, WE = wound edge. For wound treatments CS = collagen scaffold, and NT = no treatment (* = $P < 0.05$, ** = $P < 0.01$).

3.33 - Thickened epidermal bulbs contain elevated levels of connexins 43 and 26

The thickening of the wound edge epidermis is characteristic of a chronic wound, which also contains elevated levels of Cx43 (Mendoza-Naranjo et al., 2012a). Cx26 overexpression has also been found to be upregulated in chronic wounds in a recently submitted article (Sutcliffe et al.) as well as in hyperthickened skin conditions (Labarthe et al., 1998). In order to observe whether scaffolds were inducing a chronic wound-like state, wounds were stained for Cx43 and Cx26. While connexin expression in fibroblasts in the wound did not appear markedly different between treatments, wound edge keratinocyte expression differed greatly between treatments (Figure 3. 3A-B). There was a 469% increase in Cx43 expression from distal epidermis levels at D3 ($P < 0.01$, Figure 3. 3C) in scaffold-treated wound edges, significantly higher than the 38% downregulation found in untreated leading edge keratinocytes ($P < 0.01$, Figure 3. 3C). Cx43 levels were also elevated over distal epidermal levels at D5 – a 457% increase in leading edge keratinocyte expression versus the 10% increase in control wounds ($P < 0.05$, Figure 3. 3).

While a degree of Cx26 upregulation in wound edge keratinocytes is typical of healing wounds, Cx26 was upregulated by approximately 7,000% at D3, which was significantly greater than the 2,326% upregulation of non-treated wounds ($P < 0.05$, Figure 3. 3C). This feature was again observed at D5; scaffold-treated wounds had a 4,466% increase in wound edge keratinocyte Cx26 levels, which was significantly greater than the 167% detected in untreated wounds ($P < 0.05$, Figure 3. 3D).

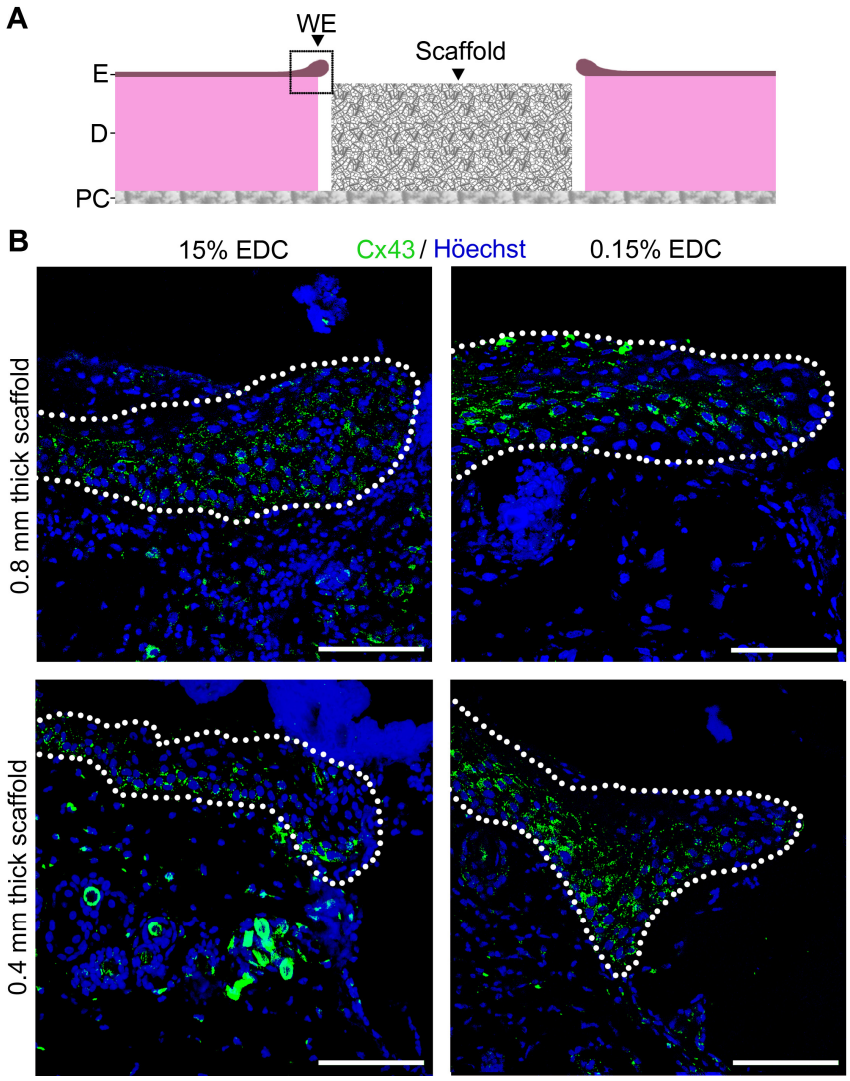

Figure 3. 4 – Wound edge Connexin 43 expression is elevated across all different collagen scaffold applications.

Cx43 staining of D1 full-thickness wound edges following treatment with varying physical properties of collagen scaffold. **(A)**: Diagram illustrating site of confocal image capture. **(B)**: High power single optical section confocal images of the boxed area in (A) of the leading edge epidermis. Scaffolds properties were varied (either 15 mM or 0.15 mM EDC used to cross-link, and scaffolds were spun to a thickness of either 0.4 mm – termed 'thin' or 0.8 mm – termed 'thick'). Dotted white lines mark the outline of the epidermis. Scale bar = 100 μm, images are typical observations of n = 5 samples per group. Diagram legend: E = epidermis, D = dermis, PC = panniculus carnosus, WE= wound edge.

3.4 – Modification of scaffolds

3.41 - Collagen scaffold design

Due to differences in reported scaffold fabrication and cross-linking methods it raised the possibility that the negative effects encountered may have been due to how it was fabricated. In particular, the 0.8 mm thick scaffolds fabricated may have been too thick for the wounds to re-epithelialise over, or the use of a high concentration (15% wt./v.) and it was postulated that the crosslinker agent EDC could have resulted in residual crosslinker remaining on the scaffolds. However, following application of scaffolds prepared to a reduced thickness (0.4 mm) or using a lower crosslinker concentration (0.15%) to full-thickness wounds, there appeared to be a strong upregulation of wound edge Cx43 in each case, even at D1 when Cx43 is typically downregulated (Figure 3. 4) (Coutinho et al., 2003). Wound edge keratinocytes also typically formed thickened bulbous areas, similar to that observed at D3 and D5 (Figure 3. 3). This suggested that the collagen scaffolds formulated in a variety of ways were all capable of retarding wound healing. The next point to address was whether other scaffold materials induced similar effects.

3.42 – Investigation into the effect of alginate applications on wound healing

In order to assess whether the negative effects observed were specific to collagen scaffolds or not, three additional polymer applications composed of alginate were applied to full-thickness wounds (Figure 3. 5A). Wounds treated with solid alginate microsphere and spun alginate dressing applications typically developed bulbs of keratinocytes at the wound edge containing upregulated levels of Cx43 at D1 (Figure 3. 5B). However, this effect was not observed in wounds treated with the alginate hydrogel, as Cx43 was typically downregulated in wound edge keratinocytes relative to distal levels, and keratinocytes migrated as a thin process of cells.

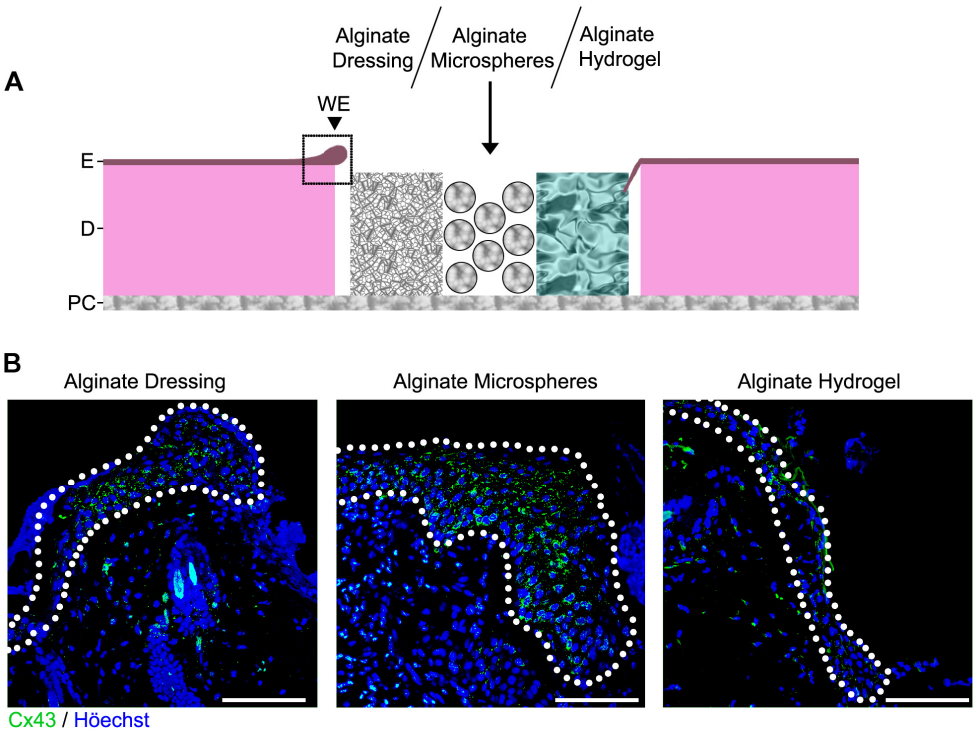

Figure 3. 5 – Connexin 43 expression in alginate treated wounds.
Alginate application to D1 full-thickness wounds. **(A)**: Diagram to illustrate the application method of one of three alginate fabrications to wounds. One type of scaffold was applied to each wound. **(B)**: Cx43 fluorescence staining of full-thickness wound edges (high power confocal single section images). Images focus on the boxed area of the wound edge illustrated in (A). Dotted white lines mark the outline of the epidermis. Scale bar = 100 μm, n = 5 samples per group. Diagram legend: E = epidermis, D = dermis, PC = panniculus carnosus, WE = wound edge.

3.5 - Bioactivation of collagen scaffolds using Cx43 asODN

3.51 – Bioactivated scaffolds macroscopically appear to integrate with wounds

The upregulation of Cx43 and Cx26 as well as wound edge epidermal thickening appeared a consistent feature associated with both solid collagen and alginate scaffolds. The alginate hydrogel, which did not produce a negative reaction, was short-lived and did not function as a supportive matrix as intended. It remained to be determined whether an integrating solid scaffold could be achieved through optimising the existing scaffold.

Elevated levels of Cx43, as found in both scaffold treated and chronic wounds, have been successfully reduced through application of antisense oligodeoxynucleotides (asODN) to Cx43 (Wang et al., 2007, Qiu et al., 2003). In an effort to overturn the negative effects associated with scaffold use, collagen scaffolds were bioactivated using a previously validated rat Cx43 asODN sequence (Qiu et al., 2003). The spread of a FITC-labelled 30% Pluronic gel throughout the scaffold structure indicated scaffolds were permeable to the drug delivery vector, suggesting that the method would incorporate asODN into the whole of the scaffold (Figure 3. 6A). Following bioactivation, scaffolds were then applied to full-thickness mouse back wounds (Figure 3. 6B). Macroscopic evaluation revealed that Cx43 asODN bioactivated scaffolds at D3 and D5 appeared to be partially integrated with the wound edge, compared with untreated scaffolds (Figure 3. 6C).

3.52 – Bioactivated scaffolds do not induce wound edge epidermal thickening

Microscopic examination of wounds revealed significant differences in wound edge epithelial thickening between bioactivated and untreated scaffolds (Figure 3. 7A, Figure 3. 8A). The wound edge epidermis following bioactive scaffold treatment was a significant 60% thinner than untreated scaffolds at D3 ($P < 0.01$, Figure 3. 7D) and 52% thinner at D5 ($P < 0.05$, Figure 3. 8D), to a level insignificantly different from untreated wounds. Although macroscopic analysis indicated that bioactive scaffolds appeared to partially integrate with the wound edge, microscopic analysis revealed keratinocytes migrated down the side and underneath scaffolds as opposed to into or over them.

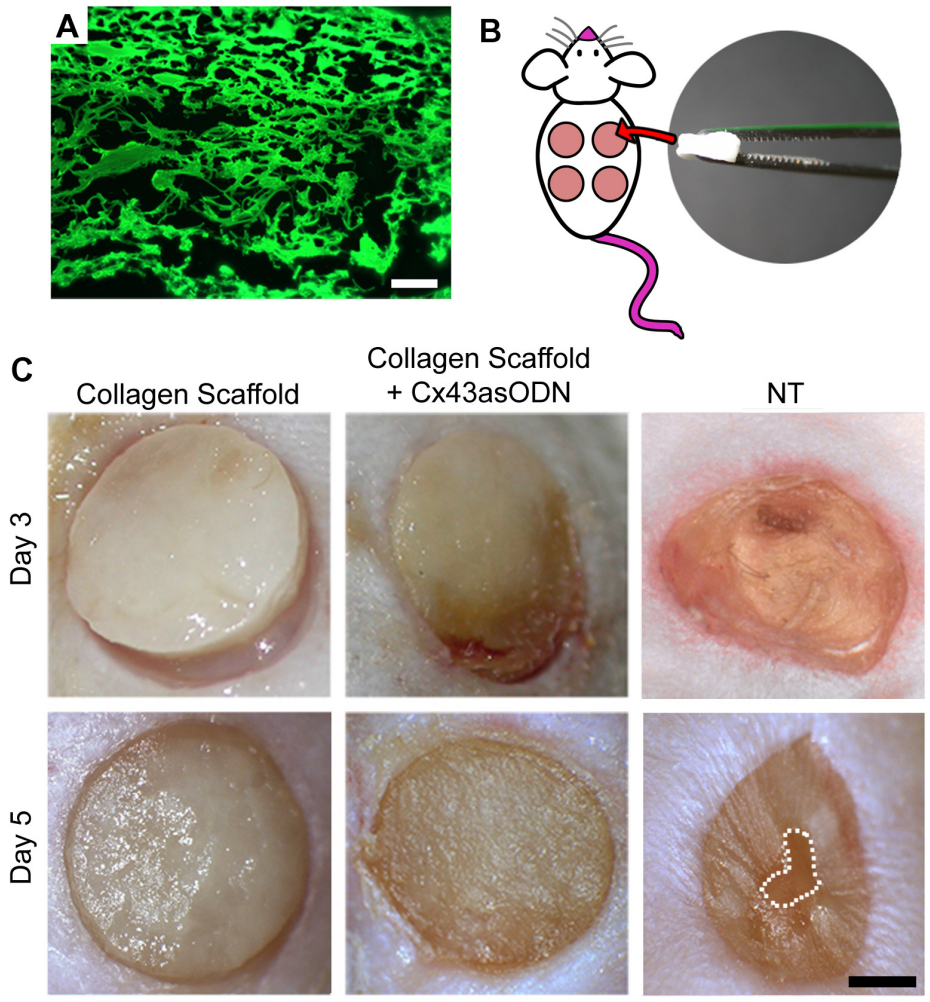

Figure 3. 6 – The *in vivo* effect of Cx43 asODN bioactivation of scaffolds.
(A): Collagen scaffolds were infused with a FITC-labelled Pluronic gel to assess scaffold permeability to the drug delivery vector. **(B-C)**: Cx43 asODN bioactivated scaffolds were applied to full-thickness wounds and compared to wounds with no treatment (NT) or control scaffolds infused with only Pluronic gel. Macroscopic images of wounds were taken at D3 and D5 post wounding. The dotted white line outlines a visible leading edge of re-epithelialisation. Images are typical representations across all mice (n = 7), Scale bar = 1.5 mm.

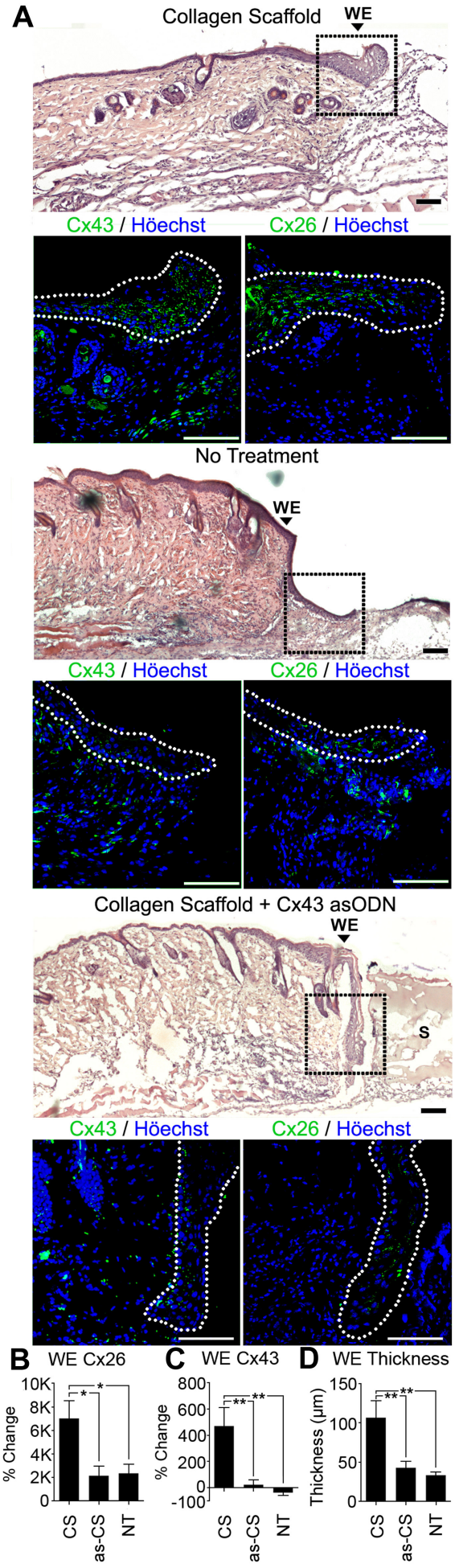

Figure 3. 7 – The microscopic effects of Cx43 asODN bioactivation of scaffolds 3 days after wounding.

H&E and Cx43 staining of D3 mouse full-thickness wounds following treatment with uncoated or Cx43 asODN infused collagen scaffolds. **(A)**: Boxed areas of representative H&E stained wound edges are magnified below in high power confocal images of sister sections. Expression of Cx26 **(B)**, Cx43 **(C)** and epithelial thickness **(D)** was quantified in keratinocytes at the wound edge. Dotted white lines mark the epidermis. Scale bar = 100 µm, n = 7 samples per group, data is plotted as mean + SEM. Diagram legend: S = scaffold, WE = wound edge. For wound treatments CS = collagen scaffold, as-CS = Cx43 asODN treated collagen scaffold and NT = no treatment (* = $P < 0.05$, ** = $P < 0.01$).

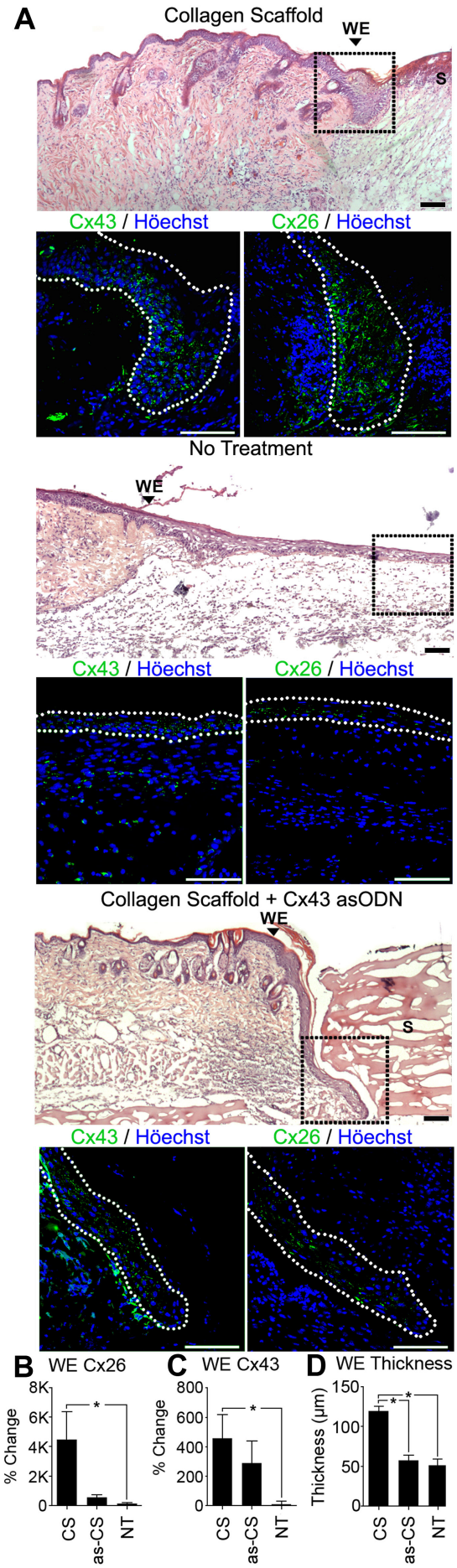

Figure 3. 8 – The microscopic effects of Cx43 asODN bioactivation of scaffolds 5 days after wounding.

H&E and Cx43 staining of D5 mouse full-thickness wounds following treatment with uncoated or Cx43 asODN infused collagen scaffolds. **(A)**: Boxed areas of representative H&E stained wound edges are magnified below in high power confocal images of sister sections. Expression of Cx26 **(B)**, Cx43 **(C)** and epithelial thickness **(D)** was quantified in keratinocytes at the wound edge. Dotted white lines mark the outline of the epidermis. Scale bar = 100 µm, n = 7 samples per group, data is plotted as mean + SEM. Diagram legend: S = scaffold, WE = wound edge. For wound treatments CS = collagen scaffold, as-CS = Cx43 asODN treated collagen scaffold and NT = no treatment (* = $P < 0.05$).

3.53 – Cx43 and Cx26 expression is downregulated following application of Cx43 asODN bioactivated scaffolds

The significant reduction in wound edge epidermal thickening indicated bioactivation had a positive effect in reducing the effect of scaffolds. There were also significant differences in wound edge connexin expression shown by immunostaining for Cx43 and Cx26 (Figure 3. 7A). Leading edge keratinocytes in bioactive scaffold treated wounds displayed a 91% significant reduction in Cx43 protein expression relative to control untreated scaffolds at D3 ($P < 0.05$, Figure 3. 7C). At D3, this level was also insignificantly different from untreated wounds. By D5, however, there was no significant difference in Cx43 expression between bioactivated and untreated scaffold treated wounds, indicating that the effect of the asODN had diminished (Figure 3. 8C). Cx26 levels were also reduced by 68% in wound edge keratinocytes at D3 ($P < 0.05$, Figure 3. 7B) and 87% at D5 ($P < 0.05$, Figure 3. 8B) following bioactive scaffold application, to levels insignificantly different from untreated wounds. Despite this, Cx26 levels were still higher in Cx43 asODN bioactivated scaffold-treated wounds than untreated wounds at D5, and throughout all treatments Cx26 expression at the wound edge was still upregulated from distal levels.

3.6 – The effect of scaffold bioactivation on inflammation

Chronic or impaired healing is typically associated with an elevated inflammatory response (Pierce, 2001), while the application of Cx43 asODN has been found to reduce inflammation (Mori et al., 2006). As such, the effect of untreated collagen and alginate scaffolds as well as Cx43 asODN bioactivated collagens scaffolds on inflammatory cell recruitment was investigated (Figure 3. 9). At 40 X magnification, the polymorphonuclear morphology of inflammatory cells could be characterised and the number of cells quantified. H&E staining of tissue sections revealed numerous polymorphonuclear leukocytes (PMNs) surrounding all solid structures including the collagen scaffold, alginate microspheres and the alginate dressing at D1 (Figure 3. 9). The effects were reduced in alginate hydrogel treated wounds, where PMNs were typically restricted to beneath the dermis in the panniculus carnosus.

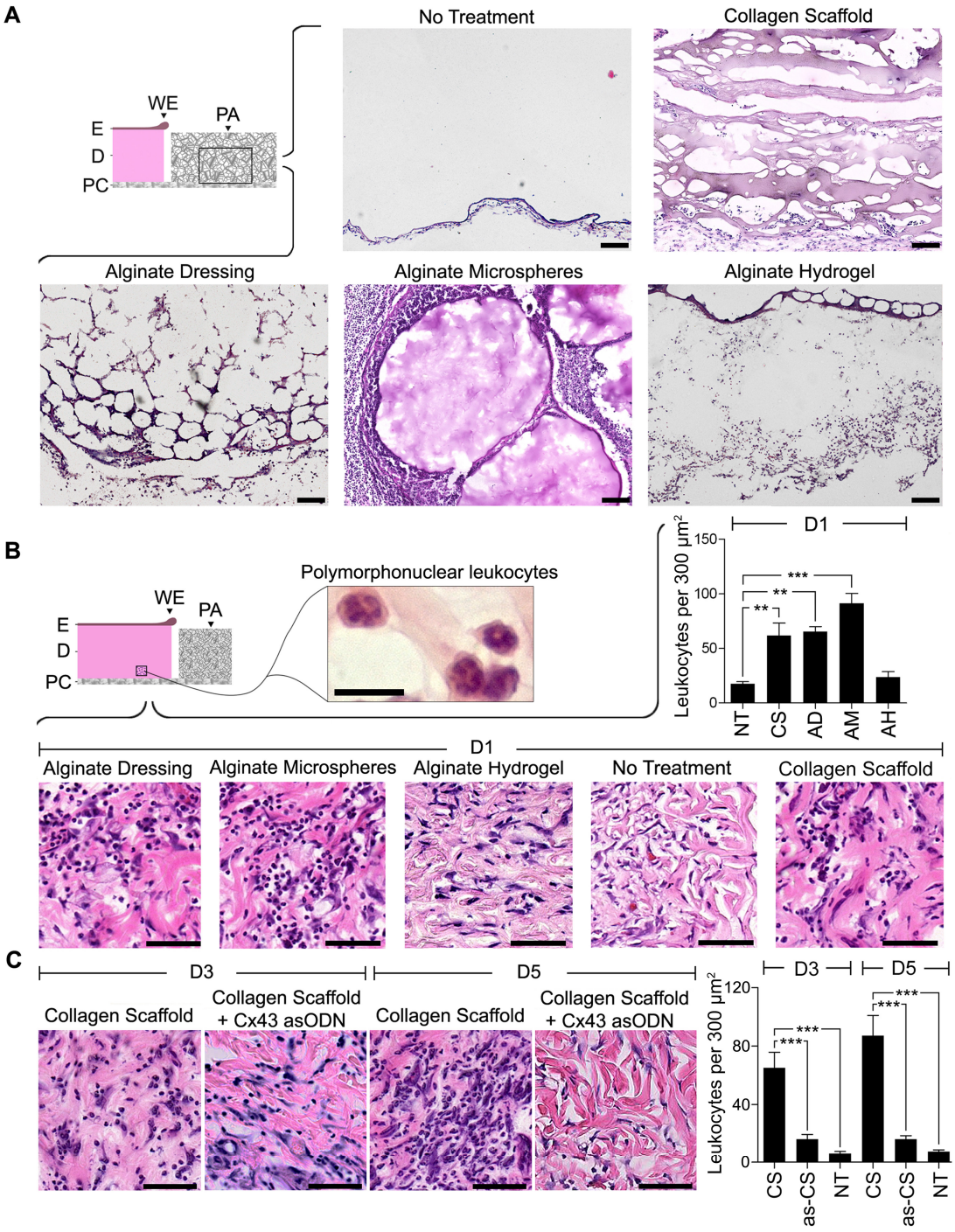

Figure 3. 9 – The effect of scaffolds on polymorphonuclear cell recruitment.
Histological assessment of cells infiltrating scaffolds and dressings. **(A)**: D1 H&E images illustrating the clustering of round cells within and surrounding polymer applications. **(B)**: High-power images focusing on a region of dermis 700 µm from the wound edge at the position indicated by the diagram at D1 following polymer application (top-left). Subsequent quantification of the number of leukocytes is also displayed (top-right). Cells were observed at high-power to identify polymorphonuclear leukocytes prior to counting

(example shown at top-left). **(C)**: High-power images of the dermis of D3 and D5 treated wounds captured identically to those in (B). Leukocyte counts at both time points were also quantified (bottom-right). (A): Scale bar = 100 μm. (B): Polymorphonuclear leukocyte image scale bar = 10 μm, all other images = 50 μm. n=5 (D1) or n=6 (D3 & D5) samples were used, data is plotted as mean + SEM. Diagram legend: E = epidermis, D = dermis, PC = panniculus carnosus, WE = wound edge, PA = polymer application. For wound treatments NT = no treatment, CS = collagen scaffold, AD = alginate dressing, AM = alginate microspheres, AH = alginate hydrogel and as-CS = Cx43 asODN treated collagen scaffold (** = $P < 0.01$, *** = $P < 0.001$).

In order to assess whether the inflammatory response induced by scaffolds extended into the tissue, the number of PMNs present in the dermis 3 fields of view from the wound edges was quantified (Figure 3. 9B). At D1 there was a significant 3.5-fold increase in numbers of invading PMNs in wounds treated with collagen scaffolds relative to untreated wounds ($P < 0.01$, Figure 3. 9B). Similarly, the alginate dressing induced a 3.8-fold increase ($P < 0.01$) and the alginate microspheres a 5.2-fold increase ($P < 0.001$) in the number of quantified PMNs. Unlike the solid structures, the number of PMNs present in this region for alginate hydrogel treated wounds was not significantly different from control wounds.

Following assessment of collagen scaffolds, untreated applications induced a 10-fold increase in dermal PMNs at D3 ($P < 0.001$) and an 11.1-fold increase at D5 ($P < 0.001$, Figure 3. 9C). Bioactivated scaffolds, however, resulted in significantly reduced numbers of dermal PMNs at D3 ($P < 0.001$) and D5 ($P < 0.001$), and were comparable to that of untreated wounds. This finding indicates that Cx43 asODN could improve the host response to implanted biomaterials *in vivo*.

3.7 – Discussion

The initial aim of the study was to determine whether scaffolds served as a temporary matrix in a full-thickness wound that had lost the dermal layer. Following fabrication and application of fibrous collagen scaffolds to full-thickness mouse wounds, healing was severely perturbed. Macroscopically, wounds did not integrate with the scaffolds and

instead appeared much larger at D3 and D5 than untreated wounds (Figure 3. 2). Wound edges in contact with scaffolds were prone to forming non-migratory, thickened bulbs of keratinocytes in which the gap junction proteins Cx43 and Cx26 were significantly upregulated (Figure 3. 3). This response was comparable to that of rats with STZ-induced diabetes, which also formed thickened bulbs of non-migratory keratinocytes at the wound edge that expressed high levels of Cx43 (Wang et al., 2007).

Cx43 is typically downregulated from moderate basal levels in wound edge keratinocytes and fibroblasts in the first 24 h of acute healing (Coutinho et al., 2003, Mendoza-Naranjo et al., 2012a, Goliger and Paul, 1995). The upregulation of Cx43 in the epidermis of scaffold-treated wounds may be the cause of the evident perturbation to healing, as Cx43 overexpression in diabetic rat wounds was found to prevent keratinocytes migration across the wound. Indeed, targeting Cx43 overexpression with Cx43 asODN restored healing to a standard rate (Wang et al., 2007, Mendoza-Naranjo et al., 2012b). It has also been shown that elevation of Cx43 expression in fibroblasts attenuates their migration by inhibiting their cytoskeletal dynamics (Mendoza-Naranjo et al., 2012a). Conversely, downregulation of Cx43 in fibroblasts reduces cell-cell adhesion and activates the small GTPases Rac1 and RhoA, enhancing cytoskeletal dynamics and promoting migration (Mendoza-Naranjo et al., 2012b). This may be in part due to the interaction of the Cx43 cytoplasmic tail with the adhesion molecules zonular occludens 1 & 2, and components of the cytoskeleton (Giepmans et al., 2001b, Laird, 2006).

While Cx43 is downregulated in wound edge keratinocytes, Cx26 is naturally upregulated and maintained at high levels during the process of cell migration (Coutinho et al., 2003). However, similar to Cx43, Cx26 expression was strongly upregulated in wound edge keratinocytes following scaffold application (Figure 3.3), to a significantly greater degree than wounds left untreated. Persistent Cx26 expression has been attributed to a hyperproliferative state in which wound healing is perturbed, and has also been strongly linked to a number of epidermal and barrier-related conditions (Djalilian et al., 2006, Labarthe et al., 1998, Lucke et al., 1999). It has also been suggested that high levels of Cx26 can result in leakage of ATP, which in turn promotes inflammation (Djalilian et al., 2006). This is in agreement with the findings in this chapter, where scaffold treated wounds that expressed high levels of Cx26 in the epidermis at the wound edge also had significantly higher levels of neutrophils infiltrating into the tissue (Figure 3.9).

Since it was not immediately apparent as to why the fabricated collagen scaffolds caused a negative reaction, a number of different scaffolds were assessed for similar outcomes. The scaffolds applied appeared somewhat thick when viewed macroscopically, and there were concerns that the crosslinker used may have left residual chemical on the scaffolds. To test whether these properties were responsible for the observed negative reaction, thinner scaffolds were fabricated and using a 100-fold reduced concentration of the cross-linker (Figure 3.4). However, none of the different scaffold thickness or crosslinker permutations resulted in a visible improvement in healing; all scaffolds resulted in a similar thickening of the wound edge and upregulation of Cx43 at D1. Next, a number of different non-collagen based applications were assessed *in vivo* to determine whether a different material or form factor may result in a more biocompatible scaffold. This led to the selection of the naturally derived alginate, which is commercially available as a fibrous wound dressing or hydrogel, and can also be electrosprayed to form microspheres (Figure 3.5). Following application to full-thickness wounds, both the solid alginate dressing and microspheres induced a negative reaction, causing a significant elevation of inflammatory cell infiltration as well as wound edge epidermal thickening and Cx43 upregulation (Figure 3.5, Figure 3.9). However, this was not the case for the alginate hydrogel, which did not induce these effects.

It appeared that the negative response observed in the presence of scaffolds might therefore be attributed to the presence of a foreign body in the wound bed rather than a specific substance inducing a reaction. Indeed, physical structures were surrounded by polymorphonuclear cells characteristic of leukocytes (Figure 3.9), typical of the early stages of a foreign body reaction (Anderson et al., 2008). Scaffolds appeared to degrade in the wound rapidly and inflammation spread beyond the wound bed into the surrounding dermis, where there is potential for PMNs to cause damage to uninjured tissue (Martin and Leibovich, 2005). Despite considerable degradation of scaffolds by D5 there were a significantly increased number of PMNs infiltrating the dermis, and continued repression of keratinocyte migration and overexpression of Cx43 and Cx26 within the thickened epidermal bulbs. The prolonged elevation of connexin expression has separately been linked to inflammation (Qiu et al., 2003). As a device to support the healing of full-thickness wounds such as chronic ulcers, association of scaffolds with inflammation could be potentially harmful. Chronic ulcers typically contain high numbers of inflammatory cells prior to treatment, so it may be questioned whether placement of scaffolds that can promote further PMN invasion is most beneficial to healing (Pierce, 2001).

Since scaffolds are intended to function as a substitute dermal layer it would be reasonable to expect scaffolds to serve as a structure for cells to migrate into and over. However, macroscopically there appeared to be minimal integration of collagen scaffolds with the surrounding tissues at D3, with little improvement at D5 (Figure 3.2). Occasionally, re-epithelialisation could be observed macroscopically in untreated wounds, yet this feature was absent in scaffold-treated wounds. Regardless of the effect of scaffolds on PMN infiltration, no fibroblast-like cells could be seen to associate with solid collagen or alginate scaffolds in this study, a finding that challenges the purported role of scaffolds as a supportive matrix for fibroblast attachment and proliferation (Zhong et al., 2010).

The targeted downregulation of Cx43 protein expression *in vivo* has been shown on multiple occasions to accelerate wound healing whilst reducing the inflammatory response (Wang et al., 2007, Mori et al., 2006, Mendoza-Naranjo et al., 2012b, Qiu et al., 2003, Mendoza-Naranjo et al., 2012a). In the case of scaffolds, which appeared to be inducing features of chronic wound healing such as upregulation of Cx43, it was questioned whether simultaneous downregulation of Cx43 using asODN specific to Cx43 mRNA could optimise them in an *in vivo* setting. Following application of Cx43 asODN bioactivated collagen scaffolds to wounds, macroscopically there appeared to be a greater degree of scaffold integration with the wound edge relative to control scaffolds at both D3 and D5 (Figure 3.6). Microscopic evaluation of H&E stained wounds revealed bioactivated scaffold-treated wounds induced fewer numbers of infiltrating polymorphonuclear cells in the dermis at both D3 and D5, which is consistent with the anti-inflammatory effects of Cx43 asODN on acute wound healing (Mori et al., 2006). Due to the observed reduction in inflammatory cell infiltration, the bioactivation of materials could be useful in both chronic ulcer and burn situations, where often dressing materials must be placed in contact with the wound as part of standard wound care procedures (Lyder, 2003).

Bioactivation with asODN appeared to reduce the negative effects associated with scaffold application. At D3, Cx43 expression was significantly reduced in wound edge keratinocytes treated with bioactivated scaffolds compared to control scaffolds (Figure 3.7). Interestingly, Cx26 levels were also reduced by 69.6% following bioactivated scaffold application relative to control scaffolds at D3. This reduction is unlikely to be due to a direct effect of the antisense sequence, however, which was designed specifically to target the Cx43 mRNA. As an unmodified single stranded DNA sequence, it is also unlikely that there would be

asODN remaining after 24 h, as unmodified DNA is rapidly degraded within minutes in the presence of sera (Agrawal, 1996). Indeed, Cx43 expression in the wound edge was not significantly lower in bioactive scaffold-treated wounds than control scaffolds at D5, suggesting that the effect of the asODN had diminished. When Cx43 and Cx26 expression was reduced in the presence of asODN, however, it occurred in conjunction with a reduction in inflammatory cell infiltration. This correlation is supported in the literature, where conditions involving upregulation of these connexins often occur in conjunction with a heightened inflammatory response (Cronin et al., 2008, Djalilian et al., 2006, Labarthe et al., 1998).

The bioactivation of scaffolds did not render them functional as a cell supportive matrix, however. By D5, bioactivated scaffold-treated wounds remained open, possibly due to the additional distance required for re-epithelialisation around scaffolds (Figure 3.6). While epithelial thickening and connexin downregulation was reduced at D5, where re-epithelialisation could be observed it occurred underneath the scaffold similar to the situation of a scab (Figure 3.7). This suggested that even though bioactivation of scaffolds with Cx43 asODN could reduce epithelial thickening and connexin overexpression, scaffolds were still perceived as a foreign body and not a matrix to grow over and into. These findings challenge the role that scaffolds are typically thought to adopt.

Conclusions

Scaffolds are intended to promote healing of full-thickness wounds, yet in this chapter it was found that the application of multiple solid scaffolds retarded healing by inducing a severe thickening of the wound edge epidermis combined with connexin overexpression. In these acute wounds, the bioactivation of scaffolds using Cx43 asODN prevented many of these occurrences; yet healing was still disadvantaged through application of the devices. In a chronic wound setting, however, wounds typically do not heal efficiently to begin with, such that scaffolds may still be rendered suitable for application. In particular, the most promising outcome of these experiments was the efficacy of Cx43 asODN in reducing symptoms of a chronic-like wound. The role of scaffolds could therefore be altered from one of function to one of drug delivery, such that scaffolds could be bioactivated to deliver asODN over a longer period of time. In this chapter, infusion of scaffolds was performed

using Pluronic gel, a hydrogel that is degraded rapidly within the wound. Investigation into vascular stents highlighted the possibility of developing a coating application capable of eluting an incorporated drug over a specified period of time. This could be particularly useful in the bioactivation of biomaterials such as dressings, which must be placed in contact with wounds as part of standard full-thickness ulcer and burn treatment. With this in mind, focus was placed on developing a coated scaffold that could elute Cx43 asODN over a longer period of time, to determine whether this would have a beneficial effect on wound healing.

CHAPTER 4

Development of a Cx43 asODN sustained release scaffold

4.1 – Introduction

In the previous chapter, following the fabrication of collagen scaffolds and subsequent *in vivo* application it became clear that scaffolds were in fact impairing acute full-thickness wound healing. The submersion of scaffolds into a Pluronic gel containing Cx43 asODN resulted in a transient bioactivation that alleviated some of the biocompatibility problems, but it still did not encourage non-inflammatory cells to associate with the scaffold matrix. This finding caused a change in direction to my research – while it may not be possible to make scaffolds function as a substitute dermal matrix, the ability of scaffolds to act as a reservoir for Cx43 asODN release appeared promising, particularly if they could be applied in a chronic or diabetic wound setting where Cx43 levels are typically highly over-expressed (Mendoza-Naranjo et al., 2012a, Mendoza-Naranjo et al., 2012b, Wang et al., 2007). This required investigation into a method to deliver asODN to the wound in a sustained manner over the time course of wound healing, since the asODN sequences used were unmodified and prone to degradation within minutes (Agrawal, 1996). While phosphorothioate modification can improve the half-life of asODN it comes at the cost of a decreased hybridisation with mRNA, as well as an increase in cell cytotoxicity and other non-specific effects (Stein, 1996).

A number of vascular stents been developed to incorporate therapeutic drugs that elute from the devices over a pre-determined period of time (Krucoff et al., 2008, Mehilli et al., 2006, Windecker et al., 2008). The first successful drug-eluting stents were developed to release the drug sirolimus to prevent restenosis. Following a clinical trial in 2002 they were approved for use in Europe, and soon after gained FDA approval for use in the US. Stents that eluted paclitaxel, another drug developed to treat restenosis, were approved soon after for clinical use in 2004. Drug-eluting stents typically comprise a polymer coating containing the drug that surrounds a traditional metal stent frame, which together provides both structural support to the blood vessel as well as a bioactive component. Many drug-eluting stents have been found to decrease the chance of restenosis occurring relative to traditional bare-metal stents (De Luca et al., 2012, Di Lorenzo et al., 2009). Since drug-eluting stents appear to be effective in the sustained and local delivery of drugs, it was hypothesised that a coating technique incorporating Cx43 asODN developed to deliver asODN to the wound may be beneficial to healing. In this way, asODN could be released over a longer period of time at the wound through diffusion as well as hydrolysis of the coating and

scaffold thus supplying the wound with asODN over the time course of healing. In the case of acute wound healing, this duration would need to be at least 5-7 days to cover the time course of re-epithelialisation (Coutinho et al., 2003).

Designing a scaffold coating required investigation into the various properties of different polymers. The choice of polymer used to generate stent coatings varies, and is selected based on biocompatibility as well as the rate at which drugs elute from them. PLGA is a copolymer of poly lactic acid (PLA) and poly glycolic acid (PGA), and is one of the most commonly used synthetic coating polymers in the field of biomaterials. One of the main reasons for its popularity is its reported level of biocompatibility, illustrated by its FDA approval status (Makadia and Siegel, 2011). The approval status of PLGA is due to the breakdown of the polymer into lactic and glycolic acid, both of which are naturally metabolised to carbon dioxide and water through the Krebs cycle. As an additional advantage, the lactide to glycolide ratio of PLGA can also be adjusted to influence the rate of drug elution (Shive and Anderson, 1997). A ratio of 50:50 lactide to glycolide will elute incorporated drugs at a higher rate than when using a 75:25 ratio, for instance. It is also important to note that the use of over 75:25 lactide to glycolide ratios have been previously shown to prevent adequate drug release over several months, demonstrating the need to carefully select the polymer used to coat devices (Khan et al., 2004). The use of PCL in drug coatings is also well documented (Acharya et al., 2012, Drachman et al., 2000), and is reported to elute incorporated drugs at a slower rate than PLGA. The choice of molecular weight of the polymer is also important, as lower molecular weight polymers release incorporated drugs faster but are linked to heightened inflammatory responses (Billinger et al., 2006).

While vascular stent coatings have been designed to release large drug molecules such as paclitaxel, the release of asODN from coatings is less common as a method to target restenosis, owing to the more common use of existing drugs used to treat patients. However, stent coatings have previously been developed to elute asODN targeting the DNA binding protein c-myb, platelet derived growth factor, and nonmuscle myosin heavy chain, and have led to positive results both *in vitro* and *in vivo* (Kipshidze et al., 2005). Results from other studies indicate that asODN may elute faster than traditional anti-restenosis drugs, yet 32-mer sequences were found to elute at a slower rate from polymer microsphere preparations than smaller 7-mer or 15-mer sequences (Khan et al., 2004).

Since the Cx43 asODN sequence is a 30-mer, this finding suggested that the selected coating polymer must not have too slow a release profile. In order to measure the rate of asODN release from scaffolds, UV spectrophotometry can be employed, which is a popular method used to determine single stranded DNA concentration. Using this technique asODN elution can be quantified at specified time points over a specified period of time (Zhang et al., 2006b).

Following a literature search into scaffold coating polymers, PLGA appeared to be a suitable choice (Makadia and Siegel, 2011). A PLGA formulation manufactured with a high molecular weight of 40,000-75,000 and a low to medium glycolide to lactide ratio (65:35) was sourced from Sigma Aldrich, UK (P2066). After focusing on the choice of polymers, a method to coat scaffolds with using the polymer as well as asODN was required. This required investigation into previously used methods employed to produce drug-eluting coatings. Complex methods specific to commercial stents have been developed to coat scaffolds such as a cobalt chromimum stent with laser-etched reservoirs that are filled using PLGA (Serruys et al., 2005). In terms of a less complex coating that could be translated to coat scaffolds, a study performed by (Kim et al., 2005) illustrated that a simple technique could also be successful. The team successfully prepared a simple polymer coating solution, and used it cover porous hydroxyapatite scaffolds. In this method, they dissolved the coating polymer in an organic solvent along with the antibiotic vancomycin then dipped the scaffolds into the crude solution. Scaffolds were then vacuum dried. However, unlike the vancomycin used in that study, asODN sequences that have been dissolved in water are not miscible with organic solvents. While this technique demonstrated the validity of a simplified coating method, a different method of preparation would be required to incorporate asODN. One technique commonly practiced in the case of immiscible liquids is to prepare an emulsion. In this approach, a water-oil emulsion is prepared whereby asODN that has been dissolved in water can be dispersed as droplets throughout the solvent. The emulsion is generated through homogenisation of the two immiscible layers and the droplets typically range in size from 10 nm - 100 μm. (Tamilvanan, 2004). With this in mind, an emulsion technique was selected for use in coating scaffolds.

Aims

After developing a protocol to coat scaffolds with PLGA and Cx43 asODN, the initial aims of this chapter were as follows:

1. To produce a polymer coating that results in asODN elution for at least the 5-7 days; the time required for re-epithelialisation to complete.

2. To establish whether the polymer coating method employed altered the incorporated asODN or the wound nuclease activity.

3. To apply coated scaffolds *in vivo* to validate the function of the devices, and to determine what effects coated scaffolds had on wound healing.

4.2 – Materials and Methods

See Chapter 2 for a detailed description of the individual methods, reagents and equipment employed. A condensed explanation of the methods used in this chapter is listed below.

4.21 – Scaffold fabrication

Collagen scaffolds were fabricated through use of the same electrospinning technique and reagents as described and used in chapter 3.

4.22 – Application of polymer coatings containing Cx43 asODN to scaffolds

Unlike the Pluronic gel infusion method used in the previous chapter, the same Cx43 asODN sequence was incorporated into polymer coatings using an emulsion technique. The rat Cx43 asODN sequence used had the sequence 5'-GTA ATT GCG GCA GGA GGA ATT GTT TCT GTC-3'. A non-functional sense (sODN) sequence to this Cx43 asODN was also incorporated to create one of the control scaffold treatments, and had the sequence: 5'- GAC AGA AAC AAT TCC TCC TGC CGC AAT TAC-3'. A modified version of this Cx43 asODN sequence was also separately obtained that had the fluorophores Cy3 and Cy5 conjugated at the 5' and 3' ends, respectively.

Either PCL or Poly(D, L-lactice-co-glycolide) (PLGA) was dissolved in the solvent dimethyl carbonate at 10% wt./v. using gentle rocking. The asODN sequences were dissolved in water and mixed with the polymer solutions to either a 100 μM or 300 μM final DNA concentration. The two immiscible layers were processed for 10 seconds using a handheld homogenizer on a medium setting at room temperature to produce an emulsion. After preparing the coating mixture, individual 6 mm collagen scaffolds were dipped for 1 second in the desired polymer-asODN solutions and immediately placed in a tube of liquid nitrogen and lyophilised overnight to remove the solvent from the scaffolds in order to maintain the structure of the scaffold. In the later scaffold experiments, this coating process, from dipping to freeze drying, was repeated 3 times to produce 4 layers of polymer + asODN, or 7 times in the case of 8-layered 'double coated' scaffolds, which in total received 4 coating layers of PCL + asODN followed by 4 layers of PLGA + asODN.

4.23 – Surgery

Six week old Sprague Dawley rats were anaesthetised using 4% isoflurane, 20% oxygen and 10% nitrous oxide, and maintained using 1.5% isoflurane by nose cone. Animals were injected subcutaneously with 0.03 mg/ml buprenorphine (Vetergesic) before operation. Rat backs were shaved and covered in a thin layer of Nair® hair removal cream, after which both the cream and hair was removed using a warm moistened gauze pad. Animals were placed on heated mats for the operation. Four full-thickness excisional biopsy punch wounds were made using a 6 mm medical biopsy punch to rodent backs, two on each side of the dorsal midline. Scaffold treatments were applied directly to wounds, after which the back was covered with a sheet of Tegaderm™ film. Post-procedure, animals were kept in a heated chamber and monitored for recovery. Once recovered, animals were re-housed in individual cages.

4.24 – Processing and histology

Harvesting wounds

Animals were culled by cervical dislocation at 1, 3, or 5 days post wounding. Wounds were macroscopically imaged as outlined in Chapter 2. Wounds were then excised and fixed in 4% paraformaldehyde (PFA)-PBS solution for 24 h at 4°C. Tissue was immersed in 20% sucrose overnight then washed in PBS, after which wounds were bisected. Half of each

wound was snap frozen in OCT medium, then sectioned using a cryostat at a thickness of either 5 μm (for H&E staining) or 10 μm (for immunofluorescence staining).

Haematoxylin and eosin staining

Frozen tissue sections were thawed for 5 min then covered completely in tap water for 5 min at room temperature. Slides were submerged in Harris' haematoxylin solution for 30 seconds followed by immersion in a container full of running tap water for 5 min. Background staining was reduced by dipping the slides in a container full of 1% acid alcohol (1% glacial hydrochloric acid, 70% ethanol, 29% distilled water) for 3 seconds, after which slides were immersed in a container of running tap water for a further 5 min. Samples were then submerged for 15 seconds in a container full of eosin B solution, followed by immersion for 5 seconds in a container full of tap water to rinse away excess stain. Slides were then immersed in 70% ethanol for 2 min, 100% ethanol for 2 min and a second container of 100% ethanol for a further 2 min, to dehydrate the sections. Slides were then submerged in a container full of xylene for 5 min, then a second container of xylene for an additional 5 min. Slides were then individually removed and covered with xylene-based DPX mountant solution, then sealed using a coverslip.

Immunofluorescence staining

Tissue sections were permeabilised in cold acetone for 5 min and then using a 0.1 M L-lysine PBS solution containing 0.1% Triton-X-100. Sections were stained for 1 h using a rabbit polyclonal antibody to Cx43 (1:2000 dilution, C6219, Sigma Aldrich UK) or Cx26 (1:200 dilution, (Diez et al., 1999). Sections were then stained using a goat anti-rabbit Alexa 488 secondary antibody (A11008, Invitrogen UK) at a 1:400 dilution for 1 h. Tissue was counterstained using Hoechst solution (both Hoechst 33528 and Hoechst 33342 dyes at 1:50,000 dilution, Sigma Aldrich UK).

4.25 – *In vitro* assays

Quantification of asODN elution

Scaffolds coated in asODN using the emulsion method were assayed for asODN release rate *in vitro*. Three coated scaffolds were immersed in 40 μl of nuclease free water at 37°C. At daily intervals, 1.5 μl of liquid was removed and assayed using a NanoDrop 2000 UV

spectrophotometer under the 'ssDNA' setting to determine DNA concentration. Scaffolds were placed in a fresh 40 µl of water to compensate for the reduction in volume following water removal for assays. Individual time point elution data was collected to produce both cumulative and daily asODN elution graphs.

Förster Resonance Energy Transfer analysis

A more detailed explanation of the Förster Resonance Energy Transfer (FRET) acceptor photobleaching technique is provided in the materials and methods chapter. Scaffolds coated with Cx43 asODN conjugated at either end to fluorophores Cy3 and Cy5 using the previously detailed emulsion method was used in this technique. Scaffolds were either left untreated or submerged in 37°C sterile foetal bovine serum (FBS) for up to 7 days. Samples were removed every 24 h then snap frozen in OCT medium, and sectioned to a thickness of 10 µm using a Leica cryostat. Samples were imaged using a confocal microscope and analysed using the incorporated Leica LAS AF software FRET wizard. Scaffolds were assessed using a FRET acceptor bleaching technique. Six randomly selected areas for each scaffold were bleached for the Cy5 acceptor fluorophore using a 633 nm laser. Using this method, Cy3 emission intensity at 570 nm is expected to increase, since energy transfer to the acceptor fluorophore was no longer occurring. The detected change in donor emission intensity was acquired and interpreted by the software package to calculate a FRET efficiency percentage ($FRET_{eff}$). The formula to calculate the $FRET_{eff}$ is stated in the software package and is as follows:

$$FRET_{eff} = (D_{post} - D_{pre}) / D_{post}$$

In this formula, D_{post} is the fluorescence intensity of the donor after photobleaching and D_{pre} is the donor fluorescence intensity prior to photobleaching. A minimum percentage of 15-20% has been considered indicative of genuine FRET occurring in other studies (Lai et al., 2014)., and the average percentage obtained in this study was around 25%. Images captured were 8-bit single optical sections with a resolution of 1024 by 1024 pixels. To determine the potency of serum in degrading asODN the wavelength emission spectra of 6 asODN regions per time point were generated by performing xyλ-mode scans on FRET labelled asODN that had been incubated in FBS at 37°C. Individual λ-scans were performed using a 543 nm laser excitation, with 19 equally sized detection steps occurring

between the wavelengths of 550 nm to 730 nm. Emission intensity values were output using the LAS AF software.

4.26 – Analysis

Imaging

Wounds were macroscopically and microscopically imaged as outlined in Chapter 2. Tissue sections immunostained for Cx26/43 and Hoechst were imaged using confocal microscopy. Single optical section 8-bit images were acquired at the wound edge and at a distal region of skin at 1024 by 1024 pixels. Image settings were consistent between treatments.

Epidermal thickening measurements

Epidermal thickness was measured on H&E stained tissue and determined by measuring the thickest point along the basal to spinous layer axis within the end 150 μm of nascent epidermis using ImageJ. The length of nascent epidermis outgrowing from the wound margin was measured at either side of the wound using ImageJ and averaged to return a re-epithelialisation distance measurement for each sample.

Connexin 26 and 43 protein quantification

Cx43 and Cx26 protein expression was quantified by counting positive pixels on binary images of wound edges using ImageJ software using the method outlined in a study by (Wang et al., 2007). Images from each experiment were identically thresholded and the number of connexin positive pixels within the end 100 μm quantified. Connexin levels were expressed per square micron of epidermis and normalised to distal levels to reduce sample variation. In the case of Cx26, distal levels were extremely low, to the extent that small fluctuations between samples could result in large differences between values. For this reason, Cx26 distal levels were averaged and these values were used to calculate the change in wound edge Cx26 expression.

Polymorphonuclear cell quantification

H&E stained D1, D3 and D5 rat full-thickness wounds were identified microscopically using a 63 X objective. At 700 μm from the wound edge in the lower dermis, rounded cells with a polymorphonuclear morphology (PMNs) were identified and counted in a single field of view using a 40 X objective were counted, a method to quantify probable inflammatory leukocytes infiltrating the uninjured tissue. Images used in figures were captured using a Zeiss Axio Scan.Z1 automated slide scanner using a 20 X objective and the brightfield image acquisition wizard settings. Images were automatically stitched together to form a montage (see chapter 2 for full details). A total of n=5 wounds were assessed per time point and treatment and values were averaged.

Measurement of granulation tissue area

Rat wounds harvested at D10 and D15 were H&E stained and loaded into an automated Zeiss Axio Scan.Z1 slide scanner. Brightfield images were captured using a 20 X objective, then automatically stitched together to form a montage. Montages were then imported into ImageJ. The granulation tissue (or wound region) was defined as the new area of tissue within the wound margins yet above the muscle and panniculus carnosus layers, and was measured using the freehand line tool within the program.

Assessment of smooth muscle actin area

Rat wounds harvested at D10 were loaded into the same Zeiss slide scanner and imaged using a 20 X objective using the built in image acquisition wizard. Hoechst and Alexa 488 fluorophores were excited to produce a montage image of the tissue. α-SMA staining in the green channel was thresholded in the software to a level that allowed visualisation of both α-SMA positive blood vessels as well as a positive staining region in the wound gap, above the panniculus carnosus. This area was drawn around using a marker tool within the proprietary ZEN 2012 software and an area in square microns was displayed. This approach was applied in the same manner to each of the 8 samples in each treatment group.

Statistical analyses

Sample size was determined using power analysis software G*Power as described in Chapter 2. Data was subjected to Kolmogorov-Smirnov tests using GraphPad Prism 5.0

software to ascertain normality, then to one-way ANOVA tests followed by Tukey's post-hoc tests to determine statistical significance.

4.3 – Design of a drug eluting polymer coating

4.31 – Investigation into coating properties

In order to design a scaffold coating to elute asODN, the literature was first assessed. It was not immediately clear what the rate of elution of Cx43 asODN would be, nor whether it would be preferable to use a higher or lower percentage of PLGA in a coating. For these reasons, scaffolds were coated using either a 10% or 15% (wt./v.) solution of PLGA (wt./v.) and Cx43 asODN dissolved in water to a final volume concentration of 100 µm (Figure 4. 1A). UV spectrophotometry revealed that over 95% of DNA had eluted by the D2 time point for both 10% and 15% PLGA coated scaffolds. Approximately 10 µg of DNA eluted over the time course studied. Both the low quantity and short duration of asODN elution using single PLGA coatings led to the requirement for an improved coating technique.

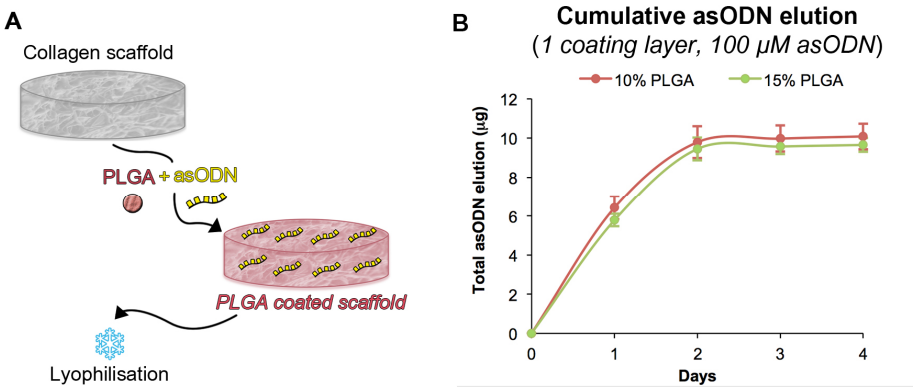

Figure 4. 1 – Coating of collagen scaffolds with a Cx43 asODN and PLGA emulsion.

(A): Collagen scaffolds were coated in an emulsion of 100 µM Cx43 asODN and either 10% or 15% PLGA and subsequently lyophilised.

(B): Cumulative Cx43 asODN elution from scaffolds was quantified in water at 37 degrees over 4 days. The average of 3 samples was recorded for all elution measurements and error bars represent SEM.

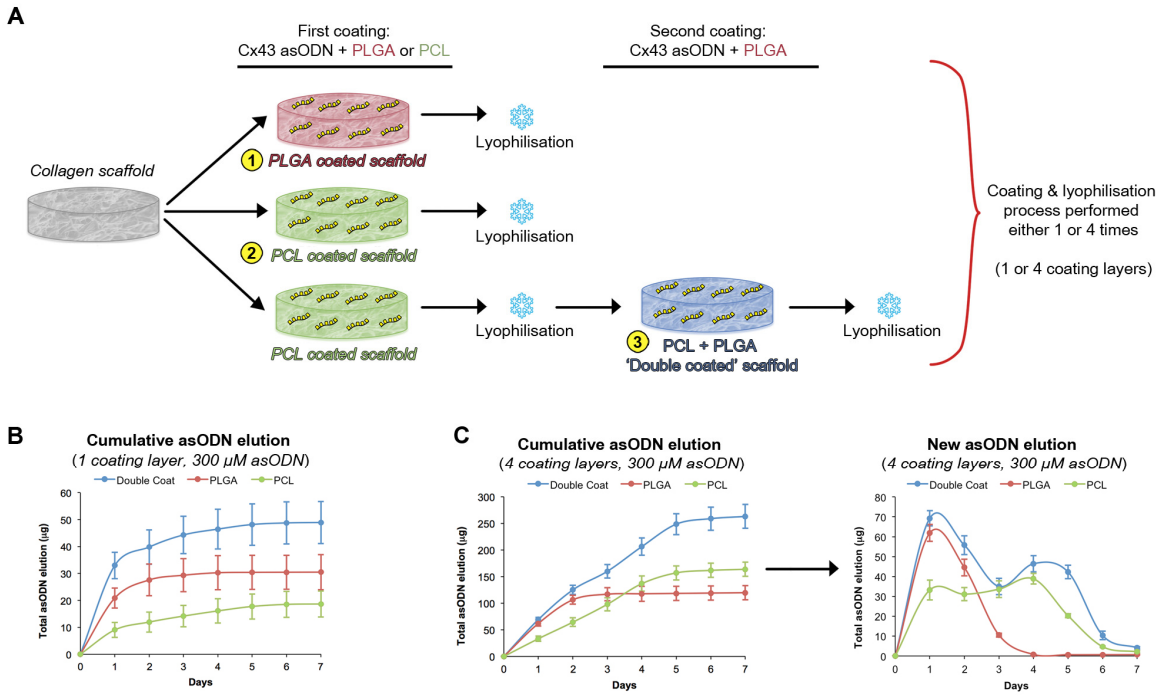

Figure 4. 2. – Cx43 asODN elution from differing combinations of scaffold coatings.

(A): Scaffolds were coated to three different specifications (labelled 1-3). Scaffolds were either coated in a single layer of PLGA mixed with 300 µM Cx43 asODN (1), a single layer of PCL mixed with 300 µM Cx43 asODN (2) or a single layer of PLGA mixed with 300 µM Cx43 asODN followed by a single layer of PCL mixed with 300 µM ('Double Coating'; 3). The coating process was performed once: '1 coating layer' (as in B) or repeated a further three times: '4 coating layers' (as in C). **(B)**: Single layer scaffolds were quantified for asODN elution for 7 days. Data is plotted as a cumulative elution. **(C)**: 4-layer scaffolds were quantified for asODN elution in water for 7 days. In the case of 'double coated' scaffolds, scaffolds received 4 coatings of each polymer (8 layers total). Data is plotted as cumulative elution (bottom left and centre) or new asODN eluted at each time point (bottom right). The average of 3 samples was recorded for all elution measurements and error bars represent SEM.

In an effort to prolong the duration and quantity of asODN release, the concentration of asODN in the coating solution used to immerse scaffolds into was increased from 100 μM to 300 μM. The literature also highlighted PCL as a polymer with a slower release profile than PLGA when used in coating (Acharya et al., 2012). Scaffolds were therefore coated in one of three ways: 1 - with 15% PLGA and Cx43 asODN, as before, 2 - with just 10% PCL and Cx43 asODN, or 3 - with both layers (PCL + asODN followed by PLGA + asODN) (Figure 4. 2A). Elution recordings ceased at D7 when new asODN release had mostly ceased.

Only 19 μg of DNA eluted from the PCL only coating within 7 days, but the release profile was more gradual than from the PLGA only coating (Figure 4. 2B). The halfway point of total release was approximately 1 day for the PCL coating, relative to nearly 15 h for the PLGA coating. Scaffolds receiving both coatings eluted approximately 48 μg in total, of which half eluted within 15 h. While the use of two coatings increased the total amount of asODN eluted, the majority still eluted within the first 24 h. It was therefore proposed that further increasing the number of coating layers may improve on the duration of release.

In order to improve the elution duration the number of individual coatings was increased from 1 to 4 (or in the case of the combined PCL and PLGA scaffold, from 2 layers to 8) (Figure 4. 2A). Further layer additions made the scaffolds too brittle and hard, which was infeasible for *in vivo* use. Individual scaffolds were then subjected to *in vitro* assays (Figure 4. 2C, left). The halfway point of release for PCL only coatings was 2.5 days, relative to just 1 day for the PLGA only coating. This represents an improvement of approximately 1.5 days for the 4-layered PCL coating relative to the single layer (Figure 4. 1). The greatest improvement was found using the PCL and PLGA double-coated scaffolds. Double coated scaffolds resulted in a total release of 265 μg, which was considerably greater than the individual PCL or PLGA coatings. Furthermore, when asODN elution from double-coated scaffolds was assessed on a day-by-day basis as opposed to cumulative release, there were two clear peaks of asODN elution - a burst release between 0 h and D1 and a later peak between D3 and D4 (Figure 4. 2C, right).

4.32 – Analysis of asODN degradation in scaffold coatings

While elution assays identified the 8-layered PCL + PLGA coating as the most suitable for *in vivo* use, it was not clear if the coating method damaged the incorporated asODN. In

order to evaluate the coating asODN integrity a series of fluorescence resonance energy transfer (FRET) experiments were carried out on sections of coated scaffolds containing Cx43 asODN labelled with Cy3 and Cy5 dyes. Using confocal microscopy, the FRET efficiency calculated by the Leica software was 25% for the coated scaffold (Figure 4. 3B, 'Day 0'). This was above the 15-20% often considered to be indicative of genuine FRET occurring (Lai et al., 2014).

Although FRET analysis of coated asODN scaffolds indicated that that the coating process did not damage the integrity of the asODN, it was unclear if the coating could also confer a level of nuclease protection to asODN within the wound. This would be necessary to ensure asODN remained intact and functional throughout the duration of wound healing. The same Cy3-Cy5 Cx43 asODN coated scaffolds were therefore submerged in foetal bovine serum (FBS) for up to 7 days and FRET efficiencies were recorded every 24 h (Figure 4. 3B). The average FRET efficiencies calculated between D1 and D7 ranged from 17.5 - 26.7%, in each case remaining above 15%, indicating the presence of intact asODN. In order to confirm the nuclease activity of the FBS used, Cy3-Cy5 labelled Cx43 asODN was dissolved in water and mixed with FBS for 6 h. A lambda scan was then performed on the solution using a 533 nm wavelength laser as well as on a control solution containing nuclease-free water in place of FBS. The lambda scans showed a second peak of emission between 650-680 nm in the control asODN solution, yet this peak was absent in the solution treated with FBS (Figure 4. 3C). The second peak of correlated with the emission range of Cy5, which indicated that FRET was occurring due to resonance.

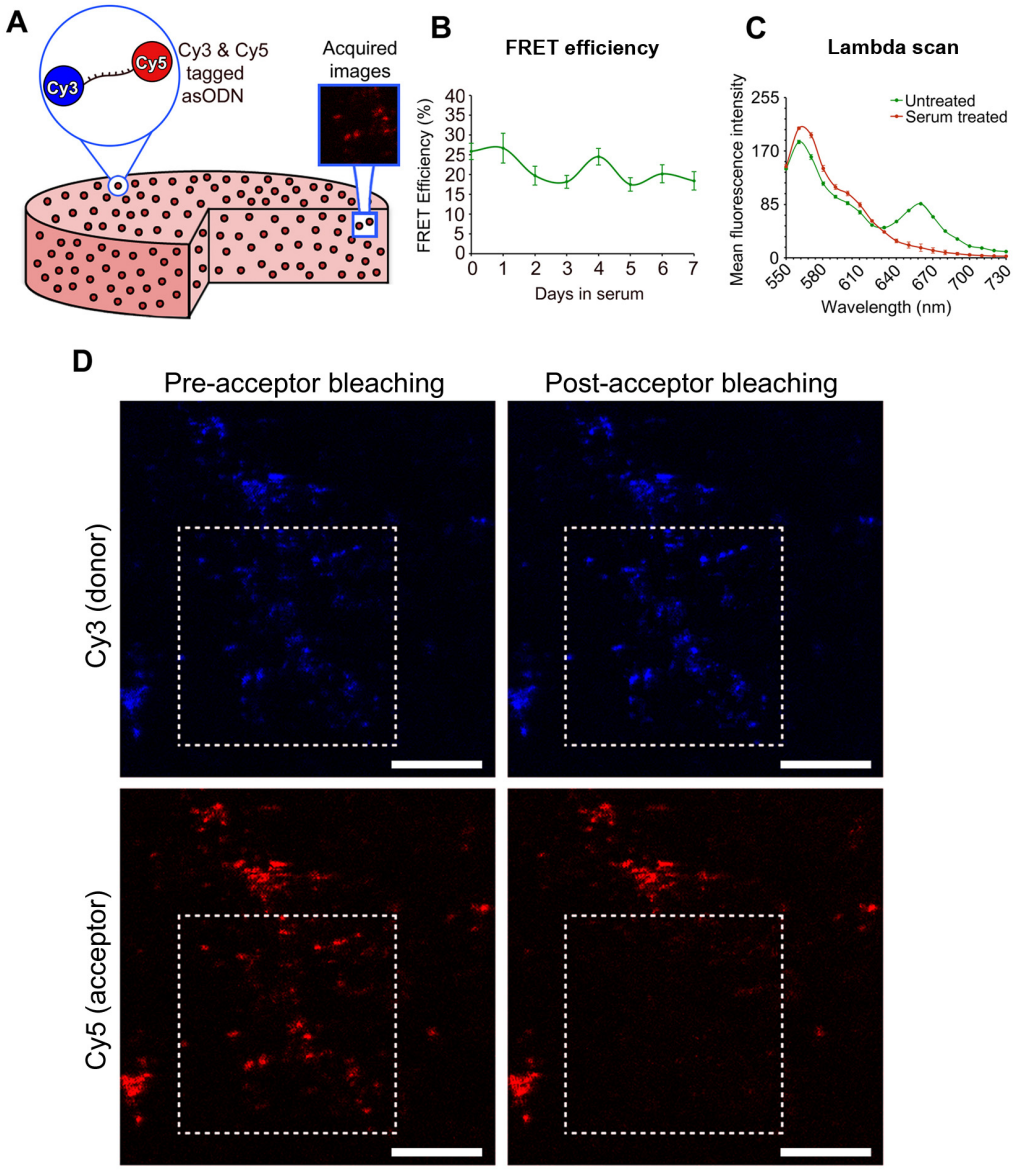

Figure 4. 3 – Cx43 asODN elution from differing combinations of scaffold coatings. PCL & PLGA double coated scaffolds containing [Cy3] [Cy5] tagged Cx43 asODN were submerged in FBS for up to 7 days. Scaffolds were then cryosectioned and subjected to FRET confocal analysis. **(A)**: A simplified diagram of a FRET-asODN coated scaffold to illustrate the stochastic dispersion of asODN clusters across the scaffold as well as the site at which images were captured in (D). **(B)**: Scaffolds were submerged in FBS for up to 7 days, after which they were sectioned and acceptor (Cy5) bleached using a confocal 633 nm wavelength laser. FRET efficiency was calculated as a percentage increase in donor fluorescence intensity after acceptor bleaching relative to before acceptor bleaching. A total of 6 regions were quantified per time point, graph data = means + SEM error bars.

(C): xyλ scans were performed on a 300 μM asODN solution either treated or untreated with FBS for 8 h to test the potency of the FBS as a nuclease effective against asODN. The mean fluorescence intensity values detected at 19 steps between 550 nm and 730 nm following excitation with a 533 nm laser were plotted. Six regions were assessed to generate averages. **(D)**: A typical confocal image of a scaffold section following immersion in FBS used to generate the FRET efficiencies plotted in (B). Images show labelled asODN clusters both before and after Cy5 bleaching. Scale bar = 20 μm.

4.4 – Using coated scaffolds to deliver Cx43 asODN to wounds

Elution and FRET assays indicated that the PCL and PLGA coated scaffolds eluted Cx43 asODN over 7 days, and that the coating protected asODN against nuclease damage. In order to test whether the scaffolds had an effect on wound healing, coated scaffolds were applied to wounds *in vivo*. Unlike the previous uncoated scaffold experiments in mice, Sprague Dawley rats were instead chosen for scaffold application. This was due to previous issues regarding epidermal fragility following Tegaderm removal from mice, owing to limited D1 data, as well as the benefits of validating scaffold findings in a second species.

4.41 – Macroscopic analysis of wounds

In order to ensure the *in vivo* effects of incorporated asODN in the polymer coated scaffolds were assessed accurately, a series of control scaffolds were devised to allow comparisons (Figure 4. 4A). These consisted of an uncoated scaffold, as used in the previous chapter, as well as two additional polymer coated scaffolds, in which one lacked any asODN ('coated scaffold') and the other contained the complementary 'sense' version of the sequence to Cx43 asODN ('coated scaffold & Cx43 sODN'). Full-thickness 6 mm wounds were made to the backs of rats and approximately 0.8 mm thick, same size individual scaffolds were applied (n=8 per treatment).

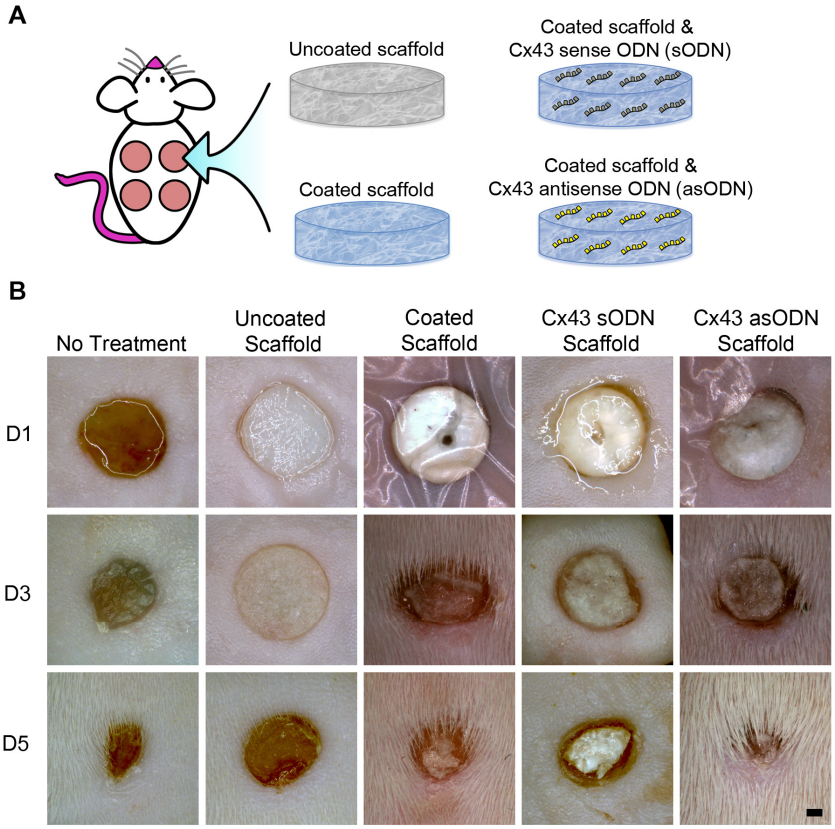

Figure 4. 4 – Macroscopic wound evaluation following coated scaffold placement. **(A)**: Full thickness rat wounds were treated with one of a number of different collagen scaffolds or left untreated. **(B)**: Animals were culled at either 1, 3 or 5 days after wounding and the wounds macroscopically imaged. Scale bar = 1 mm.

Wounds were harvested at D1 to look at the early stages of wound healing, as well as D3 and D5 to examine re-epithelialisation, as in the previous chapter. Upon examination, wounds at D1, 3 and 5 that received uncoated scaffolds were again typically larger than any of the other treatments, including those left untreated (Figure 4. 4B) At D1, all scaffold applications appeared to prevent wound contraction to some degree, following visual comparisons to untreated wounds. From macroscopic observations during processing and handling, it appeared that coating scaffolds also appeared to make them more dense and brittle. However, by D3, wounds treated with Cx43 asODN coated scaffolds appeared markedly reduced in size compared to those treated with one of the control scaffolds, to a level similar to untreated wounds. Wounds treated with uncoated scaffolds at D3 remained similar in size to the initial wounds. The coated scaffolds themselves had reduced in size by varying degrees at both D3 and D5, and wound edges did not appear to integrate with the

structures. By D5, wounds treated with the Cx43 asODN coated scaffolds had reduced in size considerably, to either the same level of untreated wounds or slightly greater.

4.42 – Re-epithelialisation analysis following scaffold placement

Coated scaffolds appeared macroscopically to be poorly integrated with the wound edge although at this level it was not clear whether the Cx43 asODN coated scaffolds improved wound healing. Wounds were therefore sectioned using a cryostat to permit histological assessment. The polymers used in coating sectioned poorly and coated scaffolds often detached from the wound during processing on account of the loose association with the tissue to begin with. For this reason, coated scaffolds were typically not present throughout the microscopic analyses. Despite this, the effect of scaffold placement on wound re-epithelialisation could still be measured.

At D1, untreated wounds had re-epithelialised on average a distance of 274 μm ± 27 μm (all re-epithelialisation data is reported as mean ± SEM, Figure 4. 5). This was greater than control scaffold-treated wounds (uncoated, coating only, and coated + Cx43 sODN), which had re-epithelialised on average a distance of 202 μm ± 25 μm, although the difference was not significant. Wounds treated with bioactivated scaffolds coated in Cx43 asODN, however, had re-epithelialised significantly further than any of the other treatments. At an average distance of 407 μm ± 32 μm, this was 67% greater than untreated wounds ($P < 0.05$) and 101% greater than the combined averages of the control scaffold-treated wounds ($P < 0.01$ and $P < 0.001$). While the actual scaffolds coated with PCL and PLGA could not be visualised due to processing, wound edge keratinocytes typically appeared to migrate down the side of the wound margins and out towards the wound bed.

Following assessment at D1, wound re-epithelialisation was also measured at D3 and D5. At D3, untreated wounds had re-epithelialised an average of 522 μm ± 52 μm, which was again higher than the average of 389 μm ± 42 μm for the combined average distances of control scaffold-treated wounds by 34%, yet this difference was not statistically significant (Figure 4. 6). Wounds treated with the Cx43 asODN bioactivated scaffolds had again re-epithelialised further than every other treatment. The average re-epithelialisation distance of 859 μm was 65% greater than untreated wounds ($P < 0.05$) and 121% greater than the averaged distance for all control treated wounds ($P < 0.01$ and $P < 0.001$). At this time point, while wound edges treated with uncoated scaffolds tended to re-epithelialise down

the side of the wound margin, some of the polymer coated scaffolds re-epithelialised outwards, across the wound bed.

Similar measurements were also recorded at D5 (Figure 4. 7). At this time point some of the wounds were close to fully re-epithelialising. Untreated wounds had re-epithelialised an average distance of 882 μm ± 47 μm, which was only 12% higher than the combined averaged distance of 779 μm ± 87 μm for the three control scaffold-treated wounds. Cx43 asODN bioactivated scaffold-treated wounds had re-epithelialised on average 1345 μm ± 98 μm, which was a 65% increase over untreated wounds ($P < 0.05$). The increase was again more pronounced over the control scaffold treatments – Cx43 asODN scaffold-treated wound re-epithelialisation was 70% increased over the average of the three control scaffold treatments ($P < 0.05$ and $P < 0.01$). Scaffolds coated with polymers containing Cx43 asODN resulted in significantly increased levels of wound re-epithelialisation across all the studied time points.

The assessment of thickening of the leading edge epidermis was also measured, since it was unknown whether coated scaffolds induced epithelial thickening similar to perturbed healing in diabetic wounds and chronic ulcers (Wang et al., 2007), (Sutcliffe et al., submitted article). All epithelial thickening measurements are reported as means of 8 animals ± SEM. At D1, the thickness of wounds treated with uncoated scaffolds (107.5 μm, ± 9.1 μm), coating only scaffolds (79.5 μm, ± 17.0 μm) and Cx43 sODN coated scaffolds (61.7 μm, ± 11 μm), which were all higher than untreated wounds (50 μm, ± 4.2 μm), although only uncoated scaffolds were deemed significantly different (Figure 4. 8). Cx43 asODN coated scaffolds resulted in the thinnest measured leading edges, at 27.8 μm, ± 6.2 μm. This was 74.1% reduced from wounds treated with uncoated scaffolds, 65% reduced from coated scaffolds, 54.9% reduced from Cx43 sODN coated scaffolds and 44.4% lower than untreated wounds. Despite this, only differences to untreated wounds ($P < 0.001$) and coating only scaffolds ($P < 0.01$) were deemed significant. This trend continued at D3; the average thickness of the leading edge following Cx43 asODN coated scaffold application was 39.7 μm, ± 3.7 μm, which was 60.5% lower than wounds left untreated (70.3 μm, ± 11.3 μm), 79.5% reduced from uncoated scaffolds (135.3 μm, ± 11.3 μm), 59.9% lower than coating only scaffolds (69.4 μm, ± 6.4 μm) and 61.8% lower than Cx43 sODN scaffolds (72.7 ± 11.3 μm). This difference was only significant against uncoated scaffolds, however ($P < 0.001$). Similar findings were evident at D5 – epithelial

thickening following Cx43 asODN coated scaffold application was 29.3 ± 3.8 μm; 41.2% lower than wounds left untreated (49.8 ± 4.7 μm), 79.3% reduced from uncoated scaffolds (141.7 ± 15.2 μm), 49.5% lower than coating only scaffolds (57.9 ± 7.2 μm) and 60.4% lower than Cx43 sODN scaffolds (74.0 ± 11.2 μm). Despite this, significance was only reported against uncoated scaffolds ($P < 0.001$) and Cx43 sODN scaffolds ($P < 0.05$).

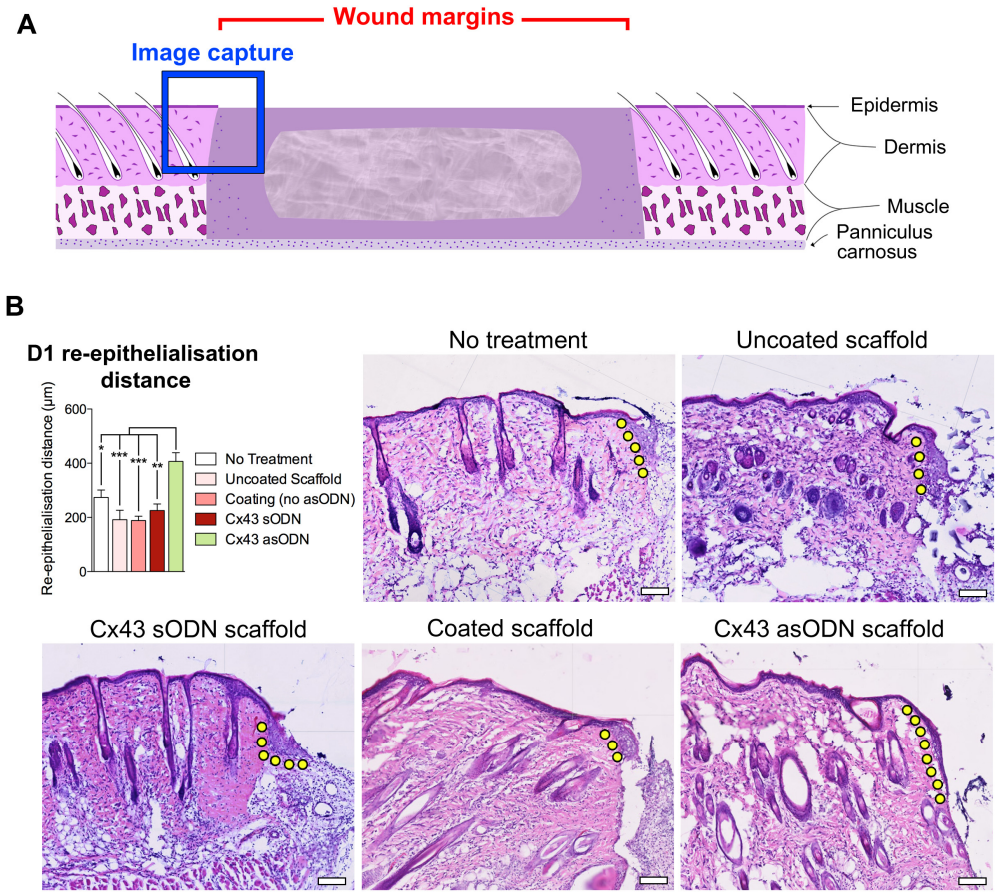

Figure 4. 5 – D1 full-thickness wound healing following application of Cx43 asODN polymer coated scaffolds.

(A): A simplified wound diagram to illustrate the site at which images were captured.

(B): Wounds were either left untreated or treated with a control scaffold (red bars) or a coated scaffold containing asODN (green bars). Wound re-epithelialisation distances outlined by dotted yellow lines were measured for each type of scaffold applied and plotted as a graph (top left). Eight rat wounds were assessed for re-epithelialisation, data is plotted as mean values + SEM error bars (* = $P < 0.05$, ** = $P < 0.01$, *** = $P < 0.001$). Scale bar = 100 μm.

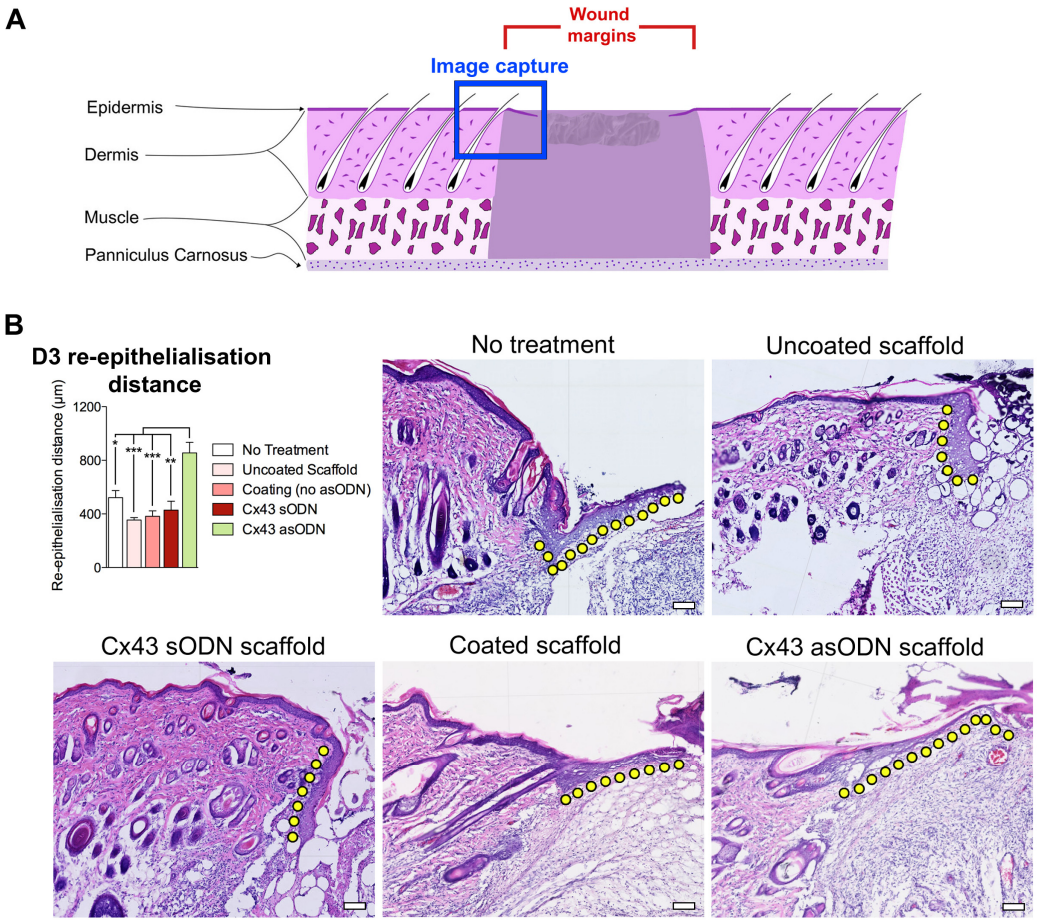

Figure 4. 6 – D3 full-thickness wound healing following application of Cx43 asODN polymer coated scaffolds

(A): A simplified wound diagram to illustrate the site at which images were captured.

(B): Wounds were either left untreated or treated with a control scaffold (red bars) or a coated scaffold containing asODN (green bars). Wound re-epithelialisation distances outlined by dotted yellow lines were measured for each type of scaffold applied and plotted as a graph (top left). Eight rat wounds were assessed for re-epithelialisation, data is plotted as mean values + SEM error bars (* = $P < 0.05$, ** = $P < 0.01$, *** = $P < 0.001$). Scale bar = 100 µm.

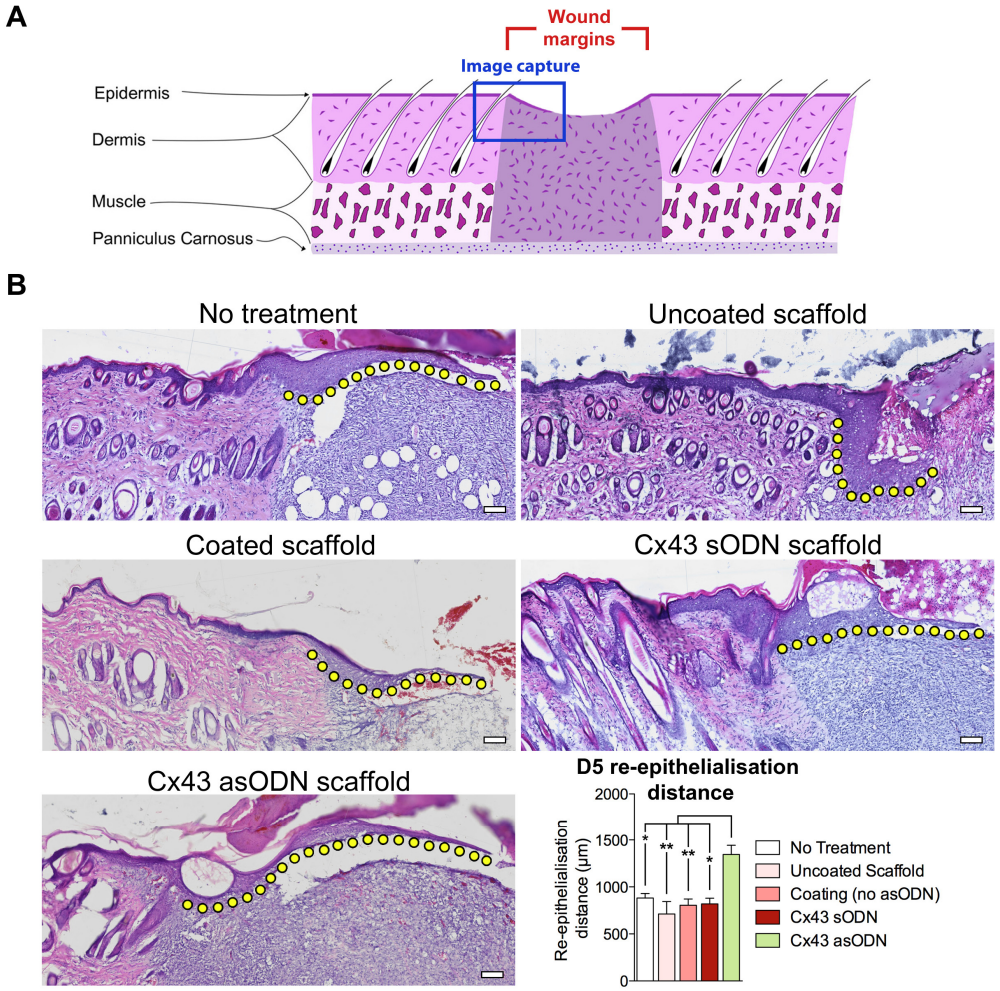

Figure 4. 7 – D5 full-thickness wound healing following application of Cx43 asODN polymer coated scaffolds

(A): A simplified wound diagram to illustrate the site at which images were captured.

(B): Wounds were either left untreated or treated with a control scaffold (red bars) or a coated scaffold containing asODN (green bar). Wound re-epithelialisation distances outlined by dotted yellow lines were measured for each type of scaffold applied and plotted as a graph (top left). Eight rat wounds were assessed for re-epithelialisation, data is plotted as mean values + SEM error bars (* = $P < 0.05$, ** = $P < 0.01$, *** = $P < 0.001$). Scale bar = 100 µm.

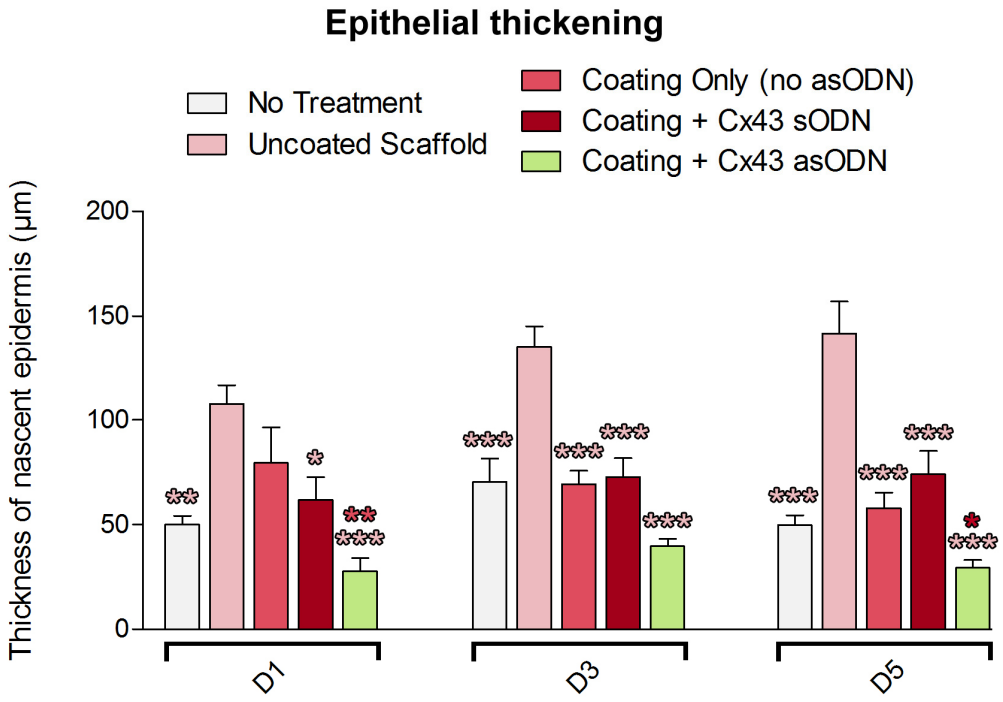

Figure 4. 8 – Leading edge epidermal thickening following Cx43 asODN scaffold application.

Full-thickness rat wounds treated with different types of scaffolds were measured for thickening of the leading edge epithelium within the end 150 µm of the nascent tip. Measurements were recorded across n=8 samples at D1, D3 and D5, and values plotted are means of 8 animals + SEM error bars (* = P<0.05, ** = $P < 0.01$, *** = $P < 0.001$). Significance stars are coloured to match the treatment that is significantly different (e.g. light pink star = significantly different to uncoated scaffold-treated wounds)

4.43 – Local inflammatory response following Cx43 asODN scaffold application

Since Cx43 knockdown has previously been shown to dampen the inflammatory response following acute wounding (Mori et al., 2006), it was questioned whether the Cx43 asODN sustained release scaffold had a similar effect over an extended period of time. Polymorphonuclear leukocytes (PMNs) were thus identified and counted in the intact dermis distal to the wound edge in order to investigate whether coated Cx43 asODN scaffolds had an effect on inflammatory cell infiltration (Figure 4. 9). All PMN counts are reported as means ± SEM. Analysis at D1 revealed that the Cx43 asODN coated scaffolds reduced PMN infiltration relative to control scaffolds. Only 15.6 ± 1.3 PMNs were

quantified for Cx43 asODN scaffolds, which was 37.1% less than untreated wounds (24.8 ± 7.4), 76.5% lower than uncoated scaffolds (66.4 ± 9.9), 60% lower than coating only scaffolds (39 ± 2.9) and 71% lower than Cx43 sODN scaffolds (53.8 ± 5.9). Significant differences were only returned against uncoated scaffolds ($P < 0.001$) and Cx43 sODN coated scaffolds ($P < 0.001$), however.

At D3, the assessed dermal regions distal to wounds had slightly elevated numbers of PMNs compared to D1 for all treatments (Figure 4. 9A-B). Cx43 asODN coated scaffolds resulted in a count of 18.8 ± 4.1 PMNs in the dermis. This was only 6.9% lower than untreated wounds (20.2 ± 2.7), 73.6% lower than uncoated scaffolds (71.2 ± 12.5), 61.3% decreased from control coated scaffolds (48.6 ± 4.3) and 69.2% reduced from Cx43 sODN scaffolds (61 ± 5.3). Differences were significant against each type of control scaffold ($P < 0.001$ = uncoated scaffold, $P < 0.001$ = Cx43 sODN scaffold, $P < 0.05$ = control coated scaffold). By D5, PMN infiltration of the distal dermis had decreased considerably across all treatments, including uncoated scaffolds. Cx43 asODN coated scaffolds still resulted in the lowest recorded PMN counts, however, with an average count of 9.4 ± 2.5 PMNs. PMNs in the dermis distal to wounds containing Cx43 asODN scaffolds were 38.16% reduced compared to untreated wounds (15.2 ± 4.3), 73.1% lower than uncoated scaffolds (35 ± 7.3), 60.5% lower than control uncoated scaffolds (23.8 ± 2.1) and 69.9% reduced from Cx43 sODN scaffolds (31.2 ± 5.4). Of these differences, Cx43 asODN treated wounds only resulted in significant differences in PMN counts between uncoated scaffolds ($P < 0.01$) and Cx43 sODN coated scaffolds ($P < 0.05$).

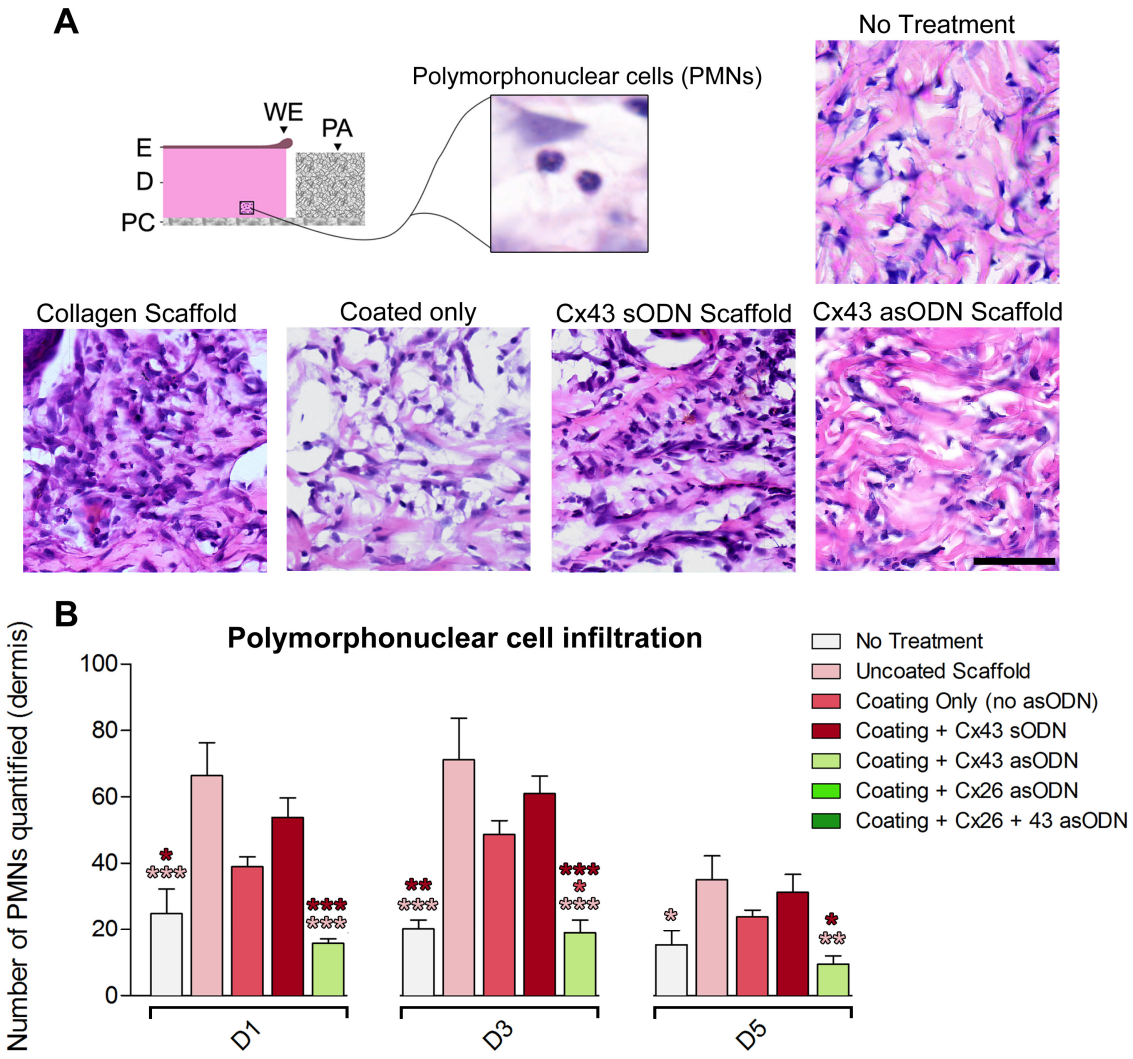

Figure 4. 9 – The effect of Cx43 asODN scaffold application on the dermal infiltration of polymorphonuclear cells

(A): Full-thickness wounds that received a scaffold treatment were assessed for polymorphonuclear cell invasion into the lower dermis 700 µm away from the wound edge as indicated in the topleft of diagram. High-power typical images of the dermal region are also shown for each scaffold treatment. The typical images shown are of the unwounded dermis distal to D3 wounds. Scale bar = 50 µm. **(B)**: Quantification of polymorphonuclear cells for each treatment across time points of D1, D3 and D5 were plotted as average values of n=5 samples. Error bars represent SEM. Diagram legend: E = epidermis, D = dermis, PC = panniculus carnosus, WE = wound edge (* = P<0.05, ** = $P < 0.01$, *** = $P < 0.001$).

4.44 – Cx26 and 43 expression in wound edge keratinocytes following scaffold application

Following H&E assessment, it was questioned whether the Cx43 asODN coating resulted in a knockdown of Cx43, and for how long, in full-thickness wound edges. Wounds were therefore immunostained for Cx43, as well as for Cx26, as in the previous chapter.

At D1, staining for Cx26 revealed a strong upregulation of protein in wound edge keratinocytes across all conditions, including wounds left untreated, with no significant differences observed between groups (Figure 4. 10). Cx26 was not significantly elevated in uncoated scaffold-treated wounds relative to untreated wounds. Despite the lack of significant differences, Cx26 levels in Cx43 asODN bioactivated scaffold-treated wound edge epidermis was 38% lower than untreated wounds and 57% less than the average of all three control scaffold-treated wounds. Staining for Cx43 revealed a different outcome, however. At D1, application of each of the control scaffolds resulted in an increase in Cx43 expression in the wound edge epidermis, with an average increase of 141% over distal levels (Figure 4. 11). Cx43 in untreated wound edges was 35% reduced, while bioactivated scaffold-treated wound edge expression decreased by an even greater degree (85%). Cx43 expression was significantly reduced in the bioactive scaffold-treated wounds relative to all three control scaffold treatments ($P < 0.05$ and $P < 0.01$).

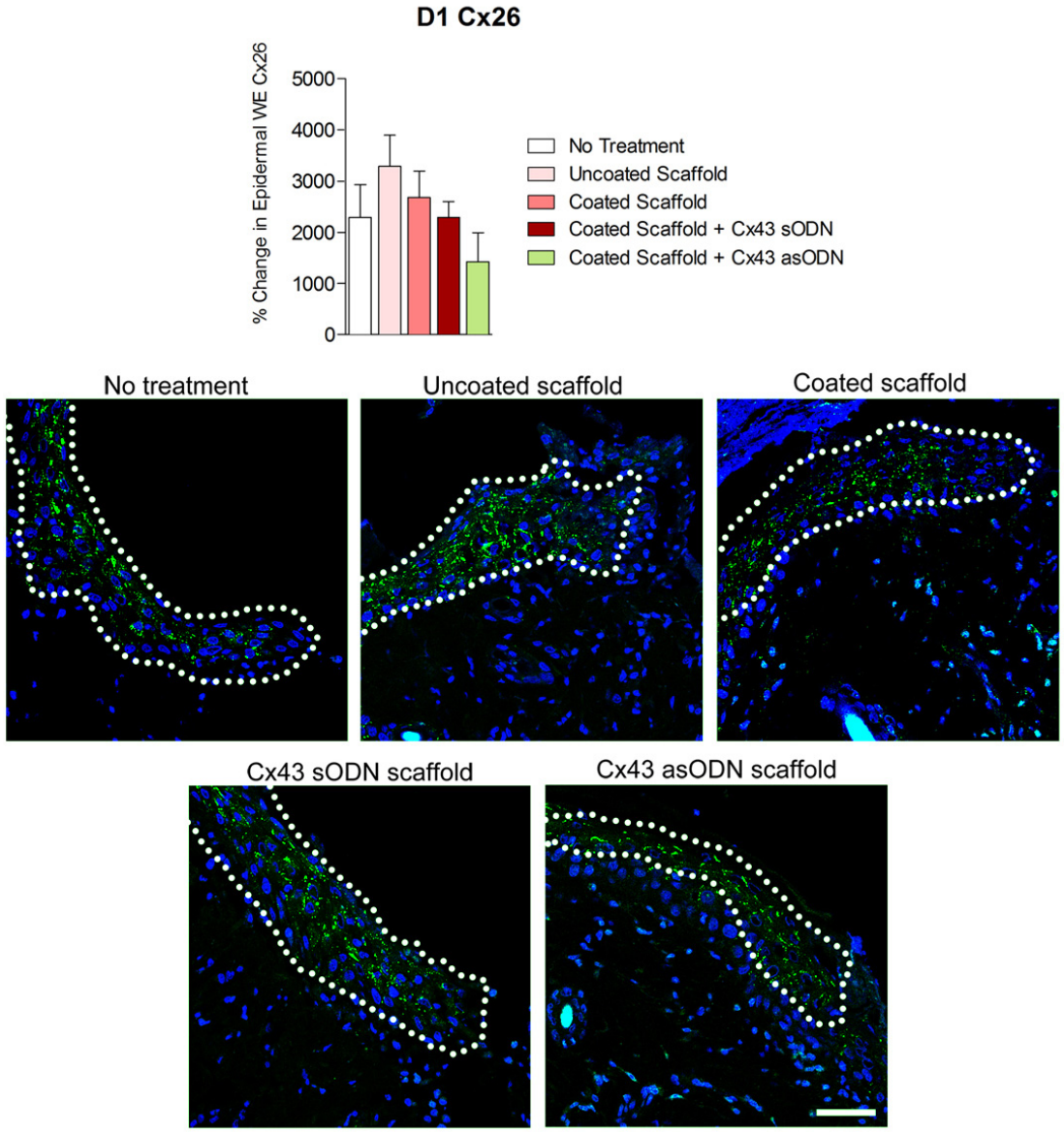

Figure 4. 10 – D1 Cx26 expression in the epidermal wound edge of scaffold-treated wounds.

Full-thickness wounds treated either left untreated or treated with a scaffold were harvested at D1. **Below**: tissue was immunostained for Cx26 (green) or Hoechst (blue) and confocal images of the nascent epidermis were captured. **Above**: positive Cx26 pixels were quantified in the end 150 μm of the wound edge epidermis as pixels per μm^2. Values were then normalised to a region of distal epidermis to calculate the percentage change (increase or decrease) from distal levels. Data plotted are means + SEM error bars. Significance stars are coloured to match the treatment that is significantly different (e.g. dark red star = significantly different to Cx43 sODN scaffold-treated wounds). Scalebar = 50 μm, n=8 rats assessed (no differences were significant in this graph).

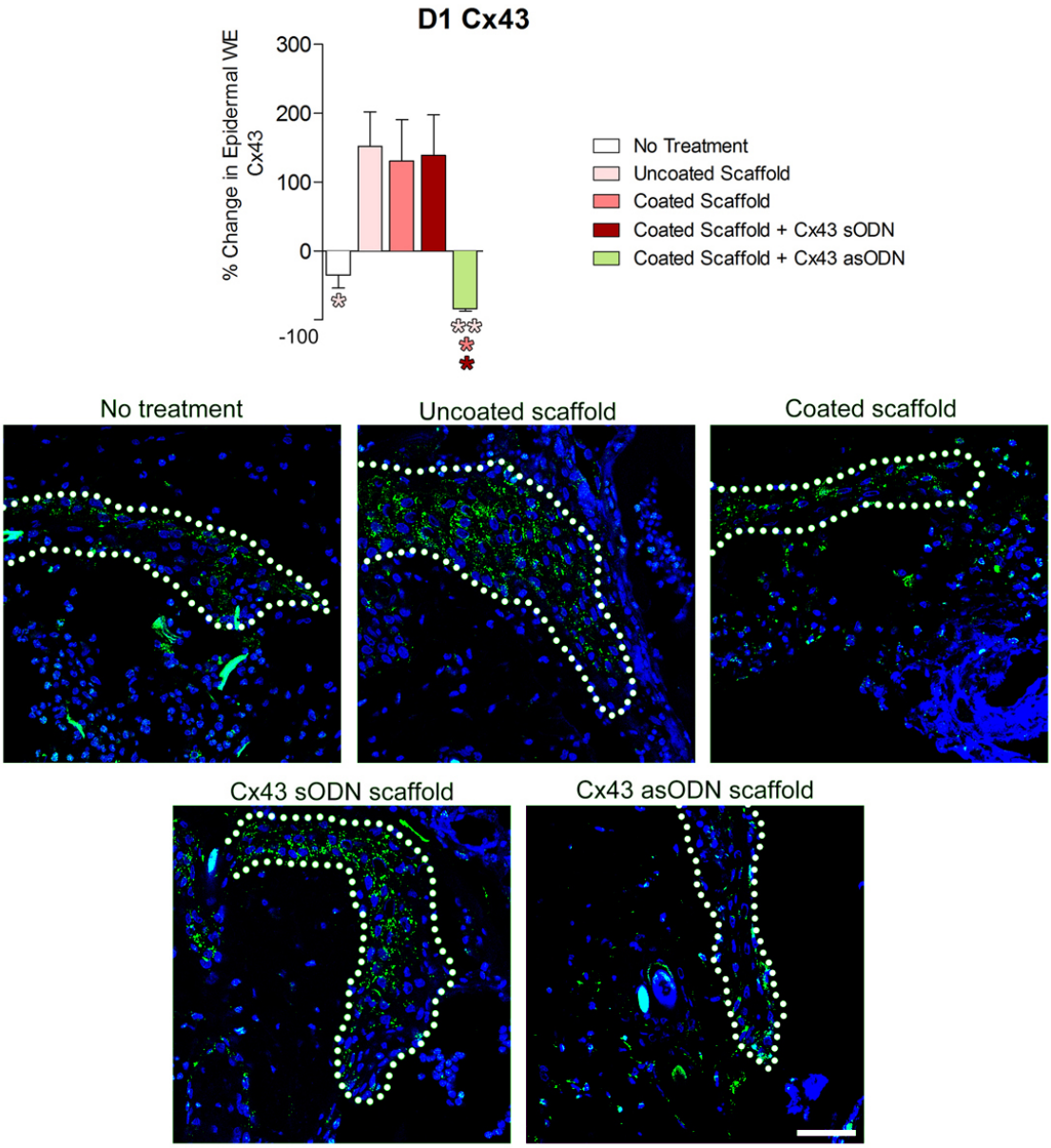

Figure 4. 11 – D1 Cx43 expression in the epidermal wound edge of scaffold-treated wounds.

Full-thickness wounds treated either left untreated or treated with a scaffold were harvested at D1. **Below**: tissue was immunostained for Cx43 (green) or Hoechst (blue) and confocal images of the nascent epidermis were captured. **Above**: positive Cx43 pixels were quantified in the end 150 μm of the wound edge epidermis as pixels per μm^2. Values were then normalised to a region of distal epidermis to calculate the percentage change (increase or decrease) from distal levels.. Data plotted are means + SEM error bars. Significance stars are coloured to match the treatment that is significantly different (e.g. dark red star = significantly different to Cx43 sODN scaffold-treated wounds). Scalebar = 50 μm, n=8 rats assessed (* = $P<0.05$, ** = $P < 0.01$).

As scaffold coatings appeared to elute asODN *in vitro* for several days, it was hypothesised that Cx43 asODN coated scaffolds might reduce Cx43 expression *in vivo* at later time points. At D3, wound edge keratinocyte Cx26 expression was increased from distal levels for all treatments (Figure 4. 12). Uncoated scaffolds produced the highest increase in wound edge Cx26 expression, at an increase of 6370%. Staining also revealed differences between species - the percentage upregulation of Cx26 in untreated rat wound edges was approximately double that found in mice (Figure 3. 3), yet was still lower than the uncoated scaffold-treated mouse wounds. In rat wounds, the uncoated scaffold did not appear to induce greater upregulation of Cx26 than the control coated scaffolds (Figure 4. 12). As with the mouse wounds, application of Cx43 asODN bioactivated scaffolds resulted in significantly lower Cx26 expression at wound edges relative to control coated and uncoated scaffolds at D3 ($P < 0.05$ and $P < 0.01$). Cx43 asODN coated scaffold-treated wound edges featured a Cx26 upregulation of only 375%.

In the case of Cx43 expression at D3, a 65% downregulation was observed in wound edges treated with bioactivated scaffolds, which was comparable to untreated wounds (Figure 4. 13). This was a significantly lower level of expression than wounds treated with uncoated scaffolds (335% increase, $P < 0.05$) and Cx43 sODN coated scaffolds (283% increase, $P < 0.05$), but not coated scaffolds, although coated scaffolds still induced Cx43 upregulation. Cx43 upregulation in uncoated scaffold-treated wound edges occurred, similar to that observed chapter 3 using mice at D3 (see Figure 3. 3).

At D5, wound edge Cx26 was markedly reduced from the levels at D3 for all treatments, while only the Cx43 asODN scaffold resulted in Cx26 downregulation from distal levels (Figure 4. 14). All three control scaffolds resulted in an increase in wound edge Cx26 expression, with an average rise of 147%. Both coated and uncoated control scaffolds resulted in significantly higher wound edge keratinocyte Cx26 levels than the Cx43 asODN bioactivated scaffold-treated wounds ($P < 0.05$), although the Cx43 sODN scaffolds did not produce a significant difference. In contrast to when Cx43 asODN was applied in Pluronic gel to mouse wounds, rat wound edges in contact with Cx43 asODN coated scaffolds still maintained a 91% downregulation of Cx43 at D5 (Figure 3. 8) & (Figure 4. 15). This was a greater downregulation than that of untreated wound edges (57%). Cx43 expression was again upregulated from distal levels at D5 across all control scaffold treatments. Wounds treated with both uncoated and coated control scaffolds resulted in

higher levels of Cx43 expression relative to the bioactive scaffold-treated wounds ($P < 0.01$ and $P < 0.001$), although significance was not achieved against the sODN coated scaffold treatment group, which had high variability.

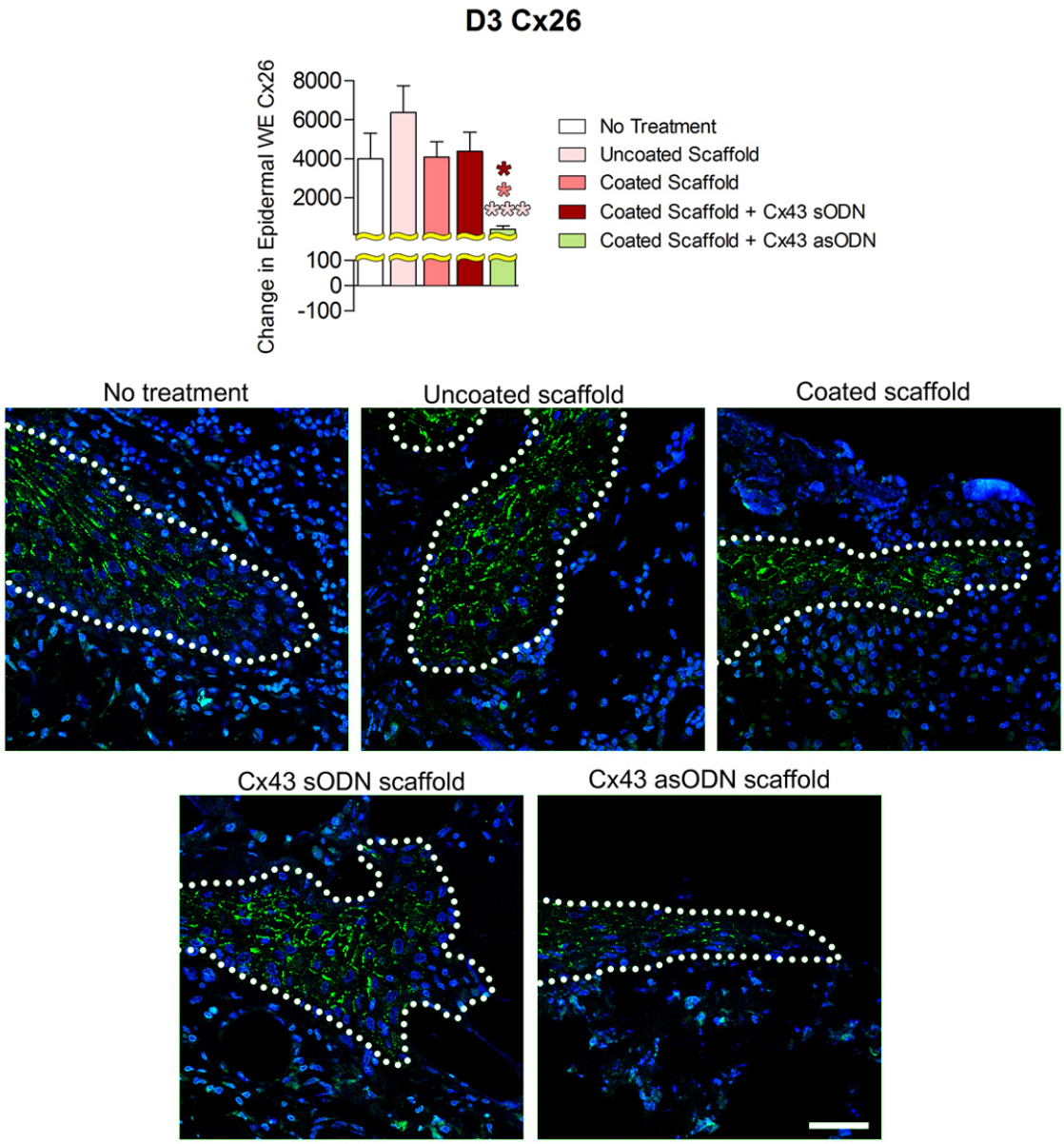

Figure 4. 12 – D3 Cx26 expression in the epidermal wound edge of scaffold-treated wounds.

Full-thickness wounds treated either left untreated or treated with a scaffold were harvested at D3. **Below**: tissue was immunostained for Cx26 (green) or Hoechst (blue) and confocal images of the nascent epidermis were captured. **Above**: positive Cx26 pixels were quantified in the end 150 μm of the wound edge epidermis as pixels per μm^2. Values were then normalised to a region of distal epidermis to calculate the percentage change (increase or decrease) from distal levels.. Data plotted are means + SEM error bars. Significance stars are coloured to match the treatment that is significantly different (e.g. dark red star = significantly different to Cx43 sODN scaffold-treated wounds). Scalebar = 50 μm, n=8 rats assessed (* = $P<0.05$, *** = $P < 0.001$).

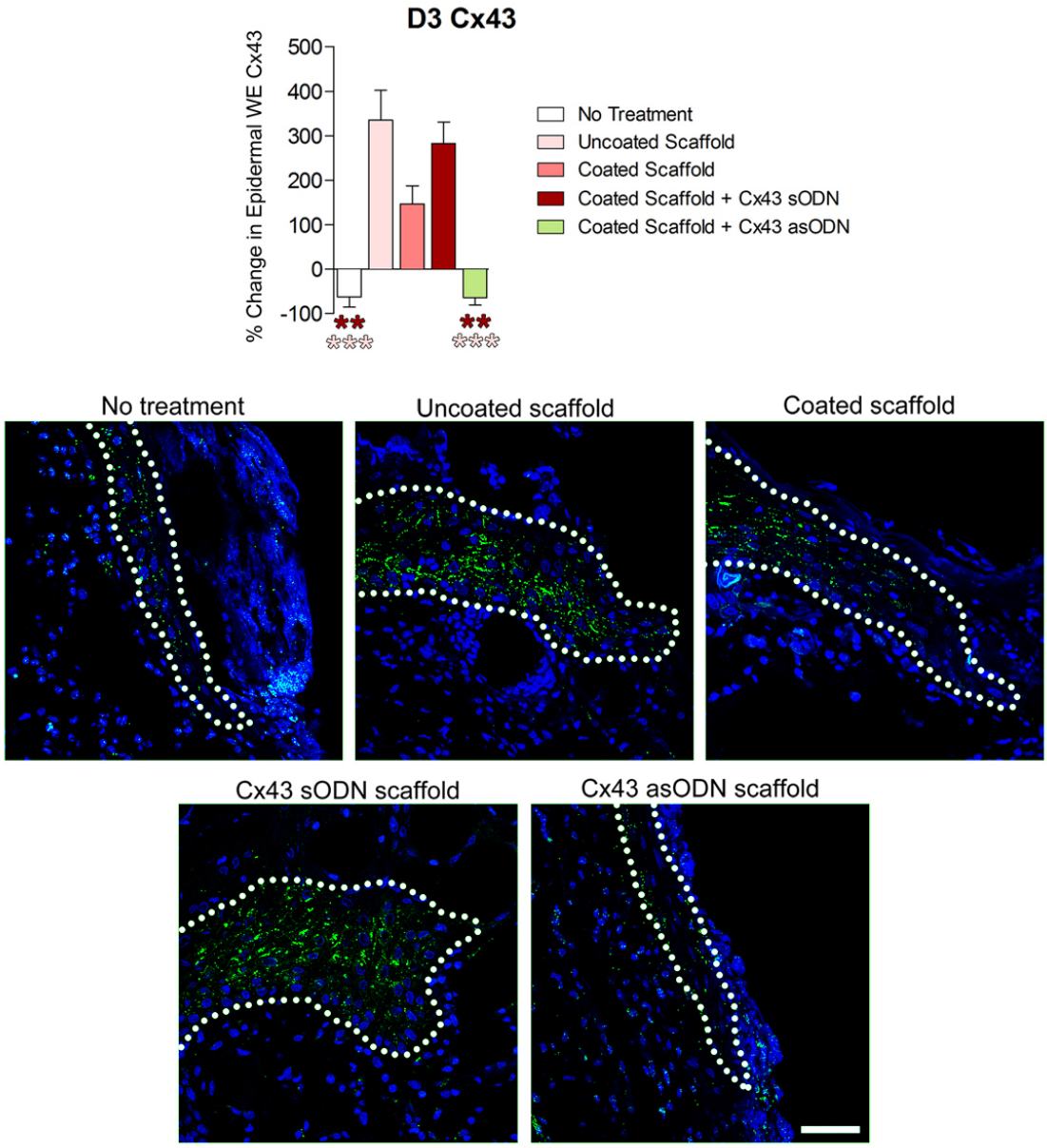

Figure 4. 13 – D3 Cx43 expression in the epidermal wound edge of scaffold-treated wounds.

Full-thickness wounds treated either left untreated or treated with a scaffold were harvested at D3. **Below**: tissue was immunostained for Cx43 (green) or Hoechst (blue) and confocal images of the nascent epidermis were captured. **Above**: positive Cx43 pixels were quantified in the end 150 μm of the wound edge epidermis as pixels per μm^2. Values were then normalised to a region of distal epidermis to calculate the percentage change (increase or decrease) from distal levels.. Data plotted are means + SEM error bars. Significance stars are coloured to match the treatment that is significantly different (e.g. dark red star = significantly different to Cx43 sODN scaffold-treated wounds). Scalebar = 50 μm, n=8 rats assessed (** = $P < 0.01$, *** = $P < 0.001$).

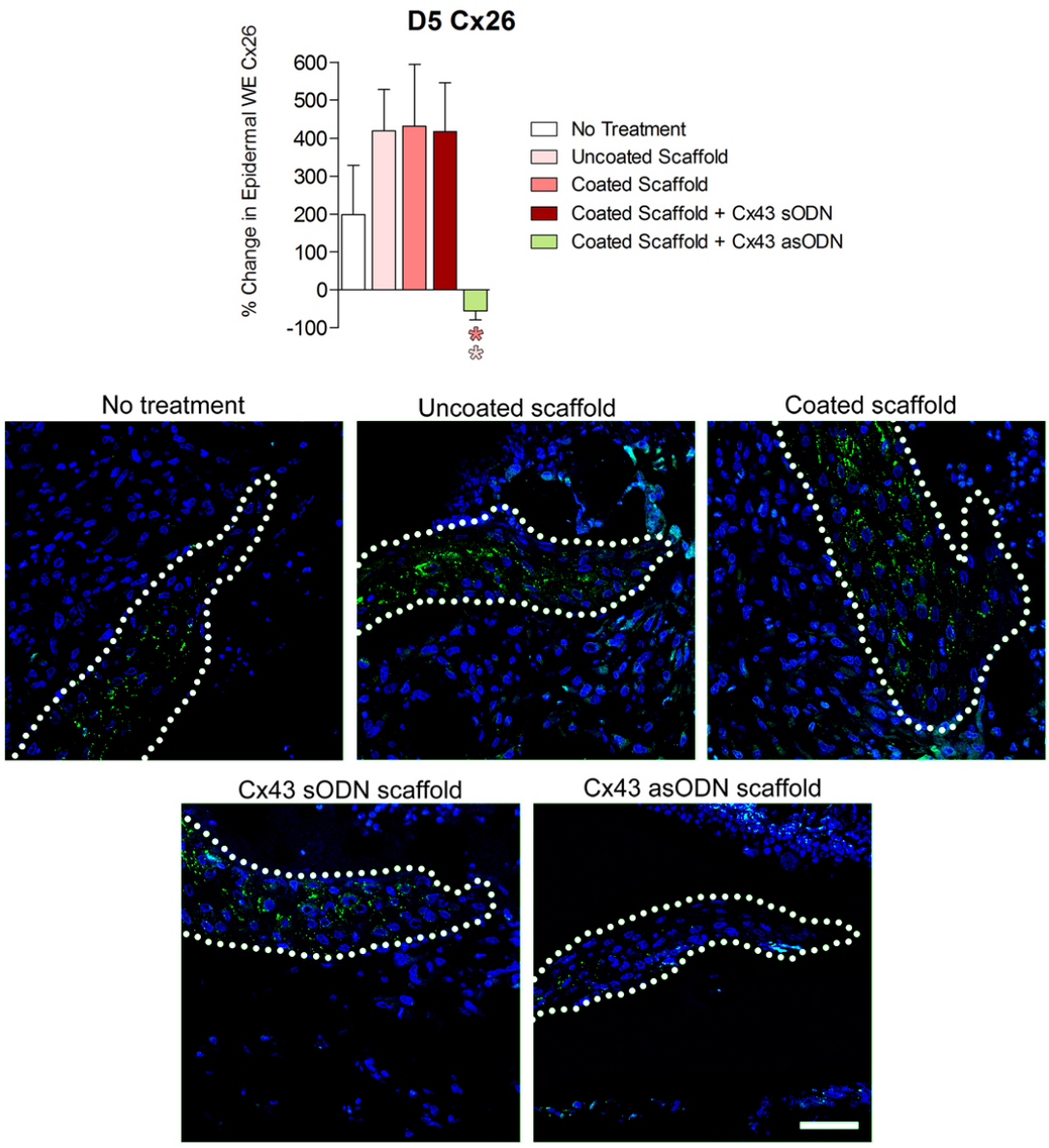

Figure 4. 14 – D5 Cx26 expression in the epidermal wound edge of scaffold-treated wounds.

Full-thickness wounds treated either left untreated or treated with a scaffold were harvested at D5. **Below**: tissue was immunostained for Cx26 (green) or Hoechst (blue) and confocal images of the nascent epidermis were captured. **Above**: positive Cx26 pixels were quantified in the end 150 µm of the wound edge epidermis as pixels per μm^2. Values were then normalised to a region of distal epidermis to calculate the percentage change (increase or decrease) from distal levels. Data plotted are means + SEM error bars. Significance stars are coloured to match the treatment that is significantly different (e.g. light pink star = significantly different to uncoated scaffold-treated wounds). Scalebar = 50 µm, n=8 rats assessed (* = $P<0.05$).

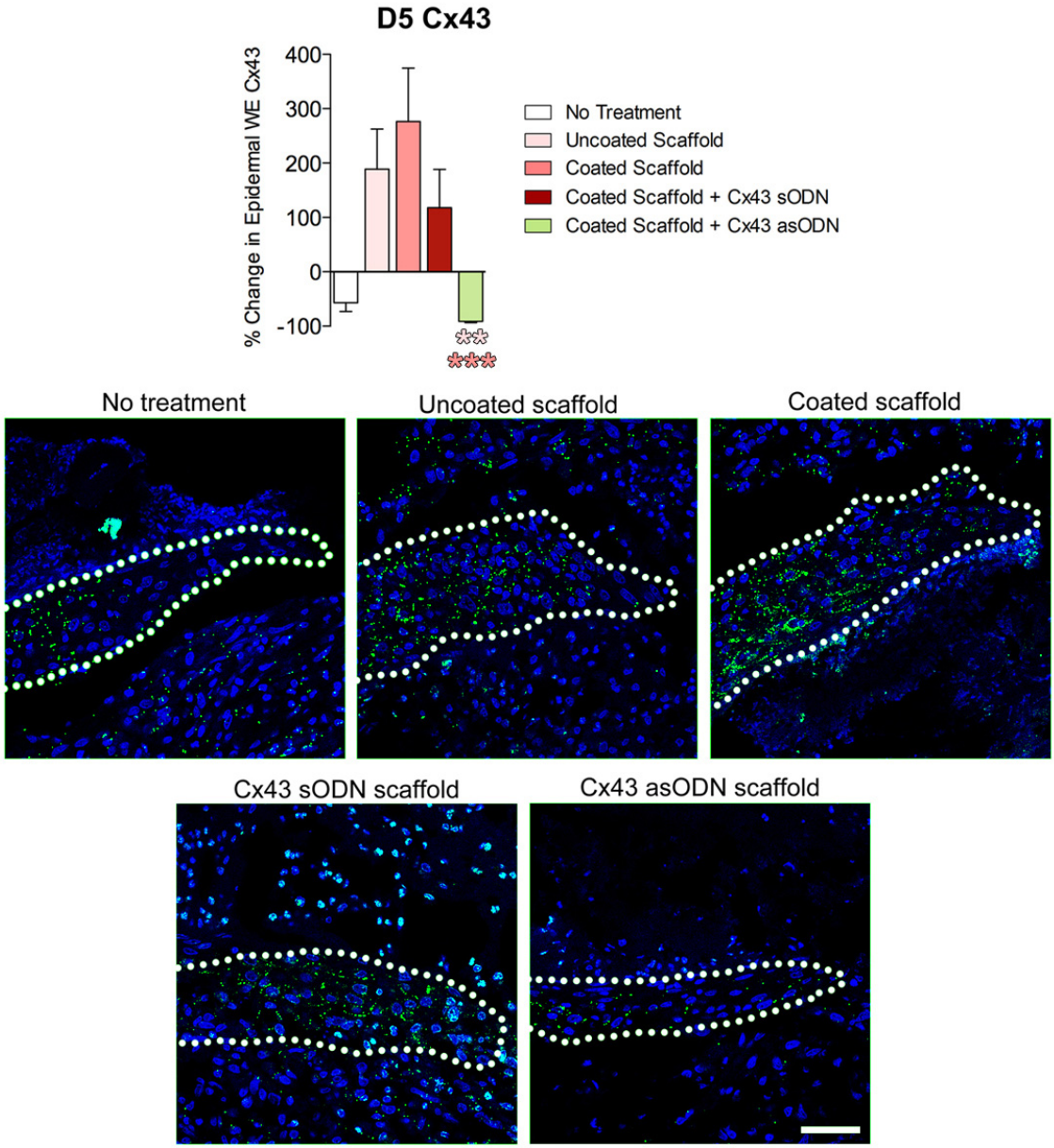

Figure 4. 15 – D5 Cx43 expression in the epidermal wound edge of scaffold-treated wounds.

Full-thickness wounds treated either left untreated or treated with a scaffold were harvested at D5. **Below**: tissue was immunostained for Cx43 (green) or Hoechst (blue) and confocal images of the nascent epidermis were captured. **Above**: positive Cx43 pixels were quantified in the end 150 μm of the wound edge epidermis as pixels per μm^2. Values were then normalised to a region of distal epidermis to calculate the percentage change (increase or decrease) from distal levels.. Data plotted are means + SEM error bars. Significance stars are coloured to match the treatment that is significantly different (e.g. light pink star = significantly different to uncoated scaffold-treated wounds). Scalebar = 50 μm, n=8 rats assessed (** = $P < 0.01$, *** = $P < 0.001$).

4.5 – The effect of Cx43 asODN coated scaffolds on the late stages of wound healing

4.51 – Granulation tissue formation following scaffold application

Because Cx43 asODN coated scaffolds appeared to affect Cx43 expression over at least 5 days, it was questioned whether their application also had an effect on the later stages of wound healing such as granulation tissue formation. Scaffolds applied to rat wounds were thus harvested at D10 and D15 (Figure 4. 16 & Figure 4. 17). Granulation tissue was then measured between the wound margins, above the panniculus carnosus layer (Figure 4. 16A).

Analysis of the now re-epithelialised wounds at D10 revealed significant differences in the region of granulation tissue formation between the scaffold treatments (Figure 4. 16B). Data for granulation tissue area measurements are reported as mean values of 8 (D10) or 7 (D15) rats ± SEM. At D10, treatment of wounds with Cx43 asODN coated scaffolds resulted in an average granulation tissue area of 2.30 ± 0.21 mm^2, which was significantly smaller than uncoated scaffold-treated wounds that measured an average of 4.47 ± 0.34 mm^2 ($P < 0.001$). The measured area for bioactive scaffold-treated wounds was also significantly smaller than wounds treated with sODN coated scaffolds (3.41 ± 0.11 mm^2, $P < 0.05$), coated scaffolds (3.47 ± 0.22 mm^2, $P < 0.05$) and untreated wounds (3.61 ± 0.18 mm^2, $P < 0.01$). Similar results were also observed at the later time point of D15. At D15, wounds that received Cx43 asODN coated scaffolds had a measured granulation tissue region of 1.391 ± 0.07 mm^2 (Figure 4. 17B), significantly lower than the 2.29 ± 0.34 mm^2 of untreated wounds ($P < 0.05$). The bioactive scaffold-treated wounds also measured significantly lower than uncoated scaffold (2.70 ± 0.31 mm^2, $P < 0.001$), coated scaffold (2.33 ± 0.20 mm^2, $P < 0.05$) and coated scaffold + Cx43 sODN-treated wounds (2.39 ± 0.23 mm^2, $P < 0.05$). Application of bioactivated scaffolds appeared to consistently reduce the area of granulation tissue present within wounds at D10 and D15.

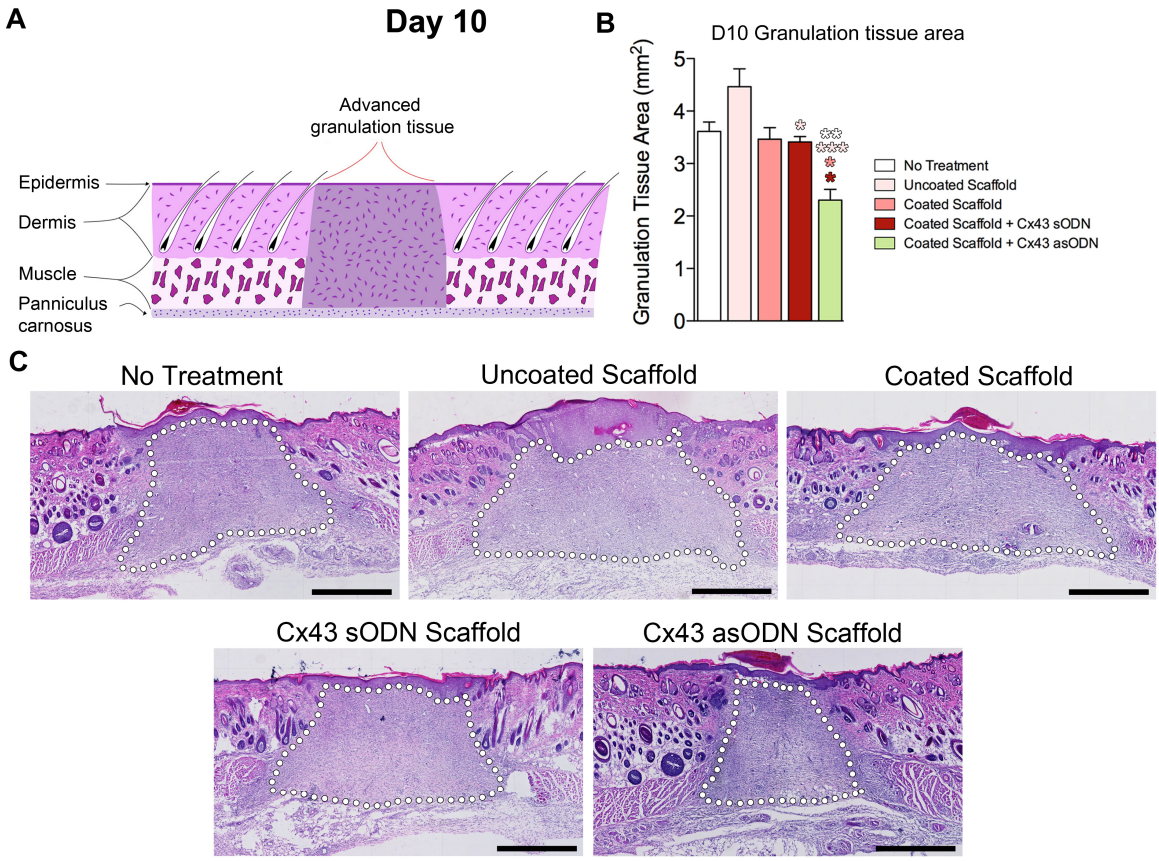

Figure 4. 16 – Full-thickness wounds treated with scaffolds at D10

Full-thickness wounds were either left untreated or treated with a scaffold. Wounds were harvested at D10.

(A): A simplified wound diagram to illustrate the granulation tissue region which was measured in (B).

(B): Wounds either left untreated or treated with a control scaffold (red bars) or a coated scaffold containing asODN (green bars) were measured for granulation tissue/wound area. Eight rat wounds were assessed, data is plotted as mean + SEM error bars (* = $P < 0.05$, ** = $P < 0.01$, *** = $P < 0.001$), scale bar = 100 μm.

(C): Typical H&E stained images illustrating the quantified granulation tissue area of the individual wounds in (white dots).

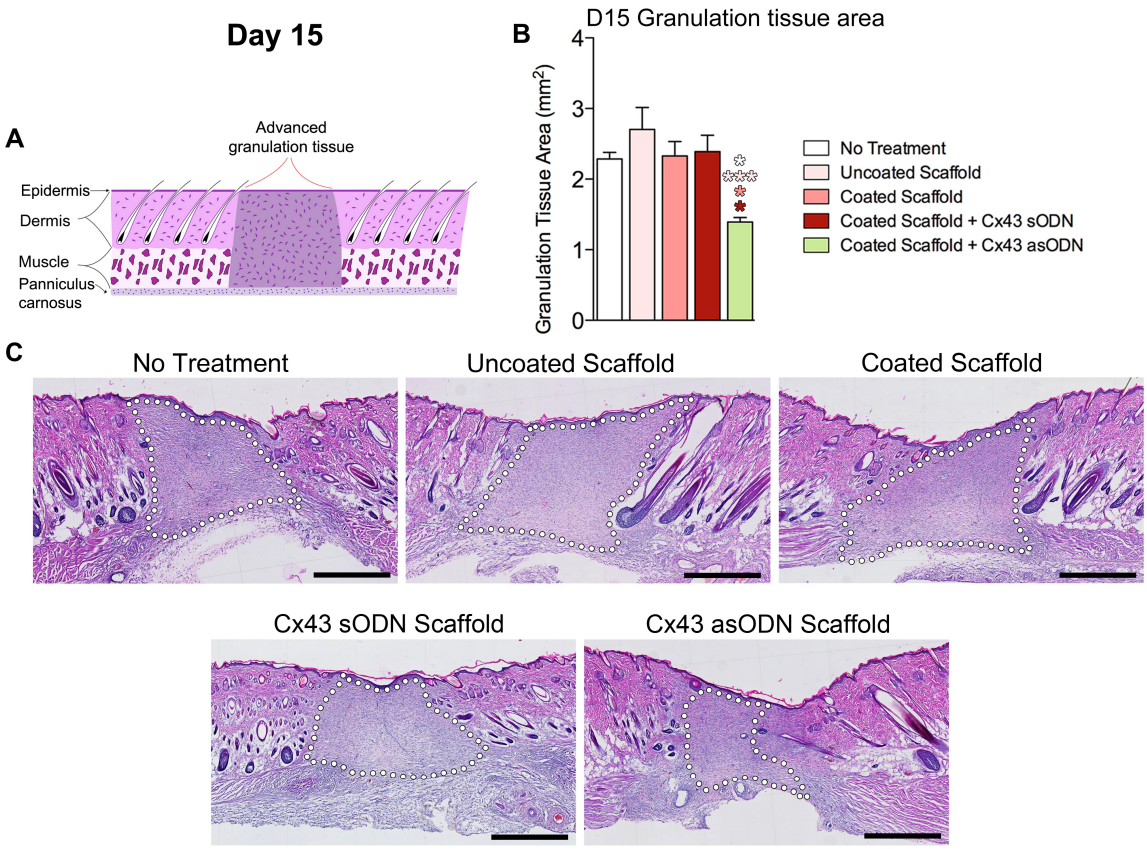

Figure 4. 17 – Full-thickness wounds treated with scaffolds at D15

Full-thickness wounds were either left untreated or treated with a scaffold. Wounds were harvested at D15.

(A): A simplified wound diagram to illustrate the granulation tissue region which was measured in (B).

(B): Wounds either left untreated or treated with a control scaffold (red bars) or a coated scaffold containing asODN (green bars) were measured for granulation tissue/wound area. Seven rat wounds were assessed, data is plotted as mean + SEM error bars (* = $P < 0.05$, ** = $P < 0.01$, *** = $P < 0.001$), scale bar = 100 µm.

(C): Typical H&E stained images illustrating the quantified granulation tissue area of the individual wounds in (white dots).

4.52 – Application of Cx43 asODN coated scaffolds reduces the region of wound alpha smooth muscle actin (α-SMA) at D10

It was postulated that the reduction in granulation tissue area following Cx43 asODN coated scaffold application could have been due to the activity of contractile myofibroblasts. This was because the use of Cx43 asODN has been shown to advance the appearance of α-SMA positive myofibroblasts in the wound by 2-3 days (Mori et al., 2006). Full-thickness rat wounds were therefore harvested at D10, when myofibroblasts are typically still contracting down the wound, and stained for the myofibroblast marker α-SMA (Figure 4. 18). Staining revealed a large α-SMA positive region in the coating only scaffold-treated wounds, relative to the Cx43 asODN scaffold-treated wounds (Figure 4. 18B). Measurement of this area (as illustrated by the dotted yellow outlines) revealed a significant 60.6% decrease in the area of positive α-SMA staining following Cx43 asODN scaffold placement, relative to the control scaffold ($P < 0.001$). Staining in the Cx43 asODN scaffold-treated wounds was more centrally localised within the wounds, compared to the extensive staining in control-scaffold treated wounds which was also found close to the wound margins.

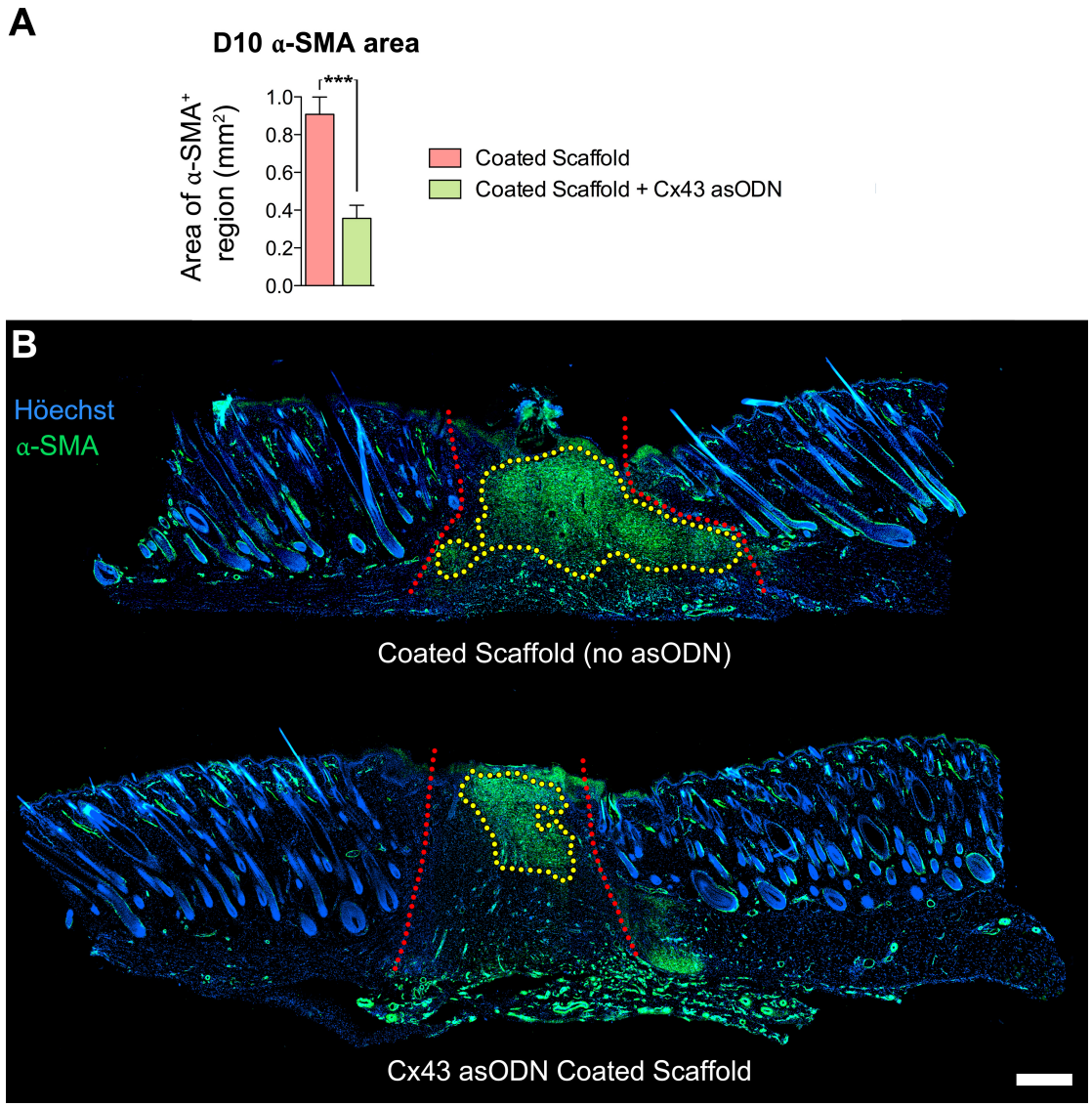

Figure 4. 18 – α-SMA expression in D10 scaffold-treated wounds

Rat full-thickness wounds treated with either control coated scaffolds (no asODN) or Cx43 asODN coated scaffolds were harvested at D10 and stained for both α-SMA (green) and Hoechst (blue). **(A)**: The α-SMA$^+$ region outlined in (B) was quantified for two different treatments on the same animals; a coated collagen scaffold without asODN and a coated scaffold coated with Cx43 asODN. This region was defined as positive stain in the wound gap above the blood vessel dense panniculus carnosus. A total of n=8 animals were assessed, values plotted are means + SEM error bars (*** = $P < 0.001$, scale bar = 500 μm). **(B)**: Typical immunofluorescence montage images illustrating the measured region of α-SMA in the wound (yellow dots) as well as the initial wound margins (red dots).

4.7 – Discussion

It became apparent that the initial method of coating scaffolds with a single layer of PLGA containing 100 μM Cx43 asODN was insufficient for sustained antisense delivery since acute wound re-epithelialisation can take between 5-7 days. Single-layer coated scaffolds released over 95% of the total eluted asODN within just the first 48 h (Figure 4. 1). The shortcomings of this method demanded further investigation into the literature. Research into other studies highlighted the possibility of utilising multiple coating layers. In one study, coating stents with three thin polymer films containing the drug S-Nitrosoglutathione was found to markedly increase the overall amount of drug eluted, although most of the additionally incorporated drug was still eluted within the first 24 h (Acharya et al., 2012). The use of multiple polymer layers containing asODN therefore appeared to be a valid method to increase the amount of asODN eluted, and it was proposed that increasing the number of layers above 3 might improve the timescale of elution relative to the other study. Indeed, when collagen scaffolds were coated with 4 layers of PLGA containing Cx43 asODN, the amount of asODN eluted within the first 3 days approximately tripled, indicating that this approach was more successful than the previous method (Figure 4. 2). Despite the improved dose delivery, over 95% of asODN that eluted in total from PLGA still eluted within the first 72 h, indicating that the PLGA used in the study may not be sufficient to achieve sustained release of Cx43 asODN. This was not the case with scaffolds coated in four layers of PCL, which resulted in a more sustained release profile in which asODN elution only began to plateau at around 6-7 days. This outcome is in agreement with the results of a study performed by (Acharya et al., 2012), where it was found that the use of PCL resulted in a more sustained release profile than PLGA or polyethylene glycol. This can be explained through differences in the molecular composition of each polymer - the chemical bonds between repeating glycolic acid units in PLGA are more sensitive to hydrolysis than those between the caproic acid monomers in PCL. In addition, PLGA breakdown occurs more rapidly since it produces acidic by-products when degraded, which promote auto-catalysis (Eglin and Alini, 2008).

While coating scaffolds with 4 layers of PCL resulted in a sustained release of asODN, coating scaffolds with 4 layers of PCL followed by an additional 4 layers of PLGA achieved the greatest overall release of Cx43 asODN across the 7-day assessment (Figure 4.2 C). Additionally, the elution profile for double coated scaffolds appeared to adopt the

characteristics of both the individual PLGA and PCL coatings. There was a large burst release of asODN in the first 24 h characteristic of the individual PLGA release profile as well as the more sustained release profile of PCL. This included a small second peak of elution around 3-4 days, which was also present in the PCL-only coated scaffold, and may have occurred due to hydrolysis of the coating layers. Second peaks of elution have also been found using other multi-layered approaches, such as with two-layered scaffold fibres containing an inner layer of PLGA mixed with gentamicin, lidocaine and vancomycin, and a blank outer layer (Chen et al., 2012). The occurrence of a second peak appears to be linked to the use of multiple layers, and could be the result of sufficient exposure of the inner coating layers occurring by this time. This can occur both through hydrolysis of chemical bonds within the outer layer polymer, as well as through enzymatic degradation of polymers within the wound. Indeed, polymer breakdown occurs more rapidly *in vivo* than *in vitro* (Eglin and Alini, 2008). The initial burst release of asODN observed could be useful in a wound setting, as Cx43 must be downregulated in the first 24 h in order for the re-epithelialisation process to initiate (Mori et al., 2006).

The finding that multiple coating layers improved the overall duration of asODN elution is also in agreement with the results of a clinical trial study that used multi-layered stent coatings. In this study, stents were coated with an inside polymer layer containing Sirolimus as well as an outer layer containing no drug (Schofer et al., 2003). The group found that the use of an outer coating provided a barrier to slow the elution of drug from the inner layer, such that up to 80% of the drug eluted over a 30-day period. The application of multiple outer layers to scaffolds may have conferred a similar effect on the elution properties of the coatings developed in this study. It is important to note, however, that the *in vitro* assessment of elution dynamics serves only as a guideline to estimate *in vivo* asODN elution. In the *in vivo* experiments performed in the previous chapter using mice it was clear that collagen scaffolds are enzymatically degraded in wounds, with significant degradation having typically occurred by D5. The wound environment may result in a greater rate of elution than that observed when performing *in vitro* assays. On the other hand, coating layers containing drugs have been widely reported to incompletely release all drug contents, with one study finding that as much as 25% of the incorporated drug tacrolimus remained in a single layered coating (Wieneke et al., 2003). In the case of scaffolds coated multiple times within this study, this could mean that an even greater proportion of asODN may have remained trapped in the coatings *in vitro*, while *in vivo* the

breakdown of scaffolds could result in a greater release due to the exposure of trapped asODN.

While spectrophotometry-based elution profiling showed that a considerable quantity of asODN eluted from PCL-PLGA double-coated scaffolds over 7 days, it did not reveal whether the homogenisation and solvent processing steps performed in the coating process damaged the structure of the incorporated DNA. FRET acceptor photobleaching was performed on sectioned scaffolds coated using a Cy3 and Cy5 dual labelled Cx43 asODN sequence (Figure 4. 3). This technique has been successfully used to study asODN integrity and is favoured for both its accuracy and simplicity (Rupenthal et al., 2012). Bleaching the Cy5 acceptor fluorophore on scaffolds sectioned immediately after coating (0 h) revealed a FRET efficiency of 25.9% (Figure 4. 3B). The fact this was above the 15-20% considered to signify that genuine FRET is occurring (Lai et al., 2014) suggested that the asODN was intact, and that the coating process did not destroy the asODN. FRET acceptor photobleaching following several days of serum immersion also resulted in high FRET efficiencies, indicating that there was intact asODN still contained within the scaffold structure (Figure 4. 3B). This indicated that that the coating conferred a degree of nuclease protection. Protection against nuclease activity is particularly important, since the wound environment is rich in DNAses; the most active of which is DNAse I (von Kockritz-Blickwede et al., 2009). The performance of a lambda scan on a solution serum-treated asODN attenuated the second peak of light emission around 640 - 700 nm following excitation, indicating that the serum was indeed effective at breaking down asODN when not contained within a coating.

In order to test whether scaffolds had an effect *in vivo* they were applied to 6 mm full-thickness wounds, this time made to the dorsum of rats. Macroscopic assessment of the scaffolds suggested that coating scaffolds with the artificial polymers appeared to reduce wound integration even further (Figure 4. 4). Coating scaffolds appeared to make scaffolds more brittle, and could perhaps explain the ease with which scaffolds disassociated from wound edges. The poor level of coated scaffold integration was also reflected by how easily scaffolds detached from wounds during processing. Despite this, coated scaffolds appeared to shrink in size in the wound, at a rate faster than the uncoated scaffolds. This was possibly through dissolution of the scaffold fibres and hydrolysis of the polymer coatings. Unlike the bioactivated scaffolds in the previous chapter, the Cx43 asODN coated scaffold

did not appear to prevent wound contraction, while the control coated scaffolds had only a mild negative effect on wound size. This could have been due to the fact that the coating method used within this chapter prevented prior cross-linking of scaffolds, allowing the collagen fibres within the scaffold to break down more rapidly in conjunction with wound contraction. The finding that Cx43 asODN bioactivated scaffolds resulted in the smallest wounds is in agreement with previous direct wound applications of Cx43 asODN in Pluronic gel, where treated wounds were found to contract to a greater degree than untreated wounds (Qiu et al., 2003). This observation could be due to enhancement of fibroblast migration into the wound due to Cx43 knockdown, which can be responsible for wound contraction following differentiation into myofibroblasts (Mori et al., 2006). Cx43 knockdown in fibroblasts, as previously discussed, can result in cytoskeletal changes to promote lamellipodia formation (Machacek et al., 2009). However, despite the possibility that Cx43 asODN may have had an effect on fibroblast migration, differences in Cx43 expression within the dermis was not visually apparent in this study. This may be due to the time points investigated or even due to additional unknown mechanisms by which Cx43 knockdown may act.

The presence of hair regrowth, scab formation and the ability of scaffolds to mask the wound prevented accurate measurements being made from macroscopic evaluations, but microscopic assessment revealed significant differences between the scaffold treatments. Because of the ease at which scaffolds separated from the wound edge, it appeared that coated scaffolds may be behaving purely as a drug delivery reservoir; acting in a different capacity to a matrix supporting cell growth and wound regeneration. The biological effect of applying Cx43 asODN coated scaffolds to wounds resulted in a clear and significant effect on wound re-epithelialisation (Figure 4. 5, Figure 4. 6 & Figure 4. 7). This finding, along with the observations that wound size reduction was slightly enhanced, suggested that coating scaffolds with Cx43 asODN in layers of PLGA and PCL may actually improve wound healing, in stark contrast to the previous chapter where bioactivation appeared to only reduce the side effects of using collagen scaffolds. The positive results obtained in this chapter are in agreement with other Cx43 asODN studies, where wound re-epithelialisation was found to be accelerated following Cx43 asODN application (Qiu et al., 2003, Wang et al., 2007). In this case, it appears to be the first time a similar result has been achieved using a sustained asODN delivery approach. The enhancement to re-epithelialisation following Cx43 asODN scaffold application was accompanied by the reduction in thickness of the

leading edge epidermis at the wound (Figure 4. 8). This mirrors the findings of the previous chapter in mice, where transient scaffold bioactivation with Cx43 asODN reduced epithelial thickening relative to unocated scaffolds. This outcome also agrees with findings in STZ diabetic rats, where diabetic wound edge epidermis thickened and re-epithelialisation was retarded, yet Cx43 asODN was found to overturn these effects (Wang et al., 2007). The control coated scaffolds also resulted in a lower degree of leading edge thickening than the uncoated scaffolds, and in some cases was not significantly different to Cx43 asODN coated scaffold-treated wounds. This could imply that the coating confers a greater degree of biocompatibility to the scaffold, or it could alternatively be the result of the reduced association and integration of coated scaffolds with the wound edge compared to uncoated scaffolds.

The application of Cx43 asODN coated scaffolds reduced the number of polymorphonuclear leukocytes (PMNs) infiltrating the dermis distal to the wound edge relative to control scaffolds (Figure 4. 9). Unlike in the previous chapter, where transiently bioactivated scaffolds still resulted in higher numbers of PMNs than untreated wounds in mice, the application of the coated bioactive scafolds to rats resulted in the lowest PMN counts across all treatments at all time points. PMN counts for bioactive scaffold-treated wounds was also lower than untreated wounds, although significance between was not obtained. In a chronic ulcer where the inflammatory phase is protracted, this could be a useful feature of an applied scaffold (Pierce, 2001).

The effects of enhanced re-epithelialisation occurred in conjunction with Cx43 downregulation at D1, D3 and D5, relative to the control-treated scaffolds where Cx43 expression was again conversely upregulated (Figure 4. 11, 13, and 15). It is reported that within 6 h after wounding Cx43 is normally downregulated in keratinocytes at the wound edge and this is a necessary step for cells to undergo migration (Coutinho et al., 2003). The enhanced knockdown of Cx43 using Cx43 asODN may help speed up this process to cause keratinocytes to initiate re-epithelialisation sooner and at an enhanced rate. The effect of Cx43 downregulation on the adoption of a migratory phenotype in keratinocytes has, similar to in fibroblasts, been linked to a reduced level of protein-protein interactions with cytoskeletal components (Hunter et al., 2005). However, Cx43 may also behave as a master regulator with the ability to influence expression of over 300 other genes (Iacobas et al., 2007). Knockdown of Cx43 may therefore also have an effect on other proteins at the

transcriptional level, which could result in acceleration of wound healing. Unlike in mouse wounds in chapter 3, Cx43 in the Cx43 asODN-treated rat wounds remained downregulated, even at the later time point of D5. This could be due to the continued effect of asODN, which would likely have been present in the wound for a considerably greater period of time than when applied using Pluronic gel. However, sODN coated scaffolds resulted in variable levels of wound edge Cx43 expression and although they caused wound edge upregulation of Cx43 relative to distal levels unlike bioactivated scaffolds, the difference was not significant. While untreated wound edges downregulated Cx43 as typical of acute wound healing, the Cx43 asODN coated scaffold appeared to downregulate Cx43 expression to a greater degree.

It was interesting to again observe that scaffolds bioactivated with Cx43 asODN influenced wound edge keratinocyte Cx26 expression, similar to in the mouse study (Figure 4. 10, Figure 4. 12 & Figure 4. 14). While Cx43 asODN coated scaffolds had no significant effect on Cx26 expression at D1, at D3 and D5 the bioactivated scaffolds resulted in significantly lower levels of expression than the other scaffold treatments. While it is not clear how Cx43 and Cx26 are linked, the two proteins have both been found to be upregulated in situations of perturbed wound healing (Labarthe et al., 1998, Mendoza-Naranjo et al., 2012a, Mendoza-Naranjo et al., 2012b, Wang et al., 2007). Immunostaining has revealed both connexin proteins to be strongly upregulated within the same non-migratory wound edge keratinocytes in the ulcer tissue. Another explanation could again be that Cx43 adopts the role of a master regulator capable of influencing Cx26 expression through downstream effects, although further investigation to support this theory is required (Iacobas et al., 2007).

While *in vitro* assays had highlighted the ability of scaffold coatings to elute asODN in a sustained manner, evaluation of treated wounds at D10 and D15 gave a clearer indication of the effects of long-term Cx43 asODN delivery on the later stages of wound healing. At the selected late stage time points scaffolds were no longer visible within wounds when they were harvested. This could be due to considerable degradation of the coating layers and scaffold fibres by this time, but may also be due to the loss of the shrunken scaffolds from the heavily contracted wounds, which had never integrated considerably with the coated scaffolds to begin with (Ishaug et al., 1994). The gradual detachment of Tegaderm film securing scaffolds to wounds before these time points also adds to this possibility.

Nevertheless, wounds that received a Cx43 asODN bioactivated coated scaffold had significantly smaller defined regions of granulation tissue, the tissue rich in cigar-shaped fibroblasts and blood vessels, than all the other treatments (Figure 4. 16 & 17).

Cx43 asODN coated scaffold-treated wounds appeared to be further ahead in the wound contraction process than the other treatments, including scaffolds that were coated identically except using sODN instead of asODN. One possible explanation for this is that Cx43 knockdown can promote fibroblast migration, which could have resulted in the appearance of myofibroblasts in the wound sooner (Mori et al., 2006). Myofibroblasts normally contract intracellular bundles of α-SMA to help pull the margins of a wound together (Hinz et al., 2001). Initially appearing at the wound margins, myofibroblasts eventually migrate towards the centre of the wound around 7-14 days and are then lost, possibly through apoptosis (Mori et al., 2006). Staining control coated scaffold wounds with an anti-α-SMA antibody revealed large regions of positive staining throughout the entirety of the wound, including close to the wound margins (Figure 4. 18). In contrast, Cx43 asODN coated scaffolds resulted in a significantly smaller area of α-SMA staining and the stained region was highly localised to the centre of the wound. The possibility that Cx43 knockdown enhances myofibroblast activity to promote wound contraction is supported by this observation; Cx43 asODN-treated wounds had both the smallest staining regions of α-SMA and myofibroblasts were centrally located, which is normally associated with myofibroblasts that are soon to be lost (Mori et al., 2006). By D15 there was no convincing staining of α-SMA to image across the two different treatments, which appeared to suggest that myofibroblasts were no longer present in the majority of wounds by this stage.

Conclusions

Using an emulsion technique a multi-layered Cx43 asODN eluting scaffold can be fabricated that released asODN over 7 days. Following application *in vivo*, the coated scaffolds appeared to offer multiple advantages over transient bioactivation with Cx43 asODN in the previous chapter. Coated scaffolds did not appear to inhibit wound contraction between D1-D5, while also maintaining Cx43 down-regulation throughout at least the first 5 days of wound healing. In both this and the previous chapter, it became

increasingly apparent that Cx26 was linked to wounds in which healing was perturbed. Cx26 up-regulation has also been linked to hyperproliferative skin conditions (Labarthe et al., 1998), and ectopic Cx26 has also been found to delay restoration of the epidermal barrier and promote the formation of an inflammatory response (Djalilian et al., 2006). By some mechanism, Cx43 asODN treated scaffolds resulted in significant decreases in wound edge keratinocyte Cx26 expression at D3-D5, although not at the onset of wound healing.

As devices intended to ultimately promote healing of full-thickness wounds such as chronic ulcers, it would also be useful to develop the coating to deliver drugs that can target other deregulated proteins such as, potentially, Cx26. However, it remained to be seen whether a potential Cx26 asODN sequence alone could also improve wound healing, especially since Cx26 is normally strongly upregulated at the wound edge of healing acute wounds (Coutinho et al., 2003).

CHAPTER 5

Targeting Cx26 expression using scaffolds

5.1 – Introduction

Following the redesign of my polymer coating for scaffolds outlined in the previous chapter, Cx43 asODN was found to elute over 7 days following a series of *in vitro* elution assays. This extended release profile had a positive effect on wound healing *in vivo*. As a means of potentially further improving scaffolds as therapeutic devices, attention was focused on Cx26.

There is currently a greater understanding of the role of Cx43 in wound healing than Cx26 – Cx43 is naturally downregulated in wound edge cells within the first 6-24 h and coincides with the adoption of a migratory phenotype both in keratinocytes and fibroblasts (Coutinho et al., 2003). In situations when Cx43 is not downregulated, such as in diabetic and chronic wounds, cell migration is significantly perturbed and wound healing is severely retarded (Mendoza-Naranjo et al., 2012a, Mendoza-Naranjo et al., 2012b, Wang et al., 2007). Throughout both chapters 3 and 4, it was clear that Cx26, as well as Cx43, was strongly upregulated in thickened bulbs of keratinocytes when wound healing was perturbed.

The role of Cx26 in wound healing is less clear. While it is known that Cx26 and Cx30 are strongly upregulated in wound edge keratinocytes within 24 h, it is not fully understood how this affects wound healing (Coutinho et al., 2003). As previously discussed, one possible explanation is that wound edge keratinocytes form a communication compartment separate to the keratinocytes further away in the uninjured epidermis. While Cx43 is downregulated in the basal layer, Cx26 and Cx30 are instead upregulated in the spinous layers of keratinocytes following injury (Coutinho et al., 2003). Since Cx26 and Cx30 can interact with each other, but not Cx43, it is possible that two connexins could establish a unique compartment with properties distinct to the rest of the epidermis (Marziano et al., 2003). In this way, it is possible that wound edge keratinocytes cannot interact with the rest of the epidermis through connexins, possibly resulting in reduced cell adhesion and the transition to a migratory cell phenotype.

It is unclear whether the Cx26 that is expressed in migratory keratinocytes during re-epithelialisation is beneficial to wound healing. In the previous chapter it was found that Cx43 asODN appeared to reduce wound edge keratinocyte Cx26 expression at D3 and D5, and this occurred alongside an improvement to re-epithelialisation (Figures 4. 10 & 4. 12).

This observation could have been due to Cx43 asODN effectively appearing to advance wound re-epithelialisation by 1-2 days, potentially to a stage where Cx26 levels begin to reduce naturally. While it is unclear what effect Cx26 downregulation may have, the ectopic overexpression of Cx26, similar to that observed following the application of uncoated scaffolds, has been shown to delay the restoration of the epithelial barrier (Djalilian et al., 2006). Cx26 up-regulation has also been linked to hyperproliferative skin conditions (Labarthe et al., 1998) and more recently, Sutcliffe et al. reported that Cx26 was strongly upregulated in chronic ulcers similar to Cx43 (journal article submitted). Because of this, it was proposed that Cx26 upregulation could be involved in the formation of thickened bulbs of keratinocytes, a possibility strengthened by the fact the bulbs express high levels of Cx26 following application of scaffolds (Figures 3. 3 & 4. 10). It has been previously postulated that Cx26 expression may be necessary in wound edge keratinocytes in order for migration to occur (Coutinho et al., 2003). However, it has separately been shown using *in vitro* scratch wound healing migration assays that mutant cells expressing nonfunctional Cx26 did not migrate slower, but nor did they migrate faster (Thomas et al., 2007). Our current understanding is insufficient to make definitive statements, but Cx26 expression in migrating keratinocytes may not actually be necessary to promote wound healing.

Despite investigations into the effects of Cx26 mutations, the role of Cx26 downregulation in wound healing has not been sufficiently analysed. Since Cx26 upregulation appears to be associated with perturbed healing and hyperproliferative skin conditions, it seemed possible that downregulation of Cx26 could actually be beneficial to healing. Targeted Cx26 downregulation could perhaps be even more effective in situations where Cx26 would be upregulated to extreme levels, such as in the epidermis of scaffold-treated wound or in a chronic ulcer (Sutcliffe et al., submitted journal article). Furthermore, if Cx26 asODN was found to have a positive effect on wound healing, it is possible that its combination with the previously tested Cx43 asODN sequence may even yield a synergistic effect. In the CoDa laboratory in New Zealand, a series of Cx26 asODN sequences have recently been designed. Following a pilot screening of a number of sequences in an *in vivo* mouse experiment performed in the laboratory, two sequences (termed 'AS3' and 'AS6') that appeared to have a mild positive effect on wound closure were previously identified. Using these two sequences, it was proposed that the scaffold coating method devised in the previous chapter could also be used to incorporate and deliver Cx26 asODN to wounds. If this resulted in Cx26 knockdown in migrating wound edge keratinocytes it could validate

the efficacy of the sequences and may also reveal what effect the knockdown of Cx26 had on wound re-epithelialisation and inflammation. Success using other asODN sequences could also highlight the potential of the developed coating method as an off-the-shelf method of delivering multiple different sequences. Since Cx43 asODN had a positive effect on wound healing, it was also proposed that if Cx26 asODN improved wound healing, the combined application of both Cx26 and Cx43 asODN in a coating might result in a synergistic effect. With this in mind, the efficacy of the new Cx26 asODN sequences on the healing of rat full-thickness wounds relative to control and Cx43 asODN scaffold treatments was investigated.

The aims of this chapter were as follows:

To adapt the scaffold coating approach to incorporate the novel Cx26 asODN sequences into a scaffold coating.

To confirm the efficacy of the asODN sequences *in vivo*, through application of coated Cx26 asODN scaffolds to rat full-thickness wounds followed by immunostaining, re-epithelialisation and inflammatory cell analysis.

To investigate whether combined Cx26 and Cx43 asODN scaffold applications had a synergistic effect on wound healing.

5.2 – Materials and Methods

See Chapter 2 for a detailed description of the individual methods, reagents and equipment employed. A condensed explanation of the methods used in this chapter is listed below.

5.21 – Scaffold fabrication

Collagen scaffolds were fabricated through use of the same electrospinning technique used throughout the previous 2 chapters, a detailed explanation of which is provided in chapter 2.

5.22 – Application of polymer coatings containing Cx26 or Cx43 asODN to scaffolds

Both Cx43 and Cx26 asODN sequences were incorporated into polymer coatings using the emulsion technique employed in chapter 4. The same rodent Cx43 asODN sequence used in both chapters 3 and 4 was used in for the purpose of coating scaffolds and had the sequence 5'-GTA ATT GCG GCA GGA GGA ATT GTT TCT GTC-3'. A non-functional sense (sODN) sequence to this Cx43 asODN was also incorporated to create one of the control scaffold treatments, and had the sequence: 5'- GAC AGA AAC AAT TCC TCC TGC CGC AAT TAC-3'.

In the case of Cx26 asODN, two different novel sequences (termed 'AS3' and 'AS6') that have been previously developed by CoDa Therapeutics Inc. in New Zealand had been identified to be potentially effective following pilot *in vivo* screening of multiple sequences. Both sequences are 20-mers (sequences currently undisclosed at the instruction of CoDa). Due to the limited time remaining in the PhD to examine each individually, both Cx26 sequences were instead combined into one coating. Cross-annealing between the two asODN sequences was first ruled out before opting to combine the sequences. Either PCL or Poly(D, L-lactice-co-glycolide) (PLGA) was dissolved in the solvent dimethyl carbonate at 10% wt./v. using gentle rocking. The individual asODN sequences were dissolved in nuclease-free water and mixed with the polymer solutions at a 300 μM final DNA concentration. In the case of Cx26 asODN, both AS3 and AS6 sequences were each dissolved at a final concentration of 300 μM, and for the combined Cx43 + Cx26 asODN scaffolds the three asODN sequences were each incorporated at a 300 μM concentration. The two immiscible layers were processed for 10 seconds using a handheld homogeniser on a medium setting at room temperature to produce an emulsion. After preparing the coating mixture, individual 6 mm collagen scaffolds were dipped for 1 second in the desired polymer-asODN solutions and immediately placed in a tube of liquid nitrogen and lyophilised overnight to remove the solvent from the scaffolds in order to maintain the structure of the scaffold. This coating process, from dipping to freeze drying, was repeated 7 times, such that each scaffold received 4 coating layers of PCL + asODN followed by 4 layers of PLGA + asODN (8 layers in total).

5.23 – Surgery

Six week old Sprague Dawley rats were anaesthetised using 4% isoflurane, 20% oxygen and 10% nitrous oxide, and maintained using 1.5% isoflurane. Animals were injected subcutaneously with 0.03 mg/ml buprenorphine (Vetergesic®) before operation. Rat backs were shaved and covered in a thin layer of Nair® hair removal cream, after which both the cream and hair was removed using a warm moistened gauze pad. Animals were placed on heated mats for the operation. Four full-thickness excisional biopsy punch wounds were made using a 6 mm medical biopsy punch to rodent backs, two on each side of the dorsal midline. Scaffold treatments were applied directly to wounds, after which the back was covered with a sheet of Tegaderm™ film. Post-procedure, animals were kept in a heated chamber and monitored for recovery. Once recovered, animals were rehoused in standard individual cages.

5.24 – Processing and histology

Harvesting wounds

Animals were culled by cervical dislocation at 1, 3, 5, 10 & 15 days post wounding. Wounds were macroscopically imaged at D1 - 5 as outlined in Chapter 2. Wounds were then excised and fixed in 4% paraformaldehyde (PFA)-PBS solution for 24 h at 4°C. Tissue was immersed in 20% sucrose overnight then washed in PBS, after which wounds were bisected. Half of each wound was snap frozen in O.C.T. medium, then sectioned using a cryostat at a thickness of either 5 μm (for H&E staining) or 10 μm (for immunofluorescence staining).

Haematoxylin and eosin staining

Frozen tissue sections were thawed for 5 min then covered completely in tap water for 5 min at room temperature. Slides were submerged in Harris' haematoxylin solution for 30 seconds followed by immersion in a container full of running tap water for 5 min. Background staining was reduced by dipping the slides in a container full of 1% acid alcohol (1% glacial hydrochloric acid, 70% ethanol, 29% distilled water) for 3 seconds, after which slides were immersed in a container of running tap water for a further 5 min. Samples were then submerged for 15 seconds in a container full of eosin B solution, followed by immersion for 5 seconds in a container full of tap water to rinse away excess

stain. Slides were then immersed in 70% ethanol for 2 min, 100% ethanol for 2 min and a second container of 100% ethanol for a further 2 min, to dehydrate the sections. Slides were then submerged in a container full of xylene for 5 min, then a second container of xylene for an additional 5 min. Slides were then individually removed and mounted using DPX mounting media.

Immunofluorescence staining

Tissue sections were permeabilised in cold acetone for 5 min and then using a 0.1 M L-lysine PBS solution containing 0.1% Triton-X-100. Sections were stained for 1 h using a rabbit polyclonal antibody to Cx43 (1:2000 dilution, C6219, Sigma Aldrich UK) or Cx26 (1:200 dilution, (Diez et al., 1999). Sections were then stained using a goat anti-rabbit Alexa 488 secondary antibody (A11008, Invitrogen UK) at a 1:400 dilution for 1 h. Tissue was counterstained using Hoechst solution (both Hoechst 33528 and Hoechst 33342 dyes at 1:50,000 dilution, Sigma Aldrich UK).

5.25 – Analysis

Imaging

Wounds were macroscopically and microscopically imaged as outlined in Chapter 2. Tissue sections immunostained for Cx26 or Cx43 and Hoechst were imaged using confocal microscopy. Single optical section 8-bit images were acquired at the wound edge and at a distal region of skin at 1024 by 1024 pixels. Image settings were consistent between treatments.

Epidermal thickening and re-epithelialisation measurements

Epidermal thickness was measured on H&E stained tissue and determined by measuring the thickest point along the basal to spinous layer axis within the end 150 μm of nascent epidermis using ImageJ. The length of nascent epidermis outgrowing from the wound margin was measured at either side of the wound using ImageJ and averaged to return a re-epithelialisation distance measurement for each sample.

Connexin 26 and 43 protein quantification

Cx43 and Cx26 protein expression was quantified on D1, D3 and D5 wounds by counting positive pixels on binary images of wound edges using ImageJ software using the method outlined in a study by (Wang et al., 2007). Images from each experiment were identically thresholded and the number of connexin positive pixels within the end 100 μm quantified. Connexin levels were expressed per square micron of epidermis and normalised to distal levels to reduce sample variation. In the case of Cx26, distal levels were extremely low, to the extent that small fluctuations between samples could result in large differences between values. For this reason, Cx26 distal levels were averaged for the group, and this averaged value was used to calculate changes in wound edge keratinocyte Cx26 expression for each animal.

Polymorphonuclear cell quantification

H&E stained D1, D3 and D5 rat full-thickness wounds were microscopically assessed at 63 X. At 700 μm from the wound edge in the lower dermis, rounded cells with a polymorphonuclear morphology (PMNs) were identified and counted in a single field of view as a means to quantify inflammatory leukocytes infiltrating the uninjured tissue. A total of n=5 wounds were assessed per time point and treatment and values were averaged.

Measurement of granulation tissue area

Rat wounds harvested at D10 and D15 were H&E stained and loaded into an automated Zeiss Axio Scan.Z1 slide scanner. Brightfield images were captured using a 20 X objective, then automatically stitched together to form a montage. Montages were then imported into ImageJ. The granulation tissue (or wound region) was defined as the new area of tissue within the wound margins yet above the muscle and panniculus carnosus layers, and was measured using the freehand line tool within the program.

Assessment of smooth muscle actin area

Rat wounds harvested at D10 were loaded into the same Zeiss slide scanner and imaged using a 20 X objective using the built in image acquisition wizard. Hoechst and Alexa 488 fluorophores were excited to produce a montage image of the tissue. SMA staining in the green channel was thresholded in the software to a level that allowed visualisation of both SMA positive blood vessels as well as a positive staining region in the wound gap, above

the panniculus carnosus. This area was drawn around using a marker tool within the proprietary ZEN 2012 software and an area in square microns was displayed. This approach was applied in the same manner to each of the 8 samples in each treatment group.

Statistical analyses

Sample size was determined using power analysis software G*Power as described in Chapter 2. Data was subjected to Kolmogorov-Smirnov tests using GraphPad Prism 5.0 software to ascertain normality, then to one-way ANOVA tests followed by Tukey's post-hoc tests to determine statistical significance.

5.3 – Wound healing response to a Cx26 asODN coated scaffold

In order to assess the efficacy of the Cx26 asODN sequences on Cx26 knockdown *in vivo*, collagen scaffolds that had been coated in two Cx26 asODN sequences were applied to 6 mm diameter full thickness wounds made to the dorsum of rats. In addition to this, some scaffolds were coated with both the Cx26 asODN sequences as well as the Cx43 asODN sequence resulting in a combined 'Cx26/43 asODN' coated scaffold. Rats treated with both scaffold types were culled at D1, 3 and 5, after which the wounds were macroscopically assessed and compared to the control and Cx43 asODN treatments (Figure 5. 1).

5.31 – Evaluation of macroscopic wound closure

At D1, wounds across all treatments appeared macroscopically similar in size to the initial 6 mm wounds made at 0 h (Figure 5. 1). At D3, both the Cx26 asODN and Cx26/43 asODN coated scaffold-treated wounds had reduced in size to a level comparable to that of untreated wounds, which was slightly smaller than control coated scaffold-treated wounds. Wounds treated with both scaffold types containing Cx26 asODN appeared markedly reduced in size relative to the uncoated scaffold, similar to the Cx43 asODN coated scaffolds. By D5, wounds treated with the Cx26 and Cx26/43 asODN coated scaffolds had considerably reduced in size, to the extent of untreated wounds or greater, although hair regrowth and the presence of scaffolds could obscure the wound margins.

Similar to the Cx43 asODN coated scaffolds, both of the Cx26 asODN containing scaffolds reduced in size over the duration of wound healing at a greater rate than the uncoated scaffolds, while also exhibiting minimal integration with the wound edge. The combined Cx26/43 asODN scaffold treated wounds did not, on average, appear markedly reduced in size relative to the Cx26 only asODN or Cx43 asODN only scaffold treatments.

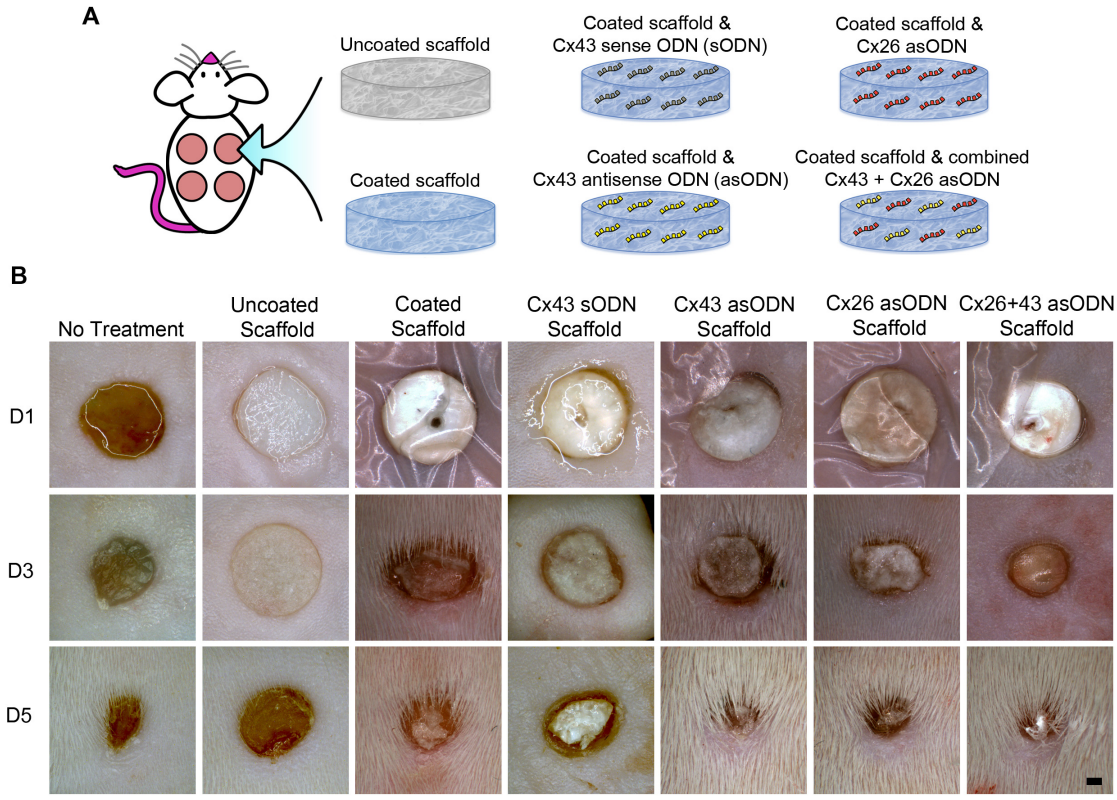

Figure 5. 1 – Effect of scaffold application on macroscopic wound appearance **(A)**: Full thickness rat wounds were treated with Cx26 asODN only coated scaffolds or scaffolds coated in both Cx26 asODN and Cx43 asODN. These treatments were compared to existing scaffold treatments as well as untreated wounds. **(B)**: Animals (n=8) were culled at either 1, 3 or 5 days (D1, D3 & D5) after wounding and the wounds macroscopically imaged. Scale bar = 1 mm.

5.32 – Cx26 asODN coated scaffolds significantly improve wound re-epithelialisation

Similar to in the previous chapter, the PLGA and PCL coated scaffolds containing Cx26 asODN sectioned poorly relative to the uncoated scaffolds, and exhibited a considerable lack of integration with the wound edge. Coated scaffolds often curled up following sectioning or became easily detached during wound processing. All re-epithelialisation values are reported as the means of n=8 animals ± SEM. Following microscopic evaluation of wound re-epithelialisation at D1, wounds treated with the Cx26 asODN only scaffold had re-epithelialised a distance of 404 ± 29 μm μm, which was a significant 47.5% increase over the 274 μm ± 27.1 μm of untreated wounds (Figure 5. 2, $P < 0.05$). This was similar to the average distance for Cx43 asODN scaffold treated wounds (407 μm ± 32 μm). Furthermore, the combined Cx26/43 asODN coated scaffolds resulted in a moderately higher re-epithelialisation distance (494 ± 40.8 μm) over scaffolds containing asODN against only one type of connexin. Combining both Cx26 and 43 asODNs in a coating increased re-epithelialisation by 22.3% over Cx43 asODN only scaffolds.

In order to assess whether Cx26 asODN and Cx26/43 asODN coated scaffolds had a similar effect on healing at later time points, wound re-epithelialisation was also measured at D3 (Figure 5. 3). The Cx26 asODN only coated scaffolds had re-epithelialised on average 791 ± 53.1 μm. This was significantly improved over the three control scaffold treatments, which had on average re-epithelialised only 50.8% as far ($P < 0.05$, $P < 0.01$ and $P < 0.001$). This distance was not significantly different from Cx43 asODN only treated wounds, however. Additionally, re-epithelialisation of the Cx26 asODN only scaffold-treated was insignificantly different from untreated wounds, in contrast to the Cx43 asODN only scaffolds. Similar to D1, wounds treated with scaffolds containing the combined Cx26 and Cx43 asODN sequences had re-epithelialised the furthest distance. At an average of 972 ± 118.3 μm, combined asODN scaffold-treated wounds had re-epithelialised significantly further than every non-asODN treatment. Wounds treated with the combined asODN scaffold had re-epithelialised 12% further than those treated with the Cx43 asODN scaffold, and 18.6% further than those treated with the Cx26 asODN only scaffold.

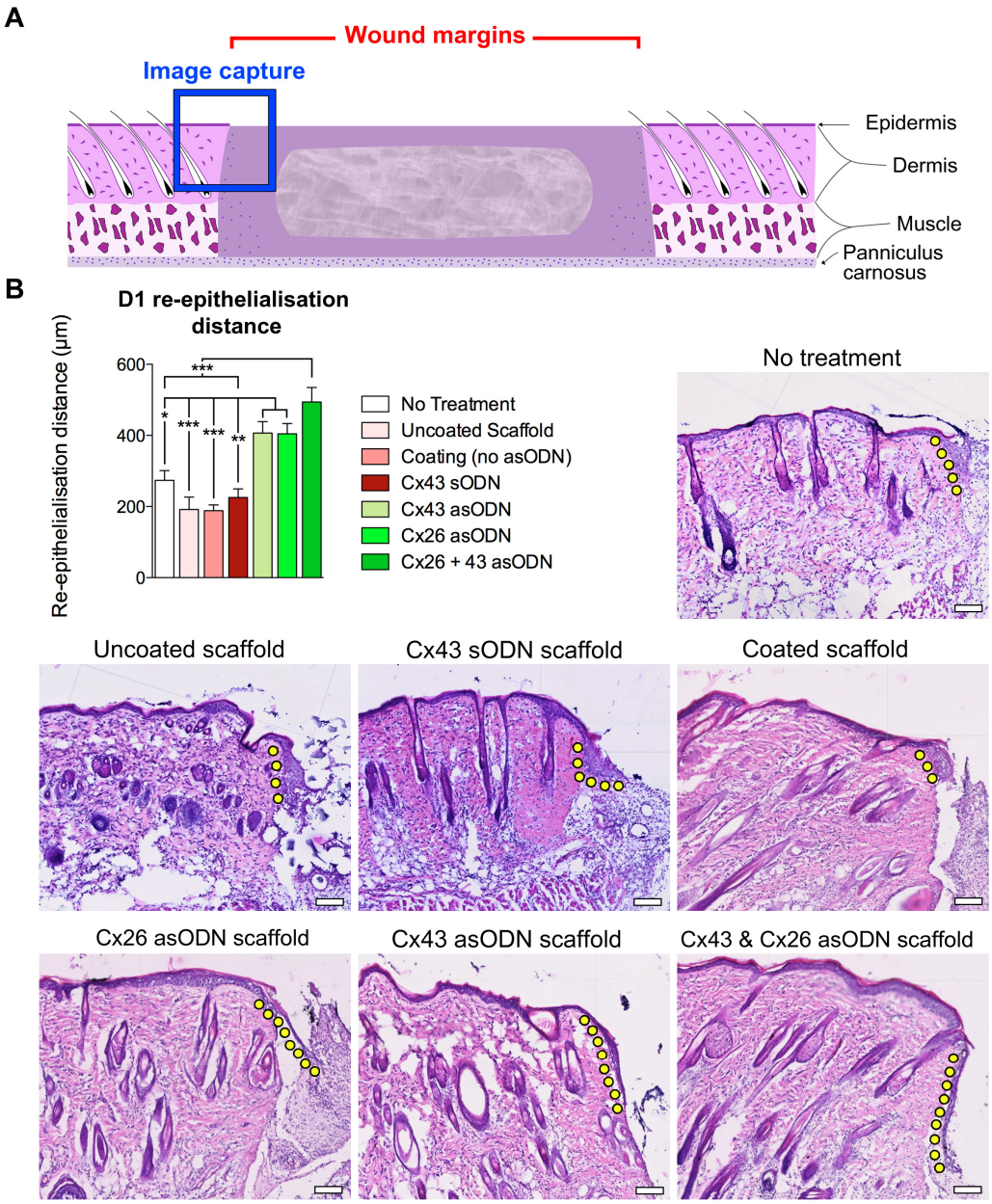

Figure 5. 2 – D1 full-thickness wound healing following application of scaffolds coated with Cx26 asODN

(A): A simplified wound diagram to illustrate the site at which images were captured.

(B): Wounds were either left untreated or treated with a control scaffold (white/red bars) or coated scaffolds containing asODN (green bars). Wound re-epithelialisation distances outlined by dotted yellow lines were measured for each type of scaffold applied and plotted as a graph (top left). Eight rat wounds were assessed for re-epithelialisation, data plotted are means + SEM error bars (* = $P < 0.05$, ** = $P < 0.01$, ** = $P < 0.001$). Scale bar = 100 µm.

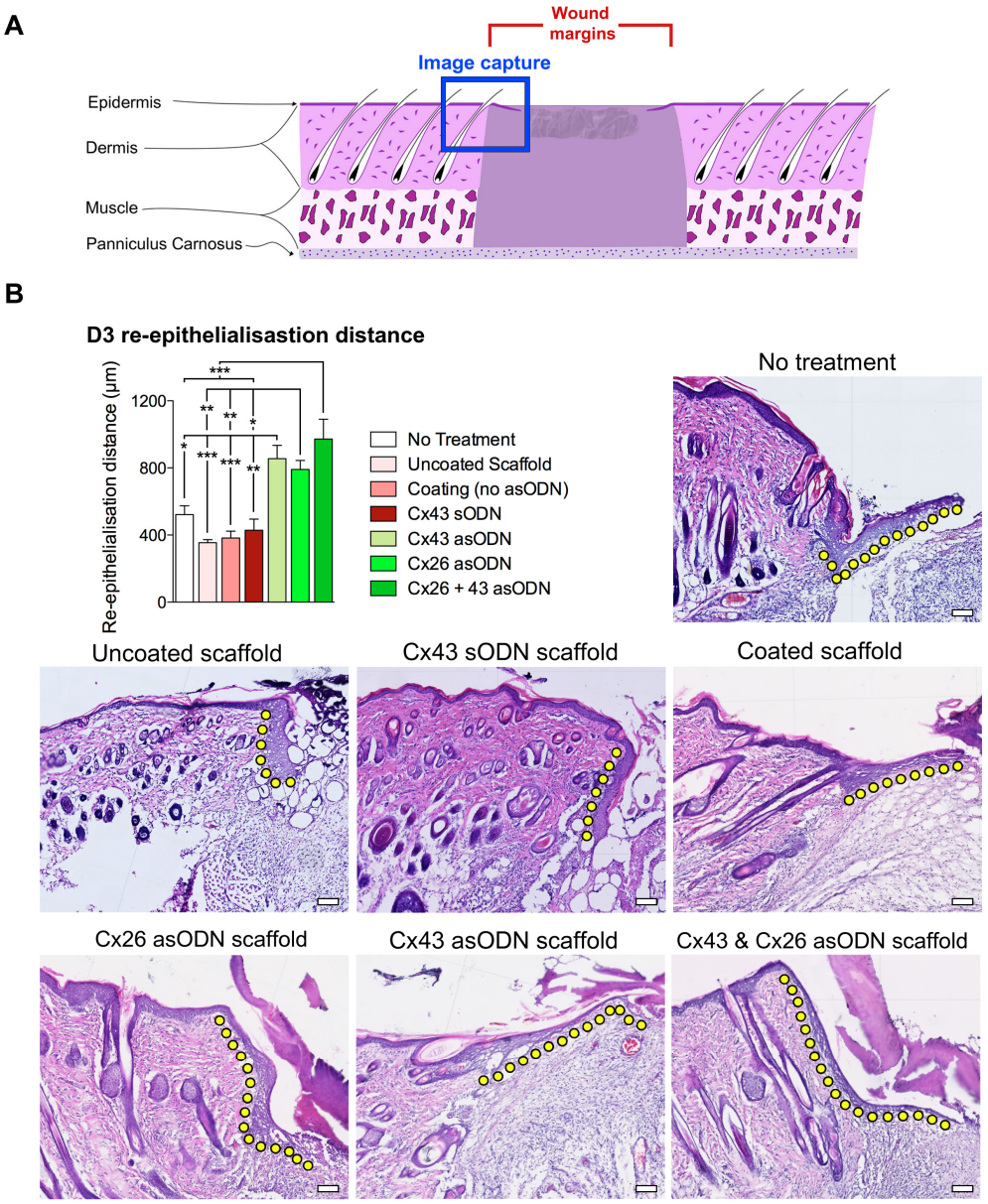

Figure 5. 3 – D3 full-thickness wound healing following application of scaffolds coated with Cx26 asODN

(A): A simplified wound diagram to illustrate the site at which images were captured.

(B): Wounds were either left untreated or treated with a control scaffold (white/red bars) or coated scaffolds containing asODN (green bars). Wound re-epithelialisation distances outlined by dotted yellow lines were measured for each type of scaffold applied and plotted as a graph (top left). Eight rat wounds were assessed for re-epithelialisation, data plotted are means + SEM error bars (* = $P < 0.05$, ** = $P < 0.01$, *** = $P < 0.001$). Scale bar = 100 µm.

Re-epithelialistion distance at D5 was also measured (Figure 5. 4). Cx26 asODN coated scaffold-treated wounds had re-epithelialised a distance of 1325 ± 43.4 μm, which was significantly further than untreated wounds (882 ± 47.3 μm, $P < 0.05$) and wounds treated with control coated scaffolds. Wounds treated with Cx26 asODN coated scaffolds had re-epithelialised significantly further than control coated scaffolds (806 ± 65.1 μm, $P < 0.01$), uncoated scaffolds (713 ± 132.1 μm, $P < 0.01$) and Cx43 sODN coated scaffolds (819 ± 62.5 μm, $P < 0.05$). The effect of Cx26 asODN on wound re-epithelialisation at D5 was similar to that of Cx43 asODN (1325 ± 43.4 μm vs. 1345 ± 97.7 μm, respectively). The combined Cx26 and Cx43 asODN scaffold again resulted in the greatest effect on re-epithelialisation, at 1695 ± 173.9 μm. This was 26% higher than wounds treated with Cx43 asODN only scaffolds and 27.9% greater than those treated with just the Cx26 asODN coated scaffolds. Across all wounds at D5, those receiving a scaffold that contained Cx43 asODN (either Cx43 asODN only scaffolds or both Cx43 and Cx26 asODN) had on 5 occasions fully re-epithelialised. Only 1 wound treated with the Cx26 asODN only scaffold had re-epithelialised, however, and only one of the control wounds had re-epithelialised.

Thickening of the nascent epidermis following Cx26 asODN scaffold application was also measured, since Cx26 expression is commonly linked to epithelial thickening disorders (Labarthe et al., 1998, Lucke et al., 1999) (Figure 5. 5). All thickening measurements are reported as means ± SEM. It was observed that at D1 ($P < 0.01$), D3 ($P < 0.001$) and D5 ($P < 0.001$) wounds treated with Cx26 asODN coated scaffolds had significantly lower epithelial thickening values than the uncoated scaffolds. Coating scaffolds with Cx26 asODN reduced epithelial thickening to a similar level of Cx43 asODN coated scaffolds at each time point. Cx26 asODN coated scaffolds resulted in measured epithelial thicknesses of 49.4 ± 7.9 μm (D1), 36.9 ± 5.5 μm (D3) and 33 ± 5 μm (D5), which were significantly thinner than the measured epithelia of most control scaffold treatments (Figure 5. 5). Cx26 asODN coated scaffold-treated wound edge epidermis was not significantly thinner than measurements for uncoated scaffold-tread wounds at D1 and D3 or Cx43 sODN scaffold-treated wounds at D1 and D5, however. The combined Cx26/43 asODN scaffold did not appear to have a synergistic effect in reducing epithelial thickening, as thickness measurements for the combined asODN scaffold were similar to the other bioactivated scaffolds. The combined Cx26 /43 asODN scaffold did, however, result in a significantly thinner measured epidermal leading edge than untreated wounds at D3 ($P < 0.05$).

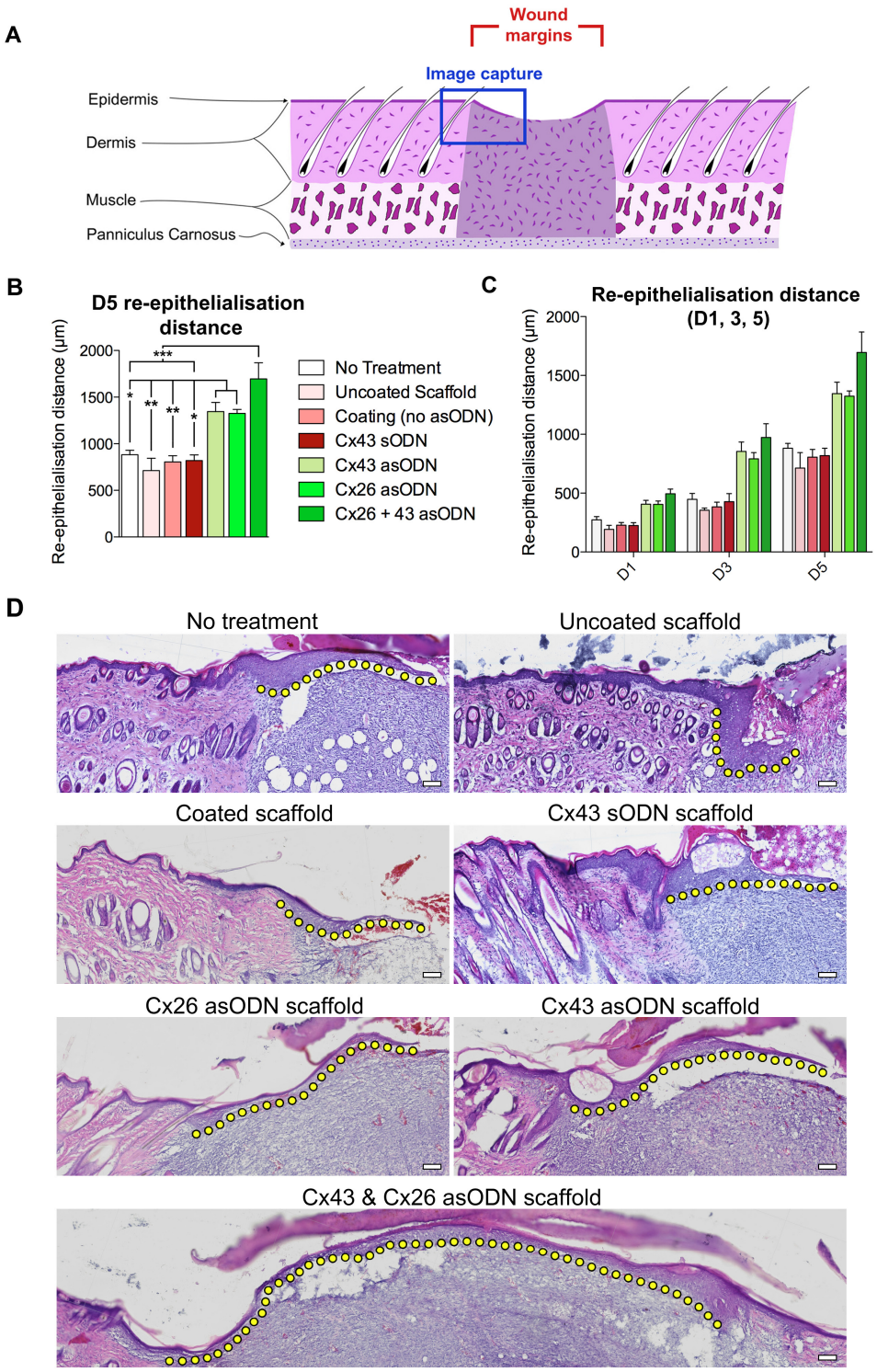

Figure 5. 4 – D5 full-thickness wound healing following application of scaffolds coated with Cx26 asODN

(A): A simplified wound diagram to illustrate the site at which images were captured.

(B): Wounds were either left untreated or treated with a control scaffold (white/red bars) or coated scaffolds containing asODN (green bars). Wound re-epithelialisation distances

outlined by dotted yellow lines were measured for each type of scaffold applied and plotted as a graph (top left). **(C)**: Each of the D1, D3 and D5 re-epithelialisation averages was individually plotted (see individual time points for significant differences). Eight rat wounds were assessed for re-epithelialisation, data plotted are means + SEM error bars (* = $P < 0.05$, ** = $P < 0.01$, *** = $P < 0.001$). Scalebar = 100 µm.

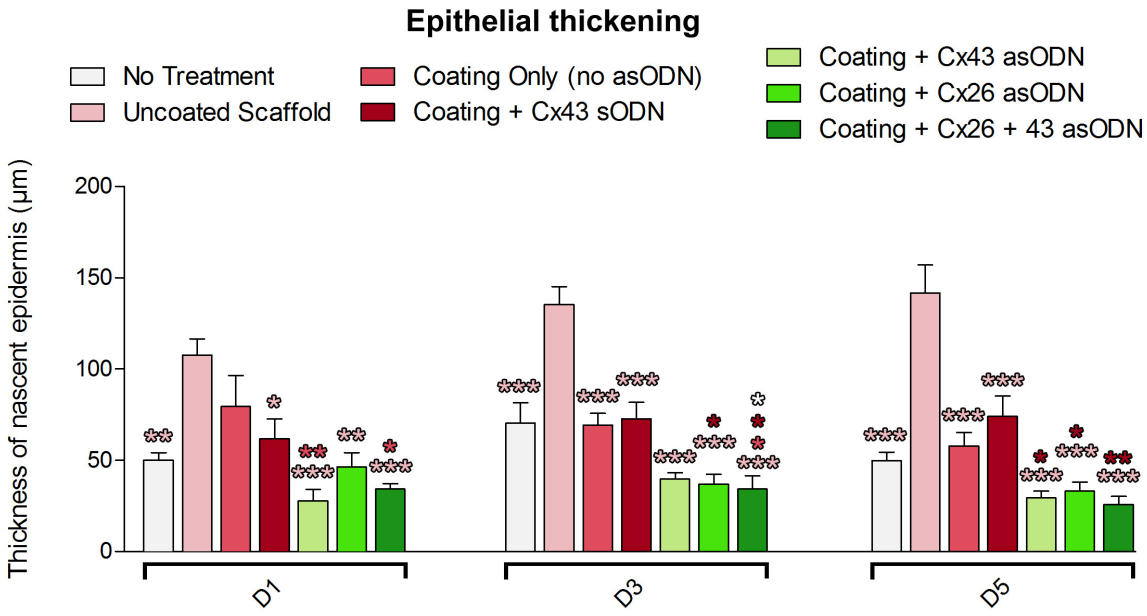

Figure 5. 5 – Thickening of the nascent epidermis following Cx26 asODN scaffold application.

The same full-thickness wounds treated with different types of scaffolds were also measured for epithelial thickness within the end 150 µm of the nascent tip of epidermis. Measurements were recorded across n=8 samples at D1, D3 and D5 (* = $P < 0.05$, ** = $P < 0.01$, *** = $P < 0.001$). Data values plotted are means + SEM error bars. Significance stars are coloured to match the treatment that is significantly different (e.g. white star = significantly different to untreated wounds).

5.33 - The effect of Cx26 asODN coated scaffolds on the local inflammatory cell response

In order to assess the effect of Cx26 asODN coated scaffolds on the infiltration of inflammatory cells, the number of individual cells with a rounded polymorphonuclear morphology characteristic of polymorphonuclear leukocytes (PMNs) were identified and measured in a region of dermis distal to the wound edge similar to the previous chapter (see chapter 2 for full method). This was performed in order to determine whether scaffolds caused extensive inflammatory cell invasion of the native tissue, and cell counts for each treatment are reported as means ± SEM (Figure 5. 6A). At D1, Cx26 asODN coated scaffolds resulted in the lowest PMN counts of any treatment, with an average of 11.6 ± 2.4 cells recorded in the region of dermis analysed (Figure 5. 6C). This was lower than that found using both Cx43 asODN coated scaffolds (15.6 ± 1.3) and the combined Cx26 + Cx43 asODN scaffolds (16 ± 4), although the differences were insignificant. Cx26 asODN scaffolds resulted in a significantly lower number of infiltrating PMNs than all control scaffold treatments at D1. The quantified number of PMNs for Cx26 asODN treated tissue were 82.5% lower than uncoated scaffolds (P <0.001), 70% lower than coating only scaffolds (P <0.05), and 78.4% lower than Cx43 sODN scaffolds (P <0.001).

At D3, the dermis distal to wounds treated with Cx26 asODN scaffolds contained a slightly higher number of PMNs relative to Cx43 asODN scaffold-treated wounds (27.4 ± 7.2 vs. 18.80 ± 14.1 cells) but this difference was insignificant (Figure 5. 6B-C). The dermis distal to Cx26 asODN scaffold treated wounds contained significantly reduced numbers of PMNs compared to uncoated scaffolds (71.2 ± 12.5, P <0.001) and coating + Cx43 sODN scaffolds (61 ± 5.3, P <0.01), but was not significantly lower than coating only scaffolds, although there was a marked difference (27.4 ± 7.2 vs. 48.6 ± 4.3 PMNs). Despite this, the combined Cx26 + Cx43 asODN scaffolds resulted in a count of 17 ± 2.6 PMNs, which was significantly lower than all three control scaffold types at D3.

Following on with measurements at D5, PMNs were greatly reduced across all treatments (Figure 5. 6C). Cx26 asODN coated scaffolds resulted in an average count of 8.2 ± 1.8 PMNs in the dermis, while the combined Cx26 + 43 asODN scaffold resulted in 9.8 ± 1.4. This was similar to the cell counts recorded for Cx43 asODN only scaffolds (9.4 ± 2.5 PMNs). Both the Cx26 and Cx26 + 43 coated scaffolds resulted in significantly lower numbers of quantified PMNs relative to control coating only scaffolds (P < 0.01) and Cx43

sODN scaffolds ($P < 0.05$), but not the control uncoated scaffolds, although the number was still lower. Cx26 asODN scaffold treated tissue PMNs were 76.6% reduced in the dermis from uncoated scaffold dermal measurements, and 73.7% reduced from the number quantified for Cx43 sODN scaffolds. These differences were similar to that of combined Cx26 + 43 asODN scaffolds. Although Cx26 asODN only, Cx43 asODN only and Cx26 + 43 asODN scaffolds did not significantly reduce PMN infiltration relative to untreated wounds, PMN counts were in a number of cases lower than wounds treated scaffolds not coated in Cx26 or Cx43 asODN.

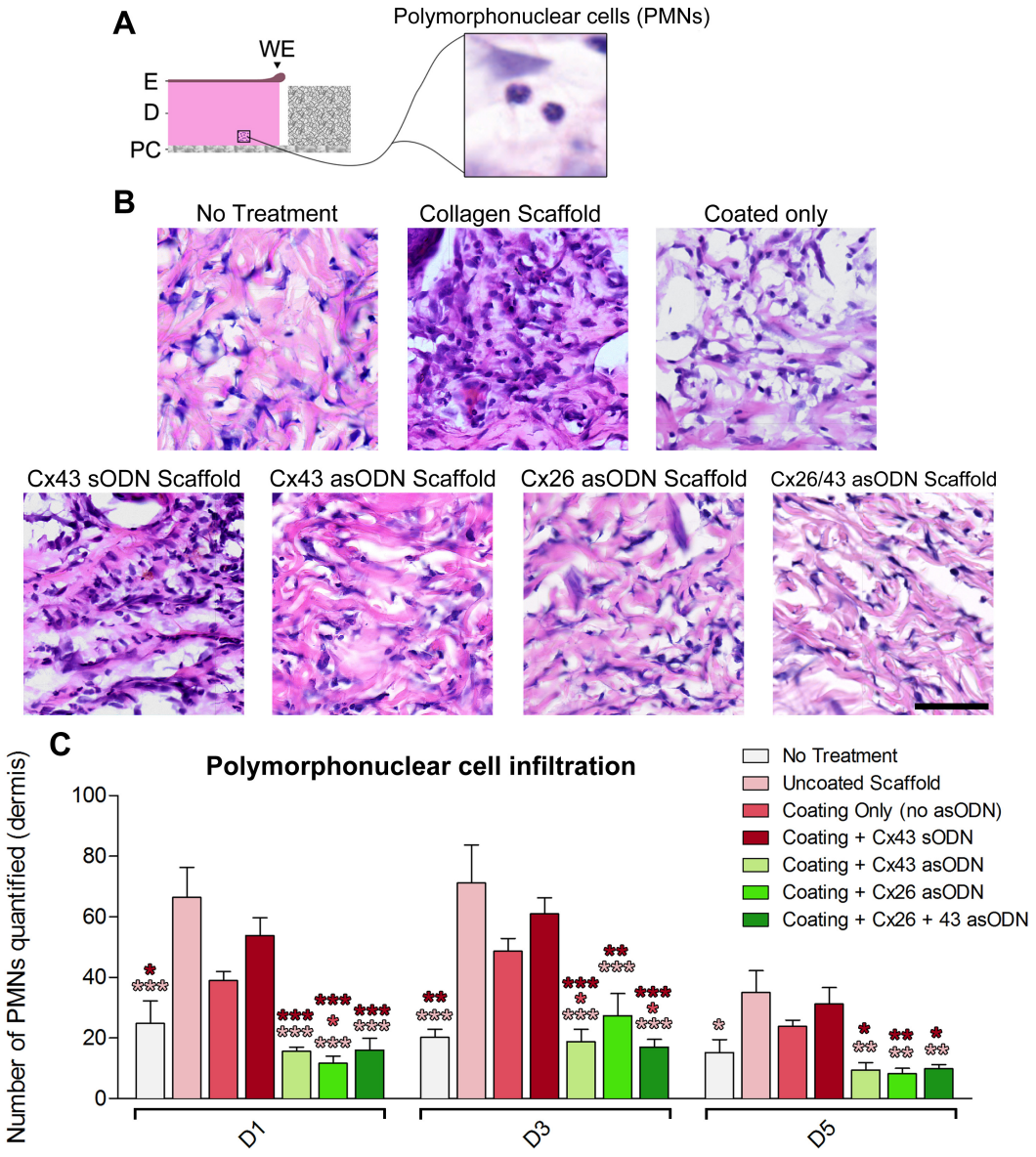

Figure 5. 6 – The effect of Cx26 asODN scaffold application on the number of polymorphonuclear cells (PMNs) infiltrating the unwound dermis.

Full-thickness wounds that received a scaffold treatment were assessed for polymorphonuclear cell invasion into the lower dermis 700 µm away from the wound edge as indicated in the diagram **(A)**. **(B)**: High-power typical images of the dermal region indicated in (A) for each scaffold treatment. The typical images shown are of the unwounded dermis distal to D3 wounds. Scale bar = 50 µm. **(C)**: Quantification of individual PMNs for each treatment across time points of D1, D3 and D5 were plotted as means + SEM error bars of n=5 samples. Diagram legend: E = epidermis, D = dermis, PC = panniculus carnosus, WE = wound edge (* = P <0.05, ** = P < 0.01, *** = P < 0.001). Significance stars are coloured to match the treatment that is significantly different (e.g. dark red star = significantly different to Cx43 sODN scaffold-treated wounds).

5.5 – Cx26 asODN promotes wound edge Cx26 downregulation

In order to examine whether the two Cx26 asODN sequences directly resulted in Cx26 knockdown at the wound, wound tissue sections were immunostained for Cx26. At D1, Cx26 was upregulated from distal levels in wound edge keratinocytes in both Cx26 asODN scaffold treated wounds (141.4% upregulation) and the combined Cx26/43 scaffold-treated wounds (225.6% upregulation) (Figure 5. 7). Despite this, the level of Cx26 upregulation was significantly lower than that measured in control treated wound edges, which were several thousand percent higher. Cx26 asODN only scaffolds did not result in a significant decrease in wound edge Cx26 expression relative to the Cx43 asODN only scaffold-treated wounds, although levels were decreased. Additionally, wound edge keratinocyte Cx26 levels were similar between both Cx26 asODN and combined Cx26/43 asODN scaffold treatments. The application of Cx26 asODN coated scaffolds did not result in a reduced level of wound edge Cx43 expression at D1 compared to untreated wounds, however; wounds exhibited a 121.9% upregulation of Cx43 similar to that found using control scaffolds (Figure 5. 8). Scaffolds containing both Cx26 and Cx43 asODN sequences however, resulted in an 85.9% downregulation of Cx43.

Wounds harvested at D3 that had been treated with a Cx26 asODN coated scaffold again featured reduced levels of Cx26 expression at the wound edge (Figure 5. 9). Wounds treated with scaffolds containing only Cx26 asODN featured a 48% downregulation of Cx26 at the wound edge, while for the combined Cx26/43 asODN scaffold this downregulation was 49.8%. For both types of scaffold this was significantly lower than untreated wounds as well as wounds treated with control scaffolds. Although Cx43 asODN coated scaffold-treated wound edges expressed significantly lower levels of Cx26 than the control treatments, expression was still upregulated and considerably higher than wound edges that had a scaffold applied containing Cx26 asODN. At D3, wounds that received Cx26 asODN scaffolds featured a 209.6% increase in Cx43 levels at the wound edge from distal levels (Figure 5. 10). Again, this was not found using scaffolds coated in both Cx26 and Cx43 asODN, which resulted in an 89% downregulation in Cx43 expression at the wound edge.

At the later time point of D5, wound edge keratinocyte Cx26 levels had considerably reduced from the levels at D3 across all treatments. Despite this, Cx26 asODN scaffolds resulted in significantly lower levels of Cx26 expression at the wound edge than other treatments (Figure 5. 11). Cx26 asODN scaffold-treated wound edge epidermis had downregulated Cx26 levels by 68.4% from distal levels, which was significantly lower than untreated wounds (199.2% upregulation), uncoated scaffolds (419.1% upregulation), control coated scaffolds (431.4% upregulation) and Cx43 sODN scaffolds (417.5% upregulation). Combined Cx26/43 asODN scaffolds resulted in a slightly greater downregulation of Cx26 asODN at the wound edge (an 87.4% downregulation) relative to the Cx26 asODN only scaffold. Although both types of scaffold containing Cx26 asODN reduced Cx26 levels compared to Cx43 asODN only scaffolds, the difference was not significant. In contrast to D1 and D3, at D5 the Cx26 asODN only scaffold resulted in a significant downregulation of Cx43 relative to the control scaffold treatments (Figure 5. 12). While control scaffolds all resulted in an upregulation of Cx43 at the wound edge epidermis, Cx26 asODN scaffolds resulted in a 62.3% downregulation of Cx43, similar to the 56.8% downregulation observed in untreated wounds. Scaffolds containing Cx43 asODN however, resulted in a greater downregulation of Cx43, although the difference was insignificant.

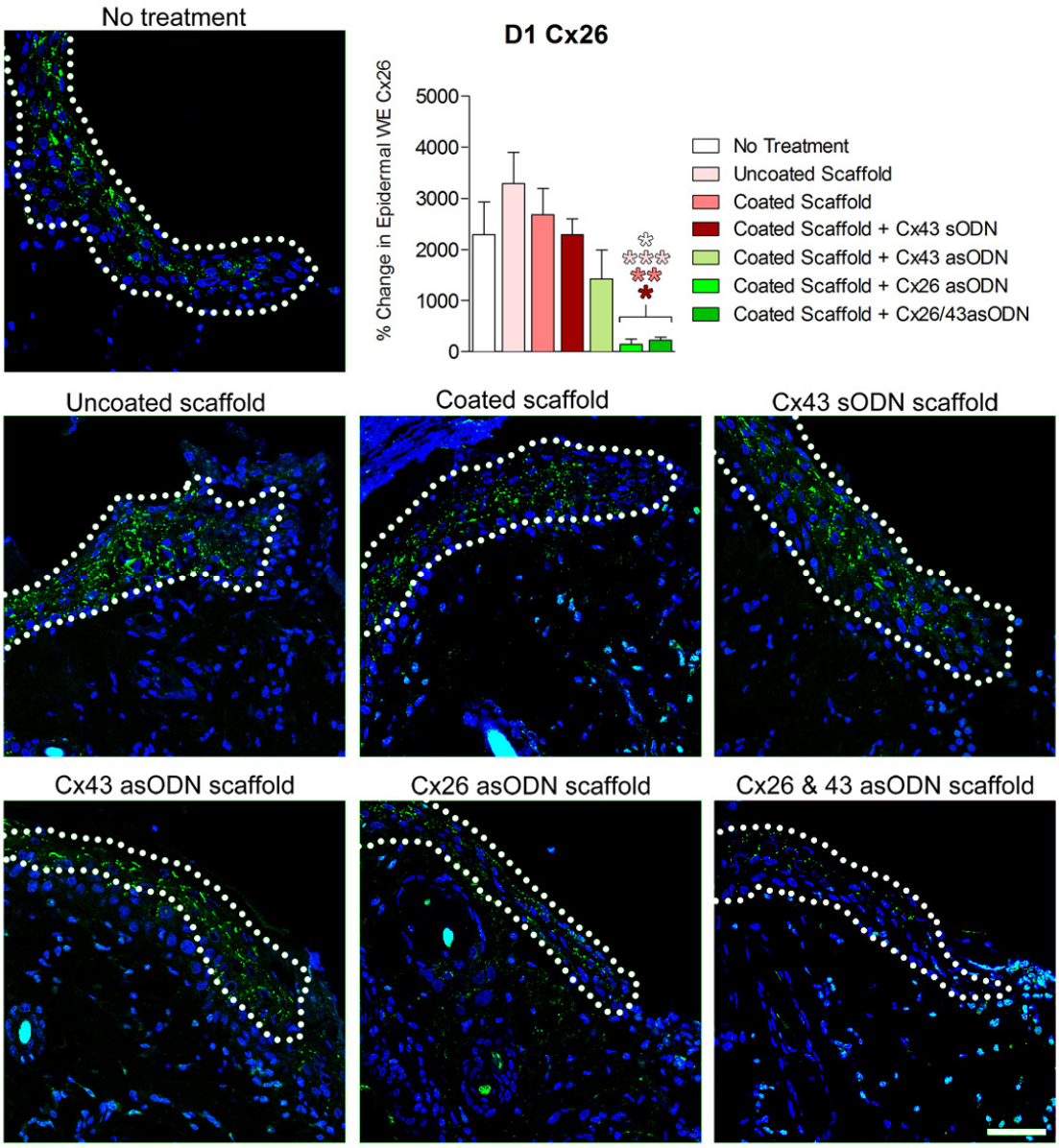

Figure 5. 7 – D1 Cx26 expression in the epidermal wound edge of scaffold-treated wounds.

Full-thickness wounds treated either left untreated or treated with a scaffold were harvested at D1. **Below**: tissue was immunostained for Cx26 (green) or Hoechst (blue) and confocal images of the nascent epidermis were captured. **Above**: positive Cx26 pixels were quantified in the end 150 μm of the wound edge epidermis as pixels per μm^2, and then normalised to a region of distal epidermis to calculate the percentage change (increase or decrease) from distal levels. Data plotted are means + SEM error bars. Significance stars are coloured to match the treatment that is significantly different (e.g. dark red star = significantly different to Cx43 sODN scaffold-treated wounds). Scalebar = 50 μm, n=8 rats assessed (* = P <0.05, ** = P < 0.01, *** = P < 0.001).

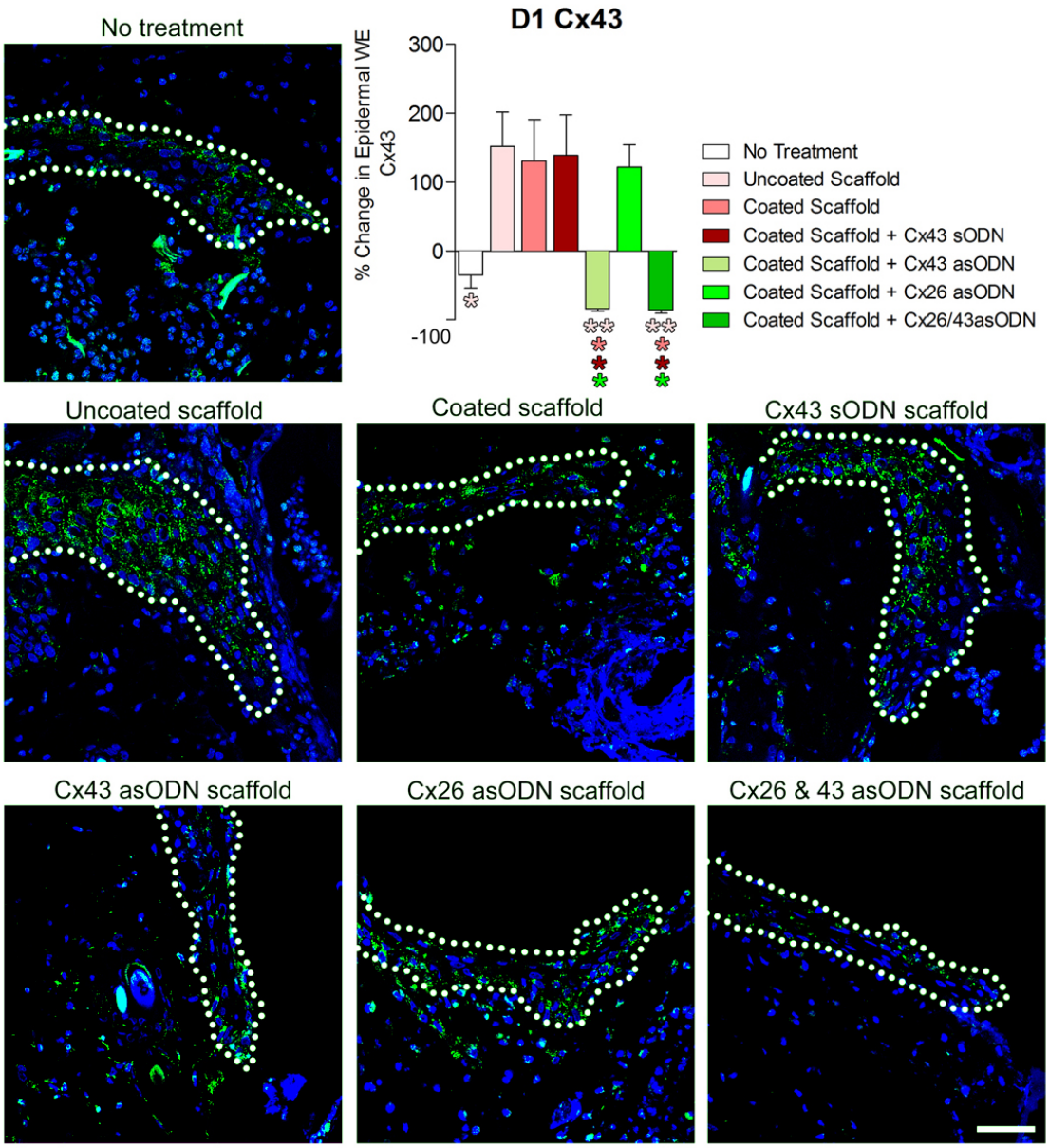

Figure 5. 8 – D1 Cx43 expression in the epidermal wound edge of scaffold-treated wounds.

Full-thickness wounds treated either left untreated or treated with a scaffold were harvested at D1. **Below**: tissue was immunostained for Cx43 (green) or Hoechst (blue) and confocal images of the nascent epidermis were captured. **Above**: positive Cx43 pixels were quantified in the end 150 μm of the wound edge epidermis as pixels per μm^2, and then normalised to a region of distal epidermis to calculate the percentage change (increase or decrease) from distal levels. Data plotted are means + SEM error bars. Significance stars are coloured to match the treatment that is significantly different (e.g. dark red star = significantly different to Cx43 sODN scaffold-treated wounds). Scalebar = 50 μm, n=8 rats assessed (* = $P < 0.05$, ** = $P < 0.01$).

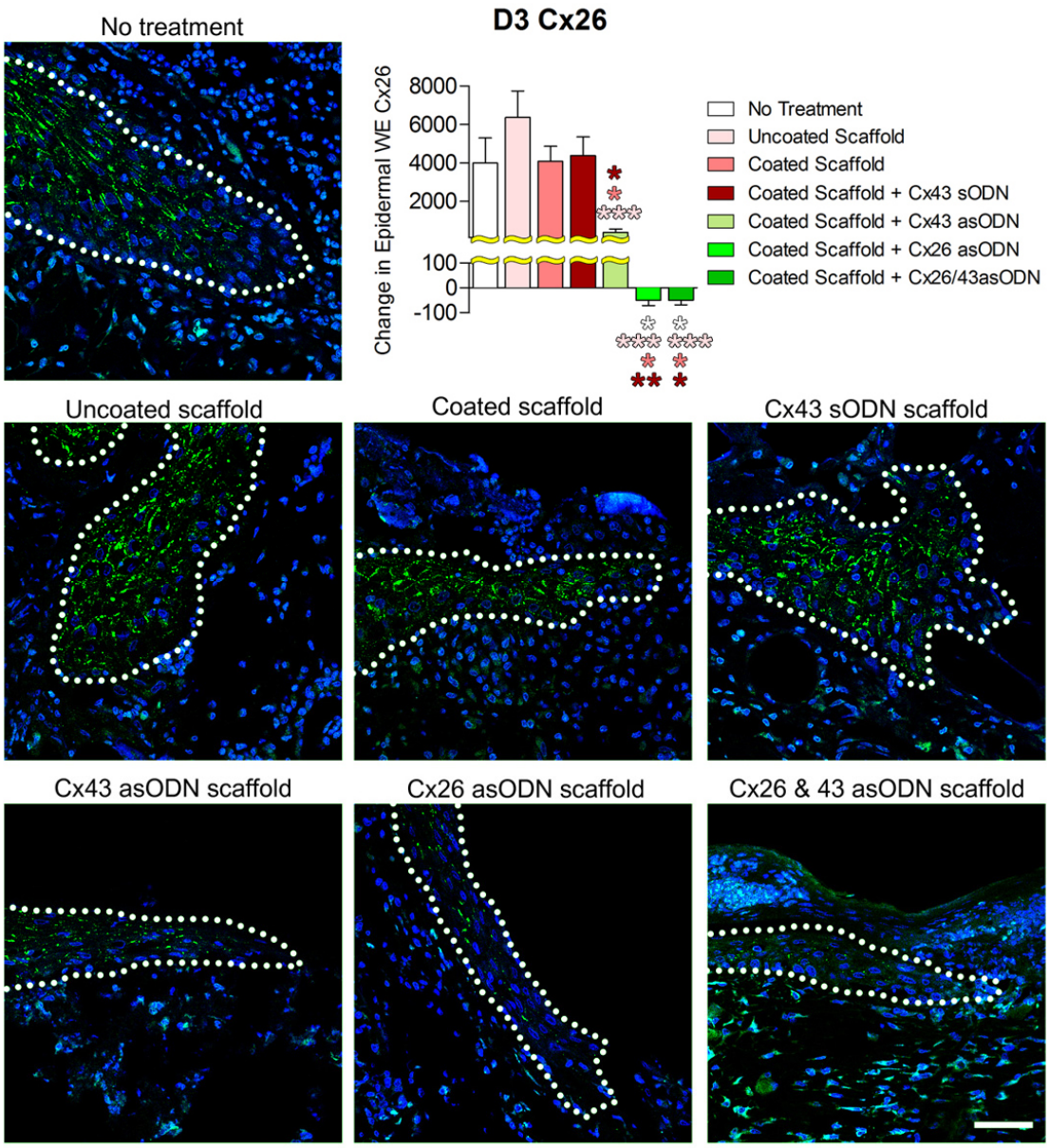

Figure 5. 9 – D3 Cx26 expression in the epidermal wound edge of scaffold-treated wounds.

Full-thickness wounds treated either left untreated or treated with a scaffold were harvested at D3. **Below**: tissue was immunostained for Cx26 (green) or Hoechst (blue) and confocal images of the nascent epidermis were captured. **Above**: positive Cx26 pixels were quantified in the end 150 μm of the wound edge epidermis as pixels per μm^2, and then normalised to a region of distal epidermis to calculate the percentage change (increase or decrease) from distal levels. Data plotted are means + SEM error bars of 8 rats. Significance stars are coloured to match the treatment that is significantly different (e.g. dark red star = significantly different to Cx43 sODN scaffold-treated wounds). Scalebar = 50 μm (* = P <0.05, ** = P < 0.01, *** = P < 0.001).

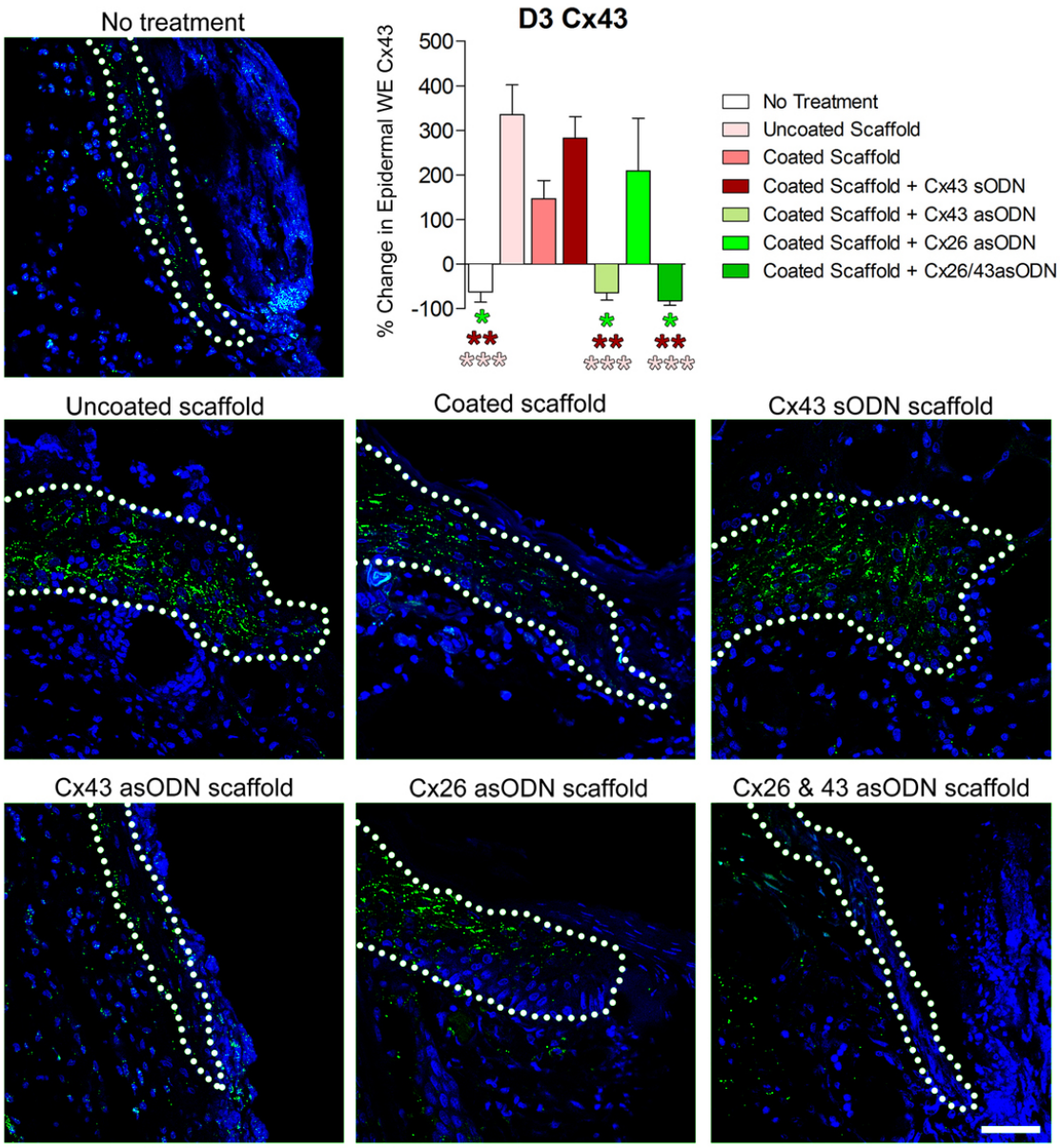

Figure 5. 10 – D3 Cx43 expression in the epidermal wound edge of scaffold-treated wounds.

Full-thickness wounds treated either left untreated or treated with a scaffold were harvested at D3. **Below**: tissue was immunostained for Cx43 (green) or Hoechst (blue) and confocal images of the nascent epidermis were captured. **Above**: positive Cx43 pixels were quantified in the end 150 μm of the wound edge epidermis as pixels per μm^2, and then normalised to a region of distal epidermis to calculate the percentage change (increase or decrease) from distal levels. Data plotted are means + SEM error bars. Significance stars are coloured to match the treatment that is significantly different (e.g. dark red star = significantly different to Cx43 sODN scaffold-treated wounds). Scalebar = 50 μm, n=8 rats assessed (* = P <0.05, ** = P < 0.01, *** = P < 0.001).

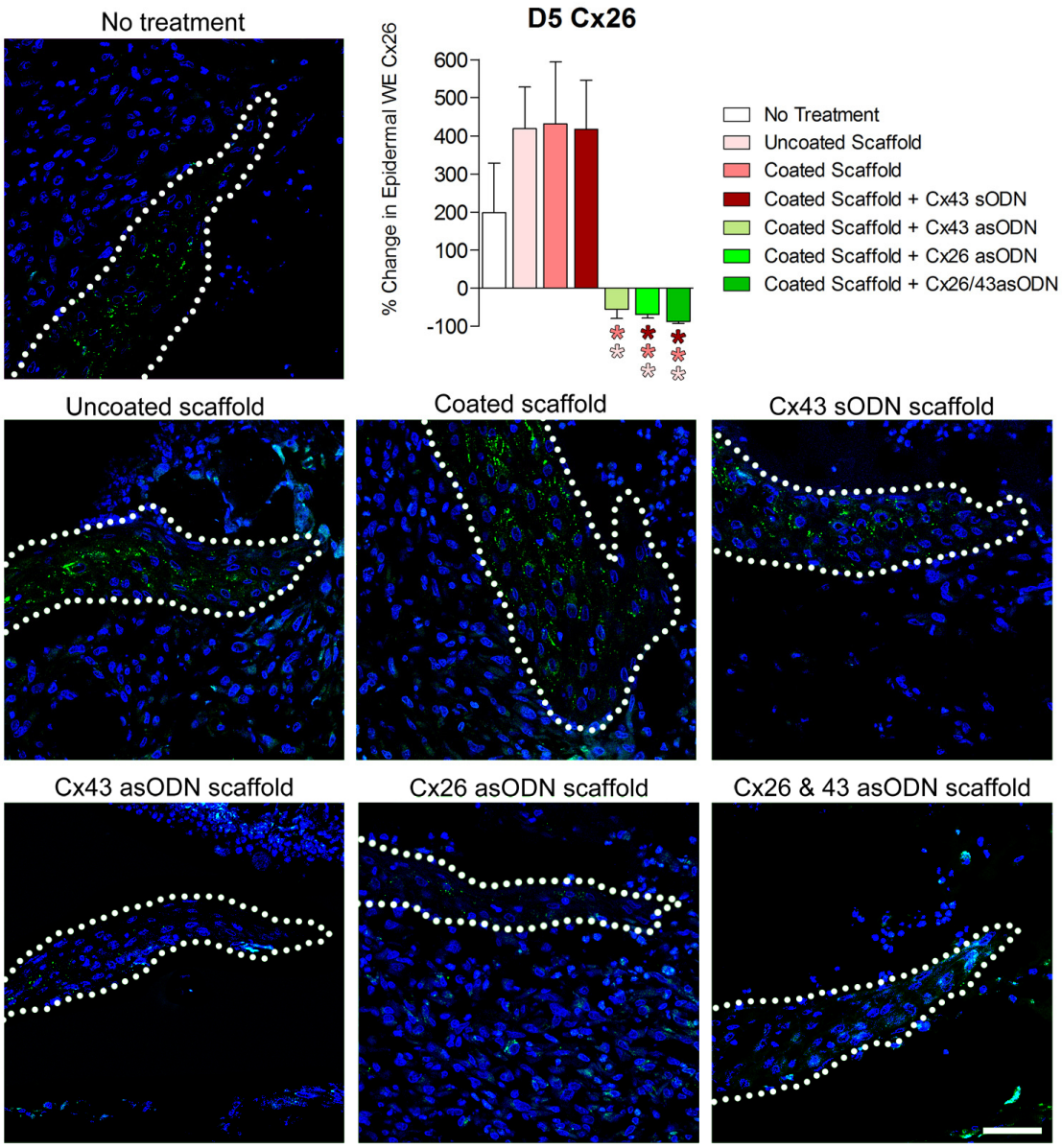

Figure 5. 11 – D5 Cx26 expression in the epidermal wound edge of scaffold-treated wounds.

Full-thickness wounds treated either left untreated or treated with a scaffold were harvested at D5. **Below**: tissue was immunostained for Cx26 (green) or Hoechst (blue) and confocal images of the nascent epidermis were captured. **Above**: positive Cx26 pixels were quantified in the end 150 μm of the wound edge epidermis as pixels per μm^2, and then normalised to a region of distal epidermis to calculate the percentage change (increase or decrease) from distal levels. Data plotted are means + SEM error bars. Significance stars are coloured to match the treatment that is significantly different (e.g. dark red star = significantly different to Cx43 sODN scaffold-treated wounds). Scalebar = 50 μm, n=8 rats assessed (* = $P < 0.05$).

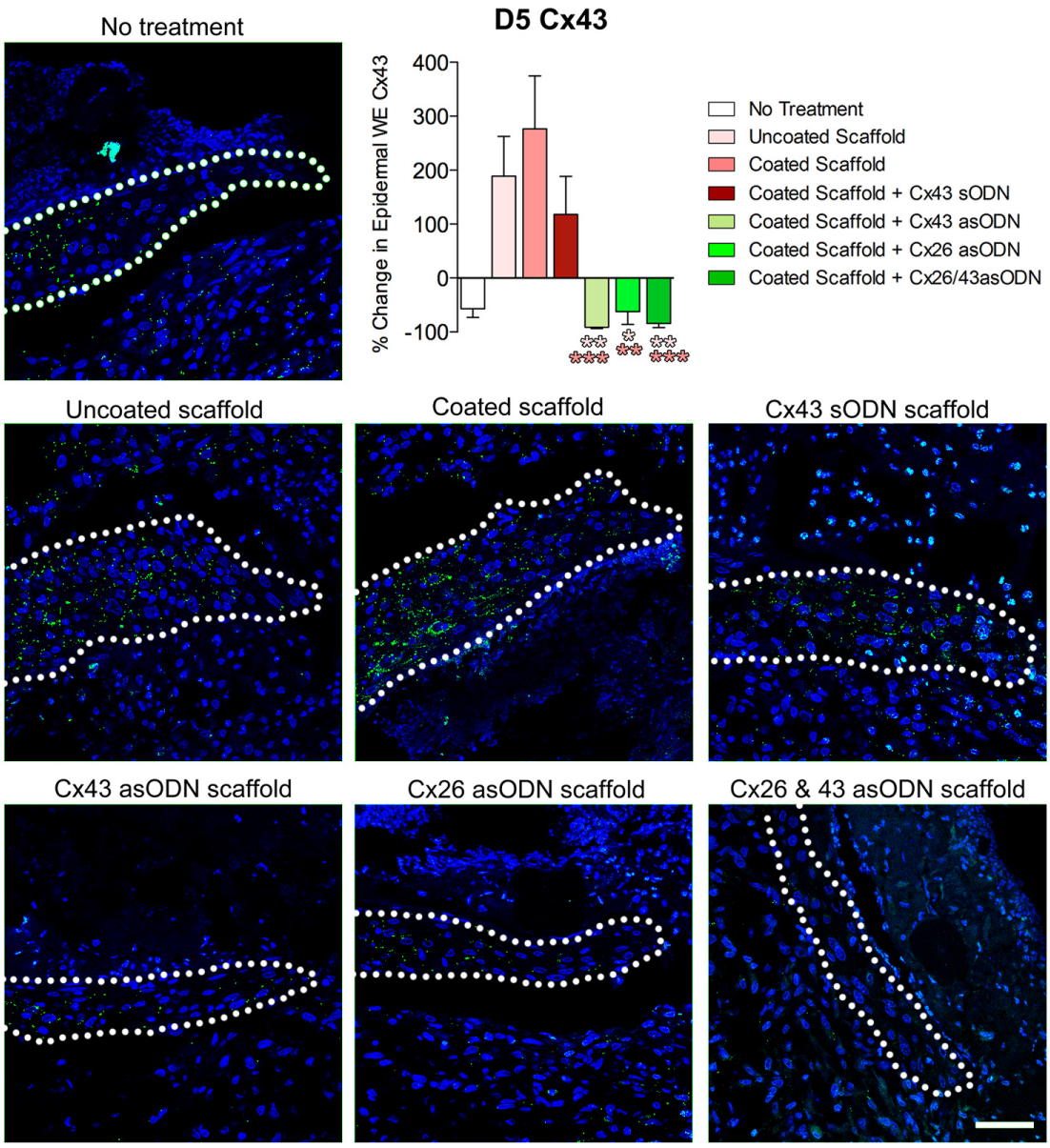

Figure 5. 12 – D5 Cx43 expression in the epidermal wound edge of scaffold-treated wounds.

Full-thickness wounds treated either left untreated or treated with a scaffold were harvested at D5. **Below**: tissue was immunostained for Cx43 (green) or Hoechst (blue) and confocal images of the nascent epidermis were captured. **Above**: positive Cx43 pixels were quantified in the end 150 μm of the wound edge epidermis as pixels per μm^2, and then normalised to a region of distal epidermis to calculate the percentage change (increase or decrease) from distal levels. Data plotted are means + SEM error bars. Significance stars are coloured to match the treatment that is significantly different (e.g. light pink star = significantly different to uncoated scaffold-treated wounds). Scalebar = 50 μm, n=8 rats assessed (* = P <0.05, ** = P < 0.01, *** = P < 0.001).

5.6 – The effect of Cx26 asODN coated scaffolds on the late stages of wound healing.

5.61 – Granulation tissue area measurements at D10 and 15.

Since the application of scaffolds coated with Cx26 asODN accelerated wound re-epithelialisation as Cx43 did, it was questioned whether, similar to Cx43, Cx26 asODN also had the effect of advancing wound healing at the later stages, including the reduction in area of wound granulation tissue. The area of granulation tissue formed in the wound was measured (for method, see Chapter 2; Materials and Methods) and is here reported as means ± SEM. H&E staining of Cx26 asODN scaffold-treated wounds at D10 had an average granulation tissue area of 2.65 ± 0.19 mm^2, which was insignificantly different from the 3.61 ± 0.18 mm^2 of untreated wounds (Figure 5. 13B-C). Cx26 asODN scaffold-treated wound areas were significantly lower than uncoated scaffold-treated wounds (4.47 ± 0.34 mm^2, $P < 0.001$), yet those wounds had considerably larger quantified areas than even untreated wounds. Similar to Cx43 asODN only scaffolds, the combined Cx26/43 scaffolds resulted in a significant reduction in the measured granulation tissue area compared to all control wounds. These observations were repeated at D15 – Cx26 asODN coated scaffolds resulted in a granulation tissue area of 1.73 ± 0.24 mm^2, which although smaller than untreated wounds (2.29 ± 0.09 mm^2) was insignificant, and significantly smaller than uncoated scaffold-treated wounds (Figure 5. 14B-C). The combined Cx26/43 asODN scaffold again resulted in a significant reduction in granulation tissue area (1.34 ± 0.10 mm^2), to a level similar to that found using Cx43 asODN only scaffolds (1.39 ± 0.07 mm^2). Across all treatments at D10 and 15, only scaffolds containing Cx43 asODN (either as Cx43 only or Cx26/43 combined applications) appeared to significantly reduce the area of granulation tissue relative to untreated wounds.

5.62 – The effect of the combined Cx26/43 asODN scaffold on the presence of myofibroblasts

While Cx26 asODN alone did not appear to significantly improve the area of wound granulation tissue, it was unclear whether the Cx26 asODN in the combined Cx26/43 asODN scaffold had a synergistic effect in reducing the size of the wound gap. As such, the two treatments that were found to significantly reduce the size of granulation tissue area (Cx43 asODN and the combined Cx43/26 asODN scaffold) were compared for α-

SMA staining. This was to determine whether there were potentially differences in the number of α-SMA positive contractile myofibroblasts relative to control uncoated scaffolds that had been applied to wounds made on the same animals (Figure 5. 15). Staining revealed a similar sized α-SMA positive region in the combined Cx26/43 asODN scaffold-treated wounds (0.39 ± 0.03 mm^2) to the Cx43 asODN only scaffolds (0.357 ± 0.07 mm^2). The combined Cx26/43 asODN scaffolds resulted in quantification of an SMA positive positive region that was 57% smaller than that measured in control scaffold-treated wounds (0.907 ± 0.09 mm^2); a difference that was statistically significant ($P < 0.001$). The localisation of -SMA staining did not appear to be more or less centrally located in wounds treated with the combined asODN scaffolds. The included Cx26 asODN sequences in the Cx26/43 scaffolds did not appear to further promote the reduction in size of the α-SMA positive region in the late time point wounds, in contrast to re-epithelialisation in which combining asODN sequences resulted in the furthest levels of re-epithelialisation.

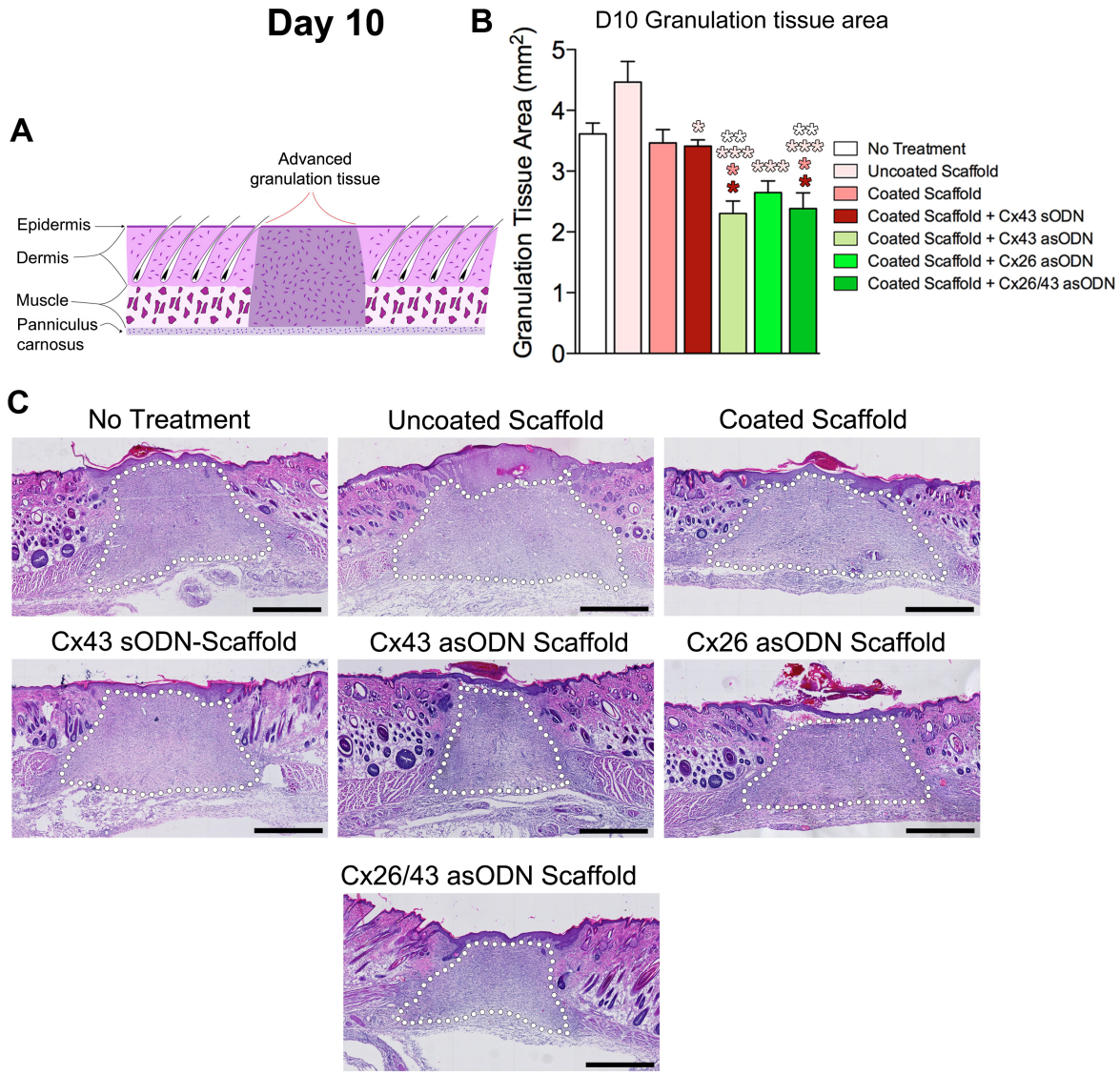

Figure 5. 13 – Full-thickness wounds treated with scaffolds at D10.
Full-thickness wounds were either left untreated or treated with a scaffold. Wounds were harvested at D10. **(A)**: A simplified wound diagram to illustrate the granulation tissue region swhich was measured in (B). **(B)**: Wounds either left untreated or treated with a control scaffold (red bars) or a coated scaffold containing asODN (green bars) were measured for granulation tissue/wound area. **(C)**: Typical H&E stained images illustrating the quantified granulation tissue area of the individual wounds in (white dots). Eight rat wounds were assessed (* = $P < 0.05$, ** = $P < 0.01$, *** = $P < 0.001$), scale bar = 100 µm. Data is plotted as means + SEM, and significance stars are coloured to match the treatment that is significantly different (e.g. dark red star = significantly different to Cx43 sODN scaffold-treated wounds).

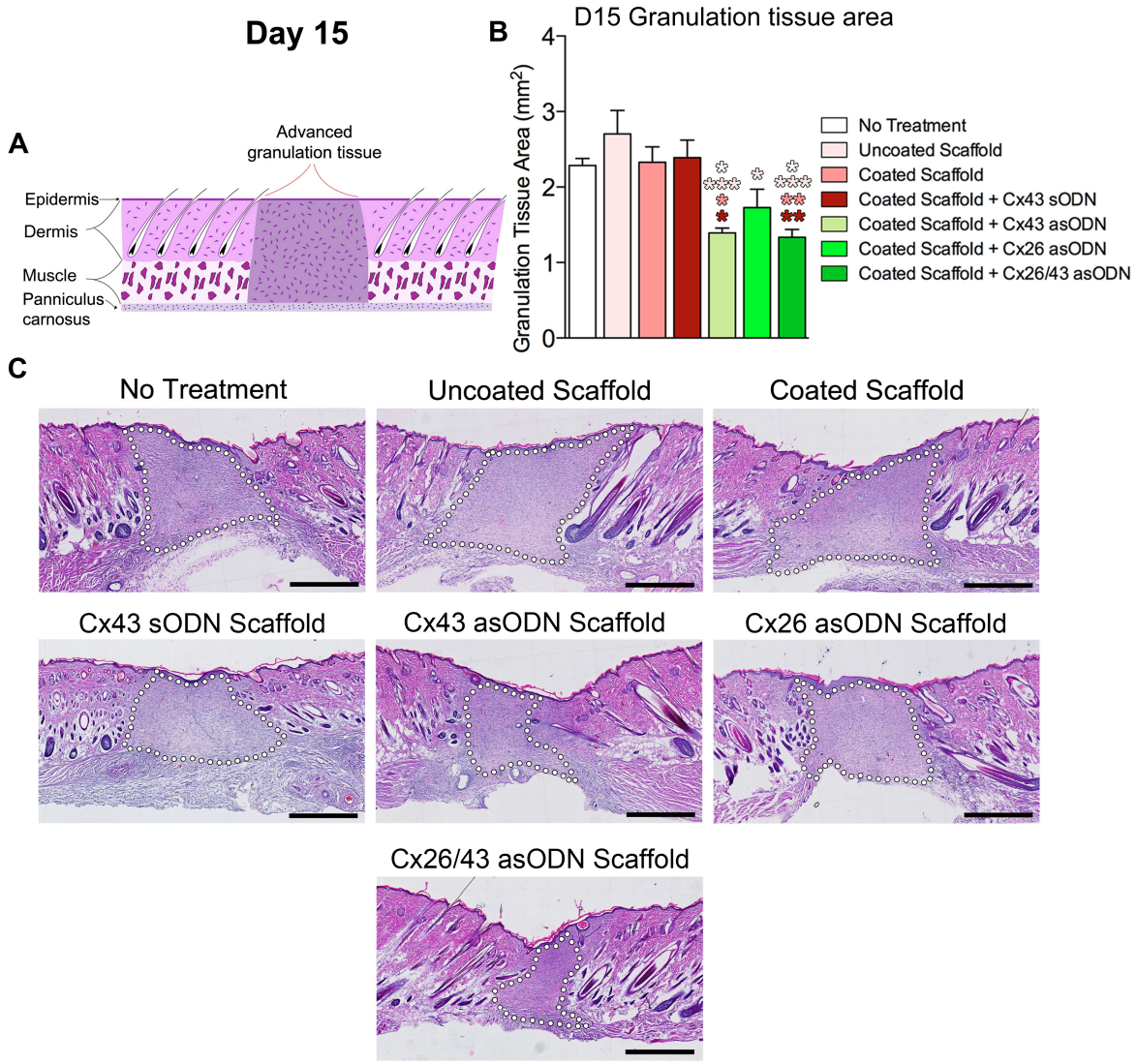

Figure 5. 14 – Full-thickness wounds treated with scaffolds at D15.
Full-thickness wounds were either left untreated or treated with a scaffold. Wounds were harvested at D15. **(A)**: A simplified wound diagram to illustrate the granulation tissue region which was measured in (B). **(B)**: Wounds either left untreated or treated with a control scaffold (red bars) or a coated scaffold containing asODN (green bars) were measured for granulation tissue/wound area. **(C)**: Typical H&E stained images illustrating the quantified granulation tissue area of the individual wounds in (white dots). Seven rat wounds were assessed (* = $P < 0.05$, ** = $P < 0.01$, *** = $P < 0.001$), scale bar = 100 µm. Data is plotted as means + SEM, and significance stars are coloured to match the treatment that is significantly different (e.g. dark red star = significantly different to Cx43 sODN scaffold-treated wounds).

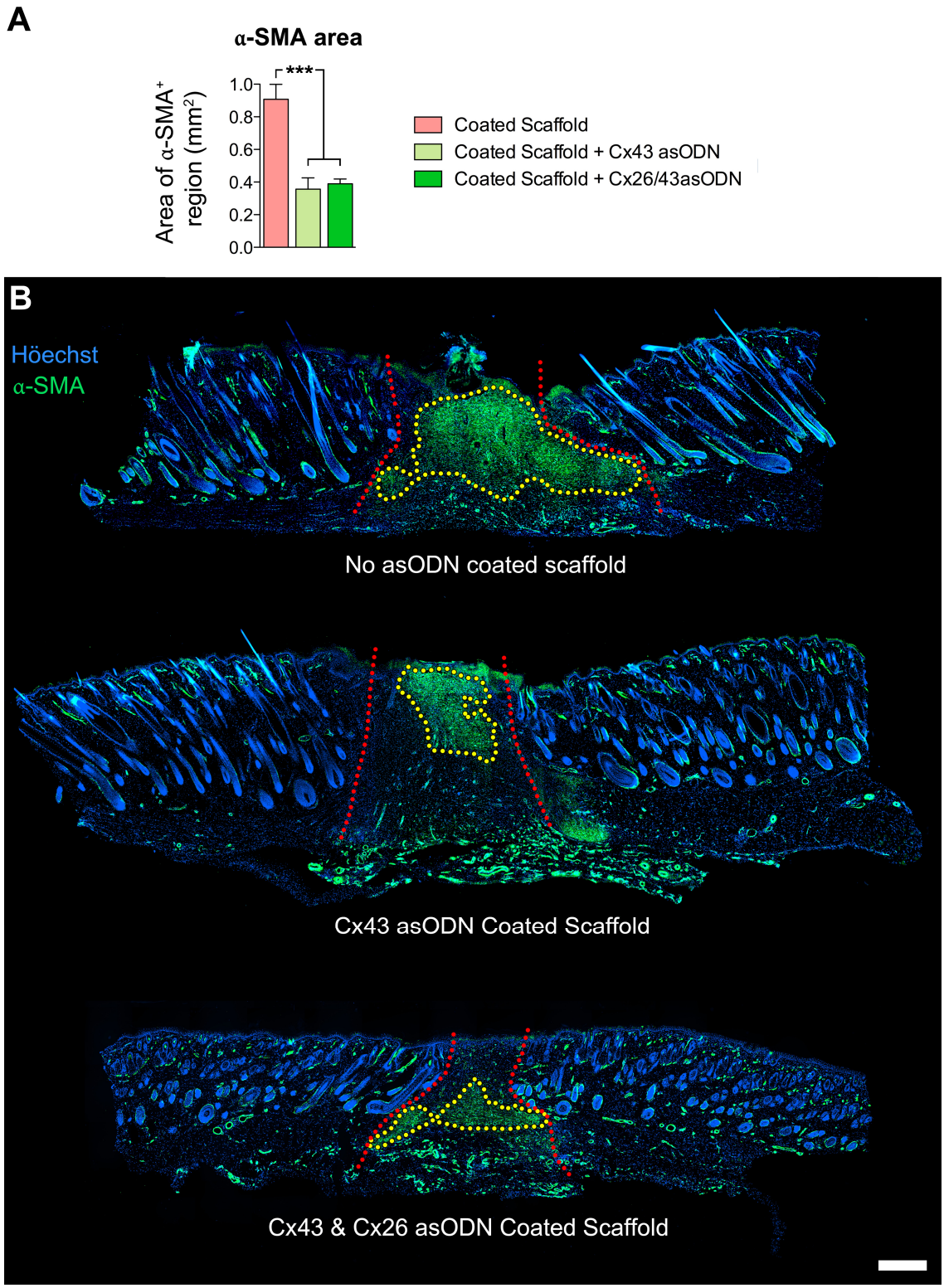

Figure 5. 15 – α-SMA expression in D10 scaffold-treated wounds.

Rat full-thickness wounds treated with either control coated scaffolds or Cx43 asODN coated scaffolds were harvested at D10 and stained for both α-SMA (green) and Hoechst (blue).

(A): The green SMA^+ region outlined in (B) was quantified for two different treatments on the same animals; a coated collagen scaffold without asODN and a coated scaffold coated with Cx43 asODN. This region was defined as positive stain in the wound gap above the blood vessel dense panniculus carnosus. A total of n=8 animals were assessed, data is plotted as means + SEM (*** = $P < 0.001$).

(B): Typical immunofluorescence montage images illustrating the measured region of α-SMA in the wound (yellow dots) as well as the initial wound margins (red dots). scale bar = 500 μm).

5.7 – Discussion

Following the results of the previous two chapters it was observed that Cx26, as well as Cx43, were each strongly upregulated in keratinocytes at the wound edge when wound healing was perturbed by the presence of a scaffold. When Cx43 was upregulated, which is a common characteristic of chronic ulcers and slow-to-heal diabetic wounds, Cx26 was frequently also significantly upregulated beyond the normal levels encountered during acute wound healing. It was unclear whether Cx26 expression was beneficial during acute wound healing, or whether Cx26 knockdown would have a negative effect on healing. It has been shown that Cx30 null mice are not wound healing impaired, and it was suggested that Cx26 may rescue this effect (Kretz et al., 2003). So it may be possible that Cx26 may not be necessary during wound healing due to a rescue effect of Cx30. While it has been shown that Cx26 may be important in controlling keratinocyte differentiation, it is unclear why Cx26 is strongly upregulated at the wound edge during re-epithelialisation (Coutinho et al., 2003, Lucke et al., 1999). To determine whether Cx26 knockdown has a positive effect on scaffold-assisted wound healing, two novel Cx26 asODN sequences designed in the CoDa Theraputics Inc. laboratory in New Zealand were applied to scaffolds following preliminary using the emulsion technique developed in the previous chapter.

Application of Cx26 asODN scaffolds to wounds did not appear to macroscopically inhibit wound closure, as wounds were similar in size to untreated wounds (Figure 5. 1). Similar to Cx43 asODN coated scaffolds, and to some extent the control scaffolds, the Cx26 asODN scaffolds did not prevent wound closure which was the opposite effect to that of the uncoated scaffolds. This could again be due to the fact that the coated scaffolds were often

only loosely associated with the wound edge and readily detached during tissue processing, to the extent that wound contraction may occur normally underneath the scaffold. The combined Cx26/43 asODN coated scaffold-treated wounds were also reduced in size to a similar degree as the other bioactivated scaffolds, although hair regrowth could often mask the actual size of the wound at D5. Unlike Cx43, Cx26 knockdown has not previously been linked to a reduction in wound area, and it still remains unclear how Cx26 knockdown could mechanistically affect wound closure.

Microscopic assessment of wounds treated with the Cx26 asODN coated scaffolds revealed significant differences in wound re-epithelialisation relative to wounds treated with scaffolds coated without asODN or with a Cx43 sODN sequence that does not cause targeted mRNA degradation (Figure 5. 2, Figure 5. 3, & Figure 5. 4). The observation that Cx26 asODN improves re-epithelialisation *in vivo* is a finding that has, to the best of my knowledge, not previously been reported before. The finding that Cx26 asODN application reduced epithelial thickening appears somewhat logical, since a somewhat 'opposite' study in which Cx26 was ectopically overexpressed resulted in the opposite effect of keratinocyte hyperproliferation and epithelial thickening (Djalilian et al., 2006). Hyperproliferation of the epidermis is also evident in individuals that have any one of a number of loss-of-function mutations in the Cx26 gene *GJB2*, and is commonly linked to deafness. A possible explanation for this hyperproliferation has been proposed following assessment of mice with a D66H Cx26 loss-of-function mutation, which are found to contain increased numbers of keratinocytes undergoing cell death (Bakirtzis et al., 2003). It has been reasoned that Cx26 may affect hyperproliferation through the triggering of a proliferative rescue response following the apoptosis of cells within the epidermis. Alternatively, it has also been suggested that overstimulation of Cx26 can lead to hyperthickening (Bakirtzis et al., 2003). It is interesting that Cx26 mutations, resulting in loss of Cx26 function, result in perturbed wound healing and epithelial thickening (Labarthe et al., 1998, Lucke et al., 1999), while knockdown of Cx26 protein appears to have had the opposite effect in this study. A possible explanation for this difference is that mutated forms of the Cx26 protein may be incorporated into connexon hemichannels, even those composed of other connexins besides Cx26, and deregulate normal signalling responsible for keratinocyte differentiation (Rouan et al., 2001).

While re-epithelialisation measurements indicated that the Cx26 asODN sequences appeared to be effective *in vivo*, immunostaining with an anti-Cx26 antibody actually confirm this knockdown at D1, 3 and 5 in the leading edge epidermis (Figure 5. 7, Figure 5. 9 & Figure 5. 11). In the previous chapters, Cx43 knockdown using Cx43 asODN also resulted Cx26 downregulation at D3 and D5 relative to uncoated scaffolds (Chapter 3 - Figure 3. 7, Figure 3. 8 & Chapter 4 - Figure 4. 10, Figure 4. 12). In the opposite fashion, here Cx26 asODN resulted in a significant downregulation of Cx43 at D3 and D5 relative to most of the control scaffolds (Figure 5. 9, Figure 5.11). This may be due to the evident acceleration of wound re-epithelialisation following Cx26 asODN application. It is known that keratinocyte Cx43 downregulation occurs in conjunction with cell migration, so it may be possible that Cx26 could indirectly affect Cx43 levels, although the mechanism by which this could occur is unknown. The finding that Cx26 can somehow interact with Cx43 has been supported by the findings of another study, however, where it was found that the Cx26 loss-of-function mutation ΔE42 resulted in a decrease in intercellular conduction of wild type Cx43 (Rouan et al., 2001). Despite this, while it has been shown that Cx26 can interact with Cx30 (Ahmad et al., 2003), it cannot form channels with Cx43 due to physiological differences between the connexins (Marziano et al., 2003). The effect of the ΔE42 mutant Cx26 on Cx43 may possibly occur through another interaction separate to the formation of gap junction channels, although such a pathway is currently unknown. While it may have previously been thought that because the Cx26 protein has a short cytoplasmic C-terminus tail it may not be able to interact with many other proteins in the way Cx43 does, a study has identified an interaction between Cx26 and the tight junction associated protein occludin (Nusrat et al., 2000). Through affinity pulldown assays, Cx26 was found to specifically interact with the coiled-coil domain of occludin (Nusrat et al., 2000). This provides a potential link between tight junctions and gap junctions through Cx26, which could explain why knockdown of Cx26 could improve wound re-epithelialisation, since occludin regulates migration of epithelial cells during wound healing (Du et al., 2010).

It was also noted that similar to Cx43 asODN, Cx26 asODN coated scaffolds had a noticeable effect in reducing the infiltration spread of cells with an inflammatory polymorphonuclear leukocyte morphology (PMNs) into the uninjured dermis. The effect of Cx26 on inflammation has partly been explored by the work by Djailian et al (2006). In the study, Cx26 was ectopically overexpressed and this led to increased hemichannel

activity, resulting in a marked increase in cellular release of ATP. Normally extracellular ATP is removed by conversion to adenosine, but excessive levels can result in its accumulation (Cauwels et al., 2014). Heightened levels of ATP have been demonstrated to have a pro-inflammatory effect, causing an increase in available pro-inflammatory cytokines such as IL-1 and, likely as a result of this, an increased number of CD4+ inflammatory cells such as leukocytes. Indeed, promoting ATP hydrolysis through supplementation with apyrase significantly reduced IL-1 levels and the quantified number of CD4+ inflammatory cells (Cauwels et al., 2014). ATP is also found to stimulate $CD39^{+}$ Langerhans cells, which typically modulate inflammation in response to chemical irritants (Mizumoto et al., 2002). It is possible that uncoated scaffolds, which cause an upregulation of Cx26, could be promoting the invasion of inflammatory PMNs through elevations in pro-inflammatory ATP, while Cx26 asODN could be preventing its extracellular accumulation. It is important to note that at some time points, not all control coated scaffolds resulted in significantly higher levels of infiltrating PMNs relative to the Cx26 asODN applications, although levels were still markedly increased by at least 50%. It is possible that the reduced level of PMN infiltration observed using control coated scaffolds relative to uncoated scaffolds was due to the fact coated scaffolds tended to be only loosely associated with the wound edge, resulting in less contact with the wound. It appears that the potential anti-inflammatory applications of Cx26 asODN may be most readily observed in situations where Cx26 is strongly upregulated, such as following uncoated scaffold application or in chronic ulcers (Sutcliffe et al. (publication submitted)).

It was interesting to observe the effect of combining both the Cx26 asODN sequences and the Cx43 asODN sequence within a single scaffold. While neither PMN infiltration (Figure 5. 6) nor granulation tissue area (Figure 5. 13 & Figure 5. 14) appeared to be further reduced following the addition of Cx26 asODN to Cx43 asODN, it was apparent that the use of asODN against both Cx26 and 43 resulted in significant downregulation of both connexins between D1 to D5 (Figure 5. 7 - Figure 5. 12). This was met by a consistent increase in re-epithelialisation distance at each time point assessed relative to the individual asODN scaffolds, with an increase as high as 27.9% at D5. Due to the observed trend it is possible that the use of both Cx26 and Cx43 asODN may have a synergistic effect, but it is important to note that the combined asODN scaffold did not significantly increase re-epithelialisation over single asODN scaffolds. Further investigation would be required to determine if a synergistic effect was indeed occurring. It is perhaps less surprising that

Cx26 asODN did not significantly reduce the area of late stage granulation tissue at D10 and D15 (Figure 5. 13 & Figure 5. 14), since Cx26 knockdown has not been linked to myofibroblast activity or their accelerated clearance from the wound, in contrast to a study that employed Cx43 asODN (Mori et al., 2006).

Conclusions

Application of the two recently developed Cx26 asODN sequences together using a scaffold coating caused significant knockdown of Cx26 in wound edge keratinocytes, a significant reduction in infiltrating PMNs relative to uncoated scaffolds and also significantly improved wound re-epithelialisation relative to a number of control scaffolds at the same time points. Considering that scaffolds are intended for application to chronic wounds where inflammation, wound re-epithelialisation and connexin expression can be perturbed, the delivery of Cx26 asODN to the wound in a sustained manner could be an effective treatment in addition to Cx43 asODN. Furthermore, it is possible that combining the asODN sequences in a scaffold may have a synergistic effect on wound re-epithelialisation, which would be of further benefit in a chronic ulcer setting. It is even possible that Cx26 and Cx43 asODN could be incorporated alongside additional drugs in other therapeutic settings, where they could act as enhancers of scaffold biocompatibility.

CHAPTER 6

Discussion

6.1 – Introduction

The findings of this study help to elucidate the previously unclear role of scaffolds when applied in an *in vivo* setting. In chapter 3 it was found that in an uncoated form, collagen scaffolds had a negative effect on the healing of acute full-thickness wounds, causing thickening of the epidermis at the wound edge, reduction of wound contraction and induction of wound edge Cx43 expression. Infusion of scaffolds with Cx43 asODN using a Pluronic gel had a positive effect in reducing Cx43 expression and wound edge epithelial thickening, but scaffolds did not appear to act as a cell supportive matrix and wound integration was not achieved. In chapter 4, a polymer coating technique was established and was found to result in Cx43 asODN elution from coatings over several days *in vitro*. Bioactivation of scaffolds in this way had a strong positive effect; application of the sustained release scaffolds to rat full-thickness wounds resulted in significant improvements to wound re-epithelialisation, and inflammation was reduced relative to uncoated scaffolds. Unlike bioactivation using Cx43 asODN in Pluronic gel, polymer coated scaffolds containing Cx43 asODN improved wound healing to a greater degree than even untreated wounds in some aspects that were investigated. Cx43 downregulation using coated scaffolds was also achieved over a longer time period than when using the transiently bioactivated scaffolds applied to mouse wounds in chapter 3. Finally, in chapter 5 it was found that the polymer coating technique could also be used to deliver more than one therapeutic agent; in this case two novel asODN sequences to Cx26, which was also found to promote wound re-epithelialisation and reduce inflammation associated with scaffold use. Following these assessments, the results of this study were assessed in light of those derived from other *in vivo* and clinical scaffold studies.

6.2 – Comparing project findings with the literature

6.21 - Downregulation of connexins 43 and 26

Downregulation of Cx43 in the acute and chronic wound model setting through the application of Cx43 asODN using a Pluronic gel has previously been shown to improve wound re-epithelialisation, reduce the severity of inflammation and promote a reduction in wound size (Mori et al., 2006, Qiu et al., 2003, Wang et al., 2007). The experimental results

of this study are in agreement with those general biological findings; Cx43 asODN coated scaffolds similarly improved wound healing across the same three aspects. Chronic wounds have been found to exhibit upregulation of Cx43 at the wound edge; a feature that has been noted to delay wound closure (Mendoza-Naranjo et al., 2012b). Using a polymer coating approach to entrap Cx43 asODN it was observed that asODN could be made to elute from collagen scaffolds over several days. The sustained delivery of asODN could be particularly beneficial in a slow-healing ulcer setting to modify deleteriously expressed proteins. A recently submitted journal article also identified Cx26 as strongly upregulated in both DFUs and VLUs, far beyond the normal levels that Cx26 is upregulated to in acute wounds (Sutcliffe et al., article submitted in 2014). To the best of my knowledge, this is the first comprehensive study of Cx26 asODN application in skin. One other study has used Cx26 siRNA *in vitro* to knockdown Cx26 in rat epidermal keratinocytes (REKs). Using an organotypic model of epidermis they reported that Cx26 knockdown had no effect on differentiation of REKs. Despite this finding, it appears that no pre-existing study has performed Cx26 knockdown using an *in vivo* wound healing model (Thomas et al., 2007). The two Cx26 asODN 20-mer sequences used in this study were combined into one scaffold coating due to the time constraints of individual testing and limited wound site availability. Testing of the two sequences individually in future would be necessary to identify the most effective sequence.

Comparisons between the findings of Cx26 knockdown in this study and the literature are difficult to make due to the lack of similar studies of Cx26 knock down *in vivo*. Loss of function mutations in Cx26 have previously been found to have no effect on rat keratinocyte cell migration or differentiation *in vitro* (Thomas et al., 2007). Cx26 is able to form gap junction channels with Cx30, and it has been shown that the expression profile of Cx30 is similar to that of Cx26 (Coutinho et al., 2003). Cx30 knockout mice have no impairment to wound healing, and it has been proposed that Cx26 may substitute for it. It is equally possible that Cx30 may substitute the function of Cx26 when Cx26 is knocked down, although what role this is remains unclear (Kretz et al., 2003). A combined Cx26 and Cx30 asODN knockdown approach may help to identify whether at least one of the two connexins is required during wound healing.

With regard to the effect of Cx26 knockdown on wound healing, as mentioned in the previous chapter, Cx26 expression has been linked to inflammation in wound healing.

Overexpression of Cx26 was found to lead to extracellular release of ATP, which can subsequently cause extracellular elevations in pro-inflammatory cytokines such as IL-1 which can serve as chemoattractants for PMNs (Cauwels et al., 2014, Djalilian et al., 2006). It may be possible, then, that downregulation of Cx26 from the high levels encountered in wound edge keratinocytes may have contributed to the reduced level of PMN infiltration of the tissue. In addition to this, re-epithelialisation could have been improved in keratinocytes in response to Cx26 asODN due to attenuation of interactions between Cx26 and the tight junction associated protein occludin. Pulldown assays revealed that the two to interact (Nusrat et al., 2000). It is possible that the downregulation of Cx26 could have led to changes in tight junction associations, which are normally rearranged in the cell during wound healing. It is also interesting that Cx26 asODN scaffolds caused a reduction in wound edge keratinocyte Cx43 expression at later time points, as it could indicate some level of interaction between the two proteins. Alternatively, this observation could be due to indirect effects on other mediators or intermediate signals. A possible interaction between the two has previously been reported when a Cx26 loss-of-function mutation decreased intercellular conduction of wild type Cx43, although it is currently unclear how such an interaction may occur (Rouan et al., 2001). Although combination of both Cx26 and Cx43 asODN sequences in a scaffold significantly improved wound re-epithelialisation over untreated or control scaffold-treated wounds, the difference was not statistically significant over single asODN applications against Cx26 or Cx43. Despite this, the combined asODN scaffold consistently resulted in the highest levels of wound re-epithelialisation at D1, 3 and 5, which may indicate a synergistic effect. However, further experiments would be required to validate such a claim.

6.22 – Scaffold design

In order to assess what the effect of scaffolds used clinically and experimentally had on wound healing it was necessary that the scaffold I developed was generated to resemble other types of scaffolds. This was particularly important so that the findings reported in this study were relevant to the scaffold types used today. The collagen scaffolds fabricated in this study using an electrospinning technique were fabricated according to a previously established protocol. Scaffold porosity and fibrosity was illustrated using SEM and FITC Pluronic gel infusion assays. Following these analyses it was evident that scaffolds were

permeable to the Pluronic gel used to deliver asODN, and that the thickness of fibres ranged from 0.03 - 4.12 μm. This diameter range of fibres measured coincide with that those generated for *in vivo* application as a full-thickness wound dermal substitute in guinea pigs. In that study, fibre diameter was measured to be between 0.25 - 2 μm (Jha et al., 2011). Additionally, the same group investigated the effect of endothelial and osteoblast cell adhesion and morphology on the scaffolds *in vitro*, finding that larger diameters supported elongation of endothelial cells and penetration of the scaffolds. The *in vivo* images shown in the study, however, did not show the cellular infiltration of scaffolds, nor did they indicate the time point at which images were captured. Fibroblast adhesion and elongation has also been observed on electrospun PCL fibres with an average diameter of approximately 0.8 - 1 μm (Mijovic et al., 2012). Given the reported diameter ranges that appear to support cell adhesion *in vitro*, it would appear that the collagen scaffolds electrospun in this study were comparable to those used elsewhere. It is likely that the negative findings observed using uncoated scaffolds are the result of the differences between *in vitro* and *in vivo* environments.

The use of electrospinning to fabricate collagen scaffolds, as performed elsewhere and in this study, has been noted that it may denature the polymer, resulting in gelatin that does not structurally resemble collagen present in the native ECM (Zeugolis et al., 2008). This argument has been further supported by the findings of Jha et al. (2011), which found that collagen fibres were altered following electrospinning of acid-soluble bovine collagen, such that they were enriched for the α2 subunit. However, despite this, the group found that cells adhered to the modified electrospun collagen, again indicating that the negative response to scaffolds *in vivo* is likely not due to the materials employed.

Scaffolds were also crosslinked using EDC hydrochloride. The use of this specific crosslinker is preferred over traditional and toxic crosslinkers such as glutaraldehyde, particularly since it is a 'zero-length' crosslinker that is not incorporated into the polymer, such that it should be easier to remove following washing steps (Girardot and Girardot, 1996). Despite this, even using a reduced concentration of crosslinker in this study (0.15% wt./v.) compared to the 15% (wt./v.) crosslinker used to develop scaffolds in a previous study did not overturn the negative effects encountered through scaffold use (Torres-Giner et al., 2009). This further increases the likeliness that dermal scaffolds are currently poorly

optimised for *in vivo* use, and not that the methods used to fabricate scaffolds in this study specifically caused a reaction.

6.23 – Wound closure

It is difficult to compare the retardation to wound re-epithelialisation witnessed following uncoated scaffold application in this study to the findings of other scaffold studies, since high power analyses of wound re-epithelialisation is not usually performed. As a typical example, an *in vivo* study of experimentally induced pressure ulcers made to mice involved the application of chitosan scaffolds to wounds, but wound closure was then measured macroscopically (Park et al., 2009). Although macroscopic images can give a general impression of wound closure, they lack the accuracy of microscopic evaluations since it is difficult to determine whether re-epithelialisation has taken place, especially under scabs. Also in rodents, wound contraction plays a far more important role in wound closure, yet this feature is less prevalent in the human wounds that scaffolds are ultimately intended to be applied to (Wong et al., 2011). Interpreting scaffold efficacy based on macroscopic wound closure alone in animal models is not a sufficient way to gauge how effective scaffolds would perform in a human chronic ulcer setting.

In many cases, human clinical trials have primarily focused on whether wounds have closed or not within a specified period of time following scaffold application as the main means to assess scaffold efficacy (Karr, 2011, Marston et al., 2003, Veves et al., 2001). In this study, uncoated bovine acid-soluble collagen scaffolds were found to inhibit wound contraction, and this result correlates with previous animal studies by other groups (Ng and Hutmacher, 2006, Soller et al., 2012, Yannas et al., 1989). The presence of a solid scaffold in the wound could present a physical obstruction to the contracting wound, such that wound closure is perturbed. Despite this, scaffolds in the present study that were polymer coated did not prevent wound closure, which may have been due to the considerable lack of integration of polymer coated scaffolds with wounds. However, it has been argued that while scaffolds may impair wound closure, they can at the same time accelerate the rate of granulation tissue development (Soller et al., 2012). Despite the authors measuring granulation tissue, neither quantification of re-epithelialisation nor assessment of leading edge cells was performed in the study, which would be necessary to support such claims. In the present study, granulation tissue was not positively affected by the application of uncoated or coated collagen scaffolds that did not contain asODN relative to untreated wounds.

Despite the results of this study that demonstrate scaffolds can delay wound contraction in mice, previous clinical applications of scaffolds to non-healing ulcers have been met with limited positive findings (Karr, 2011, Marston et al., 2003, Veves et al., 2001). Both scaffolds comprised of organised cell layers as well as dermal extracellular matrix substitutes have been applied to patient ulcers, although most data reporting is limited to wound closure rates and not detailed analysis of re-epithelialisation. The efficacy of Dermagraft, a single layer dermal scaffold consisting of both a polyglactin matrix and seeded fibroblasts, has been assessed in a randomised clinical trial, and wound healing was reported to be improved following application. The results of the trial in which 145 patient wounds were assessed showed that Dermagraft applications resulted in 30% of DFUs closing within 12 weeks, while only 18.3% of wounds receiving conventional treatment closed; a difference that was significant (Marston et al., 2003).

Cellular scaffolds comprising both epidermal and dermal layers have also been reported to be effective in promoting wound closure. This includes Apligraf, which consists of human keratinocytes overlying a bovine collagen matrix that has been seeded with human fibroblasts. Again, wound closure in DFUs was found to be significantly improved in a randomised clinical trial; 56% of wounds treated with Apligraf healed relative to 38% of controls, while the average time to heal was also significantly lower (65 vs. 90 days) (Veves et al., 2001). As well as cellular scaffolds, dermal matrix only scaffolds similar to the uncoated collagen scaffold used in this study have been clinically tested on patient DFUs and VLUs, such as the foetal bovine collagen fibrous matrix PriMatrix. A review of 68 patient ulcers found that DFUs treated with PriMatrix healed at greater than twice the speed of those treated with Apligraf (38 vs 87 days), with a similar outcome for VLUs (32 vs. 63 days) (Karr, 2011). The *in vivo* findings obtained in this project suggest that dermal scaffolds perturb acute wound healing within at least the first 5 days, yet scaffold application to chronic ulcers over many months has been frequently reported to encourage wound closure. One explanation for this difference in findings could be that the application of a scaffold to an ulcer for several weeks could provide a buffer against the highly enzymatic and ECM-degradative environment, potentially allowing the development of new granulation tissue and ECM proteins (Cullen et al., 2002). In this way, a scaffold could improve the wound environment of an ulcer but not of an acute wound as in this study. Although chronic ulcers can exhibit high levels of inflammation, microbial infections of ulcers are also common, and in some cases there may be a reduced level of cellular

infiltration of chronic ulcers (Guo and Dipietro, 2010). In neuropathic diabetic skin, for instance, it has been shown that when neuropeptides such as nerve growth factor are depleted it can result in reduced cell chemotaxis and contribute to DFU formation. Importantly, denervated skin has been found to contain reduced levels of leukocyte infiltration, such that it is possible that, in specific situations, PMN infiltration could be beneficial to the healing of a chronic ulcer (Galkowska et al., 2006). In the vast majority of ulcers this would not appear to be the case, however, since prolonged and elevated inflammation is typically associated with the pathology of chronic ulcers (Pierce, 2001). In fact, it has been argued that the continued recruitment of neutrophils and macrophages to chronic ulcers leads to damage from released reactive oxygen species, cytotoxic enzymes and proteases (Grice and Segre, 2012). For these reasons, it appears more likely that the recruitment of additional PMNs to ulcers would be detrimental to ulcer healing.

It has also been suggested that the scaffolds that have been previously used been to treat ulcers may be acting as a barrier for the wound bed against microbial infection and desiccation (Griffiths et al., 2004). This suggestion was made following the results of an Apligraf study, where it was found that Apligraf did not survive in acute wounds for longer 6 weeks, and instead may promote wound healing by serving as a temporary barrier (Griffiths et al., 2004). Regardless of how scaffolds may affect chronic ulcer closure in the long term, there still remains a need to improve existing scaffolds for use as healing devices. With only 56% of DFUs healing following the use of Apligraf in one study as well as an average healing time of 65 days, the bioactivation of similar devices might confer a considerable improvement to efficacy (Veves et al., 2001). Certainly, in this study, the bioactivation of collagen scaffolds using Cx43 asODN and Cx26 asODN considerably improved the healing of acute wounds.

Although wound edge epithelial thickening following scaffold application has not been thoroughly assessed throughout the existing scaffold literature, epithelial thickening can be observed in some cases. One group that produced electrospun collagen scaffolds and applied them to mouse full-thickness wounds claimed that their scaffolds promoted re-epithelialisation, yet the supporting images were of particularly low quality and measurement of re-epithelialisation across multiple animals was not performed (Chong et al., 2013). Despite this, clear thickening of the leading edge epidermis could be observed in some of their images in which bioactivated scaffolds were applied. Although the thickening

of the leading edge epidermis following scaffold application has not been widely reported, this negative effect was repeatedly observed in this study using a variety of different scaffold types. Uncoated collagen scaffolds, when also applied to rats, significantly increased epithelial thickening. The finding that different scaffold types induced epithelial thickening, as well as observations in both mice and rats, increase the likeliness that this is a common feature associated with scaffold application as opposed to the effect of one particular type of scaffold. The thickening of the epidermis is not only associated with hyperproliferative skin conditions, but also slow-to-heal diabetic wounds (Labarthe et al., 1998, Wang et al., 2007). The repeated observation that uncoated scaffolds induce epithelial thickening could suggest that scaffolds may prevent the transition of wound edge keratinocytes from an adherent to a migratory phenotype, since keratinocytes at the wound edge should normally migrate outwards in a thin process of cells (Laplante et al., 2001).

6.24 – Inflammation and the foreign body reaction

It was apparent that uncoated scaffolds caused a significant increase in the numbers of inflammatory cells with the characteristic morphology of neutrophils infiltrating the uninjured tissue. In this study, scaffolds were fabricated using bovine collagen, owing to it being both readily available as well as frequently selected to produce other commercial and experimental scaffolds (Clark et al., 2007). While this meant that the scaffolds fabricated in this study more closely resembled other scaffolds, in theory there was the potential that the elevated inflammatory response observed following uncoated scaffold application could have been due to a cross species immunogenic reaction to bovine collagen in mice and rats (Menkin, 1930, Opie, 1924). While this is possible, a review of collagen immunogenicity found that collagen is only mildly immunogenic, and had in fact been incorrectly believed to be non-immunogenic until 1954 (Lynn et al., 2004, Watson et al., 1954). It was found that pepsin-extracted collagen from calf skin only induced inflammatory reactions in less than 3% of human patients it was injected into humans for cosmetic purposes (Lynn et al., 2004). While pepsin-derived collagen differs in structure from the acid soluble collagen used in this study, the manufacturer Kensey Nash reports that its materials are processed to remove antigenic components, which could include processing using pepsin to remove terminal telopeptides in collagen that may be more likely to elicit inflammatory responses (Kensey-Nash, 2014). For this reason, it appears unlikely that the increased number of

infiltrating PMNs observed in the intact dermis across all animals studied is due to a cross-species reaction with collagen.

It has been previously demonstrated that implantation of biodegradable scaffolds can cause an increase in PMN infiltration in the surrounding tissue, as well there being a visible association of PMNs with the scaffolds noted (Rucker et al., 2006). Interestingly, the same group found a collagen-chitosan hydrogel induced a more severe inflammatory response over 15 days compared to a biodegradable scaffold made of PLGA. The finding that a hydrogel was less biocompatible is in direct contrast to the findings within this study, in which alginate hydrogel applications resulted in fewer PMNs invading both the dermis and wound bed. Where this study may agree with the results of my project is that the most severe response was found using a collagen application, while the PLGA scaffold was better tolerated. This mirrors the findings of my study, where exposed uncoated collagen scaffolds were found to induce a far more severe reaction than scaffolds that had an outer coating of PLGA. Although it has been argued that collagen is only mildly immunogenic (Lynn et al., 2004), uncoated scaffolds in this study are found to be rapidly degraded at the wound, and have been considerably broken down by D5.

The longer-term effects (D10 & D15 after wound treatment) of the polymer coated scaffolds were assessed in this study. I found that the coated scaffolds were no longer visible within wounds at D10 and D15. This may possibly have been due to the hydrolysis and degradation of the inner scaffold and/or dislodgement of scaffolds from the wound. As well as this, the uncoated scaffolds in this study were found to be rapidly degraded, such that they would not be present in the wound at the later time points.

It has, however, been demonstrated that the long-term application of commercial collagen sponges can cause a foreign body reaction (Cegielski et al., 2008). In particular, this response involves the fusion of macrophages to form foreign body giant cells, which associate with the scaffold and can accelerate its degradation, as well as contribute to inflammation. The foreign body reaction is not exclusive to scaffolds, and has been noted to occur on a variety of implants and medical devices (Anderson et al., 2008). The formation of foreign body giant cells has also been found to contribute to device failure (Zhao et al., 1991). In the present study, the polymer coated asODN containing scaffolds appear to behave more as a form of advanced dressing than a wound integrating scaffold;

as they were not observed to integrate with the wound. As such, if they were to be developed for clinical use it is possible that they could be frequently replaced before cells adhering to scaffolds could advance to giant cells, unlike, for instance, subdermal implants that remain within the skin for several months.

6.3 – Additional therapeutic candidates for scaffold bioactivation

In this study, the bioactivation of scaffolds using asODN to Cx43 and Cx26 was found to improve wound healing when applied either transiently using a Pluronic hydrogel, or in a sustained manner using a polymeric emulsion coating approach. In Chapter 5, it was apparent that the scaffold coating could be used to deliver more than one asODN sequence, and in doing so both Cx43 and Cx26 were found to be downregulated in the combined asODN scaffold-treated wounds. The ability to deliver multiple sequences in a sustained manner leads to the interesting possibility that the novel coating approach could be used to deliver more than one therapeutic agent, in an effort to target multiple perturbed aspects of chronic wound healing. In particular, a number of biological agents including growth factors, peptides and asODN sequences have already been investigated for their effects on wound healing, which could potentially be incorporated into a scaffold coating, as discussed below.

6.31 – Growth factors

A considerable number of studies have bioactivated scaffolds using growth factors as a means to improve wound healing or tissue regeneration. Alginate hydrogels have been designed to incorporate growth factors, including vascular endothelial growth factor (VEGF). Following application of VEGF hydrogels, it was found that angiogenesis was promoted in hypoxic ApoE-/- mouse hindlimbs relative to bollus injections of VEGF, and that the hydrogels resulted in a sustained delivery of the growth factor (Silva and Mooney, 2007). Chitsoan hydrogels incorporating fibroblast growth factor-2 (FGF-2) have also been applied to full-thickness incisional wounds, which appeared to demonstrate an improvement to wound closure (Obara et al., 2003). The authors also argued that the bioactivated hydrogels improved re-epithelialisation, although the provided images of the wounds were extremely low power and unclear. Studies using growth factors in chronic

ulcers have also been investigated, including application of a collagen-gelatine scaffold sponges containing basic FGF (bFGF), a growth factor that promotes fibroblast proliferation and angiogenesis. It was reported that wound closure and granulation tissue formation was significantly enhanced in ulcers that had not healed in over 4 weeks, although assessment of cellular interactions with scaffolds were absent (Morimoto et al., 2013). Growth factor deficiency is common in chronic ulcers, which can be attributed to the overactivity of degradative MMPs. Based on these findings, it appears that supplementing ulcers with growth factors using the sustained delivery coated scaffold could improve healing of chronic ulcers.

The potential for growth factors to improve chronic wound healing is supported to some degree by studies in which growth factors have been directly administered to ulcers (Brown et al., 1991, Steed, 2006, Tsang et al., 2003, Tuyet et al., 2009). One of the most frequently utilised growth factors in the treatment of chronic ulcers is epidermal growth factor (EGF). EGF is implicated in keratinocyte migration, fibroblast proliferation and granulation tissue formation (Hardwicke et al., 2008). Across a number of DFU clinical trials, EGF applications have been reported to improve wound closure and to promote the development of granulation tissue, although re-epithelialisation assessments were again absent in these reports (Brown et al., 1991, Tsang et al., 2003, Tuyet et al., 2009). Platelet-derived growth factor (PDGF) has also been used to treat DFUs, reporting outcomes of reduced time to heal and enhanced wound closure relative to placebo treatments (Steed, 2006).

While some studies have argued that growth factors could improve ulcer healing, a recent review of dressing and scaffold studies declared that growth factor applications did not demonstrate a significant improvement to ulcer wound healing over scaffold only treatments (Palfreyman et al., 2007). The report also highlights bias in scaffold studies and a lack of significance reporting, indicating that many current clinical studies should be interpreted with caution. Additionally, with regards to the use of growth factors over asODN sequences as therapeutic agents, targeted knockdown of specific proteins is not achieved using growth factors as they affect a multitude of proteins and processes. As well as this, safety concerns have been raised regarding the use of certain growth factors, such as the involvement of EGF and insulin growth factor-1 (IGF-1) in promoting tumour development, although a review of clinical evidence suggests that tumour initiation as a

result of growth factor application is unlikely (Berlanga-Acosta et al., 2009, Sandhu et al., 2002). Nevertheless, owing to the number of processes that growth factors can affect, it has been argued that they may be best reserved for situations where other treatments have failed (Berlanga-Acosta et al., 2009). The potential use of growth factors in a scaffold coating approach alongside the previously evaluated asODN sequences should therefore be carefully considered.

6.32 – Peptide therapy

The use of peptides, such as antimicrobial peptides used in scaffold bioactivation, could also be effective in the case of those chronic ulcers with a high bacterial content. Endogenous cationic antimicrobial peptides include cathelicidins, defensins and histatins, and have been found to be active against a broad spectrum of bacteria and fungi (Bals, 2000). The development of synthetic cationic peptides, for example such as the peptide KSL-W, appears to hold greater promise, since it requires an even lower minimum inhibitory concentration to be effective (Concannon et al., 2003). Incorporation of the KSL-W peptide into PLGA microspheres has been shown to result in peptide elution over 4-7 days when incubated in a 20% Pluronic F-127 gel (Machado et al., 2013). Of interest, the *in vitro* application of the KSL-W peptide in conjunction with a biofilm degrading enzyme (DispersinB®) has been found to inhibit the growth of biofilm embedded bacteria that are found in chronic wounds, including MRSA and *Pseudomonas aeruginosa* (Gawande et al., 2014). The combined use of an antimicrobial peptide and biofilm-degrading enzyme could be particularly effect in treating chronic ulcers, since biofilm development often underlies the ulcer resistance to antibiotics. It is important to note, however, that KSL-W has been found to promote neutrophil chemotaxis, which may be counterproductive in an already highly inflammatory wound environment. That said, the KSL-W peptide was also found to reduce oxygen radical production, which could be beneficial to ulcer healing (Williams et al., 2012).

The targeting of connexin expression, which is clinically important to the treatment of chronic ulcers, has also been achieved through the use of mimetic peptides. Unlike the use of asODN, which prevents translation of connexin mRNA transcripts to produce protein, mimetic peptides are peptide sequences that are complementary to the conserved extracellular loop regions of the connexins. These mimetic peptides prevent the opening of connexon hemichannels, and also prevent the docking of connexons to form gap junctions

(Evans and Boitano, 2001). It has also been suggested that mimetic peptides can block GJIC without affecting the connexin structure. Two mimetic peptides have been developed to target the extracellular loop of Cx43 (GAP27) and Cx32 (GAP26), although the conserved nature of the extracellular loop that they target means that they have been found to target multiple connexins (Dahl, 2007, Spray et al., 2002, Warner et al., 1995). Application of GAP27 and GAP26 *in vitro* was found to reduce GJIC in fibroblasts within 1.5 h (Wright et al., 2009), and accelerate keratinocyte and fibroblast migration (Pollok et al., 2011, Wright et al., 2009). Despite this, early passage cell cultured human diabetic keratinocytes and fibroblasts were not affected by GAP27, which appears at odds with the finding that Cx43 asODN promoted diabetic rat keratinocyte migration *in vivo* (Pollok et al., 2011, Wang et al., 2007). An alternative approach to targeting connexin expression using peptides is to target the Cx43 C-terminal tail to prevent interactions with other proteins. The internalisation protein antennapedia has been linked to the last 9 amino acids of the Cx43 tail (RPRPDDLEI) to produce the synthetic peptide ACT1. ACT1 is reported to out-compete interactions between the cytoplasmic tail of Cx43 and the PDZ2 domain of ZO-1, as well as stabilising Cx43 in the membrane and resulting in large plaque formation (Hunter et al., 2005). The use of ACT1 has been reported to accelerate wound re-epithelialisation and reduce scar tissue formation, similar to Cx43 asODN (Ghatnekar et al., 2009, Rhett et al., 2008). More recently, clinical trials investigating the effect of ACT1 found the peptide significantly enhanced wound closure relative to compression bandage therapy alone, and reduced the time taken for 50% and 100% ulcer re-epithelialisation to occur (Ghatnekar et al., 2014). It is interesting that a peptide that results in large Cx43 plaque stabilisation in the membrane has similar effects to Cx43 asODN application, since asODN instead reduces the level of Cx43. ACT1 may produce similar effects to Cx43 asODN through prevention of Cx43 interactions with other proteins, which could also be reduced in the event of Cx43 downregulation using asODN. Connexin-targeting peptides, as well asODN, could be promising therapeutic agents to bioactivate scaffolds that might be used to treat chronic ulcers.

6.33 – Antisense therapy

A number of other sequences have been applied in a wound healing setting without a scaffold that could be beneficial to ulcer healing. The application of siRNA sequences specific to MMP-9 were incorporated into a cationic polymer and reported to improve

wound closure, although the effect on re-epithelialisation or fibroblast migration was not demonstrated *in vivo* (Li et al., 2014). MMP-9 knockdown was also reported in fibroblast cells *in vitro*. The targeting of MMP activity could be particularly effective in chronic ulcers where MMP activity is often considered to be deleteriously upregulated, resulting in degradation of the ECM and growth factors (Mast and Schultz, 1996, Wysocki et al., 1993). Targeting MMP expression has also been achieved *in vitro* indirectly. Through application of asODN specific to TGF-ß1, it has been found that MMP-1 and MMP-9 expression was significantly reduced in keratinocytes and fibroblasts (Philipp et al., 2005). However, it has also been demonstrated that TGF-ß1 can upregulate both MMPs and their inhibitors, TIMPs (Gomes et al., 2012). In this case, knockdown of TGF-ß1 in a chronic ulcer setting may have the deleterious effect of removing TIMPs that are necessary to prevent matrix degradation. Another study that delivered TGF-ß1 siRNA to wounds through bioactivation of collagen-chitosan/silicone membranes argued that wound skin regeneration and scar reduction was improved (Liu et al., 2013). It was clear that TGF-ß1 downregulation was achieved in the tissue samples measured, although the study did not conclusively show that wound closure or scarring was improved. This finding supports the use of scaffold-like matrices as delivery devices for interference therapy.

Another interesting candidate protein that could be downregulated through scaffold bioactivation is the glycoprotein osteopontin (OPN). Expressed as both extracellular and intracellular variants, the complete knockout of OPN has been shown to result in viable mice with no impediment to wound healing, other than disorganisation of deposited ECM fibres following incisional wounding (Liaw et al., 1998). While it has been argued by the authors that OPN may play an important role in tissue remodelling and wound resolution, a second study identified that knockdown using asODN to OPN appears to instead have a favourable effect on healing. OPN knockdown was found to reduce scarring and granulation tissue deposition, but more importantly in the context of that which would be most beneficial in an ulcer setting is that it accelerated wound closure (Mori et al., 2008). Crucially, OPN upregulation occurs in wounds and appears to be associated with inflammation (Cooper et al., 2005). In a chronic ulcer, where inflammation is often severe and protracted, it is possible that OPN could be deleteriously upregulated, although further study would be required to confirm this. Indeed, blocking platelet-derived growth factor (PDGF), a growth factor present in the conditioned media of inflammatory macrophages and mast cells, prevented OPN upregulation (Mori et al., 2008). These findings highlight

both OPN and PDGF as potential targets for knockdown in addition to connexins to promote wound healing.

The development of a polymer coating to deliver Cx43 and Cx26 asODN had the effect of promoting wound healing across a number of different assessed areas, yet it is evident that there are number of other therapeutic agents that could be incorporated into the scaffold coating in conjunction with a cargo of connexin antisense sequences.

6.4 – A revised role for dermal scaffolds in wound healing

A number of scaffolds have been developed for use in treating various types of chronic ulcers as well as full-thickness burns. In the design of these products, it is often considered important that they mimic the native tissue, and in the case of acellular dermal scaffolds this involves the design of a fibrous matrix that can support fibroblast adhesion and proliferation as well as integrate with the wound (Chong et al., 2007). Scaffolds are also developed to be well tolerated within the wound, eliciting only a minimal inflammatory response, while also not causing a severe foreign body reaction (Figure 6. 1A). The current understanding that dermal scaffolds may serve as useful wound regenerative devices is perhaps being more readily accepted due to *in vitro* findings, in which scaffolds are often reported to accommodate seeded cells (Mo et al., 2004). Following detailed microscopic analysis of *in vivo* experiments in my study, however, it appears that collagen scaffolds, as well as alginate dressings and microspheres, do not encourage classical wound regeneration across a number of different variables that were assessed (Figure 6. 1B). The full-thickness wound application of an electrospun collagen scaffold fabricated in a similar method to previous studies (Torres-Giner et al., 2009) led instead to thickening of the epidermis at the wound edge in both mice and rats, and Cx43 and Cx26 were strongly upregulated in these regions. These findings are more in line with observations of diabetic rat wounds and chronic human ulcers, in which healing is perturbed (Mendoza-Naranjo et al., 2012b, Wang et al., 2007). The implication that scaffolds instead negatively impact wound healing is further supported by the association of PMNs with the scaffold and elevated levels of inflammation within the dermis (Chapters 3-5), (Gilmartin et al., 2013). Although this project made use of acute full-thickness wound models, the findings strongly support that

unmodified scaffolds could, instead of promoting chronic ulcer healing, have a detrimental effect on multiple aspects of healing.

The desire to produce a wound-integrating dermal scaffold could also not be achieved by addressing the deleterious overexpression of Cx43 using a Cx43 asODN Pluronic gel (Figure 6. 1C), (Gilmartin et al., 2013). Despite successfully reducing Cx43 levels in keratinocytes at the wound edge, fibroblast attachment and proliferation was not significantly observed within scaffolds, although inflammatory cell invasion was reduced. Keratinocyte migration also occurred underneath scaffolds in a manner similar to a scab. Although there was some improved biocompatibility of the scaffold, scaffolds did not act as a replacement dermal matrix as desired. These findings strongly argue against the current understanding that scaffolds may behave as good substitutes for the dermis. Despite these findings in full-thickness animal models, moderate successes have been reported following clinical use of scaffolds over several months (Schonfeld et al., 2000, Karr, 2011). It has been demonstrated that even cellular scaffolds do not integrate with wounds and serve more as a temporary barrier that could promote ulcer healing (Griffiths et al., 2004). Although scaffolds may not be useful as a dermal substitute in chronic ulcer healing, it is possible that scaffolds could adopt a new role with regards to promoting wound healing. Through the development of a novel Cx43 and Cx26 asODN scaffold coating technique, the results of this project suggest that scaffolds may better serve as a drug delivery device that does not integrate with wounds and instead acts more as a dressing overlying the wound (Figure 6. 1D). In this way, restoration of the epithelial barrier would not be obstructed while proteins that are aberrantly upregulated in cells within the ulcer could be continuously targeted through sustained drug delivery.

6.41 - Study limitations

While a number of results were obtained throughout the course of the project, the study did have certain limitations. Application of coated scaffolds to wounds for longer than 5 days (chapters 4-5) may have been affected due to the transient nature of Tegaderm film adhesiveness. In future, cyanoacrylate glues could be used, as they have been in other scaffold studies, to fix scaffolds in place on the wound (Duffy et al., 2005). The regrowth of animal hair, as well as variation in the length of time that Tegaderm remained

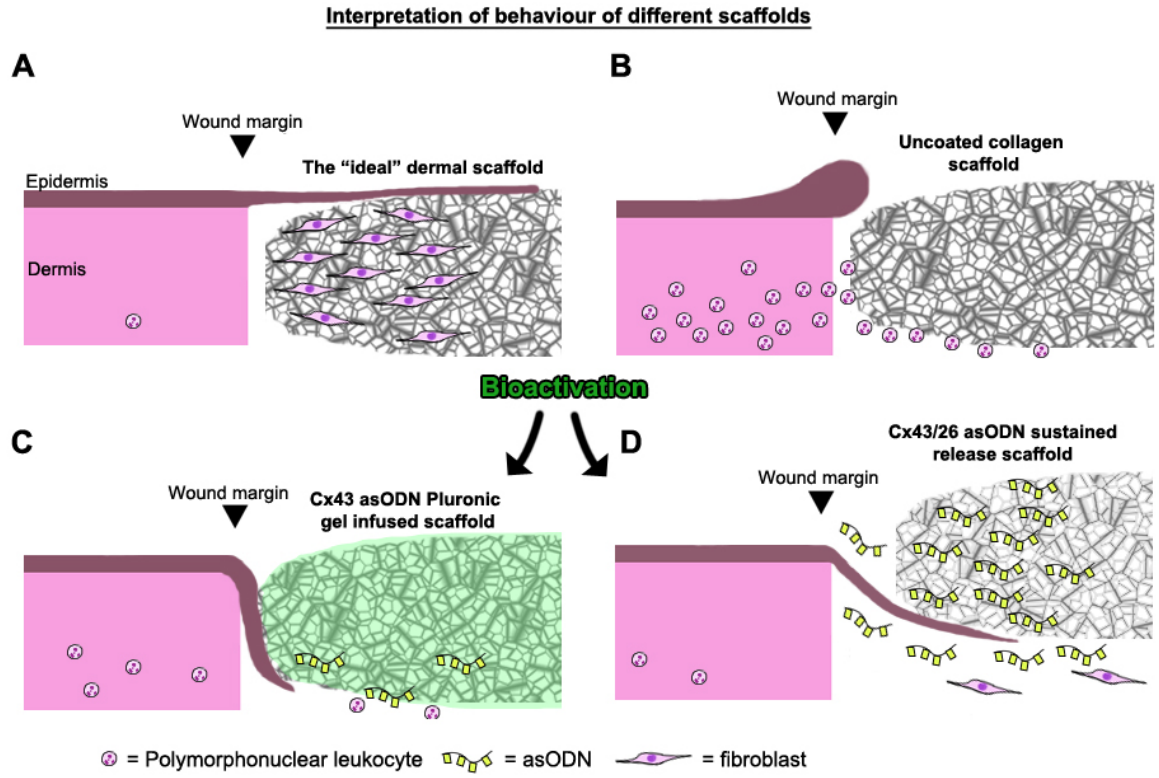

Figure 6. 1 – Interpretation of the function of uncoated and bioactive scaffolds **(A):** A model outlining the previously believed mode of scaffold action. Scaffolds were typically considered to serve in a similar capacity to native extracellular matrix, acting as a scaffold for fibroblast attachment and proliferation, while keratinocytes migrated over the matrix. **(B):** The actual observed behaviour of wounds in response to uncoated collagen scaffold application. Keratinocytes aggregate as thickened non-migratory bulbs at the wound edge in which Cx43 and Cx26 is strongly upregulated. Polymorphonuclear leukocytes (PMNs) as opposed to fibroblasts are found to associate with the scaffold, while PMNs are also found to infiltrate the dermis of uninjured tissue. **(C):** Transient bioactivation of collagen scaffolds using a Cx43 asODN Pluronic gel (green) reduced epithelial thickening and PMN infiltration, while epithelial migration occurred underneath scaffolds in a manner similar to a scab. **(D):** The function of sustained release polymer coated scaffolds bioactivated using both Cx26 and Cx43 asODN. Coated scaffolds were only loosely associated with the wound edge, and keratinocyte migration was significantly enhanced. Epithelial thickening was again prevented relative to uncoated scaffolds, while elevated PMN infiltration of the dermis was similarly prevented. In all cases, keratinocyte migration was not found to occur over scaffolds.

adherent to the animal back, meant that re-application of Tegaderm was not possible. At D10 and D15, wounds typically showed no signs of scaffolds, although it was unclear whether this was due to the hydrolysis of the inner scaffold over time or the loss of scaffolds from the open wounds. Another limiting factor regarding coated scaffolds that has previously been discussed is the fact that the polymer coated scaffolds sectioned very poorly using a cryostat. Because of this, coated scaffolds could not typically be visualised in H&E tissue sections, although scaffold presence was confirmed macroscopically prior to histological processing.

In terms of experimental limitations, the combination of two novel Cx26 asODN sequences was performed throughout chapter 5 due to the limited availability of wounds (4 per animal) as well as the time remaining in the project. Testing of the sequences individually in future could be performed in order to identify the most effective sequence. With regards to the characterisation of changes in wound edge connexin expression throughout the thesis, it has previously been shown that only a limited number of keratinocytes at the leading edge typically dynamically change in connexin levels during wound healing (Qiu et al., 2003). It would be extremely difficult to separate out these small number of cells from the rest of the tissue in order to assess changes in connexin protein quantity using western blotting approaches, for instance. The use of an immunofluoresnce staining approach was therefore used to characterise connexin expression throughout the project. This technique has been similarly practiced throughout a number of previous studies and additionally permits identification of the localisation of protein expression (Davis et al., 2013, Mendoza-Naranjo et al., 2012a, Zhai et al., 2014).

6.5 – Future experiments

6.51 – Performing a systematic review of scaffold-related literature

Over the course of the study it became clear that uncoated solid collagen scaffolds had the effect of inhibiting wound closure and re-epithelialisation, while also resulting in connexin misexpression typical of chronic wounds. These findings indicate a potential novel role for unmodified scaffolds as inducers of chronic-like wounds. Scaffolds could, in this case, instead be used as a tool to generate a chronic wound model. This possibility is particularly attractive due to the limited number of existing chronic wound animal models, which can

also be also be expensive and time consuming to develop (Ansell et al., 2012). Scaffolds can be relatively inexpensive to fabricate and the negative effects of scaffold application in this study was found to be detectable within 24 hours.

As a follow on study to this thesis, a series of future experiments to develop scaffolds as a chronic wound model would first require investigation into the most appropriate material that could be used to generate scaffolds most likely to elicit a chronic-like wound. Additionally, the scaffold form (such as an electrospun scaffold or hydrogel) would need to be selected based on its potential to cause chronic wound-like symptoms. At the outset of this thesis, collagen was selected as the base scaffold material while elctrospinning was chosen as the method to fabricate the matrices. In both cases, these choices were made following literature searches of both animal and human *in vivo* scaffold studies, as well as *in vitro* studies that reported scaffold fabrication (Buttafoco et al., 2006, Huang et al., 2003). Additionally, Dr Suwan Jayasinghe at UCL had both the means and experience to assist with the initial setup of electrospinning collagen. The primary intention of the literature searches was to identify one of the most commonly applied scaffolds that could be affordably mimicked in the laboratory, such that the results obtained in this study could address current developers of scaffolds and biomaterials journals. Collagen is not only used in a large proportion of commercial scaffolds, it is often selected for use in animal studies (Buttafoco et al., 2006, Huang et al., 2003, Shevchenko et al., 2010). Similarly, electrospinning was commonly reported throughout the literature as a relatively simple technique capable of producing fibrous matrices in an effort to mimic some of the properties of the native dermis (Huang et al., 2003). Importantly, this technique was also available to us to use in the UCL mechanical engineering department.

In a series of future experiments to develop a scaffold chronic wound model, the initial justification for using scaffolds, choice of scaffold material and method of scaffold fabrication would instead be based on a more rigorous approach than that undertaken in this thesis. In particular, performing a systematic review of existing randomised controlled trials (RCTs) in which scaffolds were applied to wounds would more accurately help identify the type of scaffold that is more likely to induce a negative effect on healing, and therefore be more useful in the setup of a chronic wound model. Performing a systematic review using Cochrane methodology will provide a comprehensive overview of the effects

of different kinds of scaffolds on wound healing, making it possible to make an informed choice of scaffold.

A Cochrane review consists of multiple sections. An abridged background and justification for performing the review, which would later be expanded on, is as follows:

Background

Chronic ulcers remain difficult to treat and have a major impact patient quality of life, while also costing the UK over £3 billion annually (Posnett and Franks, 2008). The assessment of chronic wounds at a preclinical level is hampered by the limited availability of animal models that realistically recapitulate chronic wounds (Ansell et al., 2012). Current models of impaired healing consist of animals that are diabetic, aged, treated with bacteria or subjected to anoxic insults. In the case of localised anoxia, this can be achieved through the application of magnets to form a pressure ulcer (Ansell et al., 2012). The generation of aged animals can be expensive, while diabetic wounds still heal, albeit slower, unlike many chronic wounds. The development of a new and affordable model that can better mimic chronic wounds would be extremely useful in preclinical studies as a tool for drug testing. A previous study has highlighted the potential for solid scaffolds to act as inducers of chronic-like wounds, features present in human chronic wounds. Most notably, wound re-epithelialisation was significantly perturbed, alongside severe thickening of the epidermis and misexpression of connexin proteins at the wound edge (Gilmartin et al., 2013).

Why it is important to do this review

Development of a scaffold capable of inducing chronic-like wounds requires prior investigation into the most appropriate materials and scaffold types that could be used to make a scaffold. While a systematic review of various wound dressings and scaffolds for healing wounds has been performed, this was not a Cochrane review. Additionally, it does not assess the endpoints required in order to identify the types of scaffolds have the strongest negative effect on wound healing (Snyder et al., 2012).

The objectives of the Cochrane review would be as follows:

1) To provide pooled observations and effect estimates (meta-analysis) of outcomes of the effects of different scaffold types on wound healing (including inflammation

via real time (RT)-PCR analysis/inflammatory cell counts, wound re-epithelialisation and measurements of granulation tissue formation)

2) To compare these estimates between different scaffold types in order to determine which scaffold type is most likely to elicit a negative reaction.

With regards to the methods section of the systematic review, this review will capture RCTs involving adult patients in which scaffolds (or 'advanced dressings') have been applied to chronic ulcers. When assessing RCTs for inclusion in the review, guidelines on reporting trials available on the EQUATOR (Enhancing the Quality and Transparency of Health Research; http://www.equator-network.org) network, which will be complied with where applicable during the data extraction process. The EQUATOR network was established with the primary goal to compile multiple guidelines concerning the reporting of healthcare studies. These guidelines, such as the PRISMA guidelines, are available from the EQUATOR website, and include a checklist of information to report when assessing other meta-analyses or systematic reviews (Moher et al., 2009). These include requirements for the reporting risk of bias present in studies as well as patient numbers, information sources and search strategies. Several other key reporting guidelines are also catalogued by the EQUATOR network. These include CONSORT, STROBE, STARD, COREQ, ENTREQ, SQUIRE, CARE, SAMPL and SPIRIT.

Search strategy

Searching for RCTs should be performed separately by two individuals. MEDLINE, The Cochrane Library, EMBASE and ISI Web of Science will be used to perform the searches.

RCTs will be searched for using the following keywords. As an example, the number of search records found using MEDLINE (prior to excluding any studies) is stated in square brackets after each search string, below:

'Randomized controlled trial' AND 'ulcer' AND 'matrix' [45 results]

'Randomized controlled trial' AND 'scaffold' [55 results]

'Randomized controlled trial' AND 'ulcer' AND 'dressing' [501 results]

'Randomized controlled trial' AND 'dermal' AND 'substitute' [23 results]

Searches will also be performed by substituting 'RCT' with 'CCT' in the search string. It is anticipated that additional search terms will be added to this list following general searches of scaffold studies to identify more scaffold-related search terms.

Study exclusions

Both RCTs and controlled clinical trials (CCTs) will be included, regardless of whether blinding took place or sample size. Cohort or case-control studies will not be included. Studies that do not involve the primary application of scaffold structures to wounds (e.g. systematic reviews) will also be excluded. Searching for 'scaffold' can also return results that focus on bone/cartilage repair or blood vessel stents. These focus on a different type of 'scaffold', separate to dermal scaffolds, as and such will also be excluded.

Retrieving records

As an example of performing searches, the relevant RCTs/CCTs for the search string **'randomized controlled trial' AND 'ulcer' AND 'matrix'** are presented below using PubMed to search:

Search: **'randomized controlled trial' AND 'ulcer' AND 'matrix'** [45 results]

Exclusions: [22 publications - non scaffold related, not RCT/CCTs]

Included: [23 publications]. After excluding publications, 23 records remained that met all inclusion conditions. These studies were as follows:

1. The effects of sulodexide on both clinical and molecular parameters in patients with mixed arterial and venous ulcers of lower limbs. Serra R et al. (Drug Des Devel Ther. 2014 May 13;8:519-27)

2. The influence of patient and wound variables on healing of venous leg ulcers in a randomized controlled trial of growth-arrested allogeneic keratinocytes and fibroblasts. Lantis JC 2nd et al. (J Vasc Surg. 2013 Aug;58(2):433-9)

3. [Dynamic changes of MMP-1, MMP-9 and TIMP-1 in the refractory diabetic dermal ulcers treated by autologous Platelet-rich gel]. He LP et al. (Sichuan Da Xue Xue Bao Yi Xue Ban. 2012 Sep;43(5):757-61)

4. Randomised, controlled pilot to compare collagen and foam in stagnating pressure ulcers. Piatkowski A et al. (J Wound Care. 2012 Oct;21(10):505-11)

5. A prospective, single-center, nonblinded, comparative, postmarket clinical evaluation of a bovine-derived collagen with ionic silver dressing versus a carboxymethylcellulose and ionic silver dressing for the reduction of bioburden in variable-etiology, bilateral lower-extremity wounds. Manizate F et al. (Adv Skin Wound Care. 2012 May;25(5):220-5)

6. Wound stimulation by growth-arrested human keratinocytes and fibroblasts: HP802-247, a new-generation allogeneic tissue engineering product. Goedkoop R et al. (Dermatology. 2010;220(2):114-20)

7. Randomized comparison of OASIS wound matrix versus moist wound dressing in the treatment of difficult-to-heal wounds of mixed arterial/venous etiology. Romanelli M et al. (Adv Skin Wound Care. 2010 Jan;23(1):34-8)

8. Assessment of the antimicrobial effectiveness of a new silver alginate wound dressing: a RCT. Trial C et al. (J Wound Care. 2010 Jan;19(1):20-6. Erratum in: J Wound Care. 2010 Mar;19(3):109)

9. Clinical effectiveness of an acellular dermal regenerative tissuematrix compared to standard wound management in healing diabetic foot ulcers: a prospective, randomised, multicentre study. Reyzelman A et al. (Int Wound J. 2009 Jun;6(3):196-208)

10. Clinical assessment of the effect of a matrix metalloproteinase inhibitor on aphthous ulcers. Skulason S et al. (Acta Odontol Scand. 2009;67(1):25-9)

11. Effect of oxidised regenerated cellulose/collagen matrix on proteases in wound exudate of patients with chronic venous ulceration. Smeets R et al. (Int Wound J. 2008 Jun;5(2):195-203)

12. Evaluation of the nano-oligosaccharide factor lipido-colloidmatrix in the local management of venous leg ulcers: results of a randomised, controlled trial. Schmutz JL et al. (Int Wound J. 2008 Jun;5(2):172-82)

13. The lack of reliability of clinical examination in the diagnosis of wound infection: preliminary communication. Serena TE et al. (Int J Low Extrem Wounds. 2008 Mar;7(1):32-5)

14. Effect of amelogenin extracellular matrix protein and compression on hard-to-heal venous leg ulcers: follow-up data. Romanelli M et al. (J Wound Care. 2008 Jan;17(1):17-8, 20-3)

15. Synergistic action of protease-modulating matrix and autologous growth factors in healing of diabetic foot ulcers. A prospective randomized trial. Kakagia DD et al. (J Diabetes Complications. 2007 Nov-Dec;21(6):387-91)

16. Effect of amelogenin extracellular matrix protein and compression on hard-to-heal venous leg ulcers. Vowden P et al. (J Wound Care. 2007 May;16(5):189-95)

17. The effect of amelogenins (Xelma) on hard-to-heal venous leg ulcers. Vowden P et al. (Wound Repair Regen. 2006 May-Jun;14(3):240-6)

18. Mitogenic bovine whey extract modulates matrixmetalloproteinase-2, -9, and tissue inhibitor of matrixmetalloproteinase-2 levels in chronic leg ulcers. Varelias A et al. (Wound Repair Regen. 2006 Jan-Feb;14(1):28-37. Erratum in: Wound Repair Regen. 2007 Jan-Feb;15(1):163)

19. Randomized clinical trial comparing OASIS Wound Matrix to Regranex Gel for diabetic ulcers. Niezgoda JA et al. (Adv Skin Wound Care. 2005 Jun;18(5 Pt 1):258-66)

20. Effectiveness of an extracellular matrix graft (OASIS WoundMatrix) in the treatment of chronic leg ulcers: a randomized clinical trial. Mostow EN et al. (J Vasc Surg. 2005 May;41(5):837-43)

21. Can a tissue-engineered skin graft improve healing of lower extremity foot wounds after revascularization? Chang DW et al. (Ann Vasc Surg. 2000 Jan;14(1):44-9)

22. Promotion and acceleration of diabetic ulcer healing by arginine-glycine-aspartic acid (RGD) peptide matrix. RGD Study Group. Steed DL et al. (Diabetes Care. 1995 Jan;18(1):39-46)

23. Accelerated healing of chronic sickle-cell leg ulcers treated with RGD peptide matrix. RGD Study Group. Wethers DL et al. (Blood. 1994 Sep 15;84(6):1775-9)

Data to be extracted from retrieved publications

The following data will be extracted:

1. Year and language of publication

2. Country

3. Date range that the trial took place

4. Inclusion and exclusion criteria (e.g. age, sex, grade of wound, diabetes)

5. Number of participants (both those screened and those only included in trial)

6. Details of procedure/treatment schedule

7. Outcomes. The following outcomes will be extracted:

- Primary outcome: percentage wound area reduction at 12 weeks from baseline
- Secondary outcome: re-epithelialisation percentage at 12 weeks from baseline (if such evaluation is performed)
- Secondary outcome: inflammatory reaction quantification (percentage increase in inflammatory markers/cells over controls if molecular approaches used, otherwise observational findings)

8. Methods employed to reduce bias

9. Trial funding and source

Hetereogeneity

In order to determine whether the data extracted would be suitable for statistical meta-analysis, extracted results will be subjected to heterogeneity assessments. In particular,

heterogeneity will be assessed visually using forest plots, χ^2 tests. An additional method is the interpretation of the I^2 statistic, which is calculated using the effect (Higgins et al., 2003). Using the Cochrane guidelines, meta-analysis will only be performed if the returned I^2 statistic is over 75%, in line with the recommendations of the Cochrane handbook (Higgins and Green, 2011b).

Meta-analysis

If specific outcome data is suitable for meta-analysis, the software program RevMan will be used to perform the analyses. The Cochrane handbook details common approaches to meta-analysis depending on the data obtained. In particular, the handbook outlines the available meta-analysis methods in RevMan when dealing with both dichotomous and continuous data; both fixed- or random-effects methods (Higgins and Green, 2011a). A results summary table can additionally be generated using GRADEpro software in order to grade the quality of evidence for each outcome. This is particularly important as it allows one to take into account the risk of bias within the data pool.

It is anticipated that performing a systematic review with meta-analyses will help highlight the scaffold types and materials most commonly associated with causing a negative reaction, or least frequently improving healing. This information would be useful when generating a new scaffold with the purpose of generating a novel chronic wound model.

6.52 – Establishment of a novel chronic wound model

Following the completion of a review using Cochrane methodology, it is anticipated that a number of different scaffold materials and fabrication methods will be identified as suitable to produce scaffolds that will perform well as inducers of chronic-like wounds. The first step would be to further research the scaffold processing techniques identified throughout the review, such that they could be employed to generate scaffolds composed of different materials. The different scaffolds would then be eligible for application to full-thickness excisional wounds made to the backs of rats, as performed in this thesis. The number of rats that produced significant results in the previous series of scaffold experiments would again be used in the planned experiments (n=8). The time points of D1, D3 and D5 will be selected as cull points to compare the time taken for different scaffolds to induce epithelial thickening, inflammation and Cx43/Cx26 expression. These time points will also allow

result comparisons to be made to the collagen scaffold experiments performed in this thesis.

In the first chapter of this thesis, collagen scaffolds were found to be largely degraded by day 5. The loss of the scaffold from the wound after such a short period of time would not be ideal in the generation of a chronic wound model. Polymer coated collagen scaffolds, on the other hand, appeared to shift from the position in which they were placed within the wound. One method to correct this problem could be to superglue scaffolds onto wounds (Duffy et al., 2005). This would prevent loss of the scaffold from the wound at later timepoints. Additionally, the use of higher ratios of lactide to glycolide PLGA or PCL only scaffolds, in combination with superglue, would result in scaffolds that remained within wounds for longer periods of time. These scaffolds could be applied to wounds in the same manner as the collagen scaffolds, but would allow time points of 30 days and beyond to be assessed.

Assessments

Light microscopy

As performed in this thesis, re-epithelialisation and wound edge epithelial thickening would be measured at D1, D3 and D5. Additionally, measurements will also be recorded at D10, D15 and D30, as it is anticipated that the continued presence of a scaffold will postpone re-epithelialisation. These time points would help identify the scaffolds that had the most severe impact on re-epithelialisation. A delay to wound healing on the scale of a month or more would suggest that scaffolds were capable of inducing a 'chronic-like' to partially recapitulate human chronic wounds. If, at D30, the continued presence of a scaffold has prevented re-epithelialisation from occurring, longer time points can be considered. In addition to re-epithelialisation and wound edge thickening, the histological assessment of inflammatory cells invading the dermis will again be performed on the same tissue to explore whether specific scaffold materials and forms are more likely to induce chronic wound-like inflammation. In addition, the visual detection of foreign body giant cells (FBGCs), which are fused macrophages formed in response to a foreign body, can also be performed. FBGCs typically form after a number of weeks in response to a present foreign body (Cegielski et al., 2008). The detection of these cells at the D15 and D30 time points would help further confirm the inhibitory effect of scaffolds used in this model.

Inflammation

In addition to the microscopic assessment of scaffold-treated wounds, performing real-time (RT) PCR on digested wound tissue following scaffold application would provide a more conclusive means of quantifying inflammation. The protocol to enzymatically degrade tissue followed by RNA purification has been outlined in previous studies (Jackson et al., 1990, Peirson and Butler, 2007), and would be followed to extract RNA from scaffold-treated wounds. The wounds examined histologically in the previous light microscopy section would first be bisected; one half would be fixed, frozen and cryosectioned while the other half would be stored in RNAlater and used for RNA extraction. This step would be performed using wound tissue harvested from all planned time points (D1, D3, D5, D15, D30 and potential future time points beyond 30 days).

Numerous studies have quantified pro-inflammatory cytokine gene expression in order to investigate inflammation more rigorously than is possible using histological approaches. In particular, expression of the pro-inflammatory cytokines IL-1, IFN-γ and TNF-alpha are often studied, corresponding with classically activated pro-inflammatory M1 macrophages (Autenrieth et al., 1997, Gougeon et al., 2013). Determination of expression of these genes relative to a stably expressed housekeeping gene will allow comparisons of wound inflammation following treatment with different kinds of scaffolds. On the other hand, increased expression of IL-10 and TGF-ß is more commonly associated with alternatively activated (M2) macrophages, responsible for tissue repair and attenuation of pathological inflammation (Mosser, 2003). Detection of a higher ratio of M1 to M2 cytokine expression may therefore serve as a useful indicator of inflammation in the wound bed following scaffold treatment.

Enzyme-linked immunosorbant assays (ELISA)

A common feature of chronic diabetic wounds is a reduced stability of the transcription factor hypoxia inducible factor-1 (HIF-1). The α subunit of HIF-1 is tightly regulated by cell oxygen availability; under normoxic conditions, HIF-1α has a rapid turnover of less than 5 minutes (Hofer et al., 2002). Under hypoxic conditions, HIF-1α escapes proteasomal degradation and translocates to the nucleus, whereupon it dimerises with the ß subunit. The assembled HIF-1 transcription factor can then act to regulate expression of a large number of genes, and importantly can drive VEGF expression to promote

angiogenesis (Forsythe et al., 1996). A reduced level of HIF-1 stability as found in diabetic skin can therefore result in a reduced response to anoxia, promoting the maintenance of the anoxic environment due to limited resultant angiogenesis (Botusan et al., 2008). In the case of the scaffold experiments that are planned to be performed, it may transpire that the placement of large solid scaffolds creates a localised region of anoxia, on account of the limited cellular penetration of scaffolds experienced throughout this thesis. Indeed, H&E staining revealed that vascular smooth muscle cells were not present within intact scaffolds. As such, scaffolds may be capable of creating an anoxic environment that is characteristic of chronic wounds. Anoxia could be detected in scaffold-treated wounds by measuring HIF-1α activity through ELISA. Commercially available ELISA plates containing the HIF-1α response element adherent to individual wells within a plate allow the addition of nuclear extracts (kit available from: http://www.abcam.com/hif-1-alpha-transcription-factor-assay-kit-ab133104.html). Detection of an increased level of HIF-1α would suggest that the wound environment is anoxic. Performing ELISA on nuclear extracts obtained from harvested scaffold-treated wound cells will be a useful step to confirm whether scaffolds can again induce features characteristic of human chronic wounds.

Western Blotting

Western Blotting may also be used to detect the levels of Tissue Inhibitors of matrix Metalloproteinases (TIMPs) in scaffold-treated wounds. In acute healing wounds, TIMPs act to inhibit the activity of MMPs such that the balance between deposition and degradation of new matrix proteins is finely tuned (Nagase et al., 2006). In chronic ulcer fluid, TIMP levels have been found to be significantly reduced, which may partially underlie the often severely degraded ECM present in these ulcers (Nwomeh et al., 1999). A decrease in TIMP protein in harvested wound tissue following scaffold treatment may suggest that scaffolds have the potential to disturb the normal balance between MMP and TIMPs, similar to the situation in chronic wounds. This could be due to the presence of a polymer scaffold that is systematically targeted for degradation. Western Blotting using anti-TIMP and anti-MMP antibodies on whole-cell protein extracted from wound tissue may therefore also be used to confirm whether the ratio between the two is altered, similar to chronic wounds.

Detection of cell death

It has been previously shown in VLUs that extensive cell death occurs relative to healthy skin, in conjunction with hypoxia and oxygen reperfusion. This was demonstrated through the use of terminal deoxynucleotidyl transferase dUTP nick end labeling (TUNEL) staining; fragmented DNA staining, characteristic of apoptosis, was found to be elevated in VLUs (Herouy et al., 2004). To establish whether the application of a scaffold may be causing a chronic-like wound by similarly increasing the level of apoptosis in the wound, wounds treated with scaffolds will be harvested, frozen and cryosectioned. Tissue will then be TUNEL stained. Using this method, it can be detected whether scaffolds induce apoptosis similar to in chronic ulcers, and in which specific cell types.

Impaired granulation tissue deposition using scaffolds

During the course of wound healing, the major collagen type deposited at the wound bed is type III. As the wound matures, type III collagen is gradually hydrolysed and replaced by type I collagen (Klinge et al., 2000). It has been observed that in individuals where healing is perturbed, such as diabetics, the amount of collagen type I deposited at the wound is reduced (Black et al., 2003). This finding has been explained by the decreased numbers of fibroblasts present in diabetic wounds. In this thesis, applying an obstructive scaffold resulted in very few non-inflammatory cells infiltrating the wound. It is possible, therefore, that collagen scaffolds may be recapitulating healing impaired diabetic wounds by similarly preventing fibroblast infiltration of the wound bed, resulting in decreased collagen deposition. It has been shown previously that the application of Cx43 asODN to wounds accelerates fibroblast migration both *in vitro* and *in vivo* (Mori et al., 2006). This may explain why the coating of scaffolds with Cx43 asODN resulted in faster contraction of granulation tissue at D10 and D15; due to an increased number of fibroblasts migrating into wounds and depositing collagen.

In order to determine whether the scaffold chronic-like wound model limits collagen deposition in the newly forming granulation tissue, staining for collagen type I can be performed. Immunostaining for collagen I can be performed on untreated wounds, scaffold-treated wounds and Cx43 asODN coated scaffold-treated wounds. Comparing staining levels between the different treatments will highlight whether the scaffold is preventing collagen I deposition relative to untreated wounds. Additionally, quantifying

collagen I deposition in Cx43 asODN scaffold-treated wounds can help identify whether Cx43 asODN improves collagen deposition in the wound.

In addition to this, the orientation of deposited collagen fibres can also be assessed to gauge the extent of scarring in wounds following scaffold placement. In normal skin, collagen is normally arranged in a basket-weave formation. In scarred tissue, however, collagen fibres are typically aligned with each other (Gurtner et al., 2008). Following scaffold application, assessment of collagen fibre alignment can be performed to assess the extent of scarring encountered using scaffolds. Excessive scarring may indicate that the scaffold is capable of reproducing a poorly healing wound.

6.53 – Continued development of the polymer coated drug-eluting scaffold

Characterising the role of Cx43 asODN coated scaffolds in reducing inflammation

In this thesis, although Cx43 asODN coated scaffolds were shown to reduce inflammatory PMN recruitment, it was not demonstrated how Cx43 knockdown resulted in this effect. It has been separately shown in the lung that decreasing Cx43 channel conductivity with the blocking peptide ^{43}Gap26 reduced neutrophil adhesion to endothelial cells, ultimately lowering the migration of neutrophils to the site of inflammation in the lung (Sarieddine et al., 2009). Cx43 is expressed on the surface of neutrophils and endothelial cells, such that the knockdown of Cx43 reduces communication between the two cell types. It is possible that a similar situation occurs during wound healing; Cx43 knockdown may reduce the recruitment of PMNs by reducing PMN to endothelial cell communication (and subsequently adhesion), resulting in decreased PMN transmigration to the site of injury. In order to test this hypothesis, similar *in vitro* experiments to those performed by Sarieddine et al. (2009) could be performed. In their study, they utilised lung alveolar epithelial murine pneumocyte monolayers that had been treated with the Cx43 blocking peptide, to which they applied neutrophils. To perform a similar experiment relevant to wounding, neutrophils isolated from rat skin by density gradient ultracentrifugation or flow cytometry can be treated with the Cx43 asODN sequence used in this thesis. Following the seeding of these neutrophils onto separate skin keratinocyte and endothelial cell monolayers, cells can be rinsed then fixed, after which the adhesion of cells can be visualised using a light microscope to determine the frequency of adhering neutrophils within single field of views.

This approach would be necessary to identify whether Cx43 knockdown improved healing by reducing neutrophil adhesion and, as a result, transmigration to the wound site.

Linking Cx43 knockdown to fibroblasts in the granulation tissue

One of the areas that was lacking in this thesis was the assessment of granulation tissue deposition. While it was shown that the overall area of granulation tissue and wound size was reduced following Cx43 asODN coated scaffold application, it was not shown whether Cx43 knockdown in fibroblasts resulted in this effect. It has been elsewhere demonstrated *in vitro* that Cx43 knockdown in fibroblasts improves their migration through stabilisation of the GTPases Rac1 and RhoA (Machacek et al., 2009, Mendoza-Naranjo et al., 2012a). Acceleration of granulation tissue and collagen deposition may occurr as a result of enhanced fibroblast migration through activity of Cx43 asODN. However, differences in Cx43 expression were not detectable by eye following immunofluorescence staining of both mouse and rat wounds in this thesis, mainly due to the background fluorescence often present within the wound bed.

One method to detect Cx43 levels in the wound bed would be to use an immunohistochemistry approach using horseradish peroxidase (HRP) instead of fluorescence conjugated antibodies, on account of the high background fluorescence in the wound. Another method to assess whether Cx43 asODN coated scaffolds reduced fibroblast Cx43 expression would be to use flow cytometry and Western Blotting. Harvesting scaffold-treated wound tissue at D1, D2, D3 and D5 can be performed, using the same approach as outlined in the previous sections. Enzymatic digestion of the wound tissue to release cells can be performed by following an enzymatic digestion protocol that has been successfully used in other studies (Seluanov et al., 2010). Fluorescence-Activated Cell Sorting (FACS) can then be performed to isolate cells expressing alpha smooth muscle actin (present on activated myofibroblasts) and PDGF-R. Both of these markers have been previously identified as effective in the isolation primary fibroblasts (Sharon et al., 2013). Following FACS, performing a Western Blot on the whole cell lysates of control scaffold vs Cx43 asODN scaffold treated wounds using an anti-Cx43 antibody would then reveal whether Cx43 asODN scaffolds knocked down Cx43 expression *in vivo*. This result would support previous *in vitro* findings that link Cx43 knockdown to enhanced migration in fibroblasts.

Using Cx43 asODN coated scaffolds to deliver other therapeutic agents

As detailed in section 6.3, a number of additional therapeutic agents are available that can be used to coat scaffolds in the same manner performed in this thesis. In particular, growth factors such as VEGF (Silva and Mooney, 2007), antibacterial peptides like KSL-W (Williams et al., 2012) and anti-Cx43 peptides such as ACT1 (Ghatnekar et al., 2014). The combination of the existing Cx43 and Cx26 asODN sequence with these sequences in a sustained release scaffold coating could further enhance full-thickness wound healing. The testing of these agents in conjunction with Cx asODNs would involve the same full-thickness wounding procedure that was performed on rats in this study. Four full-thickness wounds would be made to the backs of rats, and each wound would be treated with a scaffold coated in one of the new therapeutic agents. In addition, wounds can be coated in both Cx asODNs and another therapeutic agent, similar to how both Cx43 and Cx26 asODN were combined in this study. This would be done in order to detect whether there could be a synergistic effect between Cx asODNs and the other therapeutic agents being tested. The same time points of D1, D3, D5, D10 and D15 will be first assessed to determine the effect of the therapeutic agents on inflammation, re-epithelialisation, granulation tissue formation and wound closure. It is anticipated that the existing coated scaffold may serve as a useful and translatable drug delivery device to improve wound healing.

6.6 – Conclusions

At the outset of the study, little was known in terms of the biological role of dermal scaffolds and in-depth assessment of the cellular response to scaffolds was lacking. Throughout the course of the project, it was discovered that a number of scaffolds appeared to be poorly optimised in their current state as they perturbed healing and induced characteristics of slow healing diabetic wounds. Bioactivation of scaffolds with Cx43 and Cx26 asODN using a polymer coating technique had the effect of improving wound healing, yet this was not through integration of scaffolds with wounds. It is possible that this objective could be achieved in the future with further optimisation of bioactive delivery from coated scaffolds. It appears that scaffolds may currently instead best serve as sustained drug delivery devices than behaving as a temporary matrix as they were perhaps intended.

Chronic ulcers pose a challenge to treat and existing standard treatments can be ineffective. The development of an easily applicable polymer coating to scaffolds resulted in sustained delivery of asODN that would be particularly useful in a chronic ulcer where connexin expression is known to be perturbed. A number of additional asODN and siRNA sequences, as well as peptides and growth factors could also be incorporated into scaffolds andinvestigated for their effect *in vivo* to produce an even more effective drug delivery scaffold. Interestingly, Cx43 and 26 asODN improved scaffold biocompatibility, such that a Cx asODN coating might also be applicable to a number of implantable devices and dressings that could benefit from improved biocompatibility.

The developed Cx43 and Cx26 asODN coated scaffolds are potentially inexpensive, off-the-shelf devices that overcome many of the pitfalls of more expensive complex cellular scaffolds. Following the results obtained in acute wounds, it is anticipated that sustained asODN delivery to chronic ulcers using coated scaffolds may promote ulcer healing.

Publications and presentations

Publications

GILMARTIN, D. J., ALEXALINE, M. M., THRASIVOULOU, C., PHILLIPS, A. R., JAYASINGHE, S. N. & BECKER, D. L. 2013. Integration of scaffolds into full-thickness skin wounds: the connexin response. *Adv Healthc Mater,* **2,** 1151-60.

Presentations

"Using Cx43 asODN to bioactivate collagen scaffolds" – presented at the UK Gap Junction Meeting, 30th August 2012.

"The design of a synthetic, bioactive dermal scaffold to assist the healing of chronic, non-healing wounds" – presentation of the overall PhD project to take place at the Cell and Developmental PhD/Post-doc seminar series, 29th January 2014.

Bibliography

ABBASSI, O., KISHIMOTO, T. K., MCINTIRE, L. V., ANDERSON, D. C. & SMITH, C. W. 1993. E-selectin supports neutrophil rolling in vitro under conditions of flow. *J Clin Invest,* 92**,** 2719-30.

ABU-OWN, A., SCURR, J. H. & COLERIDGE SMITH, P. D. 1994. Effect of leg elevation on the skin microcirculation in chronic venous insufficiency. *J Vasc Surg,* 20**,** 705-10.

ACHARYA, G., LEE, C. H. & LEE, Y. 2012. Optimization of cardiovascular stent against restenosis: factorial design-based statistical analysis of polymer coating conditions. *PLoS One,* 7**,** e43100.

AGRAWAL, S. 1996. Antisense oligonucleotides: towards clinical trials. *Trends in biotechnology,* 14**,** 376-87.

AHMAD, S., CHEN, S., SUN, J. & LIN, X. 2003. Connexins 26 and 30 are co-assembled to form gap junctions in the cochlea of mice. *Biochem Biophys Res Commun,* 307**,** 362-8.

AKHTAR, S. 1998. Antisense technology: selection and delivery of optimally acting antisense oligonucleotides. *J Drug Target,* 5**,** 225-34.

ALEXIADOU, K. & DOUPIS, J. 2012. Management of diabetic foot ulcers. *Diabetes Ther,* 3**,** 4.

AN, H. S., SIMPSON, J. M., GLOVER, J. M. & STEPHANY, J. 1995. Comparison between allograft plus demineralized bone matrix versus autograft in anterior cervical fusion. A prospective multicenter study. *Spine (Phila Pa 1976),* 20**,** 2211-6.

ANDERSON, J. M., RODRIGUEZ, A. & CHANG, D. T. 2008. Foreign body reaction to biomaterials. *Semin Immunol,* 20**,** 86-100.

ANSELL, D. M., HOLDEN, K. A. & HARDMAN, M. J. 2012. Animal models of wound repair: Are they cutting it? *Experimental Dermatology,* 21**,** 581-585.

ARCHER, C. B. 2008. Functions of the Skin. *Rook's Textbook of Dermatology*. Blackwell Publishing, Inc.

ASHTON, R. S., BANERJEE, A., PUNYANI, S., SCHAFFER, D. V. & KANE, R. S. 2007. Scaffolds based on degradable alginate hydrogels and poly(lactide-co-glycolide) microspheres for stem cell culture. *Biomaterials,* 28**,** 5518-25.

ATIYEH, B. S. & COSTAGLIOLA, M. 2007. Cultured epithelial autograft (CEA) in burn treatment: three decades later. *Burns : journal of the International Society for Burn Injuries,* 33**,** 405-13.

AUTENRIETH, I. B., BUCHELER, N., BOHN, E., HEINZE, G. & HORAK, I. 1997. Cytokine mRNA expression in intestinal tissue of interleukin-2 deficient mice with bowel inflammation. *Gut,* 41**,** 793-800.

BAKIRTZIS, G., CHOUDHRY, R., AASEN, T., SHORE, L., BROWN, K., BRYSON, S., FORROW, S., TETLEY, L., FINBOW, M., GREENHALGH, D. & HODGINS, M. 2003. Targeted epidermal expression of mutant Connexin 26(D66H) mimics true Vohwinkel syndrome and provides a model for the pathogenesis of dominant connexin disorders. *Hum Mol Genet,* 12**,** 1737-44.

BALS, R. 2000. Epithelial antimicrobial peptides in host defense against infection. *Respir Res,* 1**,** 141-50.

BANK, D. & NIX, D. 2006. Preventing skin tears in a nursing and rehabilitation center: an interdisciplinary effort. *Ostomy/wound management,* 52**,** 38-40, 44, 46.

BAUER, F. W. & BOEZEMAN, J. B. 1986. Cell proliferation in normal and psoriatic epidermis. *The Journal of investigative dermatology,* 87**,** 678-9.

BAUER, R., LOER, B., OSTROWSKI, K., MARTINI, J., WEIMBS, A., LECHNER, H. & HOCH, M. 2005. Intercellular communication: the Drosophila innexin multiprotein family of gap junction proteins. *Chem Biol,* 12**,** 515-26.

BECKER, D. L., THRASIVOULOU, C. & PHILLIPS, A. R. 2012. Connexins in wound healing; perspectives in diabetic patients. *Biochim Biophys Acta,* 1818**,** 2068-75.

BENDY, R. H., JR., NUCCIO, P. A., WOLFE, E., COLLINS, B., TAMBURRO, C., GLASS, W. & MARTIN, C. M. 1964. Relationship of Quantitative Wound Bacterial Counts to Healing of Decubiti: Effect of Topical Gentamicin. *Antimicrob Agents Chemother (Bethesda),* 10**,** 147-55.

BENNETT, G., DEALEY, C. & POSNETT, J. 2004. The cost of pressure ulcers in the UK. *Age and Ageing,* 33**,** 230-235.

BERLANGA-ACOSTA, J., GAVILONDO-COWLEY, J., LOPEZ-SAURA, P., GONZALEZ-LOPEZ, T., CASTRO-SANTANA, M. D., LOPEZ-MOLA, E., GUILLEN-NIETO, G. & HERRERA-MARTINEZ, L. 2009. Epidermal growth factor in clinical practice - a review of its biological actions, clinical indications and safety implications. *Int Wound J,* 6**,** 331-46.

BERLOWITZ, D. R. & BRIENZA, D. M. 2007. Are all pressure ulcers the result of deep tissue injury? A review of the literature. *Ostomy/wound management,* 53**,** 34-8.

BILLINGER, M., BUDDEBERG, F., HUBBELL, J. A., ELBERT, D. L., SCHAFFNER, T., METTLER, D., WINDECKER, S., MEIER, B. & HESS, O. M. 2006. Polymer

stent coating for prevention of neointimal hyperplasia. *J Invasive Cardiol,* 18**,** 423-6; discussion 427.

BJARNSHOLT, T., KIRKETERP-MOLLER, K., JENSEN, P. O., MADSEN, K. G., PHIPPS, R., KROGFELT, K., HOIBY, N. & GIVSKOV, M. 2008. Why chronic wounds will not heal: a novel hypothesis. *Wound Repair Regen,* 16**,** 2-10.

BLACK, E., VIBE-PETERSEN, J., JORGENSEN, L. N., MADSEN, S. M., AGREN, M. S., HOLSTEIN, P. E., PERRILD, H. & GOTTRUP, F. 2003. Decrease of collagen deposition in wound repair in type 1 diabetes independent of glycemic control. *Arch Surg,* 138**,** 34-40.

BLACKWOOD, K. A., MCKEAN, R., CANTON, I., FREEMAN, C. O., FRANKLIN, K. L., COLE, D., BROOK, I., FARTHING, P., RIMMER, S., HAYCOCK, J. W., RYAN, A. J. & MACNEIL, S. 2008. Development of biodegradable electrospun scaffolds for dermal replacement. *Biomaterials,* 29**,** 3091-104.

BOBBIE, M. W., ROY, S., TRUDEAU, K., MUNGER, S. J., SIMON, A. M. & ROY, S. 2010. Reduced connexin 43 expression and its effect on the development of vascular lesions in retinas of diabetic mice. *Invest Ophthalmol Vis Sci,* 51**,** 3758-63.

BOIZIAU, C., KURFURST, R., CAZENAVE, C., ROIG, V., THUONG, N. T. & TOULME, J. J. 1991. Inhibition of translation initiation by antisense oligonucleotides via an RNase-H independent mechanism. *Nucleic Acids Res,* 19**,** 1113-9.

BOLTON, L., MCNEES, P., VAN RIJSWIJK, L., DE LEON, J., LYDER, C., KOBZA, L., EDMAN, K., SCHEURICH, A., SHANNON, R., TOTH, M. & WOUND OUTCOMES STUDY, G. 2004. Wound-healing outcomes using standardized assessment and care in clinical practice. *J Wound Ostomy Continence Nurs,* 31**,** 65-71.

BOTUSAN, I. R., SUNKARI, V. G., SAVU, O., CATRINA, A. I., GRUNLER, J., LINDBERG, S., PEREIRA, T., YLA-HERTTUALA, S., POELLINGER, L., BRISMAR, K. & CATRINA, S. B. 2008. Stabilization of HIF-1alpha is critical to improve wound healing in diabetic mice. *Proc Natl Acad Sci U S A,* 105**,** 19426-31.

BOUCHIE, A. 2002. Tissue engineering firms go under. *Nat Biotechnol,* 20**,** 1178-9.

BRANDNER, J. M., HOUDEK, P., HUSING, B., KAISER, C. & MOLL, I. 2004. Connexins 26, 30, and 43: differences among spontaneous, chronic, and accelerated human wound healing. *J Invest Dermatol,* 122**,** 1310-20.

BRANDNER, J. M., ZACHEJA, S., HOUDEK, P., MOLL, I. & LOBMANN, R. 2008. Expression of matrix metalloproteinases, cytokines, and connexins in diabetic and nondiabetic human keratinocytes before and after transplantation into an *ex vivo* wound-healing model. *Diabetes Care,* 31**,** 114-20.

BROOKS, P. C., CLARK, R. A. & CHERESH, D. A. 1994. Requirement of vascular integrin alpha v beta 3 for angiogenesis. *Science,* 264**,** 569-71.

BROWN, G. L., CURTSINGER, L., JURKIEWICZ, M. J., NAHAI, F. & SCHULTZ, G. 1991. Stimulation of healing of chronic wounds by epidermal growth factor. *Plast Reconstr Surg,* 88**,** 189-94; discussion 195-6.

BROWN, M. B., HANPANITCHAROEN, M. & MARTIN, G. P. 2001. An in vitro investigation into the effect of glycosaminoglycans on the skin partitioning and deposition of NSAIDs. *Int J Pharm,* 225**,** 113-21.

BUTKEVICH, E., HULSMANN, S., WENZEL, D., SHIRAO, T., DUDEN, R. & MAJOUL, I. 2004. Drebrin is a novel connexin-43 binding partner that links gap junctions to the submembrane cytoskeleton. *Curr Biol,* 14**,** 650-8.

BUTTAFOCO, L., KOLKMAN, N. G., ENGBERS-BUIJTENHUIJS, P., POOT, A. A., DIJKSTRA, P. J., VERMES, I. & FEIJEN, J. 2006. Electrospinning of collagen and elastin for tissue engineering applications. *Biomaterials,* 27**,** 724-734.

CALLEN, J., JORIZZO, J., BOLOGNIA, J., PIETTE, W. & ZONE, J. 2009. General Principles of Wound Care. *Dermatological Signs of Internal Disease.* 4 ed.: Elsevier.

CANDI, E., SCHMIDT, R. & MELINO, G. 2005. The cornified envelope: a model of cell death in the skin. *Nat Rev Mol Cell Biol,* 6**,** 328-40.

CASPERS, P. J., LUCASSEN, G. W. & PUPPELS, G. J. 2003. Combined *in vivo* confocal Raman spectroscopy and confocal microscopy of human skin. *Biophys J,* 85**,** 572-80.

CAUBET, C., JONCA, N., BRATTSAND, M., GUERRIN, M., BERNARD, D., SCHMIDT, R., EGELRUD, T., SIMON, M. & SERRE, G. 2004. Degradation of corneodesmosome proteins by two serine proteases of the kallikrein family, SCTE/KLK5/hK5 and SCCE/KLK7/hK7. *J Invest Dermatol,* 122**,** 1235-44.

CAUWELS, A., ROGGE, E., VANDENDRIESSCHE, B., SHIVA, S. & BROUCKAERT, P. 2014. Extracellular ATP drives systemic inflammation, tissue damage and mortality. *Cell Death Dis,* 5**,** e1102.

CENTRES FOR DISEASE CONTROL AND PREVENTION. 2011. *Diabetes, Successes and Opportunities for Population-Based Prevention and Control* [Online]. Available at: http://www.cdc.gov/chronicdisease/resources/publications/AAG/ddt.htm [Accessed 20th November 2011].

CEGIELSKI, M., IZYKOWSKA, I., PODHORSKA-OKOLOW, M., ZABEL, M. & DZIEGIEL, P. 2008. Development of foreign body giant cells in response to implantation of Spongostan as a scaffold for cartilage tissue engineering. *In Vivo,* 22**,** 203-6.

CELLA, M., SALLUSTO, F. & LANZAVECCHIA, A. 1997. Origin, maturation and antigen presenting function of dendritic cells. *Curr Opin Immunol,* 9**,** 10-6.

CHEN, D. W., LIAO, J. Y., LIU, S. J. & CHAN, E. C. 2012. Novel biodegradable sandwich-structured nanofibrous drug-eluting membranes for repair of infected wounds: an in vitro and in vivo study. *Int J Nanomedicine,* 7**,** 763-71.

CHEN, J. D., KIM, J. P., ZHANG, K., SARRET, Y., WYNN, K. C., KRAMER, R. H. & WOODLEY, D. T. 1993. Epidermal growth factor (EGF) promotes human keratinocyte locomotion on collagen by increasing the alpha 2 integrin subunit. *Exp Cell Res,* 209**,** 216-23.

CHEN, W. Y. & ROGERS, A. A. 2007. Recent insights into the causes of chronic leg ulceration in venous diseases and implications on other types of chronic wounds. *Wound Repair Regen,* 15**,** 434-49.

CHONG, C., WANG, Y., MAITZ, P., SIMANAINEN, U. & Z, L. 2013. An electrospun scaffold loaded with anti-androgen receptor compound for accelerating wound healing. *Burns & Trauma,* 1**,** 95-101.

CHONG, E. J., PHAN, T. T., LIM, I. J., ZHANG, Y. Z., BAY, B. H., RAMAKRISHNA, S. & LIM, C. T. 2007. Evaluation of electrospun PCL/gelatin nanofibrous scaffold for wound healing and layered dermal reconstitution. *Acta Biomater,* 3**,** 321-30.

CLARK, R. A., GHOSH, K. & TONNESEN, M. G. 2007. Tissue engineering for cutaneous wounds. *J Invest Dermatol,* 127**,** 1018-29.

CODA THERAPEUTICS INC. WEBSITE. 2011. *CoDa Therapeutics Achieves Positive Phase 2 Efficacy of NEXAGON® in Chronic Venous Leg Ulcers* [Online]. Available at: http://www.codatherapeutics.com/news-nexagon.html [Accessed 20th November 2011].

COLLEDGE, N., WALKER, B. & RALSTON, S. 2010. *Davidson's Principles and Practice of Medicine (21st edition)*, Churchill Livingstone.

COLLINS, L. & SERAJ, S. 2010. Diagnosis and treatment of venous ulcers. *Am Fam Physician,* 81**,** 989-96.

CONCANNON, S. P., CROWE, T. D., ABERCROMBIE, J. J., MOLINA, C. M., HOU, P., SUKUMARAN, D. K., RAJ, P. A. & LEUNG, K. P. 2003. Susceptibility of oral bacteria to an antimicrobial decapeptide. *J Med Microbiol,* 52**,** 1083-93.

COOPER, L., JOHNSON, C., BURSLEM, F. & MARTIN, P. 2005. Wound healing and inflammation genes revealed by array analysis of 'macrophageless' PU.1 null mice. *Genome Biol,* 6**,** R5.

COSTIN, G. E. & HEARING, V. J. 2007. Human skin pigmentation: melanocytes modulate skin color in response to stress. *FASEB J,* 21**,** 976-94.

COUTINHO, P., QIU, C., FRANK, S., TAMBER, K. & BECKER, D. 2003. Dynamic changes in connexin expression correlate with key events in the wound healing process. *Cell biology international,* 27**,** 525-41.

CRONIN, M., ANDERSON, P. N., COOK, J. E., GREEN, C. R. & BECKER, D. L. 2008. Blocking connexin43 expression reduces inflammation and improves functional recovery after spinal cord injury. *Molecular and cellular neurosciences,* 39**,** 152-60.

CRONIN, M., ANDERSON, P. N., GREEN, C. R. & BECKER, D. L. 2006. Antisense delivery and protein knockdown within the intact central nervous system. *Front Biosci,* 11**,** 2967-75.

CULLEN, B., WATT, P. W., LUNDQVIST, C., SILCOCK, D., SCHMIDT, R. J., BOGAN, D. & LIGHT, N. D. 2002. The role of oxidised regenerated cellulose/collagen in chronic wound repair and its potential mechanism of action. *Int J Biochem Cell Biol,* 34**,** 1544-56.

DAHL, G. 2007. Gap junction-mimetic peptides do work, but in unexpected ways. *Cell Commun Adhes,* 14**,** 259-64.

DANIEL, R. K., PRIEST, D. L. & WHEATLEY, D. C. 1981. Etiologic factors in pressure sores: an experimental model. *Arch Phys Med Rehabil,* 62**,** 492-8.

DARBY, I., SKALLI, O. & GABBIANI, G. 1990. Alpha-smooth muscle actin is transiently expressed by myofibroblasts during experimental wound healing. *Laboratory investigation; a journal of technical methods and pathology,* 63**,** 21-9.

DAVIS, N. G., PHILLIPS, A. & BECKER, D. L. 2013. Connexin dynamics in the privileged wound healing of the buccal mucosa. *Wound Repair Regen,* 21**,** 571-8.

DE LUCA, G., DIRKSEN, M. T., SPAULDING, C., KELBAEK, H., SCHALIJ, M., THUESEN, L., VAN DER HOEVEN, B., VINK, M. A., KAISER, C., MUSTO, C., CHECHI, T., SPAZIANI, G., DIAZ DE LA LLERA, L. S., PASCERI, V., DI LORENZO, E., VIOLINI, R., CORTESE, G., SURYAPRANATA, H., STONE, G. W. & DRUG-ELUTING STENT IN PRIMARY ANGIOPLASTY, C. 2012. Drug-eluting vs bare-metal stents in primary angioplasty: a pooled patient-level meta-analysis of randomized trials. *Arch Intern Med,* 172**,** 611-21; discussion 621-2.

DERMIETZEL, R., HERTBERG, E. L., KESSLER, J. A. & SPRAY, D. C. 1991. Gap junctions between cultured astrocytes: immunocytochemical, molecular, and electrophysiological analysis. *J Neurosci,* 11**,** 1421-32.

DESMOULIERE, A., REDARD, M., DARBY, I. & GABBIANI, G. 1995. Apoptosis mediates the decrease in cellularity during the transition between granulation tissue and scar. *The American journal of pathology,* 146**,** 56-66.

DI LORENZO, E., SAURO, R., VARRICCHIO, A., CAPASSO, M., LANZILLO, T., MANGANELLI, F., MARIELLO, C., SIANO, F., PAGLIUCA, M. R., STANCO, G., ROSATO, G. & DE LUCA, G. 2009. Benefits of drug-eluting stents as compared to bare metal stent in ST-segment elevation myocardial infarction: four year results of the PaclitAxel or Sirolimus-Eluting stent vs bare metal stent in primary angiOplasty (PASEO) randomized trial. *Am Heart J,* 158**,** e43-50.

DI, W. L., RUGG, E. L., LEIGH, I. M. & KELSELL, D. P. 2001. Multiple epidermal connexins are expressed in different keratinocyte subpopulations including connexin 31. *J Invest Dermatol,* 117**,** 958-64.

DIEGELMANN, R. F. & EVANS, M. C. 2004. Wound healing: an overview of acute, fibrotic and delayed healing. *Front Biosci,* 9**,** 283-9.

DIEZ, J. A., AHMAD, S. & EVANS, W. H. 1999. Assembly of heteromeric connexons in guinea-pig liver en route to the Golgi apparatus, plasma membrane and gap junctions. *European journal of biochemistry / FEBS,* 262**,** 142-8.

DIPIETRO, L. A. & POLVERINI, P. J. 1993. Angiogenic macrophages produce the angiogenic inhibitor thrombospondin 1. *Am J Pathol,* 143**,** 678-84.

DJALILIAN, A. R., MCGAUGHEY, D., PATEL, S., SEO, E. Y., YANG, C., CHENG, J., TOMIC, M., SINHA, S., ISHIDA-YAMAMOTO, A. & SEGRE, J. A. 2006. Connexin 26 regulates epidermal barrier and wound remodeling and promotes psoriasiform response. *The Journal of clinical investigation,* 116**,** 1243-53.

DOMINGUEZ-DELGADO, C., RODRIGUEZ-CRUZ, I. & LOPEZ-CERVANTE, M. 2010. The Skin: A Valuable Route for Administration of Drugs. *Current Technologies To Increase The Transdermal Delivery Of Drugs.* Bentham Science Publishers.

DRACHMAN, D. E., EDELMAN, E. R., SEIFERT, P., GROOTHUIS, A. R., BORNSTEIN, D. A., KAMATH, K. R., PALASIS, M., YANG, D., NOTT, S. H. & ROGERS, C. 2000. Neointimal thickening after stent delivery of paclitaxel: change in composition and arrest of growth over six months. *Journal of the American College of Cardiology,* 36**,** 2325-2332.

DU, D., XU, F., YU, L., ZHANG, C., LU, X., YUAN, H., HUANG, Q., ZHANG, F., BAO, H., JIA, L., WU, X., ZHU, X., ZHANG, X., ZHANG, Z. & CHEN, Z. 2010. The tight junction protein, occludin, regulates the directional migration of epithelial cells. *Dev Cell,* 18**,** 52-63.

DUFFY, M. T., BLOOM, J. N., MCNALLY-HEINTZELMAN, K. M., HEINTZELMAN, D. L., SOLLER, E. C. & HOFFMAN, G. T. 2005. Sutureless ophthalmic surgery: a scaffold-enhanced bioadhesive technique. *J AAPOS,* 9**,** 315-20.

DUMVILLE, J. C., WORTHY, G., BLAND, J. M., CULLUM, N., DOWSON, C., IGLESIAS, C., MITCHELL, J. L., NELSON, E. A., SOARES, M. O., TORGERSON, D. J. & VEN, U. S. I. I. T. 2009. Larval therapy for leg ulcers (VenUS II): randomised controlled trial. *BMJ,* 338**,** b773.

EGLIN, D. & ALINI, M. 2008. Degradable polymeric materials for osteosynthesis: tutorial. *Eur Cell Mater,* 16**,** 80-91.

EGOZI, E. I., FERREIRA, A. M., BURNS, A. L., GAMELLI, R. L. & DIPIETRO, L. A. 2003. Mast cells modulate the inflammatory but not the proliferative response in healing wounds. *Wound Repair Regen,* 11**,** 46-54.

EHRENREICH, M. & RUSZCZAK, Z. 2006. Update on tissue-engineered biological dressings. *Tissue Eng,* 12**,** 2407-24.

EL-SABBAN, M. E., SFEIR, A. J., DAHER, M. H., KALAANY, N. Y., BASSAM, R. A. & TALHOUK, R. S. 2003. ECM-induced gap junctional communication enhances mammary epithelial cell differentiation. *J Cell Sci,* 116**,** 3531-41.

EVANS, W. H. & BOITANO, S. 2001. Connexin mimetic peptides: specific inhibitors of gap-junctional intercellular communication. *Biochem Soc Trans,* 29**,** 606-12.

FALANGA, V. 1993. Venous ulceration. *J Dermatol Surg Oncol,* 19**,** 764-71.

FLETCHER, A., CULLUM, N. & SHELDON, T. A. 1997. A systematic review of compression treatment for venous leg ulcers. *BMJ,* 315**,** 576-80.

FONDER, M. A., LAZARUS, G. S., COWAN, D. A., ARONSON-COOK, B., KOHLI, A. R. & MAMELAK, A. J. 2008. Treating the chronic wound: A practical approach to the care of nonhealing wounds and wound care dressings. *J Am Acad Dermatol,* 58**,** 185-206.

FORE, J. 2006. A review of skin and the effects of aging on skin structure and function. *Ostomy Wound Manage,* 52**,** 24-35; quiz 36-7.

FORSYTHE, J. A., JIANG, B. H., IYER, N. V., AGANI, F., LEUNG, S. W., KOOS, R. D. & SEMENZA, G. L. 1996. Activation of vascular endothelial growth factor gene transcription by hypoxia-inducible factor 1. *Mol Cell Biol,* 16**,** 4604-13.

FORTICELL BIOSCIENCE WEBSITE. 2012. *OrCel Product Webpage* [Online]. Available at: http://www.forticellbioscience.com/orcel.html [Accessed 20th November 2011].

FUCHS, E. & BYRNE, C. 1994. The epidermis: rising to the surface. *Current opinion in genetics & development,* 4**,** 725-36.

GAILIT, J., WELCH, M. P. & CLARK, R. A. 1994. TGF-beta 1 stimulates expression of keratinocyte integrins during re-epithelialization of cutaneous wounds. *The Journal of investigative dermatology,* 103**,** 221-7.

GALKOWSKA, H., OLSZEWSKI, W. L., WOJEWODZKA, U., ROSINSKI, G. & KARNAFEL, W. 2006. Neurogenic factors in the impaired healing of diabetic foot ulcers. *J Surg Res,* 134**,** 252-8.

GARCIA-GIRALT, N., IZQUIERDO, R., NOGUES, X., PEREZ-OLMEDILLA, M., BENITO, P., GOMEZ-RIBELLES, J. L., CHECA, M. A., SUAY, J., CACERES, E. & MONLLAU, J. C. 2008. A porous PCL scaffold promotes the human

chondrocytes redifferentiation and hyaline-specific extracellular matrix protein synthesis. *Journal of biomedical materials research. Part A,* 85**,** 1082-9.

GAWANDE, P. V., LEUNG, K. P. & MADHYASTHA, S. 2014. Antibiofilm and antimicrobial efficacy of DispersinB(R)-KSL-W peptide-based wound gel against chronic wound infection associated bacteria. *Curr Microbiol,* 68**,** 635-41.

GHATNEKAR, G. S., GREK, C. L., ARMSTRONG, D. G., DESAI, S. C. & GOURDIE, R. G. 2014. The Effect of a Connexin43-Based Peptide on the Healing of Chronic Venous Leg Ulcers: A Multicenter, Randomized Trial. *J Invest Dermatol.*

GHATNEKAR, G. S., O'QUINN, M. P., JOURDAN, L. J., GURJARPADHYE, A. A., DRAUGHN, R. L. & GOURDIE, R. G. 2009. Connexin43 carboxyl-terminal peptides reduce scar progenitor and promote regenerative healing following skin wounding. *Regen Med,* 4**,** 205-23.

GHOLIPOUR KANANI, A. & HAJIR BAHRAMI, S. 2010. Review on electrospun nanofibers scaffold and biomedical applications. *Trends in Biomaterials and Artificial Organs,* 24**,** 93-115.

GIEPMANS, B. N., VERLAAN, I., HENGEVELD, T., JANSSEN, H., CALAFAT, J., FALK, M. M. & MOOLENAAR, W. H. 2001a. Gap junction protein connexin-43 interacts directly with microtubules. *Curr Biol,* 11**,** 1364-8.

GIEPMANS, B. N., VERLAAN, I. & MOOLENAAR, W. H. 2001b. Connexin-43 interactions with ZO-1 and alpha- and beta-tubulin. *Cell communication & adhesion,* 8**,** 219-23.

GILMARTIN, D. J., ALEXALINE, M. M., THRASIVOULOU, C., PHILLIPS, A. R., JAYASINGHE, S. N. & BECKER, D. L. 2013. Integration of scaffolds into full-thickness skin wounds: the connexin response. *Adv Healthc Mater,* 2**,** 1151-60.

GIRARDOT, J. M. & GIRARDOT, M. N. 1996. Amide cross-linking: an alternative to glutaraldehyde fixation. *J Heart Valve Dis,* 5**,** 518-25.

GOLIGER, J. A. & PAUL, D. L. 1995. Wounding alters epidermal connexin expression and gap junction-mediated intercellular communication. *Molecular biology of the cell,* 6**,** 1491-501.

GOMES, L., TERRA, L., WAILEMANN, R., LABRIOLA, L. & SOGAYAR, M. 2012. TGF-beta1 modulates the homeostasis between MMPs and MMP inhibitors through p38 MAPK and ERK1/2 in highly invasive breast cancer cells. *BMC Cancer,* 12**,** 26.

GOODCHILD, J. 1989. Inhibition of gene expression by oligonucleotides. *Oligodeoxynucleotides: antisense inhibitors of gene expression***,** 53-78.

GOODENOUGH, D. A. 1975. The structure of cell membranes involved in intercellular communication. *Am J Clin Pathol,* 63**,** 636-45.

GOUGEON, P. Y., LOURENSSEN, S., HAN, T. Y., NAIR, D. G., ROPELESKI, M. J. & BLENNERHASSETT, M. G. 2013. The pro-inflammatory cytokines IL-1beta and TNFalpha are neurotrophic for enteric neurons. *J Neurosci,* 33**,** 3339-51.

GOURDIN, F. W. & SMITH, J. G., JR. 1993. Etiology of venous ulceration. *South Med J,* 86**,** 1142-6.

GRAINGER, D. J., WAKEFIELD, L., BETHELL, H. W., FARNDALE, R. W. & METCALFE, J. C. 1995. Release and activation of platelet latent TGF-beta in blood clots during dissolution with plasmin. *Nature medicine,* 1**,** 932-7.

GREEN, K. J. & JONES, J. C. 1996. Desmosomes and hemidesmosomes: structure and function of molecular components. *Faseb J,* 10**,** 871-81.

GRICE, E. A. & SEGRE, J. A. 2012. Interaction of the microbiome with the innate immune response in chronic wounds. *Adv Exp Med Biol,* 946**,** 55-68.

GRIFFITHS, M., OJEH, N., LIVINGSTONE, R., PRICE, R. & NAVSARIA, H. 2004. Survival of Apligraf in acute human wounds. *Tissue Eng,* 10**,** 1180-95.

GUO, S. & DIPIETRO, L. A. 2010. Factors affecting wound healing. *J Dent Res,* 89**,** 219-29.

GURTNER, G. C., WERNER, S., BARRANDON, Y. & LONGAKER, M. T. 2008. Wound repair and regeneration. *Nature,* 453**,** 314-21.

HAAKE, A., SCOTT, G. & HOLBROOK, K. 2001. Stucture and function of the skin: overview of the epidermis and dermis. *In:* FREINKEL, R. & WOODLEY, D. (eds.) *The biology of skin.* The Parthenon Publishing Group.

HAFTEK, M., TEILLON, M. H. & SCHMITT, D. 1998. Stratum corneum, corneodesmosomes and ex vivo percutaneous penetration. *Microsc Res Tech,* 43**,** 242-9.

HALL, M. C., YOUNG, D. A., WATERS, J. G., ROWAN, A. D., CHANTRY, A., EDWARDS, D. R. & CLARK, I. M. 2003. The comparative role of activator protein 1 and Smad factors in the regulation of Timp-1 and MMP-1 gene expression by transforming growth factor-beta 1. *The Journal of biological chemistry,* 278**,** 10304-13.

HAN, Y. P., TUAN, T. L., HUGHES, M., WU, H. & GARNER, W. L. 2001. Transforming growth factor-beta - and tumor necrosis factor-alpha -mediated induction and proteolytic activation of MMP-9 in human skin. *J Biol Chem,* 276**,** 22341-50.

HARDWICKE, J., SCHMALJOHANN, D., BOYCE, D. & THOMAS, D. 2008. Epidermal growth factor therapy and wound healing--past, present and future perspectives. *Surgeon,* 6**,** 172-7.

HAUSMAN, G. J., CAMPION, D. R., RICHARDSON, R. L. & MARTIN, R. J. 1981. Adipocyte development in the rat hypodermis. *Am J Anat,* 161**,** 85-100.

HERMAN, L. E. & ROTHMAN, K. F. 1989. Prevention, Care, and Treatment of Pressure (Decubitus) Ulcers in Intensive Care Unit Patients. *Journal of Intensive Care Medicine,* 4**,** 117-123.

HEROUY, Y., KAHLE, B., IDZKO, M., HILDENBRAND, T., ALI, M. Y., CLEMENT, J., FERRARI, D., DI VIRGILIO, F., BRUCKNER-TUDERMAN, L. & NORGAUER, J. 2004. Venous Leg Ulcers And Apoptosis: A TIMP-3-Mediated Pathway[quest]. *J Investig Dermatol,* 123**,** 1210-1212.

HERVE, J. C., DERANGEON, M., SARROUILHE, D., GIEPMANS, B. N. & BOURMEYSTER, N. 2012. Gap junctional channels are parts of multiprotein complexes. *Biochim Biophys Acta,* 1818**,** 1844-65.

HIGGINS, J. P. & GREEN, S. 2011a. *Cochrane Handbook for Systematic Reviews of Interventions - 9.4 Summarizing effects across studies* [Online]. Available: http://handbook.cochrane.org/chapter_9/9_5_2_identifying_and_measuring_heterogeneity.htm.

HIGGINS, J. P. & GREEN, S. 2011b. *Cochrane Handbook for Systematic Reviews of Interventions - 9.5.2 Identifying and measuring heterogeneity* [Online]. Available: http://handbook.cochrane.org/chapter_9/9_5_2_identifying_and_measuring_heterogeneity.htm.

HIGGINS, J. P., THOMPSON, S. G., DEEKS, J. J. & ALTMAN, D. G. 2003. Measuring inconsistency in meta-analyses. *BMJ,* 327**,** 557-60.

HINMAN, C. D. & MAIBACH, H. 1963. Effect of Air Exposure and Occlusion on Experimental Human Skin Wounds. *Nature,* 200**,** 377-8.

HINZ, B., CELETTA, G., TOMASEK, J. J., GABBIANI, G. & CHAPONNIER, C. 2001. Alpha-smooth muscle actin expression upregulates fibroblast contractile activity. *Mol Biol Cell,* 12**,** 2730-41.

HO, S. P., BRITTON, D. H., STONE, B. A., BEHRENS, D. L., LEFFET, L. M., HOBBS, F. W., MILLER, J. A. & TRAINOR, G. L. 1996. Potent antisense oligonucleotides to the human multidrug resistance-1 mRNA are rationally selected by mapping RNA-accessible sites with oligonucleotide libraries. *Nucleic Acids Res,* 24**,** 1901-7.

HOFER, T., DESBAILLETS, I., HOPFL, G., WENGER, R. H. & GASSMANN, M. 2002. Characterization of HIF-1 alpha overexpressing HeLa cells and implications for gene therapy. *Comp Biochem Physiol C Toxicol Pharmacol,* 133**,** 475-81.

HOHN, D. C., MACKAY, R. D., HALLIDAY, B. & HUNT, T. K. 1976. Effect of O2 tension on microbicidal function of leukocytes in wounds and in vitro. *Surg Forum,* 27**,** 18-20.

HOKE, G. D., DRAPER, K., FREIER, S. M., GONZALEZ, C., DRIVER, V. B., ZOUNES, M. C. & ECKER, D. J. 1991. Effects of phosphorothioate capping on antisense oligonucleotide stability, hybridization and antiviral efficacy versus herpes simplex virus infection. *Nucleic Acids Res,* 19**,** 5743-8.

HOSGOOD, G. 1993. Wound healing. The role of platelet-derived growth factor and transforming growth factor beta. *Vet Surg,* 22**,** 490-5.

HU, S., YANG, H., CAI, R., LIU, Z. & YANG, X. 2009. Biotin induced fluorescence enhancement in resonance energy transfer and application for bioassay. *Talanta,* 80**,** 454-8.

HUANG, Z.-M., ZHANG, Y. Z., KOTAKI, M. & RAMAKRISHNA, S. 2003. A review on polymer nanofibers by electrospinning and their applications in nanocomposites. *Composites Science and Technology,* 63**,** 2223-2253.

HUNT, D. L. 2011. Diabetes: foot ulcers and amputations. *Clinical evidence,* 2011.

HUNTER, A. W., BARKER, R. J., ZHU, C. & GOURDIE, R. G. 2005. Zonula occludens-1 alters connexin43 gap junction size and organization by influencing channel accretion. *Mol Biol Cell,* 16**,** 5686-98.

IACOBAS, D. A., IACOBAS, S. & SPRAY, D. C. 2007. Connexin-dependent transcellular transcriptomic networks in mouse brain. *Prog Biophys Mol Biol,* 94**,** 169-85.

IMAI, Y., ODAJIMA, R., INOUE, Y. & SHISHIBA, Y. 1992. Effect of growth factors on hyaluronan and proteoglycan synthesis by retroocular tissue fibroblasts of Graves' ophthalmopathy in culture. *Acta Endocrinol (Copenh),* 126**,** 541-52.

INOGUCHI, T., YU, H. Y., IMAMURA, M., KAKIMOTO, M., KUROKI, T., MARUYAMA, T. & NAWATA, H. 2001. Altered gap junction activity in cardiovascular tissues of diabetes. *Med Electron Microsc,* 34**,** 86-91.

ISHAUG, S. L., YASZEMSKI, M. J., BIZIOS, R. & MIKOS, A. G. 1994. Osteoblast function on synthetic biodegradable polymers. *J Biomed Mater Res,* 28**,** 1445-53.

JACKSON, D. P., LEWIS, F. A., TAYLOR, G. R., BOYLSTON, A. W. & QUIRKE, P. 1990. Tissue extraction of DNA and RNA and analysis by the polymerase chain reaction. *J Clin Pathol,* 43**,** 499-504.

SCALLAN, J., HUXLEY, V. H. & Korthuis, R. J. 2010. Pathophysiology of Edema Formation. *Capillary Fluid Exchange: Regulation, Functions, and Pathology.* San Rafael (CA): Morgan & Claypool Life Sciences.

JALIFE, J., MORLEY, G. E. & VAIDYA, D. 1999. Connexins and impulse propagation in the mouse heart. *J Cardiovasc Electrophysiol,* 10**,** 1649-63.

JHA, B., AYRES, C., BOWMAN, J., TELEMECO, T., SELL, S., BOWLIN, G. & SIMPSON, D. 2011. Electrospun Collagen: A Tissue Engineering Scaffold with Unique Functional Properties in a Wide Variety of Applications. *Journal of Nanomaterials,* 2011.

JI, Y., GHOSH, K., SHU, X. Z., LI, B., SOKOLOV, J. C., PRESTWICH, G. D., CLARK, R. A. & RAFAILOVICH, M. H. 2006. Electrospun three-dimensional hyaluronic acid nanofibrous scaffolds. *Biomaterials,* 27**,** 3782-92.

JONES, D. A., ABBASSI, O., MCINTIRE, L. V., MCEVER, R. P. & SMITH, C. W. 1993. P-selectin mediates neutrophil rolling on histamine-stimulated endothelial cells. *Biophys J,* 65**,** 1560-9.

JONES, J. E. & NELSON, E. A. 2007. Skin grafting for venous leg ulcers. *Cochrane Database Syst Rev***,** CD001737.

JONES, V. & MILTON, T. 2000. When and how to use hydrogels. *Nurs Times,* 96**,** 3-4.

JORNESKOG, G., BRISMAR, K. & FAGRELL, B. 1995. Skin capillary circulation is more impaired in the toes of diabetic than non-diabetic patients with peripheral vascular disease. *Diabet Med,* 12**,** 36-41.

KALININ, A. E., KAJAVA, A. V. & STEINERT, P. M. 2002. Epithelial barrier function: assembly and structural features of the cornified cell envelope. *Bioessays,* 24**,** 789-800.

KARR, J. C. 2011. Retrospective comparison of diabetic foot ulcer and venous stasis ulcer healing outcome between a dermal repair scaffold (PriMatrix) and a bilayered living cell therapy (Apligraf). *Adv Skin Wound Care,* 24**,** 119-25.

KENSEY-NASH. 2014. *Kensey Nash - Wound Repair (product description)* [Online]. 2014].

KHAN, A., BENBOUBETRA, M., SAYYED, P. Z., NG, K. W., FOX, S., BECK, G., BENTER, I. F. & AKHTAR, S. 2004. Sustained polymeric delivery of gene silencing antisense ODNs, siRNA, DNAzymes and ribozymes: in vitro and in vivo studies. *J Drug Target,* 12**,** 393-404.

KHIL, M. S., CHA, D. I., KIM, H. Y., KIM, I. S. & BHATTARAI, N. 2003. Electrospun nanofibrous polyurethane membrane as wound dressing. *J Biomed Mater Res B Appl Biomater,* 67**,** 675-9.

KIM, H. W., KNOWLES, J. C. & KIM, H. E. 2005. Hydroxyapatite porous scaffold engineered with biological polymer hybrid coating for antibiotic Vancomycin release. *J Mater Sci Mater Med,* 16**,** 189-95.

KIPSHIDZE, N., TSAPENKO, M., IVERSEN, P. & BURGER, D. 2005. Antisense therapy for restenosis following percutaneous coronary intervention. *Expert Opin Biol Ther,* 5**,** 79-89.

KLINGE, U., SI, Z. Y., ZHENG, H., SCHUMPELICK, V., BHARDWAJ, R. S. & KLOSTERHALFEN, B. 2000. Abnormal collagen I to III distribution in the skin of patients with incisional hernia. *European surgical research. Europaische chirurgische Forschung. Recherches chirurgicales europeennes,* 32**,** 43-8.

KLOKK, T. I. & MELVIK, J. E. 2002. Controlling the size of alginate gel beads by use of a high electrostatic potential. *J Microencapsul,* 19**,** 415-24.

KNIGHTON, D. R., HUNT, T. K., THAKRAL, K. K. & GOODSON, W. H., 3RD 1982. Role of platelets and fibrin in the healing sequence: an in vivo study of angiogenesis and collagen synthesis. *Ann Surg,* 196**,** 379-88.

KOSIAK, M. 1959. Etiology and pathology of ischemic ulcers. *Arch Phys Med Rehabil,* 40**,** 62-9.

KOSIAK, M., KUBICEK, W. G., OLSON, M., DANZ, J. N. & KOTTKE, F. J. 1958. Evaluation of pressure as a factor in the production of ischial ulcers. *Arch Phys Med Rehabil,* 39**,** 623-9.

KRETZ, M., EUWENS, C., HOMBACH, S., ECKARDT, D., TEUBNER, B., TRAUB, O., WILLECKE, K. & OTT, T. 2003. Altered connexin expression and wound healing in the epidermis of connexin-deficient mice. *J Cell Sci,* 116**,** 3443-52.

KRUCOFF, M. W., KEREIAKES, D. J., PETERSEN, J. L., MEHRAN, R., HASSELBLAD, V., LANSKY, A. J., FITZGERALD, P. J., GARG, J., TURCO, M. A., SIMONTON, C. A., 3RD, VERHEYE, S., DUBOIS, C. L., GAMMON, R., BATCHELOR, W. B., O'SHAUGHNESSY, C. D., HERMILLER, J. B., JR., SCHOFER, J., BUCHBINDER, M., WIJNS, W. & GROUP, C. I. I. 2008. A novel bioresorbable polymer paclitaxel-eluting stent for the treatment of single and multivessel coronary disease: primary results of the COSTAR (Cobalt Chromium Stent With Antiproliferative for Restenosis) II study. *J Am Coll Cardiol,* 51**,** 1543-52.

KUROKI, T., INOGUCHI, T., UMEDA, F., UEDA, F. & NAWATA, H. 1998. High glucose induces alteration of gap junction permeability and phosphorylation of connexin-43 in cultured aortic smooth muscle cells. *Diabetes,* 47**,** 931-6.

KUWAHARA, M., HATOKO, M., TADA, H. & TANAKA, A. 2001. E-cadherin expression in wound healing of mouse skin. *J Cutan Pathol,* 28**,** 191-9.

LABARTHE, M. P., BOSCO, D., SAURAT, J. H., MEDA, P. & SALOMON, D. 1998. Upregulation of connexin 26 between keratinocytes of psoriatic lesions. *The Journal of investigative dermatology,* 111**,** 72-6.

LADIN, D. A., HOU, Z., PATEL, D., MCPHAIL, M., OLSON, J. C., SAED, G. M. & FIVENSON, D. P. 1998. p53 and apoptosis alterations in keloids and keloid

fibroblasts. *Wound repair and regeneration : official publication of the Wound Healing Society [and] the European Tissue Repair Society,* 6**,** 28-37.

LAI, X. J., YE, S. Q., ZHENG, L., LI, L., LIU, Q. R., YU, S. B., PANG, Y., JIN, S., LI, Q., YU, A. C. & CHEN, X. Q. 2014. Selective 14-3-3gamma induction quenches p-beta-catenin Ser37/Bax-enhanced cell death in cerebral cortical neurons during ischemia. *Cell Death Dis,* 5**,** e1184.

LAIRD, D. W. 2006. Life cycle of connexins in health and disease. *The Biochemical journal,* 394**,** 527-43.

LAPLANTE, A. F., GERMAIN, L., AUGER, F. A. & MOULIN, V. 2001. Mechanisms of wound reepithelialization: hints from a tissue-engineered reconstructed skin to long-standing questions. *FASEB J,* 15**,** 2377-89.

LEBRUN, E., TOMIC-CANIC, M. & KIRSNER, R. S. 2010. The role of surgical debridement in healing of diabetic foot ulcers. *Wound Repair Regen,* 18**,** 433-8.

LEITHE, E., BRECH, A. & RIVEDAL, E. 2006. Endocytic processing of connexin43 gap junctions: a morphological study. *Biochem J,* 393**,** 59-67.

LI, J., ZHANG, Y. P. & KIRSNER, R. S. 2003. Angiogenesis in wound repair: angiogenic growth factors and the extracellular matrix. *Microsc Res Tech,* 60**,** 107-14.

LI, N., LUO, H. C., YANG, C., DENG, J. J., REN, M., XIE, X. Y., LIN, D. Z., YAN, L. & ZHANG, L. M. 2014. Cationic star-shaped polymer as an siRNA carrier for reducing MMP-9 expression in skin fibroblast cells and promoting wound healing in diabetic rats. *Int J Nanomedicine,* 9**,** 3377-87.

LIAW, L., BIRK, D. E., BALLAS, C. B., WHITSITT, J. S., DAVIDSON, J. M. & HOGAN, B. L. 1998. Altered wound healing in mice lacking a functional osteopontin gene (spp1). *J Clin Invest,* 101**,** 1468-78.

LINGEN, M. W. 2001. Role of leukocytes and endothelial cells in the development of angiogenesis in inflammation and wound healing. *Archives of pathology & laboratory medicine,* 125**,** 67-71.

LIU, X., MA, L., LIANG, J., ZHANG, B., TENG, J. & GAO, C. 2013. RNAi functionalized collagen-chitosan/silicone membrane bilayer dermal equivalent for full-thickness skin regeneration with inhibited scarring. *Biomaterials,* 34**,** 2038-48.

LO, S. F. 2010. Antimicrobial silver dressings beneath compression for venous ulceration are not cost-effective compared with standard dressings. *Evid Based Nurs,* 13**,** 120-1.

LOBMANN, R., SCHULTZ, G. & LEHNERT, H. 2005. Proteases and the diabetic foot syndrome: mechanisms and therapeutic implications. *Diabetes Care,* 28**,** 461-71.

LODISH H, BERK A & SL, Z. 2000. Collagen: The Fibrous Proteins of the Matrix. *Molecular Cell Biology.* 4 ed. New York: W. H. Freeman.

LOOTS, M. A., LAMME, E. N., MEKKES, J. R., BOS, J. D. & MIDDELKOOP, E. 1999. Cultured fibroblasts from chronic diabetic wounds on the lower extremity (non-insulin-dependent diabetes mellitus) show disturbed proliferation. *Arch Dermatol Res,* 291**,** 93-9.

LUCKE, T., CHOUDHRY, R., THOM, R., SELMER, I. S., BURDEN, A. D. & HODGINS, M. B. 1999. Upregulation of connexin 26 is a feature of keratinocyte differentiation in hyperproliferative epidermis, vaginal epithelium, and buccal epithelium. *The Journal of investigative dermatology,* 112**,** 354-61.

LYDER, C. H. 2003. Pressure ulcer prevention and management. *JAMA,* 289**,** 223-6.

LYNN, A. K., YANNAS, I. V. & BONFIELD, W. 2004. Antigenicity and immunogenicity of collagen. *J Biomed Mater Res B Appl Biomater,* 71**,** 343-54.

MACHACEK, M., HODGSON, L., WELCH, C., ELLIOTT, H., PERTZ, O., NALBANT, P., ABELL, A., JOHNSON, G. L., HAHN, K. M. & DANUSER, G. 2009. Coordination of Rho GTPase activities during cell protrusion. *Nature,* 461**,** 99-103.

MACHADO, H. A., ABERCROMBIE, J. J., YOU, T., DELUCA, P. P. & LEUNG, K. P. 2013. Release of a wound-healing agent from PLGA microspheres in a thermosensitive gel. *Biomed Res Int,* 2013**,** 387863.

MAKADIA, H. K. & SIEGEL, S. J. 2011. Poly Lactic-co-Glycolic Acid (PLGA) as Biodegradable Controlled Drug Delivery Carrier. *Polymers (Basel),* 3**,** 1377-1397.

MAKINO, A., PLATOSHYN, O., SUAREZ, J., YUAN, J. X. & DILLMANN, W. H. 2008. Downregulation of connexin40 is associated with coronary endothelial cell dysfunction in streptozotocin-induced diabetic mice. *Am J Physiol Cell Physiol,* 295**,** C221-30.

MAKOWSKI, L., CASPAR, D. L., PHILLIPS, W. C. & GOODENOUGH, D. A. 1977. Gap junction structures. II. Analysis of the x-ray diffraction data. *J Cell Biol,* 74**,** 629-45.

MAN, Y. K., TROLOVE, C., TATTERSALL, D., THOMAS, A. C., PAPAKONSTANTINOPOULOU, A., PATEL, D., SCOTT, C., CHONG, J., JAGGER, D. J., O'TOOLE, E. A., NAVSARIA, H., CURTIS, M. A. & KELSELL, D. P. 2007. A deafness-associated mutant human connexin 26 improves the epithelial barrier in vitro. *J Membr Biol,* 218**,** 29-37.

MARGADANT, C., CHARAFEDDINE, R. A. & SONNENBERG, A. 2010. Unique and redundant functions of integrins in the epidermis. *FASEB J.*

MARGOLIS, D. J., BERLIN, J. A. & STROM, B. L. 2000. Which venous leg ulcers will heal with limb compression bandages? *Am J Med,* 109**,** 15-9.

MARICICH, S. M., WELLNITZ, S. A., NELSON, A. M., LESNIAK, D. R., GERLING, G. J., LUMPKIN, E. A. & ZOGHBI, H. Y. 2009. Merkel cells are essential for light-touch responses. *Science,* 324**,** 1580-2.

MARSTON, W. A., HANFT, J., NORWOOD, P., POLLAK, R. & DERMAGRAFT DIABETIC FOOT ULCER STUDY, G. 2003. The efficacy and safety of Dermagraft in improving the healing of chronic diabetic foot ulcers: results of a prospective randomized trial. *Diabetes Care,* 26**,** 1701-5.

MARTIN, P. 1997. Wound healing--aiming for perfect skin regeneration. *Science,* 276**,** 75-81.

MARTIN, P., D'SOUZA, D., MARTIN, J., GROSE, R., COOPER, L., MAKI, R. & MCKERCHER, S. R. 2003. Wound healing in the PU.1 null mouse--tissue repair is not dependent on inflammatory cells. *Curr Biol,* 13**,** 1122-8.

MARTIN, P. & LEIBOVICH, S. J. 2005. Inflammatory cells during wound repair: the good, the bad and the ugly. *Trends in cell biology,* 15**,** 599-607.

MARZIANO, N. K., CASALOTTI, S. O., PORTELLI, A. E., BECKER, D. L. & FORGE, A. 2003. Mutations in the gene for connexin 26 (GJB2) that cause hearing loss have a dominant negative effect on connexin 30. *Hum Mol Genet,* 12**,** 805-12.

MAST, B. A. & SCHULTZ, G. S. 1996. Interactions of cytokines, growth factors, and proteases in acute and chronic wounds. *Wound Repair Regen,* 4**,** 411-20.

MCMANUS, M. C., BOLAND, E. D., SIMPSON, D. G., BARNES, C. P. & BOWLIN, G. L. 2007. Electrospun fibrinogen: feasibility as a tissue engineering scaffold in a rat cell culture model. *Journal of biomedical materials research. Part A,* 81**,** 299-309.

MEHILLI, J., KASTRATI, A., WESSELY, R., DIBRA, A., HAUSLEITER, J., JASCHKE, B., DIRSCHINGER, J., SCHOMIG, A., INTRACORONARY, S. & ANGIOGRAPHIC RESTENOSIS--TEST EQUIVALENCE BETWEEN 2 DRUG-ELUTING STENTS TRIAL, I. 2006. Randomized trial of a nonpolymer-based rapamycin-eluting stent versus a polymer-based paclitaxel-eluting stent for the reduction of late lumen loss. *Circulation,* 113**,** 273-9.

MENDOZA-NARANJO, A., CORMIE, P., SERRANO, A. E., HU, R., O'NEILL, S., WANG, C. M., THRASIVOULOU, C., POWER, K. T., WHITE, A., SERENA, T., PHILLIPS, A. R. & BECKER, D. L. 2012a. Targeting cx43 and N-cadherin, which are abnormally upregulated in venous leg ulcers, influences migration, adhesion and activation of rho GTPases. *PloS one,* 7**,** e37374.

MENDOZA-NARANJO, A., CORMIE, P., SERRANO, A. E., WANG, C. M., THRASIVOULOU, C., SUTCLIFFE, J. E., GILMARTIN, D. J., TSUI, J., SERENA, T. E., PHILLIPS, A. R., BECKER, D. L., ..3 & 33 2012b. Overexpression of the gap junction protein Cx43 as found in diabetic foot ulcers can retard fibroblast migration. *Cell biology international.*

MENKIN, V. 1930. Studies on Inflammation : Iv. Fixation of Foreign Protein at Site of Inflammation. *J Exp Med,* 52**,** 201-13.

MIDWOOD, K. S., WILLIAMS, L. V. & SCHWARZBAUER, J. E. 2004. Tissue repair and the dynamics of the extracellular matrix. *Int J Biochem Cell Biol,* 36**,** 1031-7.

MIJOVIC, B., TRCIN, M., AGIC, A., ZDRAVEVA, E., BUJIC, M., SPOLJARIC, I. & KOSEC, V. 2012. Study on Cell Adhesion Detection onto Biodegradable Electrospun PCL Scaffolds. *Journal of Fiber Bioengineering & Informatics,* 5**,** 33-40.

MIZUMOTO, N., KUMAMOTO, T., ROBSON, S. C., SEVIGNY, J., MATSUE, H., ENJYOJI, K. & TAKASHIMA, A. 2002. CD39 is the dominant Langerhans cell-associated ecto-NTPDase: modulatory roles in inflammation and immune responsiveness. *Nat Med,* 8**,** 358-65.

MO, X. M., XU, C. Y., KOTAKI, M. & RAMAKRISHNA, S. 2004. Electrospun P(LLA-CL) nanofiber: a biomimetic extracellular matrix for smooth muscle cell and endothelial cell proliferation. *Biomaterials,* 25**,** 1883-90.

MOHER, D., LIBERATI, A., TETZLAFF, J., ALTMAN, D. G. & GROUP, P. 2009. Preferred reporting items for systematic reviews and meta-analyses: the PRISMA statement. *PLoS Med,* 6**,** e1000097.

MORI, R., POWER, K. T., WANG, C. M., MARTIN, P. & BECKER, D. L. 2006. Acute downregulation of connexin43 at wound sites leads to a reduced inflammatory response, enhanced keratinocyte proliferation and wound fibroblast migration. *Journal of cell science,* 119**,** 5193-203.

MORI, R., SHAW, T. J. & MARTIN, P. 2008. Molecular mechanisms linking wound inflammation and fibrosis: knockdown of osteopontin leads to rapid repair and reduced scarring. *J Exp Med,* 205**,** 43-51.

MORIMOTO, N., YOSHIMURA, K., NIIMI, M., ITO, T., AYA, R., FUJITAKA, J., TADA, H., TERAMUKAI, S., MURAYAMA, T., TOYOOKA, C., MIURA, K., TAKEMOTO, S., KANDA, N., KAWAI, K., YOKODE, M., SHIMIZU, A. & SUZUKI, S. 2013. Novel collagen/gelatin scaffold with sustained release of basic fibroblast growth factor: clinical trial for chronic skin ulcers. *Tissue Eng Part A,* 19**,** 1931-40.

MOSSER, D. M. 2003. The many faces of macrophage activation. *J Leukoc Biol,* 73**,** 209-12.

MOSSER, D. M. & EDWARDS, J. P. 2008. Exploring the full spectrum of macrophage activation. *Nat Rev Immunol,* 8**,** 958-69.

MOWAT, A. & BAUM, J. 1971. Chemotaxis of polymorphonuclear leukocytes from patients with diabetes mellitus. *N Engl J Med,* 284**,** 621-7.

MOYER, K. E., DAVIS, A., SAGGERS, G. C., MACKAY, D. R. & EHRLICH, H. P. 2002. Wound healing: the role of gap junctional communication in rat granulation tissue maturation. *Exp Mol Pathol,* 72**,** 10-6.

MULLER, M., TROCME, C., LARDY, B., MOREL, F., HALIMI, S. & BENHAMOU, P. Y. 2008. Matrix metalloproteinases and diabetic foot ulcers: the ratio of MMP-1 to TIMP-1 is a predictor of wound healing. *Diabet Med,* 25**,** 419-26.

MUTO, T., TIEN, T., KIM, D., SARTHY, V. P. & ROY, S. 2014. High glucose alters Cx43 expression and gap junction intercellular communication in retinal Muller cells: promotes Muller cell and pericyte apoptosis. *Invest Ophthalmol Vis Sci,* 55**,** 4327-37.

NAGASE, H., VISSE, R. & MURPHY, G. 2006. Structure and function of matrix metalloproteinases and TIMPs. *Cardiovasc Res,* 69**,** 562-73.

NARAYANAN, A. S., PAGE, R. C. & SWANSON, J. 1989. Collagen synthesis by human fibroblasts. Regulation by transforming growth factor-beta in the presence of other inflammatory mediators. *Biochem J,* 260**,** 463-9.

NELSON, E. A., BELL-SYER, S. E. & CULLUM, N. A. 2000. Compression for preventing recurrence of venous ulcers. *Cochrane Database Syst Rev***,** CD002303.

NG, K. W. & HUTMACHER, D. W. 2006. Reduced contraction of skin equivalent engineered using cell sheets cultured in 3D matrices. *Biomaterials,* 27**,** 4591-8.

NGUYEN, B. P., RYAN, M. C., GIL, S. G. & CARTER, W. G. 2000. Deposition of laminin 5 in epidermal wounds regulates integrin signaling and adhesion. *Curr Opin Cell Biol,* 12**,** 554-62.

NIESSEN, C. M. 2007. Tight junctions/adherens junctions: basic structure and function. *J Invest Dermatol,* 127**,** 2525-32.

NISHIDA, T., YASUMOTO, K., OTORI, T. & DESAKI, J. 1988. The network structure of corneal fibroblasts in the rat as revealed by scanning electron microscopy. *Invest Ophthalmol Vis Sci,* 29**,** 1887-90.

NURDEN, A. T., NURDEN, P., SANCHEZ, M., ANDIA, I. & ANITUA, E. 2008. Platelets and wound healing. *Front Biosci,* 13**,** 3532-48.

NUSRAT, A., CHEN, J. A., FOLEY, C. S., LIANG, T. W., TOM, J., CROMWELL, M., QUAN, C. & MRSNY, R. J. 2000. The coiled-coil domain of occludin can act to organize structural and functional elements of the epithelial tight junction. *J Biol Chem,* 275**,** 29816-22.

NWOMEH, B. C., LIANG, H. X., COHEN, I. K. & YAGER, D. R. 1999. MMP-8 is the predominant collagenase in healing wounds and nonhealing ulcers. *J Surg Res,* 81**,** 189-95.

OBARA, K., ISHIHARA, M., ISHIZUKA, T., FUJITA, M., OZEKI, Y., MAEHARA, T., SAITO, Y., YURA, H., MATSUI, T., HATTORI, H., KIKUCHI, M. & KURITA, A. 2003. Photocrosslinkable chitosan hydrogel containing fibroblast growth factor-2 stimulates wound healing in healing-impaired db/db mice. *Biomaterials,* 24**,** 3437-44.

OPIE, E. L. 1924. Inflammatory Reaction of the Immune Animal to Antigen (Arthus Phenomenon) and Its Relation to Antibodies. *The Journal of Immunology,* 9**,** 231-245.

ORGANOGENESIS WEBSITE. 2012. *Apligraf Product Webpage* [Online]. Available at: http://www.apligraf.com/professional/what_is_apligraf/index.html [Accessed 20th November 2011].

PADDLE-LEDINEK, J. E., CRUICKSHANK, D. G. & MASTERTON, J. P. 1997. Skin replacement by cultured keratinocyte grafts: an Australian experience. *Burns : journal of the International Society for Burn Injuries,* 23**,** 204-11.

PALFREYMAN, S., NELSON, E. A. & MICHAELS, J. A. 2007. Dressings for venous leg ulcers: systematic review and meta-analysis. *BMJ,* 335**,** 244.

PANCHIN, Y., KELMANSON, I., MATZ, M., LUKYANOV, K., USMAN, N. & LUKYANOV, S. 2000. A ubiquitous family of putative gap junction molecules. *Curr Biol,* 10**,** R473-4.

PARK, C. J., CLARK, S. G., LICHTENSTEIGER, C. A., JAMISON, R. D. & JOHNSON, A. J. 2009. Accelerated wound closure of pressure ulcers in aged mice by chitosan scaffolds with and without bFGF. *Acta Biomater,* 5**,** 1926-36.

PASYK, K. A., THOMAS, S. V., HASSETT, C. A., CHERRY, G. W. & FALLER, R. 1989. Regional differences in capillary density of the normal human dermis. *Plast Reconstr Surg,* 83**,** 939-45; discussion 946-7.

PAUS, R. & COTSARELIS, G. 1999. The biology of hair follicles. *N Engl J Med,* 341**,** 491-7.

PEIRCE, S. M., SKALAK, T. C. & RODEHEAVER, G. T. 2000. Ischemia-reperfusion injury in chronic pressure ulcer formation: a skin model in the rat. *Wound Repair Regen,* 8**,** 68-76.

PEIRSON, S. N. & BUTLER, J. N. 2007. RNA extraction from mammalian tissues. *Methods Mol Biol,* 362**,** 315-27.

PEPPER, M. S. 2001. Role of the matrix metalloproteinase and plasminogen activator-plasmin systems in angiogenesis. *Arterioscler Thromb Vasc Biol,* 21**,** 1104-17.

PHILIPP, K., RIEDEL, F., GERMANN, G., HORMANN, K. & SAUERBIER, M. 2005. TGF-beta antisense oligonucleotides reduce mRNA expression of matrix metalloproteinases in cultured wound-healing-related cells. *Int J Mol Med,* 15**,** 299-303.

PHILLIPS, T. J. & GILCHREST, B. A. 1991. Cultured epidermal allografts as biological wound dressings. *Prog Clin Biol Res,* 365**,** 77-94.

PIERCE, G. F. 2001. Inflammation in nonhealing diabetic wounds: the space-time continuum does matter. *The American journal of pathology,* 159**,** 399-403.

POLADIA, D. P., SCHANBACHER, B., WALLACE, L. J. & BAUER, J. A. 2005. Innervation and connexin isoform expression during diabetes-related bladder dysfunction: early structural vs. neuronal remodelling. *Acta Diabetol,* 42**,** 147-52.

POLLOK, S., PFEIFFER, A. C., LOBMANN, R., WRIGHT, C. S., MOLL, I., MARTIN, P. E. & BRANDNER, J. M. 2011. Connexin 43 mimetic peptide Gap27 reveals potential differences in the role of Cx43 in wound repair between diabetic and non-diabetic cells. *J Cell Mol Med,* 15**,** 861-73.

POSNETT, J. & FRANKS, P. J. 2008. The burden of chronic wounds in the UK. *Nurs Times,* 104**,** 44-5.

POWELL, H. M. & BOYCE, S. T. 2006. EDC cross-linking improves skin substitute strength and stability. *Biomaterials,* 27**,** 5821-7.

QIU, C., COUTINHO, P., FRANK, S., FRANKE, S., LAW, L. Y., MARTIN, P., GREEN, C. R. & BECKER, D. L. 2003. Targeting connexin43 expression accelerates the rate of wound repair. *Current biology : CB,* 13**,** 1697-703.

RAFFETTO, J. D. & MARSTON, W. A. 2011. Venous ulcer: what is new? *Plast Reconstr Surg,* 127 Suppl 1**,** 279S-288S.

REDD, M. J., COOPER, L., WOOD, W., STRAMER, B. & MARTIN, P. 2004. Wound healing and inflammation: embryos reveal the way to perfect repair. *Philos Trans R Soc Lond B Biol Sci,* 359**,** 777-84.

REN, Y., GU, G., YAO, M. & DRIVER, V. R. 2014. Role of matrix metalloproteinases in chronic wound healing: diagnostic and therapeutic implications. *Chin Med J (Engl),* 127**,** 1572-81.

RHETT, J. M., GHATNEKAR, G. S., PALATINUS, J. A., O'QUINN, M., YOST, M. J. & GOURDIE, R. G. 2008. Novel therapies for scar reduction and regenerative healing of skin wounds. *Trends Biotechnol,* 26**,** 173-80.

RHO, K. S., JEONG, L., LEE, G., SEO, B. M., PARK, Y. J., HONG, S. D., ROH, S., CHO, J. J., PARK, W. H. & MIN, B. M. 2006. Electrospinning of collagen nanofibers: effects on the behavior of normal human keratinocytes and early-stage wound healing. *Biomaterials,* 27**,** 1452-61.

RICHARD, G. 2000. Connexins: a connection with the skin. *Exp Dermatol,* 9**,** 77-96.

RISEK, B., KLIER, F. G. & GILULA, N. B. 1992. Multiple gap junction genes are utilized during rat skin and hair development. *Development,* 116**,** 639-51.

ROBINSON, R. 2004. RNAi therapeutics: how likely, how soon? *PLoS Biol,* 2**,** E28.

ROSEEUW, D. I., DE CONINCK, A., LISSENS, W., KETS, E., LIEBAERS, I., VERCRUYSSE, A. & VANDENBERGHE, Y. 1990. Allogeneic cultured epidermal grafts heal chronic ulcers although they do not remain as proved by DNA analysis. *J Dermatol Sci,* 1**,** 245-52.

ROUAN, F., WHITE, T. W., BROWN, N., TAYLOR, A. M., LUCKE, T. W., PAUL, D. L., MUNRO, C. S., UITTO, J., HODGINS, M. B. & RICHARD, G. 2001. trans-dominant inhibition of connexin-43 by mutant connexin-26: implications for dominant connexin disorders affecting epidermal differentiation. *J Cell Sci,* 114**,** 2105-13.

RUCKER, M., LASCHKE, M. W., JUNKER, D., CARVALHO, C., SCHRAMM, A., MULHAUPT, R., GELLRICH, N. C. & MENGER, M. D. 2006. Angiogenic and inflammatory response to biodegradable scaffolds in dorsal skinfold chambers of mice. *Biomaterials,* 27**,** 5027-38.

RUPENTHAL, I. D., R., G. C. & ALANY, R. G. 2012. Evaluation of Fluorescence Resonance Energy Transfer approaches as a tool to quantify the stability of antisense oligodeoxynucleotides. *Current Pharmaceutical Analysis,* 8**,** 2-10.

SABOLINSKI, M. L., ALVAREZ, O., AULETTA, M., MULDER, G. & PARENTEAU, N. L. 1996. Cultured skin as a 'smart material' for healing wounds: experience in venous ulcers. *Biomaterials,* 17**,** 311-20.

SANDHU, M. S., DUNGER, D. B. & GIOVANNUCCI, E. L. 2002. Insulin, insulin-like growth factor-I (IGF-I), IGF binding proteins, their biologic interactions, and colorectal cancer. *J Natl Cancer Inst,* 94**,** 972-80.

SANTORO, S. W. & JOYCE, G. F. 1997. A general purpose RNA-cleaving DNA enzyme. *Proc Natl Acad Sci U S A,* 94**,** 4262-6.

SARIEDDINE, M. Z., SCHECKENBACH, K. E., FOGLIA, B., MAASS, K., GARCIA, I., KWAK, B. R. & CHANSON, M. 2009. Connexin43 modulates neutrophil recruitment to the lung. *J Cell Mol Med,* 13**,** 4560-70.

SATRIANO, J., MANSOURY, H., DENG, A., SHARMA, K., VALLON, V., BLANTZ, R. C. & THOMSON, S. C. 2010. Transition of kidney tubule cells to a senescent phenotype in early experimental diabetes. *Am J Physiol Cell Physiol,* 299**,** C374-80.

SCHERER, L. J. & ROSSI, J. J. 2003. Approaches for the sequence-specific knockdown of mRNA. *Nat Biotechnol,* 21**,** 1457-65.

SCHMITZ, G. & MULLER, G. 1991. Structure and function of lamellar bodies, lipid-protein complexes involved in storage and secretion of cellular lipids. *J Lipid Res,* 32**,** 1539-70.

SCHOFER, J., SCHLUTER, M., GERSHLICK, A. H., WIJNS, W., GARCIA, E., SCHAMPAERT, E., BREITHARDT, G. & INVESTIGATORS, E. S. 2003. Sirolimus-eluting stents for treatment of patients with long atherosclerotic lesions in small coronary arteries: double-blind, randomised controlled trial (E-SIRIUS). *Lancet,* 362**,** 1093-9.

SCHONFELD, W. H., VILLA, K. F., FASTENAU, J. M., MAZONSON, P. D. & FALANGA, V. 2000. An economic assessment of Apligraf (Graftskin) for the treatment of hard-to-heal venous leg ulcers. *Wound repair and regeneration : official publication of the Wound Healing Society [and] the European Tissue Repair Society,* 8**,** 251-7.

SCHREIER, T., DEGEN, E. & BASCHONG, W. 1993. Fibroblast migration and proliferation during in vitro wound healing. A quantitative comparison between various growth factors and a low molecular weight blood dialysate used in the clinic to normalize impaired wound healing. *Res Exp Med (Berl),* 193**,** 195-205.

SEAH, C. C., PHILLIPS, T. J., HOWARD, C. E., PANOVA, I. P., HAYES, C. M., ASANDRA, A. S. & PARK, H. Y. 2005. Chronic wound fluid suppresses proliferation of dermal fibroblasts through a Ras-mediated signaling pathway. *J Invest Dermatol,* 124**,** 466-74.

SEKAR, R. B. & PERIASAMY, A. 2003. Fluorescence resonance energy transfer (FRET) microscopy imaging of live cell protein localizations. *J Cell Biol,* 160**,** 629-33.

SELUANOV, A., VAIDYA, A. & GORBUNOVA, V. 2010. Establishing primary adult fibroblast cultures from rodents. *J Vis Exp*.

SEMENZA, G. L. 2001. Regulation of hypoxia-induced angiogenesis: a chaperone escorts VEGF to the dance. *J Clin Invest,* 108**,** 39-40.

SEPHEL, G. C. & DAVIDSON, J. M. 1986. Elastin production in human skin fibroblast cultures and its decline with age. *J Invest Dermatol,* 86**,** 279-85.

SERRUYS, P. W., SIANOS, G., ABIZAID, A., AOKI, J., DEN HEIJER, P., BONNIER, H., SMITS, P., MCCLEAN, D., VERHEYE, S., BELARDI, J., CONDADO, J., PIEPER, M., GAMBONE, L., BRESSERS, M., SYMONS, J., SOUSA, E. & LITVACK, F. 2005. The effect of variable dose and release kinetics on neointimal hyperplasia using a novel paclitaxel-eluting stent platform: the Paclitaxel In-Stent Controlled Elution Study (PISCES). *J Am Coll Cardiol,* 46**,** 253-60.

SHAH, J. B. 2011. The history of wound care. *J Am Col Certif Wound Spec,* 3**,** 65-6.

SHARON, Y., ALON, L., GLANZ, S., SERVAIS, C. & EREZ, N. 2013. Isolation of normal and cancer-associated fibroblasts from fresh tissues by Fluorescence Activated Cell Sorting (FACS). *J Vis Exp***,** e4425.

SHAW, J. P., KENT, K., BIRD, J., FISHBACK, J. & FROEHLER, B. 1991. Modified deoxyoligonucleotides stable to exonuclease degradation in serum. *Nucleic Acids Res,* 19**,** 747-50.

SHAW, R. M., FAY, A. J., PUTHENVEEDU, M. A., VON ZASTROW, M., JAN, Y. N. & JAN, L. Y. 2007. Microtubule plus-end-tracking proteins target gap junctions directly from the cell interior to adherens junctions. *Cell,* 128**,** 547-60.

SHEVCHENKO, R. V., JAMES, S. L. & JAMES, S. E. 2010. A review of tissue-engineered skin bioconstructs available for skin reconstruction. *Journal of the Royal Society, Interface / the Royal Society,* 7**,** 229-58.

SHIVE, M. S. & ANDERSON, J. M. 1997. Biodegradation and biocompatibility of PLA and PLGA microspheres. *Adv Drug Deliv Rev,* 28**,** 5-24.

SILVA, E. A. & MOONEY, D. J. 2007. Spatiotemporal control of vascular endothelial growth factor delivery from injectable hydrogels enhances angiogenesis. *J Thromb Haemost,* 5**,** 590-8.

SILVER, F. H., FREEMAN, J. W. & DEVORE, D. 2001. Viscoelastic properties of human skin and processed dermis. *Skin Res Technol,* 7**,** 18-23.

SINGH, A., HALDER, S., MENON, G. R., CHUMBER, S., MISRA, M. C., SHARMA, L. K. & SRIVASTAVA, A. 2004. Meta-analysis of randomized controlled trials on hydrocolloid occlusive dressing versus conventional gauze dressing in the healing of chronic wounds. *Asian J Surg,* 27**,** 326-32.

SMITS, E., BURVENICH, C., GUIDRY, A. J. & MASSART-LEEN, A. 2000. Adhesion receptor CD11b/CD18 contributes to neutrophil diapedesis across the bovine blood-milk barrier. *Vet Immunol Immunopathol,* 73**,** 255-65.

SNYDER, D. L., SULLIVAN, N. & SCHOELLES, K. M. 2012. *Skin Substitutes for Treating Chronic Wounds*. Rockville (MD).

SOHL, G. & WILLECKE, K. 2004. Gap junctions and the connexin protein family. *Cardiovasc Res,* 62**,** 228-32.

SOLLER, E. C., TZERANIS, D. S., MIU, K., SO, P. T. & YANNAS, I. V. 2012. Common features of optimal collagen scaffolds that disrupt wound contraction and enhance regeneration both in peripheral nerves and in skin. *Biomaterials,* 33**,** 4783-91.

SOSINSKY, G. 1995. Mixing of connexins in gap junction membrane channels. *Proc Natl Acad Sci U S A,* 92**,** 9210-4.

SOUTSCHEK, J., AKINC, A., BRAMLAGE, B., CHARISSE, K., CONSTIEN, R., DONOGHUE, M., ELBASHIR, S., GEICK, A., HADWIGER, P., HARBORTH, J., JOHN, M., KESAVAN, V., LAVINE, G., PANDEY, R. K., RACIE, T., RAJEEV, K. G., ROHL, I., TOUDJARSKA, I., WANG, G., WUSCHKO, S., BUMCROT, D., KOTELIANSKY, V., LIMMER, S., MANOHARAN, M. & VORNLOCHER, H. P. 2004. Therapeutic silencing of an endogenous gene by systemic administration of modified siRNAs. *Nature,* 432**,** 173-8.

SPRAY, D. C., ROZENTAL, R. & SRINIVAS, M. 2002. Prospects for rational development of pharmacological gap junction channel blockers. *Curr Drug Targets,* 3**,** 455-64.

STADELMANN, W. K., DIGENIS, A. G. & TOBIN, G. R. 1998. Physiology and healing dynamics of chronic cutaneous wounds. *Am J Surg,* 176**,** 26S-38S.

STEED, D. L. 2006. Clinical evaluation of recombinant human platelet-derived growth factor for the treatment of lower extremity ulcers. *Plast Reconstr Surg,* 117**,** 143S-149S; discussion 150S-151S.

STEIN, C. & KUCHLER, S. 2013. Targeting inflammation and wound healing by opioids. *Trends Pharmacol Sci,* 34**,** 303-12.

STEIN, C. A. 1996. Phosphorothioate antisense oligodeoxynucleotides: questions of specificity. *Trends Biotechnol,* 14**,** 147-9.

STEPHENSON, M. L. & ZAMECNIK, P. C. 1978. Inhibition of Rous sarcoma viral RNA translation by a specific oligodeoxyribonucleotide. *Proc Natl Acad Sci U S A,* 75**,** 285-8.

STRASSMANN, G., PATIL-KOOTA, V., FINKELMAN, F., FONG, M. & KAMBAYASHI, T. 1994. Evidence for the involvement of interleukin 10 in the differential deactivation of murine peritoneal macrophages by prostaglandin E2. *J Exp Med,* 180**,** 2365-70.

TAMILVANAN, S. 2004. Oil-in-water lipid emulsions: implications for parenteral and ocular delivering systems. *Prog Lipid Res,* 43**,** 489-533.

THANNICKAL, V. J., LEE, D. Y., WHITE, E. S., CUI, Z., LARIOS, J. M., CHACON, R., HOROWITZ, J. C., DAY, R. M. & THOMAS, P. E. 2003. Myofibroblast differentiation by transforming growth factor-beta1 is dependent on cell adhesion and integrin signaling via focal adhesion kinase. *The Journal of biological chemistry,* 278**,** 12384-9.

THEISS, C. & MELLER, K. 2002. Microinjected anti-actin antibodies decrease gap junctional intercellular commmunication in cultured astrocytes. *Exp Cell Res,* 281**,** 197-204.

THOMAS, T., AASEN, T., HODGINS, M. & LAIRD, D. W. 2003. Transport and function of cx26 mutants involved in skin and deafness disorders. *Cell Commun Adhes,* 10**,** 353-8.

THOMAS, T., SHAO, Q. & LAIRD, D. W. 2007. Differentiation of organotypic epidermis in the presence of skin disease-linked dominant-negative Cx26 mutants and knockdown Cx26. *J Membr Biol,* 217**,** 93-104.

TOBIN, D. J. 2006. Biochemistry of human skin--our brain on the outside. *Chem Soc Rev,* 35**,** 52-67.

TONNESEN, M. G., FENG, X. & CLARK, R. A. 2000. Angiogenesis in wound healing. *The journal of investigative dermatology. Symposium proceedings / the Society for Investigative Dermatology, Inc. [and] European Society for Dermatological Research,* 5**,** 40-6.

TORRES-GINER, S., GIMENO-ALCANIZ, J. V., OCIO, M. J. & LAGARON, J. M. 2009. Comparative performance of electrospun collagen nanofibers cross-linked by means of different methods. *ACS applied materials & interfaces,* 1**,** 218-23.

TREUTING, P., DINTZIS, S., FREVERT, C. & MONTINE, K. 2012. Skin and Adnexa. *Comparative Anatomy and Histology: A Mouse and Human Atlas.* Academic Press.

TSANG, M. W., WONG, W. K., HUNG, C. S., LAI, K. M., TANG, W., CHEUNG, E. Y., KAM, G., LEUNG, L., CHAN, C. W., CHU, C. M. & LAM, E. K. 2003. Human epidermal growth factor enhances healing of diabetic foot ulcers. *Diabetes Care,* 26**,** 1856-61.

TUYET, H. L., NGUYEN QUYNH, T. T., VO HOANG MINH, H., THI BICH, D. N., DO DINH, T., LE TAN, D., VAN, H. L., LE HUY, T., DOAN HUU, H. & TRAN TRONG, T. N. 2009. The efficacy and safety of epidermal growth factor in treatment of diabetic foot ulcers: the preliminary results. *Int Wound J,* 6**,** 159-66.

UBBINK, D. T., WESTERBOS, S. J., EVANS, D., LAND, L. & VERMEULEN, H. 2008. Topical negative pressure for treating chronic wounds. *Cochrane Database Syst Rev***,** CD001898.

USUI, M. L., UNDERWOOD, R. A., MANSBRIDGE, J. N., MUFFLEY, L. A., CARTER, W. G. & OLERUD, J. E. 2005. Morphological evidence for the role of suprabasal keratinocytes in wound reepithelialization. *Wound repair and regeneration : official publication of the Wound Healing Society [and] the European Tissue Repair Society,* 13**,** 468-79.

VACANTI, J. P., LANGER, R., UPTON, J. & MARLER, J. J. 1998. Transplantation of cells in matrices for tissue regeneration. *Adv Drug Deliv Rev,* 33**,** 165-182.

VEVES, A., FALANGA, V., ARMSTRONG, D. G., SABOLINSKI, M. L. & APLIGRAF DIABETIC FOOT ULCER, S. 2001. Graftskin, a human skin equivalent, is effective in the management of noninfected neuropathic diabetic foot ulcers: a prospective randomized multicenter clinical trial. *Diabetes Care,* 24**,** 290-5.

VINCENT, A. M., RUSSELL, J. W., LOW, P. & FELDMAN, E. L. 2004. Oxidative stress in the pathogenesis of diabetic neuropathy. *Endocr Rev,* 25**,** 612-28.

VOGEL, H. G. 1974. Correlation between tensile strength and collagen content in rat skin. Effect of age and cortisol treatment. *Connect Tissue Res,* 2**,** 177-82.

VON KOCKRITZ-BLICKWEDE, M., CHOW, O. A. & NIZET, V. 2009. Fetal calf serum contains heat-stable nucleases that degrade neutrophil extracellular traps. *Blood,* 114**,** 5245-6.

WAGNER, C. 2008. Function of connexins in the renal circulation. *Kidney Int,* 73**,** 547-55.

WAINWRIGHT, D. J. 1995. Use of an acellular allograft dermal matrix (AlloDerm) in the management of full-thickness burns. *Burns : journal of the International Society for Burn Injuries,* 21**,** 243-8.

WANG, C. M., LINCOLN, J., COOK, J. E. & BECKER, D. L. 2007. Abnormal connexin expression underlies delayed wound healing in diabetic skin. *Diabetes,* 56**,** 2809-2817.

WARNER, A., CLEMENTS, D. K., PARIKH, S., EVANS, W. H. & DEHAAN, R. L. 1995. Specific motifs in the external loops of connexin proteins can determine gap junction formation between chick heart myocytes. *J Physiol,* 488 (Pt 3)**,** 721-8.

WATSON, R. F., ROTHBARD, S. & VANAMEE, P. 1954. The antigenicity of rat collagen. *J Exp Med,* 99**,** 535-50.

WEBER, L., KIRSCH, E., MULLER, P. & KRIEG, T. 1984. Collagen type distribution and macromolecular organization of connective tissue in different layers of human skin. *J Invest Dermatol,* 82**,** 156-60.

WEI, C. J., FRANCIS, R., XU, X. & LO, C. W. 2005. Connexin43 associated with an N-cadherin-containing multiprotein complex is required for gap junction formation in NIH3T3 cells. *J Biol Chem,* 280**,** 19925-36.

WEINSTEIN, G. D., MCCULLOUGH, J. L. & ROSS, P. 1984. Cell proliferation in normal epidermis. *The Journal of investigative dermatology,* 82**,** 623-8.

WHO WEBSITE. 2011. *World Health Organisation - Ageing and Life Course Statistics* [Online]. Available at: http://www.who.int/ageing/en/ [Accessed 20th November 2011].

WIENEKE, H., DIRSCH, O., SAWITOWSKI, T., GU, Y. L., BRAUER, H., DAHMEN, U., FISCHER, A., WNENDT, S. & ERBEL, R. 2003. Synergistic effects of a novel nanoporous stent coating and tacrolimus on intima proliferation in rabbits. *Catheter Cardiovasc Interv,* 60**,** 399-407.

WILKE, K., MARTIN, A., TERSTEGEN, L. & BIEL, S. S. 2007. A short history of sweat gland biology. *Int J Cosmet Sci,* 29**,** 169-79.

WILLIAMS, R. L., SROUSSI, H. Y., LEUNG, K. & MARUCHA, P. T. 2012. Antimicrobial decapeptide KSL-W enhances neutrophil chemotaxis and function. *Peptides,* 33**,** 1-8.

WINDECKER, S., SERRUYS, P. W., WANDEL, S., BUSZMAN, P., TRZNADEL, S., LINKE, A., LENK, K., ISCHINGER, T., KLAUSS, V., EBERLI, F., CORTI, R., WIJNS, W., MORICE, M. C., DI MARIO, C., DAVIES, S., VAN GEUNS, R. J., EERDMANS, P., VAN ES, G. A., MEIER, B. & JUNI, P. 2008. Biolimus-eluting stent with biodegradable polymer versus sirolimus-eluting stent with durable

polymer for coronary revascularisation (LEADERS): a randomised non-inferiority trial. *Lancet,* 372**,** 1163-73.

WINTER, G. D. 1962. Formation of the scab and the rate of epithelization of superficial wounds in the skin of the young domestic pig. *Nature,* 193**,** 293-4.

WITTE, M. B., THORNTON, F. J., KIYAMA, T., EFRON, D. T., SCHULZ, G. S., MOLDAWER, L. L. & BARBUL, A. 1998. Metalloproteinase inhibitors and wound healing: a novel enhancer of wound strength. *Surgery,* 124**,** 464-70.

WONG, V. W., SORKIN, M., GLOTZBACH, J. P., LONGAKER, M. T. & GURTNER, G. C. 2011. Surgical Approaches to Create Murine Models of Human Wound Healing. *Journal of Biomedicine and Biotechnology,* 2011**,** 8.

WOO, K., AYELLO, E. A. & SIBBALD, R. G. 2007. The edge effect: current therapeutic options to advance the wound edge. *Adv Skin Wound Care,* 20**,** 99-117; quiz 118-9.

WRIGHT, C. S., BECKER, D. L., LIN, J. S., WARNER, A. E. & HARDY, K. 2001. Stage-specific and differential expression of gap junctions in the mouse ovary: connexin-specific roles in follicular regulation. *Reproduction,* 121**,** 77-88.

WRIGHT, C. S., VAN STEENSEL, M. A., HODGINS, M. B. & MARTIN, P. E. 2009. Connexin mimetic peptides improve cell migration rates of human epidermal keratinocytes and dermal fibroblasts in vitro. *Wound Repair Regen,* 17**,** 240-9.

WU, S. C., JENSEN, J. L., WEBER, A. K., ROBINSON, D. E. & ARMSTRONG, D. G. 2008. Use of pressure offloading devices in diabetic foot ulcers: do we practice what we preach? *Diabetes Care,* 31**,** 2118-9.

WYSOCKI, A. B., STAIANO-COICO, L. & GRINNELL, F. 1993. Wound fluid from chronic leg ulcers contains elevated levels of metalloproteinases MMP-2 and MMP-9. *J Invest Dermatol,* 101**,** 64-8.

YAGIHASHI, S., YAMAGISHI, S. & WADA, R. 2007. Pathology and pathogenetic mechanisms of diabetic neuropathy: correlation with clinical signs and symptoms. *Diabetes Res Clin Pract,* 77 Suppl 1**,** S184-9.

YANG, Y., ZHU, X. L., CUI, W. G., LI, X. H. & JIN, Y. 2009. Electrospun Composite Mats of Poly[(D,L-lactide)-co-glycolide] and Collagen with High Porosity as Potential Scaffolds for Skin Tissue Engineering. *Macromolecular Materials and Engineering,* 294**,** 611-619.

YANNAS, I. V., LEE, E., ORGILL, D. P., SKRABUT, E. M. & MURPHY, G. F. 1989. Synthesis and characterization of a model extracellular matrix that induces partial regeneration of adult mammalian skin. *Proc Natl Acad Sci U S A,* 86**,** 933-7.

YEAGER, M. & NICHOLSON, B. J. 1996. Structure of gap junction intercellular channels. *Current opinion in structural biology,* 6**,** 183-92.

YUAN, X., CHEN, Z., YANG, Z., GAO, J., ZHANG, A., WU, S. M. & JACOBY, R. 2009. Expression pattern of connexins in the corneal and limbal epithelium of a primate. *Cornea,* 28**,** 194-9.

ZENILMAN, J., VALLE, M. F., MALAS, M. B., MARUTHUR, N., QAZI, U., SUH, Y., WILSON, L. M., HABERL, E. B., BASS, E. B. & LAZARUS, G. 2013. AHRQ Comparative Effectiveness Reviews. *Chronic Venous Ulcers: A Comparative Effectiveness Review of Treatment Modalities*. Rockville (MD): Agency for Healthcare Research and Quality (US).

ZEUGOLIS, D. I., KHEW, S. T., YEW, E. S., EKAPUTRA, A. K., TONG, Y. W., YUNG, L. Y., HUTMACHER, D. W., SHEPPARD, C. & RAGHUNATH, M. 2008. Electro-spinning of pure collagen nano-fibres - just an expensive way to make gelatin? *Biomaterials,* 29**,** 2293-305.

ZHAI, J., WANG, Q. & TAO, L. 2014. Connexin expression patterns in diseased human corneas. *Exp Ther Med,* 7**,** 791-798.

ZHANG, J. & HILL, C. E. 2005. Differential connexin expression in preglomerular and postglomerular vasculature: accentuation during diabetes. *Kidney Int,* 68**,** 1171-85.

ZHANG, J. H., KAWASHIMA, S., YOKOYAMA, M., HUANG, P. & HILL, C. E. 2006a. Increased eNOS accounts for changes in connexin expression in renal arterioles during diabetes. *Anat Rec A Discov Mol Cell Evol Biol,* 288**,** 1000-8.

ZHANG, X. X., CUI, C. C., XU, X. G., HU, X. S., FANG, W. H. & KUANG, B. J. 2004. In vivo distribution of c-myc antisense oligodeoxynucleotides local delivered by gelatin-coated platinum-iridium stents in rabbits and its effect on apoptosis. *Chin Med J (Engl),* 117**,** 258-63.

ZHANG, Y., OUYANG, H., LIM, C. T., RAMAKRISHNA, S. & HUANG, Z. M. 2005. Electrospinning of gelatin fibers and gelatin/PCL composite fibrous scaffolds. *J Biomed Mater Res B Appl Biomater,* 72**,** 156-65.

ZHANG, Z., CAO, X., ZHAO, X., WITHERS, S. B., HOLT, C. M., LEWIS, A. L. & LU, J. R. 2006b. Controlled delivery of antisense oligodeoxynucleotide from cationically modified phosphorylcholine polymer films. *Biomacromolecules,* 7**,** 784-91.

ZHAO, Q., TOPHAM, N., ANDERSON, J. M., HILTNER, A., LODOEN, G. & PAYET, C. R. 1991. Foreign-body giant cells and polyurethane biostability: in vivo correlation of cell adhesion and surface cracking. *J Biomed Mater Res,* 25**,** 177-83.

ZHONG, S. P., ZHANG, Y. Z. & LIM, C. T. 2010. Tissue scaffolds for skin wound healing and dermal reconstruction. *Wiley interdisciplinary reviews. Nanomedicine and nanobiotechnology,* 2**,** 510-25.

ZOU, A. P. & COWLEY, A. W., JR. 2003. Reactive oxygen species and molecular regulation of renal oxygenation. *Acta Physiol Scand,* 179**,** 233-41.